CHARACTERISATION OF BIOCATALYST PRODUCTION WITHIN AN INTEGRATED BIOREFINERY CONTEXT

Nurashikin Binti Suhaili

A thesis submitted for the degree of

Doctor of Philosophy

to

University College London

The Advanced Centre for Biochemical Engineering

Department of Biochemical Engineering

University College London

2017

DECLARATION

I, Nurashikin Binti Suhaili, confirm that the work presented in this thesis is my own. Where information has been derived from other sources, I confirm that this has been indicated in the thesis.

Signature: _____ Date: _____

In loving memory of my Dad

And to my Mum

ABSTRACT

With the emerging interest in integrated biorefinery concepts, there is a need to identify and develop profitable product streams and ensure the utilisation of as many waste streams as possible. Early stage bioprocess development for these processes can be facilitated by the use of high throughput bioreactor platforms that enables rapid, quantitative and scalable data acquisition. This thesis aims to establish high throughput methodologies for the production and characterisation of industrial biocatalysts within an integrated biorefinery context. Specifically, the work focuses on the production of the CV2025 ω-Transaminase (CV2025 ω-TAm) in *Escherichia coli* BL21 (DE3) using sugar beet vinasse, a bioethanol waste stream, as a fermentation feedstock. The high throughput platform to be explored is a 24-well, controlled microbioreactor (MBR) that provides individual monitoring and control of process parameters at the well level.

Initially, batch *E. coli* BL21 (DE3) fermentations expressing CV2025 ω-TAm were established in the controlled MBR using a synthetic medium to provide benchmark data on cell growth and enzyme expression. These cultures indicated a good degree of monitoring and control with respect to process parameters as well as culture reproducibility across the wells. Significant enhancements in relation to maximum biomass concentration (X_{max}), yield of biomass on substrate ($Y_{X/S}$) and CV2025 ω-TAm specific activity of 3.7, 1.9 and 2.2-fold, respectively, were shown in the MBR compared to conventional shake flask system, also representing a 31-fold volumetric reduction. Optimisation of CV2025 ω-TAm production in the MBR showed that the best cell growth and enzyme titre was achieved with an early induction (6 h), 0.1 mM IPTG and 0.024 mmol IPTG g_{dcw}^{-1}, yielding enhancements in X_{max}, $Y_{X/S}$ and CV2025 ω-TAm specific activity of 1.04, 1.2 and 1.4-fold, respectively, over the non-optimised cultures. Control of dissolved oxygen (DO) levels between 30 - 50% oxygen saturation had no significant impact on cell growth and CV2025 ω-TAm titre.

Evaluation of vinasse as a fermentation feedstock for CV2025 ω-TAm production has led to several novel findings. Characterisation of vinasse showed that the feedstock comprised mainly of glycerol along with several reducing sugars, sugar alcohols, acetate, polyphenols and protein. Preliminary results showed *E. coli* BL21 (DE3) cell growth and CV2025 ω-TAm production were feasible in cultures using 17 to 25% (v/v) vinasse with higher concentrations demonstrating inhibitory effects. The D-galactose in vinasse was shown to facilitate auto-induction of the pQR801 plasmid leading to comparable CV2025 ω-TAm expression as obtained in IPTG-induced cultures. Assessment of different vinasse pre-processing options confirmed the relevance of the dilution step in reducing polyphenol concentrations to below inhibitory levels. Moreover, the use of pasteurised vinasse was found to be promising for large scale applications.

Further medium optimisation studies in the MBR showed the benefit of supplementing vinasse with specific media components. Supplementation of diluted vinasse medium with 10 g L^{-1} yeast extract enabled enhancements of 2.8, 2.5, 5.4 and 3-fold in specific growth rate, X_{max}, CV2025 ω-TAm volumetric and specific activity, respectively, over those achieved in non-supplemented

cultures. Additionally, the CV2025 ω-TAm titre attained here represented 81% of that obtained using an optimised synthetic medium. Investigation into the metabolic preferences of *E. coli* BL21 (DE3) when grown on a complex carbon source like vinasse showed the sequential metabolism of D-mannitol before glycerol utilisation, which was followed by the simultaneous metabolism of glycerol, D-xylitol, D-dulcitol and acetate thereafter.

Finally, scale-up of the optimal conditions for CV2025 ω-TAm production using both synthetic and vinasse-based media, from the controlled MBR to a 7.5 L stirred tank reactor (STR) was shown based on matched $k_L a$ values and specific aeration rates. Results showed a good reproducibility with respect to cell growth, substrate consumption and CV2025 ω-TAm production between the scales, representing a 769-fold volumetric scale translation. The feasibility of further intensification of CV2025 ω-TAm production in STR at higher $k_L a$ values using both synthetic and vinasse-based media was also demonstrated leading to enhancements of 1.4 and 1.9-fold in enzyme titre, respectively. Overall, this work has established high throughput methodologies for the characterisation, optimisation and scale-up of industrial biocatalyst production. The approach was demonstrated within the context of an integrated sugar beet biorefinery. However, the utility of the high throughput approach is considered generally applicable across the industrial biotechnology sector.

IMPACT STATEMENT[†]

This research has established a high throughput platform and methodologies for production of industrial biocatalysts. The utility of the approach has been demonstrated for production of CV2025 ω-TAm by *E. coli* BL21 (DE3) within an integrated sugar beet biorefinery using vinasse from bioethanol production as a fermentation feedstock. There are several potential benefits arising from this work that will have impact across academia, the environment and industry.

From the academic perspective, the accomplishment of this project will facilitate exploration of the enzymes produced using vinasse for bioconversion studies, and also the valorisation of vinasse for production of other target products from fermentations. These will be potential spin off projects from this research. The results from this work can also be written up for publication, to facilitate wider dissemination, and serve to support creation of teaching materials for courses related to industrial biotechnology, biocatalysis and fermentation.

Moreover, the research could have considerable impact on the environment and sustainability. With the increasing demand of bioethanol in future, utilisation of the increased amount of vinasse generated, as the bioethanol by-product, could help to overcome environmental pollution otherwise associated with vinasse. The exploitation of renewable feedstocks such as vinasse may also help to reduce society's reliance on expensive and diminishing fossil-based resources. This could help further reduce greenhouse gas emission. From a broader perspective, the present research gives useful insights into adoption of green technologies for industrial production.

Another benefit arising from this research is the potential for commercial exploitation leading to wealth and job creation. For biorefinery the procedures established in this work, if implemented, may help to increase the overall revenues from biorefinery operation. This subsequently may enhance the sustainability of future biorefinery operations. Moreover, the present research may also create promising opportunities in biorefineries using other crops such as sugar cane and starchy plants. Considering the biocatalyst (CV2025 ω-Transaminase) focused in this research, development of its cost effective production as shown by the utilisation of renewable feedstocks, such as vinasse, may help to enhance the importance of the biocatalyst for its further industrial applications as well as the viability of its commercialisation. Meanwhile, concerning the high throughput technology explored in this work, further development and validation of the procedures such as the scale-up procedure for aerobic fermentation from microbioreactors to large scale reactors, will help companies that utilise the technology to reduce the costs and timescales of bioprocess development.

Overall, this research has generated outputs at several levels that could have real impact either immediately or incrementally in future. This process could be accelerated through disseminating research outputs such as journal papers, conference posters/presentations and course materials.

_____

[†]Included as part of the requirements for publication of a UCL doctoral thesis.

ACKNOWLEDGEMENTS

TABLE OF CONTENTS

LIST OF FIGURES

15

LIST OF TABLES

NOMENCLATURE

Symbol		Units
A	Gas liquid interfacial area	m^{-1}
C_L	Dissolved oxygen concentration in the liquid phase	$kg.m^{-3}$
C_{LO}	Dissolved oxygen concentration in the liquid phase at t=0	$kg.m^{-3}$
C_L^*	Saturated oxygen concentration in the liquid phase	$kg.m^{-3}$
d	Path of light	cm
D_i	Impeller diameter	m
D_t	Tank diameter	m
D_w	Well diameter	m
H_i	Impeller height	m
H_t	Tank height	m
H_w	Well height	m
k	Degree of reduction per carbon	-
k_La	Volumetric mass transfer coefficient	h^{-1}
m	Mass	kg
N	Agitation / shaking frequency	min^{-1}
P/V	Specific power input	$kg\ m^{-1}s^{-3}$
Q	Airflow rate	$L\ min^{-1}$
R^2	Coefficient of determination	-
rpm	Revolutions per minute	min^{-1}
T	Temperature	^oC
t	Time	s
t_m	$1/k_La$	s
U	Unit of enzyme activity	$\mu mol\ min^{-1}$
V	Volume	L
v_s	Superficial velocity	ms^{-1}
vvm	Gas volume flow per unit of liquid volume per minute	min^{-1}
v/v	Volume by volume	-
X	Biomass concentration	$g_{dcw}\ L^{-1}$
X_{max}	Maximum biomass concentration	$g_{dcw}\ L^{-1}$
$Y_{X/S}$	Biomass yield on substrate used	$g_{dcw}\ g^{-1}$

Greek symbols

μ	Specific growth rate	h^{-1}
τ_p	Probe response time	s
ε	Extinction coefficient	$mM^{-1}\ cm^{-1}$

ABBREVIATIONS

Abs	Absorbance
ABT	2-amino-1, 3, 4-butanetriol
AC	Activated carbon
ADP	Adenosine diphosphate
AP	Acetophenone
ATP	Adenosine triphosphate
AV	Autoclaved vinasse
BFL	Direct sparged miniature bioreactor plate format with baffles
BOD	Biological oxygen demand
BSA	Bovine Serum Albumin
cAMP	Cyclic adenosine monophosphate
CCR	Carbon catabolite repression
CDA	Clean dry air
CFD	Computational Fluid Dynamics
CHO	Chinese hamster ovary
CH_4	Methane
COD	Chemical oxygen demand
CO_2	Carbon dioxide
CV2025	*Chromobacterium violaceum* 2025
DFA	Difructose anhydride
DISMT	Dual indicator system for mixing time (DISMT)
DMSO	Dimethyl sulfoxide
DO	Dissolved oxygen
DoE	Design of experiment
DV	Dilute vinasse
dcw	Dry cell weight
FC	Follin-Ciocalteu
FV	Filtered vinasse
GA	Gallic acid
glpF	Glycerol transporter
glpK	Glycerol kinase
glpD	Glycerol-3-phosphate dehydrogenase
glpABC	Glycerol-3-phosphate dehydrogenase
GS-CHO	Glutamine-synthetase Chinese hamster ovary
HEPES	4-(2-hydroxyethyl)-1-piperazineethanesulfonic acid buffer
His 6-tag	6x Histidine-tagged
HPLC	High performance liquid chromatography
HTP	High throughput
H_3PO_4	Phosphoric acid
H_2SO_4	Sulphuric acid
ICS	Ion chromatography system
IgG	Immunoglobin G
IPTG	Isopropyl-β-D-thiogalactopyranoside
kDa	Kilo Dalton
KH_2PO_4	Monopotassium phosphate
K_2HPO_4	Dipotassium phosphate
KOH	Potassium hydroxide
LB	Luria Bertani
LED	Light emitting diodes
MBA	Methylbenzylamine
MBR	Microbioreactor

mtlA	Mannitol operon gene responsible for the production of mannitol specific enzyme II of the phosphotransferase
mtlC	Cis-dominant regulatory gene
mtlD	Mannitol-1-phosphate dehydrogenase
MWP	Microwell plate
NADH	Nicotinamide adenine dinucleotide
NH_3	Ammonia
$(NH_4)HPO_4$	Ammonium hydrogen phosphate
NaH_2PO_4	Monosodium phosphate
NH_4Cl	Ammonium Chloride
NH_4OH	Ammonium hydroxide
$(NH_4)SO_4$	Ammonium sulphate
N_2O	Nitrous oxide
OD	Optical density
OD_{600}	Optical density at 600 nm
OTR	Oxygen transfer rate (kg_{O2} $m^{-3}s^{-1}$)
OUR	Oxygen uptake rate (kg_{O2} $m^{-3}s^{-1}$)
PCR	Polymerase chain reaction
PID	Proportional integral derivative
P&ID	Piping and instrumental diagram
PERC	Headspace sparged miniature bioreactor plate format
PHA	Polyhydroxyalkanoate
PLP	Pyridoxal 5'phosphate
PMP	Pyridoxamine 5'phosphate
PPG	Poly propylene glycol
PTS	Phosphotransferase
PV	Pasteurised vinasse
REG	Direct sparged miniature bioreactor plate format
RO	Reverse osmosis
sccm	Standard cubic centimetre per minute
SDS-PAGE	Sodium dodecyl sulfate polyacrylamide gel electrophoresis
STR	Stirred tank reactor
TB	Terrific broth
TE	Trace elements
TK	Transketolase
TP	Therapeutic protein
YE	Yeast extract
ω-TAm	ω-Transminase

CHAPTER 1

INTRODUCTION

1.1 Overview of industrial biocatalysis

With the global trend towards greener approaches to industrial product synthesis, there is a growing interest in the application of biocatalysis. This is due to several benefits of biocatalysis such as high enantioselectivity and regioselectivity in aqueous solution, no requirement for protection and deprotection of functional groups and milder reaction conditions i.e. pH and temperature (Buchholz *et al.*, 2005; Tao and Xu, 2009; Sanchez and Demain, 2011). In contrast chemical syntheses are now often seen as unfavourable from an environmental perspective. This is because these routes normally involve the use of toxic and hazardous solvents and compounds, leading to non-recyclable wastes and thus making the process unsustainable (Halim, 2012).

Owing to the advantages offered by biocatalysis, its industrial implementation is becoming increasingly widespread. Both whole cells and purified enzymes play important roles in the industrial biocatalysis (Schmidt *et al.*, 2001) and their selection is dependent on the specific needs and applications. Whole cells biocatalysts are particularly useful for reactions that require regeneration of cofactors as it is much easier and less costly than it is under *in vitro* conditions (Schmidt *et al.*, 2001). Additionally, the natural environment provided by the whole cells is more likely to be conducive for the enzymes, reducing the risk of activity loss due to conformational alterations in the protein structure in an *in vitro* environment (de Carvalho and da Fonseca, 2007). The major challenge in whole cells biocatalysis, however, lies in the access of the substrates to the enzymes which is hindered by the cell wall and the cell membrane. This may reduce the efficiency of the enzymatic reactions contrary to those by isolated enzymes (de Carvalho, 2011). On the other hand, the major advantages of using purified enzymes in biocatalysis include high specificity of reactions, less complex protocols and higher tolerance to co-solvents used for solubilising poorly water soluble substrates (Roberts *et al.*, 1995). Among the limitations associated with this form of biocatalyst are the isolation and purification of enzymes that could be costly and labour intensive, in addition to the requirement for co-factors addition (de Carvalho, 2011).

It is reported that the application of biocatalysis at an industrial scale, which is on an annual basis of commercialised products of more than 100 kg, has showed a two-fold increase every decade (Fernandes, 2010). In the fine and bulk chemical industries, several compounds have been produced via enzymatic synthesis such as glycolic acid (Panova *et al.*, 2007), acrylamide (Cui *et al.*, 2014; Kang *et al.*, 2014), 1, 3-propanediol (Nakamura and Whited, 2003; Sabra *et al.*, 2010; Riekenberg *et al.*, 2014), cyclodextrins (Duan *et al.*, 2013; Wang *et al.*, 2013) and (R), (S)-epichlorohydrin (Jin *et al.*, 2012). Generally, the bioconversion processes described for these

compounds were found to be advantageous in circumventing limitations related to the chemical synthesis such as use of environmental pollutants (Choi *et al.*, 2015), requirement for high pressure and temperature (Panova *et al.*, 2007) and product instability and low solubility (Jin *et al.*, 2012).

Moreover, in the pharmaceutical industry the application of biocatalysis is also attractive for the synthesis of several drugs. In the synthesis of an anti-diabetic compound, Sitagliptin, the biocatalytic reaction was found to give several benefits such as reduction in total wastes, exclusion of heavy metal use, increase in product yield and feasibility for enzyme recycling (Desai, 2011; Truppo *et al.*, 2012; Ghislieri and Turner, 2013). Meanwhile, in the production of an anti-asthmatic drug (Montelukast), atorvastatin, duloxetine, phenylephrine, ezetimibe and crizotinib, the biocatalytic reactions catalysed by a keto reductase from *Lactobacillus kefir* were found to be beneficial in eliminating the use of a hazardous chemical catalyst (Huisman *et al.*, 2010; Huisman and Collier, 2013).

In the production of 2-amino-1, 3, 4-butanetriol (ABT), a chiral synthon for the synthesis of protease inhibitors such as Nelfinavir™, transaminase (TAm) was exploited for the transamination of L-Erythrulose (Kwon and Ko, 2002). Other pharmaceuticals including boceprevir (Li *et al.*, 2012), telaprevir (Znabet *et al.*, 2010), solitenacin, levocetirizine (Ghislieri and Turner, 2013) have all been synthesised by monoamine oxidase from *Aspergillus niger*. Generally, the increasing demand of biocatalysis in the pharmaceutical industry is partly due to the continued need for compounds with structural complexity, which are otherwise difficult to be synthesised by conventional chemical routes (Pollard and Woodley, 2006).

There is also an interest in adopting biocatalysis in the food industry particularly in the production of functional foods like prebiotics, low-calorie sweeteners and rare sugars (Akoh *et al.*, 2008). Some examples include difructose anhydride (DFA) III (Hang *et al.*, 2011) and galacto-oligosaccharides (Rodriguez-Colinas *et al.*, 2011; Vera *et al.*, 2012). Likewise in the aforementioned applications, the biocatalytic processes in most food industries promote high production yields and simpler processes with lower cost (Choi *et al.*, 2015).

Furthermore, biocatalysis is also of interest in other fields such as cosmetics, textile, pulp and paper industries. In cosmetics, production of arbutin, a glycosylated hydroquinone, by a spectrum of enzymes including α-amylases, α-glucosidase, transglucosidase, sucrose phosphorylase and dextransucrase has been reported (Wang *et al.*, 2006). Other examples include myristyl myristate that is synthesised via an esterification reaction catalysed by lipase (Hilterhaus *et al.*, 2008). In the textile industry, cellulases and proteases play important roles in several processes such as jeans staining, colour enhancement and wrinkle minimisation (Yachmenev *et al.*, 2002; Silva *et al.*, 2005; Dincer and Telefoncu, 2007). Meanwhile, in the pulp and paper industries, several enzymes are of importance such as xylanases and ligninases that are exploited for improving the pulp quality by lignin and hemicellulose removal (Maijala *et al.*, 2008). Moreover, the recycling of printed papers is facilitated by the biocatalytic reaction of cellulase (Patrick, 2004).

Numerous studies have focused on development of new biocatalytic activities and aspects such as alleviating the downsides associated with the use of naturally occurring enzymes and ultimately in generating the maximum possible level of product synthesis (Ingram *et al.*, 2007; Valetti and Gilardi, 2013). Moreover, various technologies have been proposed to further enhance the biocatalytic process among which are continuous reaction and separation bioreactors (De Roode *et al.*, 2001), packed bed reactors (Jeong *et al.*, 2000), immobilised enzyme reactors (Krenkova and Foret, 2004; Urban *et al.*, 2006; Matosevic *et al.*, 2011) and microscale and high throughput (HTP) platforms (Baboo *et al.*, 2012; Halim *et al.*, 2013). With the increasing technology and process development to overcome limitations related to biocatalytic reactions, the future direction of biocatalysis is promising and it continues to serve as an efficient tool, replacing the roles of the traditional chemical processes in many areas.

Generally, the growing application of biocatalysis has also prompted an increased demand for biocatalysts supply. Acquisition of economical and stable biocatalysts has emerged as one of the challenges alongside other issues around the biocatalytic systems such as design methods and productivity (Lye and Woodley, 1999). In order to facilitate the implementation of biocatalysis in industry, a good knowledge of suitable biocatalysts and their process development is indispensable. One of the significant classes of biocatalysts used in the pharmaceutical industry are transaminases (TAm) which are particularly relevant to this work. Further details of TAm will be discussed in Section 1.2.

1.2 Introduction to Transaminases (TAm)

TAm catalyzes the transfer of an amine group from an amino-donor, to an acceptor ketone, yielding a secondary amino compound and a ketone by-product (Brunhuber and Blanchard, 1994; Hyun and Davidson, 1995). The catalytic reaction is mediated by a cofactor, pyridoxal 5' phosphate (PLP) that binds as a prosthetic group. The ω-TAm from *Chromobacterium violaceum* is a homodimeric enzyme with a molecular weight of 50 kDA (Halim, 2012). Figure 1.1 illustrates the reaction scheme of a TAm-mediated bioconversion in the presence of a co-factor PLP. The reaction mechanism is known as ping-pong bi-bi mechanism that is divided into two reactions (Christen and Metzler, 1985). During the first half reaction or oxidative deamination, the amino group is transferred to an enzyme-bound PLP, yielding a pyridoxamine 5'-phosphate (PMP) and the respective keto product. Subsequently, during the second half reaction, the PLP is restored via the reductive amination of the carbonyl compound.
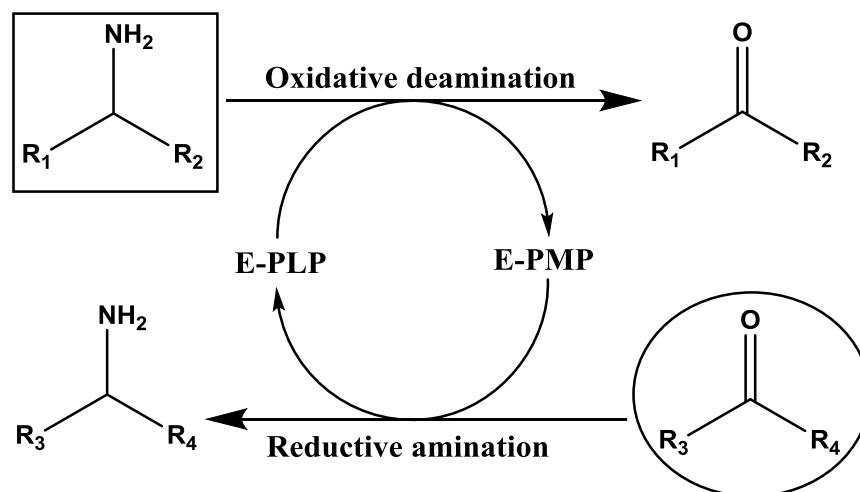
Figure 1.1. Reaction scheme of a TAm-mediated bioconversion in the presence of co-factor PLP. The compounds in the box and circle denote amino donor and amino receptor respectively. Abbreviations: E-PLP – Enzyme bound PLP; E-PMP – Enzyme bound PMP. Adapted from Park and Shin (2013).

This class of enzyme exhibits significant potential for industrial synthesis of amino acids and chiral amines, which are important in the pharmaceutical industry (Shin and Kim, 2001) as preparative materials for production of neuorological, immunological, anti-hypertensive and anti-infective drugs (Sutin *et al.*, 2007; Koszelewski *et al.*, 2008). Generally, chiral compounds comprised of either single enantiomers or racemates constitute over half of the worldwide approved drugs (Caner *et al.*, 2004). It is revealed that about 70% of the drugs are synthesised in routes that have an amino group reaction (Halim, 2012).

There are four different groups of TAm based on their different primary structure (Mehta *et al.*, 1993; Sayer *et al.*, 2007). However the type of a cofactor needed to facilitate the reaction by all the TAms is similar. Further division of TAm into subgroups is based on the types of substrate accessed. TAm from Group II, which is generally recognized as ω-TAm has a notable superiority whereby it can utilise an array of substrates that are not accepted by aminotransferases present in other TAms from Groups I, III and IV (Stirling, 1992). Other visible advantages of ω-TAm include elimination of the need for redox cofactor recycling (Stewart, 2001).

ω-TAms are found in a number of microorganisms and higher organisms where the enzymes are responsible for amino-acid metabolism (Christen and Metzler, 1985). Previous work reported their basic characteristics in *Vibrio fluvialis* JS17, *Klebsiella pneumoniae* JS2F, and *Bacillus thuringiensis* JS64 (Shin and Kim, 2001). Among the advantages demonstrated by the ω-TAm from these microorganisms are high enantioselectivity for several chiral amine enantiomers (Shin and Kim, 2001; Sayer *et al.*, 2007) and high reactivity of amino receptor for pyruvate (Shin and Kim, 2001). In comparison with *K. pneumoniae* JS2F, and *B. thuringiensis* JS64, *V. fluvialis* JS17

was revealed as the best strain for exhibiting better kinetic resolution and asymmetric synthesis. In a more recent work by Kaulmann *et al.* (2007), they have successfully cloned an ω-TAm gene from *C. violaceum* DSM30191 into a pET29a vector and expressed this in an *E. coli* BL21 (DE3) host whereby the resulting plasmid was later designated as pQR801. Figure 1.2 illustrates the structure of the plasmid pQR801. The plasmid has an inducible T7 promoter, lac repressor and codes for kanamycin as the selective marker. The protein sequence of the *C. violaceum* CV2025 enzyme demonstrates a 38% resemblance with that from *V. fluvialis* JS17. Additionally, the *C. violaceum* enzymes were also revealed to favour the transamination in the forward direction, making them promising candidates for the synthesis of chiral amino alcohols. The use of CV2025 ω-TAm will be of a specific interest in this study.
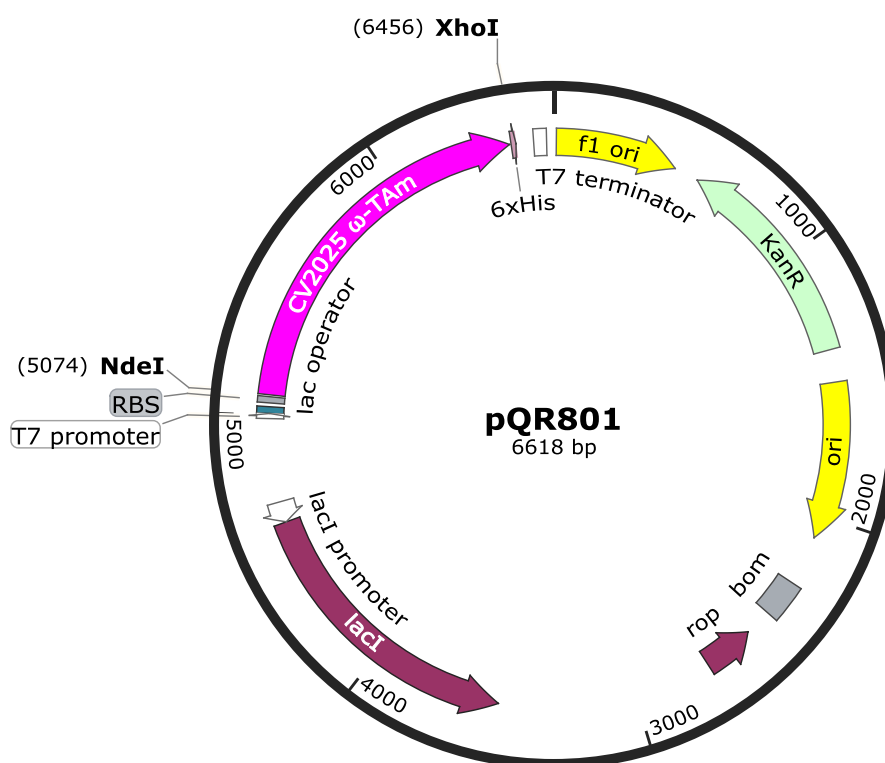
Figure 1.2. Structure of the plasmid pQR801.

In many multi step catalytic reactions involving CV2025 ω-TAm, its low activity often becomes the bottleneck in overall bioconversion productivity (Halim *et al.*, 2013). Apart from enhancements in CV2025 ω-TAm activity during the enzymatic reaction, another possible way to overcome this problem is by intensifying the enzyme expression during the upstream stage. Rios-Solis *et al.* (2015) have highlighted the importance of manipulating the induction conditions to increase CV2025 ω-TAm production in a whole cell *E. coli* BL21 (DE3) biocatalyst harbouring Transketolase (TK) and CV2025 ω-TAm. Their findings led to a high ratio of CV2025 ω-TAm to TK, yielding an efficient multi-step synthesis of amino alcohols. Moreover, their study is among a

few that highlighted the strategies for increasing the expression of dual enzymes in a single strain where the particular focus was on CV2025 ω-TAm.

Future studies should also consider in-depth investigations into the expression of a single enzyme in order to gain a thorough understanding of factors influencing the level of enzyme production. In particular, the development of ω-TAm production has not been specifically emphasised in any previous work that mostly focused on its catalytic reaction (Halim *et al.*, 2013; Park and Shin, 2013; Gustavsson *et al.*, 2014). Hence, key information about optimal production of ω-TAm remains limited.

1.3 *E. coli* culture process development

Over the years, *E. coli* has been the most extensively used microbial platform for producing heterologous proteins due to the fact that it is well characterised in relation to its molecular genetics, physiology and protein synthesis (Makrides, 1996; Choi and Lee, 2004). This includes the expression of CV2025 ω-TAm (as discussed in Section 1.2) whereby *E. coli* BL21 (DE3) with a pET-expression system was used (Kaulmann *et al.*, 2007). Establishing a high cell density culture of *E. coli* is a foremost concern in achieving a maximum CV2025 ω-TAm titre. As most of *E. coli* recombinant proteins, including CV2025 ω-TAm are produced in the cytoplasm, the overall productivity of their production depends greatly on the cell density and amount of protein formed per unit cell mass (Lee, 1996). Over the decades, a large number of works have been dedicated to developing high cell density cultures of *E. coli* with numerous determining aspects being highlighted. Several specific strategies will be highlighted in the following sub sections.

1.3.1 Possible strategies for achieving high cell density and protein titre

1.3.1.1 Media development

Nutrition is one the factors that exerts notable impacts on the metabolic regulation and growth of any microorganism including *E. coli*. A basic understanding of nutrient requirements along with the cell growth behaviour is crucial in determining suitable growth media. Table 1.1 outlines the fundamental elements in *E. coli* dried cells that signify the important nutrients required for the cell metabolism.

Table 1.1. Elemental composition of *E. coli* dried cells. Adapted from Bunch (1994).

Element	Proportion (%)
Carbon	50 – 70
Nitrogen	15 – 20
Oxygen	10 – 20
Hydrogen	6 – 8
Phosphorus	2 – 4
Sulphur	1 – 3
Potassium	1 – 2
Iron	0.1 – 0.3
Calcium	0.01 – 0.05
Magnesium	0.01 – 0.05
Chlorine	0.02 – 0.03
Trace elements	0.2 – 0.5

Generally, cultivation media can be categorised into three types: defined, semi-defined and complex. Defined media have a definite concentration of each nutrient whereas in complex media, the composition of the components such as yeast extract and peptone may be inconsistent (Lee, 1996). Despite the variation of those components, semi-defined and complex media are normally exploited for accelerating product formation (Lee, 1996). In general, suitable media consisting sufficient components in accordance with the metabolic requirement of the microorganism for instance *E. coli*, as outlined in Table 1.1, should be designed in attempting optimal production of the protein of interest.

It is shown in Table 1.1 that carbon is the major element found in *E. coli*, which implies the significance of carbon source in the media formulation. Different types of carbon source have been widely exploited for growing *E. coli*. In early studies, glucose is commonly used in most *E. coli* cultures. In later works, glycerol has been increasingly exploited for *E. coli* cultivations owing to several benefits such as low cost, higher reduction ability and low generation of acetate (Oh and Liao, 2000; Shiloach and Fass, 2005). Whilst an inhibitory threshold of 50 g L^{-1} was reported for glucose in *E. coli* fermentations (Lee, 1996), none is reported for glycerol thus far in the literature. Comparative analyses between glucose and glycerol for *E. coli* fermentations have been widely discussed (Korz *et al.*, 1995; Macaloney *et al.*, 1996; Martínez-Gómez *et al.*, 2012) suggesting the potential of glycerol in substituting glucose as a carbon source to achieve high cell densities. Table 1.2 summarises the applications of both carbon sources alongwith other major medium components for production of various recombinant proteins in *E. coli.* Exploitation of waste glycerol from biofuel industry as fermentation feedstocks will be discussed further in Section 1.6.2.

Several works reported the benefits of certain medium components in alleviating some limitations that normally occur in basic media like Luria Bertani (LB) and Terrific Broth (TB), which could consequently increase the cell density. The maximum achievable *E. coli* cell density in pH, temperature and oxygen-controlled cultivations using LB medium for example is only 1 g_{dcw} L^{-1} (Shiloach and Fass, 2005). A number of works addressed the addition of trace elements like $FeCl_3.6H_2O$, $MnSO_4.H_2O$, $CaCl_2.2H_2O$, $CoCl_2$, $ZnSO_4.7H_2O$, $Na_2MoO_2.2H_2O$, $CuCl_2.2H_2O$ and H_3BO_3, which are important for achieving high cell densities (Shiloach and Bauer, 1975; Riesenberg, 1991; Sivakesava *et al.*, 1999; García-Arrazola *et al.*, 2005; Shiloach and Fass, 2005; Siurkus *et al.*, 2010; Marisch *et al.*, 2013). Furthermore, some elements like selenium, nickel and molybdenum were found essential in reducing the accumulation of formate, which has a similar inhibitory effect as acetate, in *E. coli* cultures (Soini *et al.*, 2008). Incorporation of the aforementioned elements is beneficial as they can serve as cofactors in the degradation of formate to carbon dioxide and hydrogen, catalysed by a formate hydrogen lyase (Soini *et al.*, 2008).

Some components of a complex medium may naturally act as inducers of heterologous protein expression and thus may trigger automatic induction (auto-induction) despite the absence of a typical inducer like isopropyl-β-D-thiogalactopyranoside (IPTG) during protein expression (Studier, 2005). Xu and co-workers (2012) reported a considerable amount of galactose in peptone (7.07 g kg^{-1}) while a trace amount of lactose was detected in peptone, yeast extract and tryptone. The feasibility of lactose to cause induction has been demonstrated in a number of works pertaining to the production of various recombinant proteins by different *E. coli* strains (Tyler *et al.*, 2005; Giomarelli *et al.*, 2006; Gordon *et al.*, 2008; Nishi *et al.*, 2010). In contrast to lactose, galactose has a similarity with IPTG whereby it is not metabolised during the cell growth upon its addition to the culture medium (Xu *et al.*, 2012). However, unlike IPTG, galactose does not hamper the cell metabolism despite its presence throughout the cultivation (Mattanovich *et al.*, 1998), which enables a high cell density to be attained (Xu *et al.*, 2012). The feasibility of galactose in mediating induction in *E. coli* expression systems has also been reported in several other works (De Leon *et al.*, 2003; Menzella and Gramajo, 2004). Both lactose and galactose are regarded as weak inducers and hence, they are needed in a high concentration to allow optimal protein expression (Xu *et al.*, 2012).

Table 1.2. Applications of several medium components in various *E. coli* cultivations.

Medium component	Function	Product	Reference
Glucose	Carbon source	Human tumor necrosis factor-related apoptosis-inducing ligand (Apo2L/TRAIL)	Shen *et al.* (2004)
		Human epidermal growth factor (hEGF)	Sivakesava *et al.* (1999)
		Human tumor necrosis factor-*α* (rhTNF*α*)	Poo *et al.* (2002)
		Uricase	Nakagawa *et al.* (1995)
		Ribonuclease inhibitor	Siurkus *et al.* (2010)
		Mycobacterium tuberculosis	Piubelli *et al.* (2013)
Glycerol		Human interleukin-7	Ouellette *et al.* (2003)
		Protective antigen protein	Chauhan *et al.* (2001)
		Antifungal peptides	Gavit and Better (2000)
		Insulin-like growth factor-1 fusion protein	Choi *et al.* (2003)
Yeast extract	Nitrogen source	Human tumor necrosis factor-*α* (rhTNF*α*)	Poo *et al.* (2002)
		Human tumor necrosis factor-related apoptosis-inducing ligand (Apo2L/TRAIL)	Shen *et al.* (2004)
		Benzoylformate decarboxylase	Losen *et al.* (2004)
		Alcohol dehydrogenase and formate dehydrogenase	Hortsch and Weuster-Botz (2011)
		CV2025 ω-TAm	Halim *et al.* (2013), Rios-Solis *et al.* (2011)
		Pectate lyase	Matsumoto *et al.* (2002)
Peptone		Human tumor necrosis factor-*α* (rhTNF*α*)	Poo *et al.* (2002)
		Isoprenoid	Zhang *et al.* (2013)
		Glyceraldehyde-3-phosphate dehydrogenase	Nancib *et al.* (1993)
		Alcohol dehydrogenase and formate dehydrogenase	Hortsch and Weuster-Botz (2011)
Tryptone		Human tumor necrosis factor-related apoptosis-inducing ligand (Apo2L/TRAIL)	Shen *et al.* (2004)
		Isoprenoid	Zhang *et al.* (2013)

		Ribonuclease inhibitor	Siurkus et al. (2010)
		CV2025 ω-TAm	Halim et al. (2013), Rios-Solis et al. (2011)
		Benzoylformate decarboxylase	Losen et al. (2004)
K_2HPO_4 / KH_2PO_4 $(NH_4)_2HPO_4$ / NaH_2PO_4	Phosphate source, buffer	Ribulose 1, 5-Biphosphate carboxylase / oxygenase	Kleman et al. (1996)
		Alcohol dehydrogenase and formate dehydrogenase	Hortsch and Weuster-Botz (2011)
		Mycobacterium tuberculosis	Piubelli et al. (2013)
		Benzoylformate decarboxylase	Losen et al. (2004)
		Thioredoxin (Trx) and human parathyroid hormone (hPTH)	Fu et al. (2006)

1.3.1.2 Inoculum development

The inoculum is another important factor that contributes to the attainment of high cell density cultures. Several aspects are considered important such as inoculum medium, age and initial cell concentration for a fermentation. In any case, the primary aim is to shorten the lag phase of the subsequent fermentation to achieve optimal cell growth. Some generic approaches have been adopted in previous works including supplementation with amino acids (Marchlis, 1957) and elimination of inhibitory compounds (Yamamoto et al., 1993). Moreover, inoculum age has also been reported as a critical factor that determines the duration of the lag phase in fermentations (Ginovart et al., 2011; Xia and Wu, 2012).

In several studies involving E. coli cultures, the medium used for the seed culture is similar to that used for the subsequent production cultures (Wang and Lee, 1998; Paliy and Gunasekera, 2007; Casablancas et al., 2013). Although the reason was not explicitly discussed in those studies, the underlying reason is believed to ease the adaptibility of the cells when transfering from the seed culture to the fresh production medium that in turn may possibly shorten the lag phase of the fermentations.

1.3.1.3 Optimisation of induction conditions

Induction of the expression system in a recombinant microorganism leads to the regulation of the genes for the energy synthesis, transcription and translation, which are all responsible for protein production (Haddadin and Harcum, 2005). The induction can be performed by using a chemical inducer like IPTG or by manipulating the physical conditions of the cultures such as temperature (Donovan et al., 1996). IPTG is commonly preferred due to its inherent efficiency in inducing

expression even at a low concentration. Other possible inducers include lactose and galactose (Xu *et al*., 2012) as discussed previously in Section 1.3.1.1.

Among factors that influence induction efficiency are inducer concentration and induction time. The optimal concentration of inducer depends greatly on the promoter strength, availability of the plasmid secretory repressor genes, cellular sites of production, cell interaction upon expression of the recombinant protein, protein solubility and protein features (Cserjan-Puschmann *et al*., 2002). The usual range of IPTG concentration used in most of *E. coli* cultivations lies between 0.1 and 1.0 mM (Losen *et al*. 2004; Krause *et al*. 2010; Fang *et al*. 2011; Hortsch and Weuster-Botz 2011; Rios-Solis *et al*. 2011). Normally, induction is performed during the exponential phase of cell growth. As claimed by Rios-Solis (2012), the best induction time and temperature for the expression of CV2025 ω-TAm by *E. coli* BL21 (DE3) is during the early exponential phase at a temperature of 37 °C. In other scenarios, where cell growth is severely hampered by the addition of the inducer, induction can be performed during the late exponential or early stationary phase (Donovan *et al*., 1996).

Another way to manipulate induction is by adjusting the culture temperature. This has been demonstrated by Schmidt *et al*. (1999) whereby a thermally inducible expression vector was used for expressing human insulin fusion proteins in a recombinant *E. coli*. The expression of the insulin fusion proteins was induced by shifting the temperature from 30 to 42 °C. This induction approach is another alternative in replacing the use of the costly IPTG.

At present, the trend in studying protein expression in *E. coli* has shifted towards utilising high throughput (HTP) platforms to facilitate parallel experiments during process development and optimisation studies. As *E. coli* continues to be exploited as a prominent host for production of numerous recombinant proteins, future research may need to constantly focus on the aspects related to the throughput efficiency and process sustainability. The former will be discussed in detail in the following section.

1.4 High throughput (HTP) technology

In facilitating early stage process development of microbial fermentations, the exploitation of HTP models is of great interest. Miniaturisation and parallel operation promotes HTP experimentation and low material requirements leading to rapid data acquisition and in general, shortens the process development timelines (Long *et al*., 2014). Primarily, the technology is heavily used for analytical purposes (Persidis, 1998) but lately it has been further exploited for other applications. The use of laboratory automation platforms and conventional microwell plate (MWP) has become widespread in various applications such as microbial (Duetz *et al*., 2000; Minas *et al*., 2000; Elmahdi *et al*., 2003; Islam *et al*., 2008) and mammalian cell culture (Girard *et al*., 2001),

biocatalysis (Stahl *et al.*, 2000; John and Heinzle, 2001; Ferreira-Torres *et al.*, 2005; Baboo *et al.*, 2012) and downstream processes (Welch *et al.*, 2002; Jackson *et al.*, 2006; Rayat *et al.*, 2010).

Despite the advantages of HTP, one limitation of conventional MWPs lies in the absence of in-situ measurement of certain process paramaters such as pH and DO although controlled microbioreactor (MBR) technologies are now becoming available. In the following sections, applications of conventional MWP and controlled MBRs for fermentations will be discussed further.

1.4.1 Conventional microwell plate (MWP) technologies

Over the last decade, several works have addressed the use of MWP for optimisation studies of various microbial and cell cultures. For instance, Ferreira-Torres *et al.* (2005) reported the use of 96-deep square well plates for a linked sequence of microscale operations involving fermentation, enzyme induction and bioconversion for cyclohexanone monoxygenase production by *E. coli* and *Acinetobacter calcoaceticus*. Throughout their study, the potential of the microscale platform in quantitatively distinguishing between different strains was demonstrated. Furthermore, the fermentation and bioconversion microscale kinetics were found to be predictive for a 1400 and 2800-fold scale translation, respectively, confirming the potentials of the microscale platform for the whole process operation.

In another investigation, optimisation studies based on a statistical Design of Experiment (DoE) approach using 24-well and 48-well plates was demonstrated for firefly luciferase production by *E. coli* (Islam, 2007). The results proposed the reliable role of the microscale platform to facilitate rapid data collection for the optimisation studies and also scalability of the process to laboratory and pilot scales. Meanwhile, the application of MWP for murine hybridoma cell culture expressing IgG1 was reported by Barett and co-workers (2010). Their findings suggested the reproducibility of the culture performance with respect to the standard shake flask culture while presenting a 30-fold scale reduction of the operation.

There are fewer works dealing with the implementation of fed-batch operations in shaken MWPs. Silk and co-workers (2010) evaluated the use of a bolus feed for cultivating a Glutamine-Synthetase-Chinese hamster ovary (GS-CHO) cell line. The results obtained were equivalent to those attained in shake flask cultures in relation to cell growth, viability and antibody titre. The use of EnBase™ or enzyme-based-substrate delivery technology in MWPs has been addressed by several researchers. Siurkus *et al.* (2010) and Li *et al.* (2015) have examined the technology for *E. coli* fermentations in MWPs and translation of the processes, to laboratory scale reactors. A good equivalency of the fermentation kinetics between the fed MWP and laboratory scale reactor cultures was reported. Despite the simple solution that these substrate-release systems have offered for carrying out fed-batch operations in the microscale platforms, a significant

challenge with respect to the MWP system itself at this point is the integration of a feeding system that can regulate the feed more effectively as in the conventional reactors. This may solve the limitation associated with the fast release rate of the substrate using the aforementioned fed-batch approaches, which might be challenging for cell cultures that have a relatively lower substrate uptake rate than the microbial cultures (Hegde *et al.*, 2012).

Whilst there are several inherent advantages offered by MWPs over the conventional shake flask system such as HTP and low materials requirement, the unavailability of monitoring and control for certain process parameters particularly pH and dissolved oxygen (DO) limits their application. A number of works have reported several approaches to overcome the limitations in MWP of which only a few are given a particular mention here. For example, the benefit of pH control in microscale fermentations of *S. erythraea* for erythromycin production was demonstrated by Elmahdi and co-workers (2003). The implementation of a pH control system, which was initially introduced at the 7 L scale, was successfully reproduced at the microwell scale yielding to an increase in both maximum specific growth rate and biomass concentration in comparison with the uncontrolled pH cultures.

The development of MWPs with the incorporation of oxygen sensors has been discussed in several works. Hynes *et al.* (2003) and Deshpande and Heinzle (2004) demonstrated the application of oxygen sensors for cell cultures in microplates that enables the determination of the oxygen uptake rates and specific uptake rates of the cells. In another study by O'Riordon *et al.* (2000), they investigated the use of a disposable phosphorescent sensor in the microwell fermentation for cultivating *Schizosaccharomyces pombe* in order to determine the DO levels in the culture. The study has shown the benefits of the incorporated oxygen sensors, which are non-consumptive and non-invasive, for monitoring the respiration of the cells. Generally, all the abovementioned studies on the intensification of MWPs have given early insights into the feasibility and importance of the incorporation of process control, ensuring the benefits of HTP platforms to be further extended.

1.4.2 Controlled microbioreactor (MBR) technologies

The growing interest in conventional MWPs over the past decade has led to the development of controlled MBR technologies, which are equipped with a real-time monitoring and control of process parameters such as pH, DO and temperature. Figure 1.3 depicts the comparison of features between a standard shake flask, a HTP controlled MBR and a conventional scale, stirred reactor. As clearly illustrated, the controlled MBR combines the advantages featured by shake flasks and conventional scale, stirred reactors along with its HTP and automation capabilities. On the other hand, the limitation of the conventional MWPs lies in the absence of the environmental control that is available in the laboratory reactors. Having the integrated benefits of the shake flasks and laboratory reactors, the use of controlled MBRs is highly desirable to support early

process development such as strain screening and process optimisation, replacing the typical role of the two former systems.
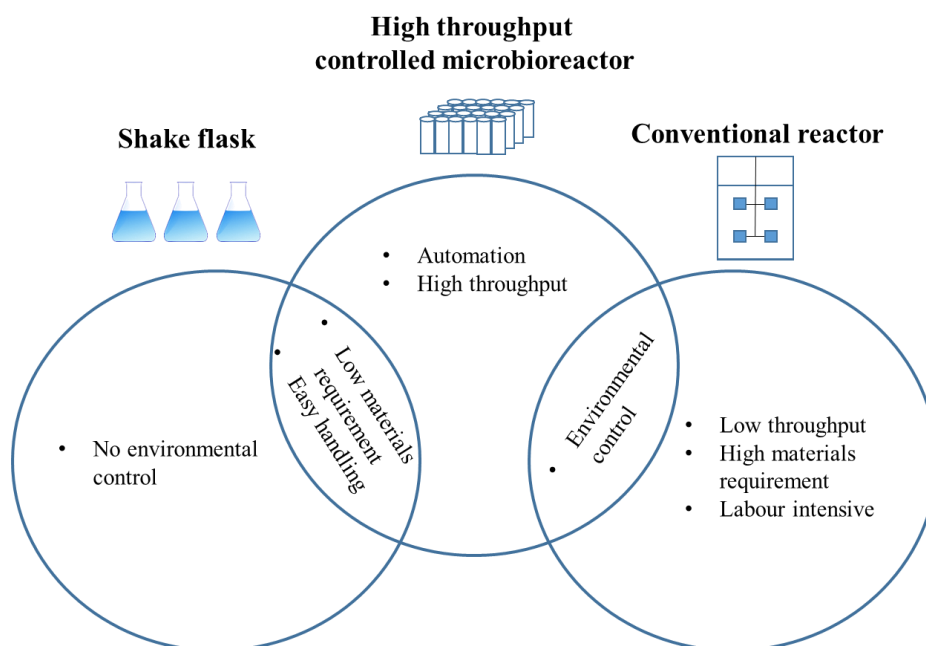
Figure 1.3. Comparison of features between a standard shake flask, HTP controlled MBR and conventional scale, stirred reactor.

There are now a number of commercialised controlled MBRs that are available in different geometries, sizes and functionalities. Over the past decade, a number of works have reported the applications of these commercialised systems. One of the popular MBRs is the Micro-24 (Pall Corporation, USA). It is a 24-well miniature single-use MBR featuring independent control of pH, DO and temperature in every well. The working volume ranges between 3 and 7 ml. This MBR is one of its kind to have the monitoring and control of the process parameters at individual well level (Isett *et al.*, 2007). The use of Micro-24 has been discussed by several researchers. Tang *et al.* (2006) first evaluated its use for optimising the growth of *Shewanella oneidensis* MR-1 and further evaluated it for the reduction of chromium (Cr (VI)) by investigating the influence of several determinants of the process.

In a study by Isett *et al.* (2007), an initial assessment of the Micro-24 was carried out for cultivating *S. cerevisae*, *P. pastoris* and *E. coli* apart from the characterisation of volumetric mass transfer coefficient (k_La) and mixing time. A good reproducibility of the process parameters namely pH, DO and temperature was observed between the wells. Comparing the cultivation performance between Micro-24 and a 20 L stirred tank reactor (STR) for *S. cerevisae* and *E. coli*, the authors found that the growth and metabolite kinetics between the scales were reproducible for the former strain while in the latter case, there were limitations encountered with respect to pH and DO

profiles although the dextrose consumption was found to be reproducible during the exponential phase. Meanwhile for *P. pastoris*, a high cell density culture was successfully cultivated under batch and fed-batch operations with a good reproducibility of pH, DO and temperature profiles.

The application of Micro-24 for Chinese hamster ovary (CHO) cell culture was first discussed by Chen and colleagues (2009). Among the findings reported include the interwell reproducibility in relation to process parameters, cell growth, metabolites, protein titre and quality and the feasibility of a 400-fold scale translation. In a later study by Betts *et al.* (2014), the impact of aeration strategies on CHO cell culture was investigated using direct sparged cassette (REG) and headspace sparged cassette (PERC) along with some characterisation studies with respect to $k_L a$ and mixing time. Whilst a superior cultivation performance was reported for PERC cassette, the authors highlighted the pronounced role of the REG cassette for scale-up application due to its similarity with the STR in terms of the dispersed gas phase. Generally, these two studies suggest the promising application of Micro-24 as a scale-down platform for cell culture process development.

Holmes *et al.* (2009) further evaluated the application of the Micro-24 for optimising recombinant protein production in *P. pastoris* through a DoE approach. The proposed model from their study was found to predict well the protein yield in both Micro-24 and 7 L STR under fed-batch operation. Their study was the first attempt that used the DoE strategy for optimisation studies in Micro-24. Recently, Ramirez-Vargas *et al.* (2014) investigated the respirometric potential of Micro-24 by examining the DO fluorescent quenching sensors. The studies suggested that the capability of the MBR to determine oxygen uptake rate (OUR) from 0.038 to 3390 mg $L^{-1}h^{-1}$ when pure oxygen is used where that range spans over the typical OURs reported for most bacteria, yeast and cell cultures.

Another type of MBR is the BioLector system (m2p-Labs, Germany), a miniature 48-shaken microtitre plate that also operates with non-invasive optical sensors. It provides an online monitoring technique for quantifying biomass concentration and fluorescence. The system allows integration with a liquid handling system, enabling a fully automated MBR unit. Among early applications of this MBR system include the cultivation of *E. coli* and *Hansenula polymorha* (Kensy *et al.*, 2009b). The work reported the feasibility of the MBR to facilitate studies related to media and clone screening for both microorganisms. Huber *et al.* (2009) first reported the integration of BioLector with a liquid handling robot (Robolector) for cultivating *E. coli* BL21 (DE3) pRhotHi-2-EcFbFP, expressing the fluorescence protein EcFbFP. The use of the RoboLector has further extended the capability of BioLector to facilitate a HTP and fully automated experimentation with a rapid collection of high content kinetic data.

Scale-up works involving the BioLector have been discussed in several studies. Kensy and co-workers (2009a) reported the feasibility of a 7000-fold scale translation from the BioLector to a 1.4 L STR based on a matched $k_L a$ value where reproducible growth and protein expression kinetics were observed between the scales. In a later study by Rohe *et al.* (2012), the scalability

of an optimal production of cutinase by *Corynebacterium glutamicum* has been demonstrated between BioLector and 1 L and 20 L STR. In line with the report by Kensy *et al.* (2009a), identical growth and product titre were reported although the scale-up basis was not explicitly discussed.

A fed-batch approach based on enzymatic release of polymeric glucose has been demonstrated in the BioLector by Toeroek *et al.* (2015) for *E. coli* based production processes. The results suggested the feasibility of the fed-batch process to support a high cell density *E. coli* culture without any limitations in oxygen supply, which is also transferable to larger scales. Other applications of the BioLector include optimisation of lipid accumulation in *Yarrowia lipolytica* (Back *et al.*, 2016), recombinant virus-like particle production for chimeric vaccines in *E. coli* (Effio *et al.*, 2016), screening of cellulases for biofuel production (Jager *et al.*, 2011), and evaluation of inducible promoter / repression systems for recombinant protein expression in *Lactobacillus plantarum* (Heiss *et al.*, 2016).

One of the latest additions to the controlled MBRs is the ambr^{TM} system (TAP Biosystems, Royston, Cambridge) a micro stirred bioreactor that comes up with 24 single-use individual vessel, equipped with a closed loop control of pH and DO with an independent control of O_2 and CO_2. The system is integrated with an automated liquid handling unit that aids reactor set up, feeding and sampling. Initial assessments of this MBR were mostly centered for cell culture application. The application of the ambr^{TM} system for cultivating CHO cell lines was discussed by Hsu *et al.* (2012), Nienow *et al.* (2013) and Rameez *et al.* (2014) whereby the reproducibility of the process parameters and cultivation performance between ambr^{TM} and laboratory scale reactors has been highlighted. Additionally, in these studies the superiority of the cultivation performance in ambr^{TM} over that in the shake flask system was reported, implying the benefits of the control system provided in the former system.

An extensive evaluation of the ambr^{TM} system for process characterisation, process parameters classification and development of process parameters control strategy for a manufacturing process of a cell culture was first reported by Janakiraman and Kwiatkowski (2015). The results suggested the transferability of the cell culture performance from the ambr^{TM} system to a bench (5 L) and manufacturing (15 000 L) scale reactor under a defined specific aeration rate. The comparability of the DoE data between the ambr^{TM} system and bench scale reactor indicated the promising role of the former system to facilitate rapid data collection for early process development. Generally, the application of the ambr^{TM} system for microbial cultivations is still limited. Further studies concerning options for scaling up as well as the characterisation of the MBR will be beneficial.

The most recent controlled MBR to enter the market is the micro-Matrix (Applikon Biotechnology B. V., Holland). Sani (2016) reported the initial evaluation of the micro-Matrix system for cultivating CHO cell lines. Throughout the study, the best strategies comprising controlled addition and continuous feeding have been identified to favour high cell concentration and viability. Moreover,

the feasibility of a 1000-fold scale translation of the CHO cultivation was demonstrated between the micro-Matrix and a 5 L STR based on a matched mixing time whereby an equivalent performance was observed between the two geometries in relation to viable cell concentration and IgG titre. This initial report has validated the promising application of micro-Matrix for screening and optimisation studies particularly for cell culture application.

The application of the micro-Matrix for microbial cultures nonetheless, remained to be explored. One challenge that might lie in its application for microbial cultures is in terms of its aeration system, which is based on head space aeration that is unlikely to support highly aerobic microbial cultures. Nevertheless, the availability of the feeding system in this MBR may enable efficient fed-batch operations to be conducted. A summary of the basic features of all the abovementioned controlled MBRs is outlined in Table 1.3.

The integration of HTP and single-use technologies has further enhanced their significant role in early stage bioprocess development. The application of single-use reactors has eliminated the need for the laborious steps before and after the production stage such as the set up, sterilisation and cleaning. Other advantages include minimal risk of contamination, reduced turn-around time and enhanced flexibility and productivity (Allison and Richards, 2014; Gao and Allison, 2015). Although there may be a trade-off with the cost of the disposable reactors, in general, adoption of both HTP and single-use technologies can accelerate the process development timeline with significant labour and energy savings. In Chapter 3 of this thesis, a particular approach of the exploitation of a HTP single-use controlled MBR (Micro-24) for *E. coli* BL21 (DE3) culture will be explored in detail.

Table 1.3. Specification of selected commercially available HTP controlled MBRs. Adapted from Long *et al.* (2014).

Characteristic	Controlled microbioreactor			
	BioLector	Micro-24	Ambr	micro-Matrix
Working volume	0.8 – 1.5 mL per well	3 – 7 mL per well	10-15 mL per vessel	1 – 7 mL per well
Mixing mechanism	Orbital shaking	Orbital shaking	Agitation	Orbital shaking
Aeration strategy	Headspace	Headspace / Dispersed	Dispersed	Headspace
Throughput	48 wells	24 wells per cassette	24 or 48 vessels	24 wells per unit
Process parameters / information	Online monitoring and control of pH, DO, T, biomass and fluorescence protein	Online monitoring and control of pH, DO, T,	Online monitoring and control of pH, DO, T,	Online monitoring and control of pH, DO, T,
Oxygen transfer rate (mmol L^{-1} h^{-1})	>100	>300	n.a.	>300
Feed availability	Possible integration with a liquid handling system	Possible integration with a liquid handling system	Automated liquid handling robot for set up, feeding and sampling	Automated liquid handling robot for set up, feeding and sampling
Manufacturer	m2p-Labs	Pall Corporation	TAP Biosystems,	Applikon Biotechnology

n.a. – not available

Note: Headspace aeration – refers to aeration provided to the culture from the liquid surface alone; dispersed aeration – refers to aeration provided from the gas bubbles that pass through the culture (in addition to any headspace aeration).

1.5 Scale-up of fermentation processes

One of the concerns regarding the application of HTP cultivation systems is the reproducibility of the optimal process conditions established in those platforms at larger scales of production. Generally, the ultimate aim of a scale-up is to acquire a larger quantity of product with an increase or at least reproducible specific yield and product quality (Schmidt, 2005). Among the key challenges in scale-up is the variation between the scales in terms of the system geometries and the prevailing mechanisms of heat and mass transfer. This has led to studies on the characterisation of reactor systems prior to scale-up in order to gain insights into the identification and validation of the critical scale-up parameters.

The selection of the scaling parameter generally depends on the factors that affect the specific process behaviour such as oxygen supply, mass transfer, mixing, aeration and power input (Najafpour, 2007; Burke, 2008). There is no generic scale-up rule that fits all cultivations; therefore the possibility of achieving a successful scale-up via different strategies is usually possible. The combination of more than two scaling parameters is commonplace in many fermentations with both of them being fixed during scale translation (Schmidt 2005; Najafpour, 2007; Marques *et al.*, 2010). Several typical scale-up parameters are described in detail below.

1.5.1 Concepts and strategies of scale-up

1.5.1.1 Volumetric mass transfer coefficient ($k_L a$)

Oxygen serves as one of the main substrates in any aerobic bioprocesses for cell growth, maintenance and metabolites production (Buchs, 2001; Liu *et al.*, 2006). The transfer of oxygen normally from bubbles or the liquid surface to cultures is typically hindered by the low oxygen solubility in water of approximately 0.272 mmol L^{-1} at 25 ^{o}C and 101 kPa air pressure, making it a limiting substrate in aerobic fermentations (Doran, 1995). Hence, the subsequent challenge lies in supplying adequate amount of oxygen to the cultures.

Oxygen transfer rate (OTR) is characterised in terms of the combined, overall volumetric mass transfer coefficient ($k_L a$) and the oxygen concentration gradient (C_L^*-C_L) (Doran, 1995; Burke, 2008) as outlined in Equation 1.1.

$$\text{OTR} = k_L a(C_L^* - C_L) \qquad \text{(Equation 1.1)}$$

Where k_L represents mass transfer coefficient, a is interfacial area, C_L is the dissolved oxygen concentration in the liquid phase (kg.m^{-3}) and C_L^* is the saturated oxygen concentration in the liquid phase (kg.m^{-3}). Due to the difficulty in measuring k_L and a separately, their product, k_La is often regarded as a single variable. Increasing the OTR is often crucial in overcoming high oxygen demand during fermentations, normally regarded as oxygen uptake rate (OUR) (Marques *et al.*, 2010). In increasing OTR, (C_L^*-C_L) renders less possibilities for enhancement since the C_L^* value is typically small (Rao, 2010). Thus, k_La plays a relatively important role in determining the OTR. Both k_L and a are influenced by several factors, among which are power consumption, gas superficial velocity, liquid phase properties that include ionic strength, surface tension and viscosity (Van't Riet, 1979).

Due to the low solubility of oxygen in water despite its high demand during aerobic bioprocesses, oxygen transfer appears to be a limiting factor in these cases. Hence, maintaining a constant OTR, which is mainly governed by k_La, is a typical basis for scaling aerobic bioprocesses. The oxygen uptake rate (OUR) of bacterial cells ranges from 0.46 - 2.33 x 10^{-3} g cell^{-1} h^{-1}, in contrast to 2 to 10 x 10^{-12} g cell^{-1} h^{-1} for mammalian cells (Michelletti *et al.*, 2006). As the oxygen may not adversely impact the growth of mammalian cell cultures (Lavery and Nienow, 1987), most works involving cell cultures normally do not consider k_La as the scaling basis.

There are several ways to directly measure k_La, which can be categorised into chemical and physical methods of which the latter case will be of concern in this study. Chemical methods include sodium sulphite oxidation (Cooper *et al.*, 1944) and absorption of CO_2 (Danckwerts and Gillham, 1966). One of the limitations of these chemical methods is that the chemicals addition may vary the physicochemical properties of the fluid; the mass transfer coefficient may also be over predicted due to the increased oxygen absorption rate caused by the chemical reaction (Garcia-Ochoa and Gomez, 2009).

Physical methods, on the other hand, involve direct measurement of changes in DO levels using an oxygen-selective probe (Garcia-Ochoa and Gomez, 2009). This approach is known as the dynamic gassing-out method and is a widely adopted technique for k_La determination due to its simplicity and accuracy (Marques *et al.*, 2010). The dynamic method of absorption involves purging the oxygen from the liquid phase, usually by sparging nitrogen gas until the oxygen concentration reaches 0%. Subsequently, air is sparged into the reactor under appropriate agitation and aeration conditions and the change of the DO with time is recorded. Meanwhile, the dynamic method of desorption comprises first sparging the liquid phase with air until a saturation level of oxygen concentration is attained. Following that, the oxygen is purged by sparging the nitrogen until the concentration reaches 0% and the change of the DO with time is recorded. In either method, the influence of the probe response time (τ_p) needs to be incorporated into the k_La measurement (Garcia-Ochoa and Gomez, 2009). τ_p is defined as the time taken to achieve 63% of the saturation level of DO (Van't Riet, 1979). The relationship between k_La, dissolved oxygen concentration and time during the absorption and desorption techniques is represented by

Equations 1.2 and 1.3, respectively; in both cases, k_La represents the slope of the graph of ln f (C_L) versus time.

$$\ln\left(1 - \frac{C_L}{C_L^*}\right) = -k_La(t) \qquad\qquad \text{(Equation 1.2)}$$

$$\ln\frac{C_{L0}}{C_L} = k_La(t) \qquad\qquad \text{(Equation 1.3)}$$

Where C_{L0} is the dissolved oxygen concentration in the liquid phase at 0 h (kg.m^{-3}). Apart from the experimental methods, k_La can also be predicted using empirical correlations. The variation of the types of fluid used, type and size of reactor, operational conditions and measuring methods applied in the development of the empirical correlations are likely to influence the accuracy between the experimental and calculated k_La values (Garcia-Ochoa and Gomez, 1998; Gogate *et al.*, 2000).

The most widely used k_La correlation was proposed by Van't Riet (1979), which is represented by Equation 1.4.

$$k_La = a\left(\frac{P}{V}\right)^b(V_s)^c \qquad\qquad \text{(Equation 1.4)}$$

Where (P/V) denotes volumetric power consumption (kg m^{-1}s^{-3}), v_s is superficial velocity (ms^{-1}) and a, b and c are correlation coefficients. The use of Equation 1.4 to predict k_La in STRs has been reported extensively in the literature (Montes *et al.*, 1999; Weuster-Botz *et al.*, 2002; Islam *et al.*, 2008; Baboo *et al.*, 2012).

1.5.1.2 Mixing time

Scale-up can also be based on constant mixing time between the scales. Mixing time is defined as the time needed to achieve a certain uniformity level of the reactor contents upon tracer injection (Marques *et al.*, 2010). The rationale of adopting mixing time as a scale-up basis is to ensure a similar homogeneity of the culture composition across the scales. Experimental determination of mixing time in a reactor is commonly performed based on colorimetric methods. Generally, these are based on a colour-decolourisation concept where a liquid tracer is injected into the reactor containing liquid and the dispersion of the tracer within the reactor content is observed and recorded over time (Ascanio, 2015). As the method was initially developed for a conventional laboratory reactor, there lies a challenge in quantifying the mixing time in a shaken

microscale platform. Thus, certain modifications need to be carried out. In a study by Nealon and co-workers (2006), they established a high-speed video method to measure the jet macro-mixing times in a static MWP. The technique also allows visualisation of the jet formation and liquid flow patterns throughout the wells. Meanwhile, Rodriguez *et al.* (2014) used the Dual Indicator System for Mixing Time (DISMT) approach for the quantification of mixing time in orbital shaken reactors. They demonstrated the incorporation of a critical Froude number as promising for the development of the scaling law for mixing time between the shaken reactors of different scales.

1.5.1.3 Volumetric power consumption

Constant ungassed (P_o) or gassed power (P_g) per unit volume between the scales can be used as bases for scale-up. For stirred reactors of standard geometry, according to Rushton *et al.* (1950a) and Rushton *et al.* (1950b), empirical determination of P_o is based on Equation 1.5:

$$P_o = N_p N^3 D_i^5 \rho \qquad \text{(Equation 1.5)}$$

Where N_p is the impeller power number, N is agitation speed (rpm), D_i is impeller diameter (m) and ρ is density of broth (kg m^{-3}). Meanwhile, P_g can be determined based on Equation 1.6 that is proposed by Michel and Miller (1962):

$$P_g = m \left(\frac{P_o^2 N D_i^3}{Q^{0.56}} \right)^{0.45} \qquad \text{(Equation 1.6)}$$

Where m is impeller constant and Q denotes airflow rate (L min^{-1}). A wide number of other correlations for determining power consumption are available in the literature (Hughmark, 1980; Buchs *et al.*, 2000a; Buchs *et al.*, 2000b). Indirect determination of specific power input in an STR can also be based on torque measurements (Ojo, 2014). The scarcity of suitable methods for the measurement of power consumption in small scale HTP reactors, of non-standard geometry, has limited the application of the specific power input as a scale-up basis (Marques *et al.*, 2010). Moreover, most empirical correlations were developed based on STR systems that incorporate direct mechanical agitation via an impeller. Additionally, there is still lack of information concerning correlations involving power consumption in MWPs or other microscale reactors. The use of Computational Fluid Dynamics (CFD) was highlighted by several researchers as a tool to estimate power consumption in shaken microwells (Zhang *et al.*, 2008; Barrett *et al.*, 2010). In a more recent report by Durauer *et al.* (2016), a novel colorimetric method to quantify the power input in shaken microtitre plates has been introduced. The method facilitated a direct measurement of the specific power input in the microtitre plate, which may potentially be applied further for the scale-up purposes where this has yet to be demonstrated.

1.5.1.4 Specific aeration rate (Q/V_L or vvm)

Standardisation of the specific aeration rate is another possible approach for scale-up. The rationale for this approach is that a similar volumetric ratio of air to the working volume of the culture will ensure a fair provision of the oxygen to the culture. A compromise should be made concerning the Q value as excessive air supply may result in foaming and high gas hold up in the reactor. The typical values of Q/V_L used for a scale-up range between 1 and 1.67 with lower values normally adopted for larger scales (Junker, 2004).

1.5.2 Scalability of HTP fermentations

Ever since HTP reactors began to be used as optimisation platforms for microbial and cell cultures, significant attention has also been paid to the feasibility of scale translation of culture performance. Certain traditional scale-up approaches such as similar reactor geometry and constant impeller tip speed are generally not applicable to most HTP reactor formats (Table 1.3) due to the preference for shaken systems at small scale.

Table 1.4 summarises several works that reported the scalability of the cultivation processes in various HTP platforms to laboratory scale, stirred reactors using defined scale-up criteria. As already suggested in Section 1.5.1.1 for most aerobic cultivations such as *E. coli* fermentations, constant k_La is widely adopted as the basis of the scale translation.

One of the challenges in using k_La as the scaling basis is that it is a process-dependent parameter; therefore, it is subjected to change throughout different phases of a fermentation (Buckland, 1984). Nevertheless, this limitation may be alleviated by the standardisation of the optimal C_L during the scale translation (Ju and Chase, 1992) whereby maintenance of C_L above the minimum level required for an optimal cell growth may help to ensure a sufficient supply of oxygen to the culture. In the case of a viscous mycelial culture, the C_L value of between 30 and 70% saturation is required whereas for less viscous cases such as yeast and *E. coli* cultures, the minimum level of C_L ranges from 10 to 30% (Junker, 2004).

In scale-up works involving cell cultures, the use of mixing time as a scaling basis is commonplace compared to other scaling parameters. This is due to the fact that cell cultures grow relatively slowly compared to microbial cultures thus, provision of a well-mixed environment is crucial in ensuring a good quality of the cell suspension as well as the regulation of the incoming and outgoing gases from the cultures (Ozturk, 1996; Serrato *et al.*, 2004; Lara *et al.*, 2006). In addition, scale-up based on a matched mixing time may also be potentially applied for fed-batch *E. coli* and yeast cultures as the high cell densities may challenge the mixing performance within the cultures (Junker, 2004).

Alternatively, the feasibility of maintaining a specific power consumption as the scale-up basis for VPM8 hybridoma cell culture between MWP and a laboratory reactor has been demonstrated by Michelletti and co-workers (2006). The equivalency of the cultivation performance between the scales indicates the practicability of the estimated power consumption by CFD as a scaling criterion apart from the commonly used mixing time.

Overall, there is usually a need to elaborate a specific scale-up strategy for each specific fermentation and product type. Here, a particular approach of scaling up an *E. coli* BL21 (DE3) fermentation process from a HTP controlled MBR to a laboratory STR will be described in Chapter 5 of this thesis.

Table 1.4. Summary of scale-up studies under defined engineering criteria using HTP platforms.

Scaling parameter	High throughput platform	Microorganism	Reference
k_La	Conventional MWP	*E. coli*	Ferreira-Torres *et al.* (2005), Michelleti *et al.* (2006), Islam *et al.* (2008), Zhang *et al.* (2008), Baboo *et al.* (2012), Marques *et al.* (2012)
	BioLector	*E. coli, Hansenula polymorpha*	Kensy *et al.* (2009a)
	24-well miniature photobioreactor (mPBr)	*Chlorella sorokiniana, Chlorella protothecoides*	Ojo (2015)
Mixing time	Micro-24	CHO	Betts (2014)
	Micro-Matrix	CHO	Sani (2016)
Specific aeration rate	Ambr	CHO	Janakiraman and Kwiatkowski (2015)
Power consumption	Conventional MWP	VPM8 hybridoma cells	Michelleti *et al.* (2006)

1.6 Exploration of renewable feedstocks for industrial fermentations

In addition to establishment of efficient and reliable cultivation platforms to facilitate early stage and scalable bioprocess development (Section 1.4), another generic challenge is the high cost associated with the feedstock. Typically, 38 - 73% of the total production cost attributed to the feedstock cost alone (Stansbury *et al.*, 1999). Conventionally, there is still a high reliance on fossil-fuel based feedstocks in many industries. The continual depletion of fossil fuels has resulted in

an increased price and thus, making any associated process dependent on the source as expensive.

Recently, there has been a growing interest in exploiting renewable feedstocks for production of value-added products by fermentation. Valorisation of renewable feedstocks helps to reduce overall production cost, increase process sustainability and minimise environmental hazards such as the emission of greenhouse gases such as CO_2, CH_4 and N_2O (Maity, 2014). Among examples of potential renewable feedstocks for bioproductions are wastes generated from biorefineries, food, agricultural and agro-based industries. One such source, sugar beet vinasse, is the focus of this thesis.

1.6.1 Introduction to vinasse

One of the potential biorefinery waste stream is vinasse, the stillage discharged following the distillation of industrial bioethanol fermentation broths (Fitzgibbon *et al.*, 1995). Ethanol produced from fermentation process constitutes 90 – 95% of the global production, leaving only a small proportion produced via chemical synthesis (Sarris and Papanikolaou, 2016). With the growing demand for bioethanol, due to a multitude of applications, the production of vinasse is also expected to increase. Conventionally, vinasse is mainly exploited for soil mineralisation and as an additive for fertilizers and animal feeds due to its high content of organic nutrients (Parnaudeau *et al.*, 2008). However, application of vinasse on soil may lead to severe water and soil pollution as a result of the leaching of metals to groundwater, variation of soil texture, a rise of phytotoxicity and generation of bad odours due to production of methane and nitrous oxide gases (Christofoletti *et al.,* 2013; De Oliveira *et al.*, 2013). Additionally, the market for soil mineralisation is relatively small. A large portion of vinasse is still disposed into the water streams, causing an adverse impact on the aquatic ecosystem due to the presence of toxic compounds such as phenols, polyphenols and heavy metals, which resulted in high biological oxygen demand (BOD) (15-46 g L^{-1}) and chemical oxygen demand (COD) (26-91 g L^{-1}) (Espana-Gamboa *et al.*, 2011).

Over the years, a number of studies have focused on vinasse pre-treatment using several methods with the aim of removing toxic substances before disposal. Early work by Coca and Gonzalez (2006) highlighted the treatment of vinasse via a chemical route. Meanwhile, biological treatment of vinasse has been reported widely in the literature. Cibis *et al.* (2011) and Ryznar-Luty *et al.* (2015) have focused on the assimilation of betaine, a major pollutant in vinasse during aerobic biodegradation using a mixed culture of *Bacillus* species. Other studies reported the same approach but using different microorganisms (Lutoslawski *et al.*, 2011). On the other hand, vinasse treatment via anaerobic biodegradation has also been discussed. The major advantage of treatment via this method, apart from being cheaper than the preceding techniques, is the production of biogas such as methane and CO_2 whereby the former can be utilised as fuels for use within the refinery plant itself (Benitez *et al.*, 2003; Beltran *et al.*, 2005). Janke and co-workers (2016) reported the enhancement in methane gas production by 79% during anaerobic

biodegradation of sugarcane vinasse by supplementation with trace elements, nitrogen and phosphate. The on-site production of biogas that can potentially contribute to the overall revenue of the biorefinery is one of the early solutions that can help to ensure the sustainability of the industry in general apart from minimising the ecological impact associated with vinasse disposal.

Other works have addressed the exploitation of vinasse for production of various value-added products such as polyhydroxyalkanoate (PHA) (Bhattacharyya *et al.*, 2012; Pramanik *et al.*, 2012), biohydrogen and volatile fatty acids (Sydney, 2013) and xylitol (Salgado *et al.*, 2010). Furthermore, vinasse has also been used as one of the medium components for the production of *Spirulina maxima* biomass (Barrocal *et al.*, 2010). Meanwhile, the recycling of vinasse for ethanol fermentation has also been addressed (Navarro *et al.*, 2000; Fadel *et al.*, 2014). Overall, these works denoted the potential utilisation of vinasse as an alternative fermentation feedstock to synthetic media. The findings also provide useful insights into the potential use of vinasse for growing other microorganisms that have yet to be explored, such as *E. coli*, which is one of the preferred hosts for recombinant enzyme production.

Furthermore, there are several studies that reported the extraction of valuable components from vinasse. For example, Caqueret and colleagues (2008) reported the separation of betaine, which has amphoteric surfactant properties making it valuable for production of toiletries and health care products. In their study, the removal of polyphenolics and coloured compounds was initially investigated in order to facilitate the separation of betaine by ion-exchange. Apart from that, the recovery of the polyphenolic compound itself from vinasse has also become of interest. Diaz *et al.* (2012) reported the recovery of polyphenols from white wine vinasse where the compound was found to possess a potent ability as an antioxidant and therefore has potential applications such as in the food industry. The study reported the extraction of about 45% dry weight phenolics from 1 L of wine vinasse that generated 42 grams of dry product.

All of the aforementioned studies suggest the potential of vinasse in creating value-added opportunities that can enhance the economics of the overall biorefinery industry. Nonetheless, there is still an ongoing demand for more profitable process streams to be developed utilising vinasse in overcoming its bulk abundance as a result of the increasing demand of bioethanol in future.

1.6.2 Potential of waste glycerol as a biorefinery feedstock

The biofuel industry generally produces glycerol-based waste streams (Li *et al.*, 2013). Likewise, vinasse that is generated from the bioethanol industry, comprises mainly glycerol that is co-produced during ethanol fermentation by yeast (Figure 1.4). Despite the environmental hazards that the stillage might pose, the presence of glycerol in vinasse has enhanced the economic viability of the stillage due to various potential uses of the carbon source. The increasing production of biofuels over the years has resulted in a surplus of waste glycerol and therefore a

reduction of its price, which is about 6 times cheaper than refined glycerol (Yang *et al.*, 2012). This factor, along with the high cost of petrochemical precursors, has reduced the proportion of glycerol produced via chemical synthesis to about 10% of the total production (Yazdani and Gonzalez, 2007), making waste glycerol from the biofuel industry as an important contributor to the overall market. Waste glycerol presents several potential uses such as for direct application as a simple carbon source, chemical transformations and bioproductions (Johnson *et al.*, 2007; Siles *et al.*, 2010; Bohon *et al.*, 2011; Yang *et al.*, 2012). The latter application will be given a particular concern in this study.
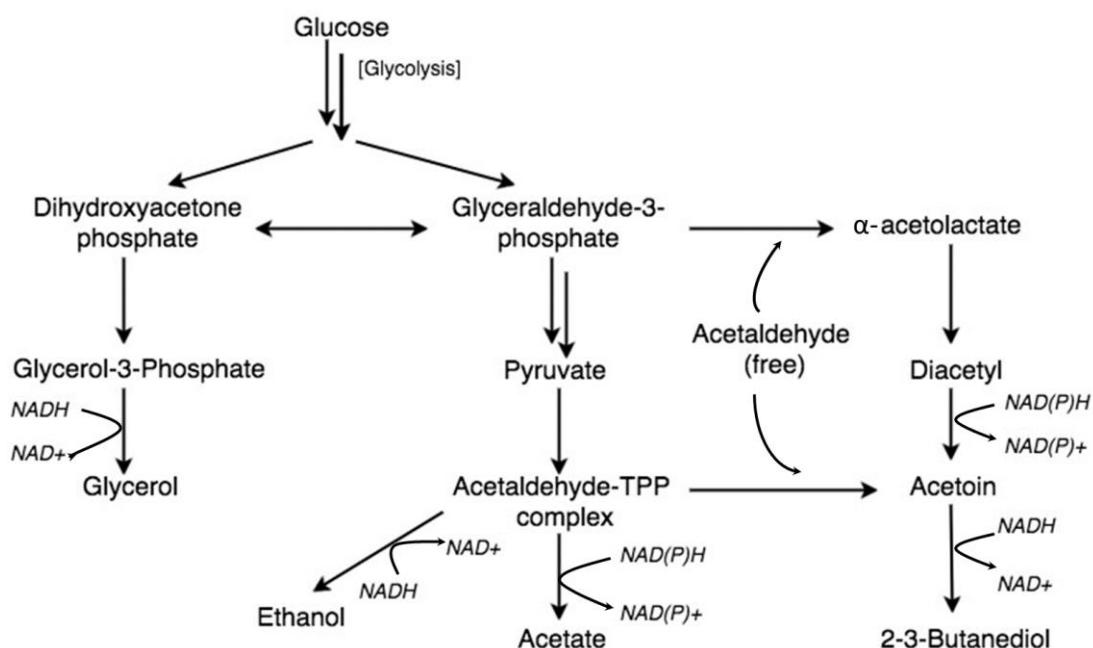
Figure 1.4. Metabolic pathway during a typical ethanol fermentation by *Saccharomyces cerevisae* indicating glycerol production as a by-product. Adapted from Macedo and Brigham (2014).

In microbial fermentations, the use of glycerol as a carbon source has several advantages over other carbon sources including glucose. Apart from being a non-food feedstock with a low cost, glycerol has a higher degree of reduction per mole of carbon, k (4.67) in comparison with glucose and sucrose where k=4 (Adnan *et al.*, 2014). Additionally, the rate of nicotinamide adenine dinucleotide (NADH) generation is also higher during glycerol metabolism whereby consumption of 1 mole of glycerol ($C_3H_8O_3$) generates 2 moles of NADH in contrast to only 1 mole of NADH when half a mole of glucose ($C_6H_{12}O_6$) is metabolised (Neijssel *et al.*, 1975; Lin, 1976). This has made glycerol a favourable carbon source for microbial growth, which can potentially lead to a higher yield of the products in comparison to glucose and sucrose (Yazdani and Gonzalez, 2007). The metabolic pathway of glycerol utilisation in *E. coli*, the host studied in this work, is illustrated in Figure 1.5. The metabolism is mediated by a glycerol transporter (*glpF*), a glycerol kinase (*glpK*) and two respiratory glycerol-3-phosphate dehydrogenases (*glpD* and *glpABC*) (Pettigrew *et al.*,

1990; Borgnia and Agre, 2001; Walz *et al.*, 2002). Moreover, unlike glucose, the use of glycerol in a fermentation also minimises the production of acetate during the metabolism as cell growth is relatively lower that in turn can prevent the overflow of carbon flux (Oh and Liao, 2000).
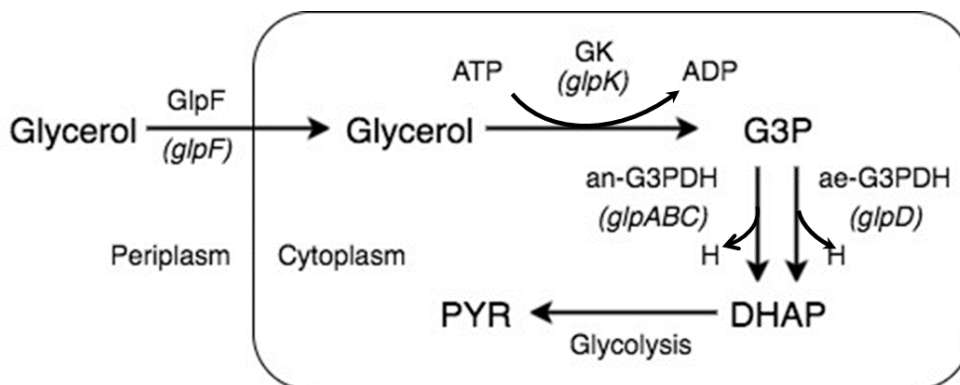
Figure 1.5. Metabolic pathway of glycerol utilisation in *E. coli* in the presence of electron acceptors facilitated by an ATP-dependent glycerol kinase (GK, coded for by glpK) and respiratory aerobic glycerol-3-phosphate dehydrogenase (ae-G3PDH) and anaerobic glycerol-3-phosphate dehydrogenase (an-G3PDHs), encoded by *glpD* and *glpABC*, respectively. Abbreviations: G3P - Glycerol-3-Phosphate; DHAP – Dihydroxyacetone phosphate; PYR – Pyruvate; ATP – adenosine triphosphate; ADP – adenosine diphosphate; H – reducing equivalents. Adapted from Murarka *et al.* (2008).

Extraction of waste glycerol from biofuel stillage may be beneficial in certain applications that attempt to minimise the problems arising from the complexity of the stillage composition when it is used as a fermentation feedstock. Nonetheless, reports on the use of glycerol extracted from bioethanol stillage are still scarce in comparison with those from biodiesel. The use of biodiesel derived glycerol is mainly discussed in this section although some generic issues will be highlighted. Several works have reported the application of extracted glycerol from the biofuel industry as feedstocks for production of various biochemical products as outlined in Table 1.5. A number of studies have highlighted the superior performance of waste glycerol over pure glycerol in terms of the product yield (Li *et al.*, 2013; Adnan *et al.*, 2014). The higher product titre is due to the existence of additional carbon or electron sources, nitrogen and some metals that may present in a trace amount in waste glycerol (Thompson and He, 2006; Lee *et al.*, 2012).

Table 1.5. Production of various value-added products from glycerol extracted from the biofuel industry.

Product	Microorganism	Reference
1,3-propanediol	*Klebsiella pneumoniae*	Hiremath *et. al.* (2011)
	Clostridium butyricum	Chatzifragkou *et. al.* (2011)
Citric acid	*Yarrowia lypotica*	Rywińska *et al.* (2009)
Erythritol	*Yarrowia lypotica*	Rymowicz *et al.* (2009)
D-lactic acid	*Escherichia coli*	Mazumdar *et al.* (2010)
Polyhydroxyalkanoate	*Cupriavidus necator*	Cavalheiro *et al.* (2009)
	Zobellella denitrificans	Ibrahim *et al.* (2009)
Phytase	*Pichia pastoris*	Tang *et al.* (2009)
Propionic acid	*Propionibacterium acidipropionici*	Zhang and Yang (2009)
Lipase	*Staphylococcus caseolyticus*	Volpato *et al.* (2008)
Succinic acid	*Basfia succiniciproducens*	Scholten *et al.* (2009)
Ethanol	*E. coli*	Adnan *et al.* (2014)
	Kluyvera cryocrescens	Choi *et al.* (2011)
	Klebsiella pneumoniae	Oh *et al.* (2011)
Lipid	*Schizochytrium limacinum*	Liang *et al.* (2010)
	Chlorella protothecoide	O'Grady *et al.* (2011)
Butanol	*Clostridium pasteurianum*	Taconi *et al.* (2009)
		Kao *et al.* (2013)
Hydrogen	*Enterobacter aerogenes* and *Clostridium butyricum*	Pachapur *et al.* (2015)

In comparison to the whole stillage, one of the advantages of using extracted glycerol lies in the downstream processing stages used for end-product recovery; fewer impurities are expected with extracted glycerol. However, there is an additional cost that needs to be invested in order to separate or further purify the glycerol from biofuels in the first place. Depending on the purpose and cost that need to be invested, purification of glycerol to a high-quality grade may be beneficial for critical applications related to the pharmaceutical and food industries where the removal of impurities is a prerequisite (Wan Isahak *et al.*, 2015).

Another advantage of using extracted glycerol as a fermentation feedstock could be in terms of the elimination of several potential cell growth inhibitors such as acetate, polyphenols and furfural, which are generally present in biofuel wastes including vinasse. Typically, the composition of waste glycerol largely depends on the process operations related to biofuel production (Yang *et al.*, 2012). It has been reported that extracted glycerol from biofuels generally does not contain the aforementioned cell growth inhibitors (Hansen *et al.*, 2009). In the case where the whole

vinasse is to be considered for bioproduction, suitable strategies such as pre-treatment for polyphenol removal are necessary in order to exclude the impact of these growth inhibitors. This has been addressed by Bhattacharyya *et al.* (2012) and Pramanik *et al.* (2012) whereby they incorporated a pre-treatment with activated carbon (AC) in order to eliminate the polyphenols from vinasse prior to the use of the feedstock for PHA production.

Generally, the abovementioned studies highlight the potential of waste glycerol, the major component of bioethanol stillage, as a potential fermentation feedstock. A comparative analysis between whole vinasse and extracted glycerol from vinasse for use in bioproduction may be beneficial in evaluating different process options. Essentially, a compromise should be made considering the process economics and viability in defining the relevant use of extracted glycerol and whole vinasse for any particular fermentation.

1.7 Integrated biorefinery concept: Opportunities and future direction

A biorefinery is defined as a production plant that utilises biomass as a starting material to generate a multitude of products particularly fuels, chemicals and energy (Kamm and Kamm, 2004a; Kamm *et al.*, 2006). The shortage of fossil fuels and also the emerging trend in the exploitation of biomass for the production of non-food products has led to the evolvement of the biorefinery concept since the 1990s (Ohara, 2003; Kamm and Kamm, 2004a; Kamm and Kamm, 2004b; Fernando *et al.*, 2006; Kamm *et al.*, 2006). There are three broad categories of a biorefinery, which are defined by the biomass utilised namely triglycerides, lignocellulosic and sugar/starchy materials (Maity, 2014). In the present study, the latter type will be discussed in detail with a specific focus on sugar beet.

Over the years, routes to several bioproducts have been developed within existing biorefineries. Use of a side stream to generate biogas, such as methane by anaerobic digestion, is among early examples of an integrated biorefinery concept. The methane gas produced can potentially be used as a source of energy within the biorefinery plant that consequently may open up opportunities for energy integration. Furthermore, in a typical sugar beet biorefinery, apart from sugar as the principal product, there are a number of co-products resulting from the side process streams among which are bioethanol, animal feed, power supply and liquid CO_2. At the Wissington factory in the UK, they also incorporated a horticulture business within the sugar beet biorefinery whereby the glasshouse is heated by the combustion of gases in a power station, yielding about 140 million tonnes of tomatoes per year. The framework comprising a spectrum of process streams within the Wissington factory is shown in Figure 1.6.

From a more holistic perspective, a fully integrated biorefinery should aim to utilise the maximum possible amount of intermediates and by-products, where the output of one process may serve as an input for another, with the aim of producing sustainable products and minimise unnecessary wastes generated from the whole facility. One of the generic challenges however, still lies in the

effective utilisation of the wastes generated. Among the principal wastes generated in a sugar beet biorefinery are sugar beet pulp and vinasse, which are identified as among the main causes of the environmental hazards (Vaccari *et al.*, 2005).
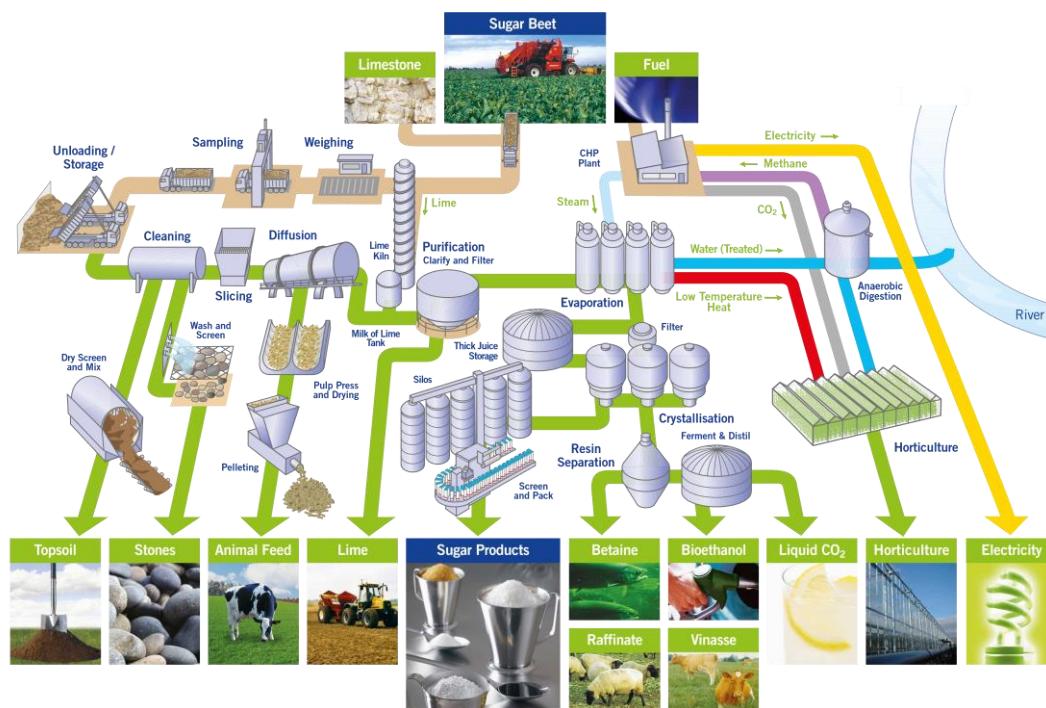
Figure 1.6. AB Sugar Wissington biorefinery (Norfolk, UK) indicating the sugar beet processing for sugar production and also various integrated process streams. Reproduced with permission from AB Sugar.

Sugar beet pulp (SBP) is generated upon the extraction of sugars in the crop during the early stage of sugar production. With over 8 million tonnes of sugar beet being harvested yearly in the UK, there is a significant amount of pulp generated following the crop processing (Ward *et al.*, 2015). Conventionally, the pulp is processed as an animal feed via a costly and energy intensive drying process to remove water (Zheng *et al.*, 2012). Having a high content of carbohydrates mainly cellulose and pectin (Micard *et al.*, 1996), SBP could potentially serve as a promising source of useful monomers derived upon the separation process. Recently, Cárdenas-Fernández *et al.* (2017) have reported the purification of L-arabinose and D-galacturonic acid, main components of pectin from SBP, which have many potential industrial applications. L-arabinose is an important substrate for production of biopolymers following esterification (Borges and Balaban, 2014). Apart from that, L-arabinose in its reduced form, arabinitol is useful for the construction of the unsaturated polyester resins (Werpy and Petersen, 2004). D-galacturonic acid on the other hand, is normally utilised for the production of hyperbranched polyesters and plasticisers (Werpy and Petersen, 2004). Moreover, both L-arabinose and D-galacturonic acid could serve as attractive substrates for biocatalysis, yielding novel chiral aminopolyols (Ingram *et*

al., 2007; Smith *et al.*, 2010; Rios-Solis *et al.*, 2015) that have important applications as pharmaceutical intermediates.

The work on the bioconversion of SBP has driven an interest in the development of on-site biocatalyst production within an integrated biorefinery like Wissington. The abundance of both SBP and vinasse offers a continuous supply chain thus ensuring the sustainability of the potential process streams while eliminating the current challenges and environmental hazards associated with their disposal. Figure 1.7 illustrates the integration of existing sugar and bioethanol production with the aforementioned proposed novel process streams within an integrated sugar beet biorefinery framework. In a broader context, these two on-site process streams may serve as promising process options for the development of a fully integrated sugar beet biorefinery in future. Exploration into the feasibility of developing a process for on-site biocatalyst production using vinasse will be discussed in Chapter 4 of this thesis.
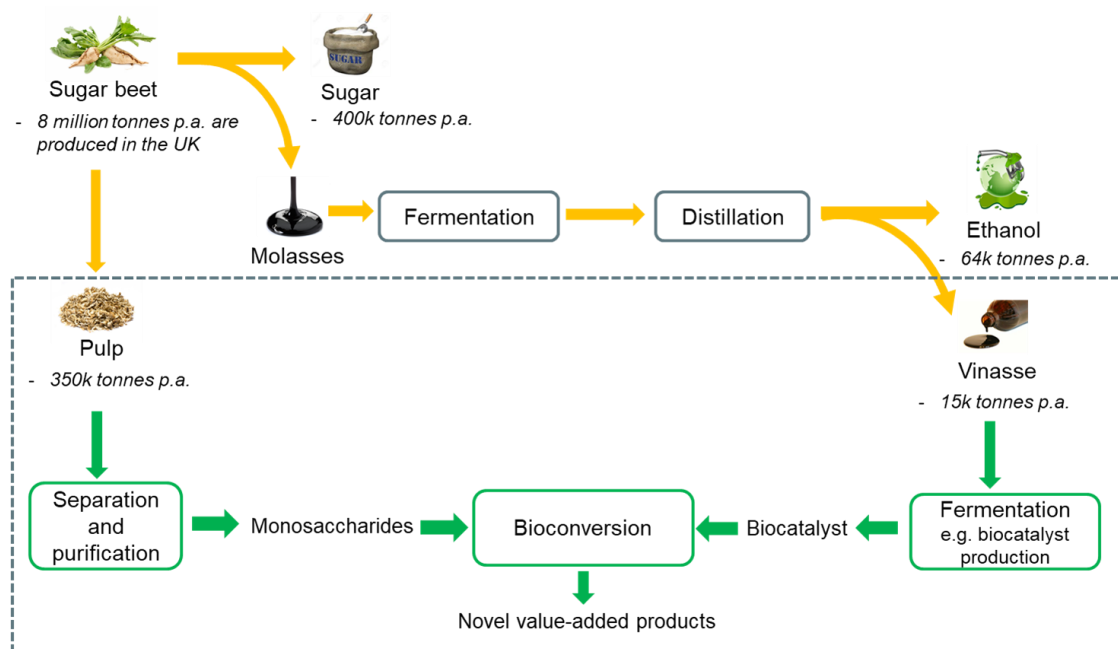
Figure 1.7. Diagram showing the potential integration of the existing and novel process streams within a sugar beet biorefinery context. Novel process streams are enclosed in the box with dashed lines. The quantitative information is provided by British Sugar (personal communication, 2017) based on operations at Wissington biorefinery. Abbreviation: p.a. – per annum.

1.8 Critical appraisal of the published literature

Whilst various studies related to the use of HTP microreactors have been reported for both microbial and cell culture applications (Section 1.4), there remains a need to understand the flexibility and scalability of the platforms for real-world applications. A number of works have highlighted the use of conventional MWPs on defined media over the past decade as detailed in Section 1.4.1. Nonetheless the absence of monitoring and control for key environmental parameters, particularly pH and DO limits the quality of the data that can be attained. The most recent studies have focused on controlled MBRs for mammalian cell cultures (Section 1.4.2) however, there remains a need for additional studies on microbial cultures in these systems and in particular mixing and oxygen mass transfer characteristics under microbial culture conditions.

Most scale-up studies from microwell to STR scales have either focused on conventional MWPs or mammalian cell culture (Section 1.5.2). There is therefore a need to study microbial cultivation in controlled MBRs and scale-up to laboratory and pilot scale STRs. The few studies that have addressed microbial scale-up (Isett *et al.*, 2007; Chen *et al.*, 2009; Holmes *et al.*, 2009) have generally been empirical and not defined specific engineering bases for scale translation. The challenge here lies in understanding the fundamental engineering characteristics of the emerging controlled MBRs that come in various geometries and subsequently, the reproducibility of the cultivation at larger scales.

With regards to the biocatalyst used in this study, CV2025 ω-TAm (Section 1.2), the optimisation of its production during fermentation has not been a major focus in previous works (Kaulmann *et al.*, 2007; Rios-Solis *et al.*, 2011; Halim *et al.*, 2013). As most proteins are produced intracellularly in *E. coli,* including CV2025 ω-TAm, there is a proportionality between the cell density and product titre, which implies the importance of achieving high cell density cultures. This in turn will facilitate the subsequent bioconversion stage where a high biocatalyst concentration is of an immense interest. The application of HTP platforms such as controlled MBRs for optimisation of biocatalysts production is again rarely described in the literature. Apart from that, there is also a need for cheap and sustainable feedstocks to replace the expensive fossil-based media for bioproductions. To date, exploitation of renewable feedstocks such as vinasse (Section 1.6.1) for industrial biocatalysts production particularly is still scarcely reported.

In the context of vinasse, which is the renewable feedstock explored in this work, although there have been several works in the literature, generally, the scope of studies is still limited. As elaborated in Section 1.6.1, a number of works have discussed the pre-treatment of vinasse by various methods (Coca and Gonzalez, 2006; Ghosh *et al.*, 2007; Cibis *et al.*, 2011; Luty *et al.*, 2015). Other aspects addressed include removal of polyphenols (Caqueret *et al.*, 2012), recycling for ethanol fermentation (Fadel *et al.*, 2014) and also bioproductions involving several types of microorganisms (Barrocal *et al.* 2010; Salgado *et al.*, 2010; Bhattacharyya *et al.*, 2012; Pramanik *et al.*, 2012). Undoubtedly, these studies provide initial insights into the promising applications of vinasse however, to date, there is no work reporting the utilisation of vinasse for *E. coli* growth

and biocatalyst production. As *E. coli* is a typical host exploited for production of many invaluable recombinant proteins, it is interesting to investigate the feasibility of developing a cost effective fermentation process by utilising a renewable feedstock such as vinasse.

Another interesting aspect is the exploration of potential process streams using vinasse within an integrated biorefinery approach. As discussed in Section 1.7, the feasibility of deriving monosaccharides from SBP has led to an interesting concept of linking the process of bioconversion and biocatalyst production within an integrated sugar beet biorefinery framework.

1.9 Aim and objectives

Based on the above consideration (Section 1.8) the aim of this thesis is to establish HTP methodologies for the production and characterisation of industrial biocatalysts for use within an integrated biorefinery context. A 24-well single-use, controlled microbioreactor platform (Micro-24) will be utilised in this work (Table 1.3). As described in Section 1.4.2, the direct gas sparging and oxygen blending capacity are expected to provide adequate oxygen transfer rates to support microbial cell growth above the levels achievable in shaken flasks. The focus will be on optimising the production of the CV2025 ω-TAm in *E. coli* BL21 (DE3), as this has been shown to be an important biocatalyst for chiral amine synthesis (Section 1.2). The biorefinery context is provided from related studies on the creation of an integrated biorefinery for SBP utilisation (Section 1.7). The work here will address methods for the utilisation of sugar beet vinasse, the side-stream of bioethanol distillation, as an inexpensive and renewable source of nutrients for *E. coli* BL21 (DE3) growth and CV2025 ω-TAm production. The key objectives of the project are outlined below.

- The initial objective will be to establish a small scale fermentation system as a platform for parallel studies of biocatalyst production in microbial hosts. Preliminary studies will involve media screening in batch flask cultures. The performance of the controlled MBR will be initially assessed in terms of the measurement and control of the process parameters and culture reproducibility. Subsequently, the basic culture conditions for CV2025 ω-TAm production will be established in the controlled MBR using a synthetic medium (a model system) and compared to the standard shake flask cultures. Once the experimental methodologies are developed, the utility of the controlled MBR will be then demonstrated in optimisation studies for *E. coli* BL21 (DE3) growth and CV2025 ω-TAm production. The optimal levels of cell growth and CV2025 ω-TAm activity achieved here will serve as the benchmark for subsequent studies on vinasse utilisation and scale-up. The results of this work are presented and discussed in Chapter 3.

- The second objective will be to explore the integration of the controlled MBR technology within a biorefinery context using sugar beet vinasse as a fermentation feedstock. Preliminary studies will involve characterisation of vinasse with an emphasis on the

composition of fermentable sugars and related compounds. Following that, several possible vinasse pre-processing techniques will be evaluated. In addition, pre-treatment of vinasse by AC adsorption will be studied. Initial studies using vinasse as a fermentation medium will be performed in shake flasks whereby the influence of several parameters such as vinasse concentration and IPTG induction will be determined. The use of the pre-treated vinasse will also be evaluated over the untreated vinasse for the CV2025 ω-TAm production. Additionally, the reproducibility of vinasse between different batches will be assessed in terms of the fermentation performance and product titre. Further optimisation of fermentation and CV2025 ω-TAm production using vinasse will be carried out in the controlled MBR. The influence of supplementation with trace elements and nitrogen-containing substrates on the fermentation performance will be studied. Additionally, the metabolism of *E. coli* BL21 (DE3) in vinasse medium that links to sugar utilisation and selectivity will also be elucidated. The results of this work are elaborated in Chapter 4.

- The third objective will be to scale-up the optimised fermentation processes using both synthetic and vinasse-based media (based on the results in Chapter 3 and 4). Scale-up demonstrated from the controlled MBR (6.5 ml) to a conventional STR scale (5 L) representing a 769-fold volumetric scale translation. The scale-up studies will be based on matched k_La values and specific aeration rates (Section 1.5.1). Experimental quantification of k_La values will be first undertaken in both controlled MBR and 7.5 L STR using water, synthetic and vinasse media in order to establish the correlations for prediction of k_La values. For the vinasse medium, additional studies will be performed related to options for vinasse pre-processing procedures suitable for a large scale application. Finally, optimum conditions for cell growth and CV2025 ω-TAm production will be scaled-up and evaluated in a 7.5 L STR. The results of this work are described in Chapter 5.

In addition to the above, Chapter 2 describes the equipment and experimental methods established during this work; in particular Micro-24 operation and control and assays for the quantification of the complex carbohydrate mixtures present in sugar beet vinasse. Finally, general conclusions from these studies and suggestions for future work are discussed in Chapter 6.

CHAPTER 2

MATERIALS AND METHODS

2.1 Microorganism

E. coli BL21 (DE3) containing plasmid pQR801 that incorporates the ω-transaminase gene from *Chromobacterium violaceum* (CV2025 ω-TAm) with an N-Terminal His$_6$-tag (GenBank accession no. NP_901695), as established in earlier work (Kaulmann *et al.*, 2007), was used throughout this study. Working stock cultures were stored in a 20% (v/v) glycerol solution at -80 °C.

2.2 Materials

All chemicals used in this work were obtained from Sigma-Aldrich (Gillingam, UK) unless otherwise stated and were of the highest purity available. The sugar beet vinasse was provided by AB Sugar Wissington biorefinery. It was received in chilled form, i.e. with the temperature approximately below 5 °C. Two batches were received during the study, named thereafter as Batch 1 and 2, which were supplied on 15 September 2014 and 27 November 2015, respectively. Reverse Osmosis (RO) water was used in all experimental procedures.

2.3 Media Preparation

2.3.1 Synthetic medium

The compositions of the media used in this work are as follows. Luria Bertani (LB) – glycerol medium, as reported by Rios-Solis *et al.* (2011), contained (g L^{-1}): glycerol, 10; yeast extract, 5; tryptone, 10 and sodium chloride, 10. Defined medium and complex medium were modified from that described by Hortsch and Weuster-Botz (2011). Defined medium consisted of (g L^{-1}): glycerol, 30; KH_2PO_4, 13; K_2HPO_4, 10; $MgSO_4.7H_2O$, 1; NH_4Cl, 0.2; $(NH_4)_2SO_4$, 2; NaCl, 5 and trace elements, 150 µL L^{-1}. Complex medium consisted of (g L^{-1}): glycerol, 30; yeast extract, 5; KH_2PO_4, 13; K_2HPO_4, 10; $MgSO_4.7H_2O$, 1; NH_4Cl, 0.2; NaCl, 5 and trace elements, 150 µL L^{-1}. The trace element solution was made up as described by Marisch *et al.* (2013) and was prepared in 5 N HCl. The composition is as follows (g L^{-1}): $FeCl_3.6H_2O$, 10; $MnSO_4.H_2O$, 10; $CaCl_2.2H_2O$, 2; $CoCl_2$, 0.2; $ZnSO_4.7H_2O$, 2; $Na_2MoO_2.2H_2O$, 5; $CuCl_2.2H_2O$, 30; H_3BO_3, 30.

Before sterilisation the pH of all the media was adjusted to 7 using 1 M NaOH or1 M HCl whenever required. The trace element solution was sterilised by filtration through a 0.22 µm pre-sterilised filter (Milipore, USA). All other media components were autoclaved at 121 °C for 20 minutes using a Denley autoclave (Thermo Fischer Scientific, USA). Phosphate components were also autoclaved separately. These and the trace element solutions were added to the other media components aseptically prior to fermentation.

2.3.2 Vinasse medium

A typical composition of vinasse as provided by AB Sugar Wissington biorefinery is shown in Table 2.1. Prior to its use in this work, suspended solids were removed by centrifuging the raw vinasse at 4000 rpm for 30 minutes at 4 ^{o}C (Avanti J-E Centrifuge, Beckman Coulter, USA). The resulting liquid fraction was then stored in -20 ^{o}C. In this work, vinasse medium was prepared by a number of pre-treatment routes as illustrated in Figure 2.1. Five different options were considered. For pre-treatment Option 1, clarified vinasse was diluted as required using RO water and then adjusted to pH 7 before it was filtered through a 0.22 µm sterile filter (Millipore Express Plus, Merck, UK). In Option 2, pre-treatment with AC (Section 2.10) was included while the remaining procedures were as in Option 1. In Option 3, the vinasse was autoclaved after the pH adjustment before being used for fermentation. In Option 4, D-galactose was added to the autoclaved vinasse prior to fermentation. Finally, in Option 5, the vinasse was used directly after the pH adjustment without any sterilisation.

Table 2.1. Summary of vinasse on a dry mass basis. Data is provided by AB Sugar.

Component	Percentage (%)
Sugars	8.77
Glycerol	34.89
Crude protein	31.03
Ash	23.4
Total	98.10
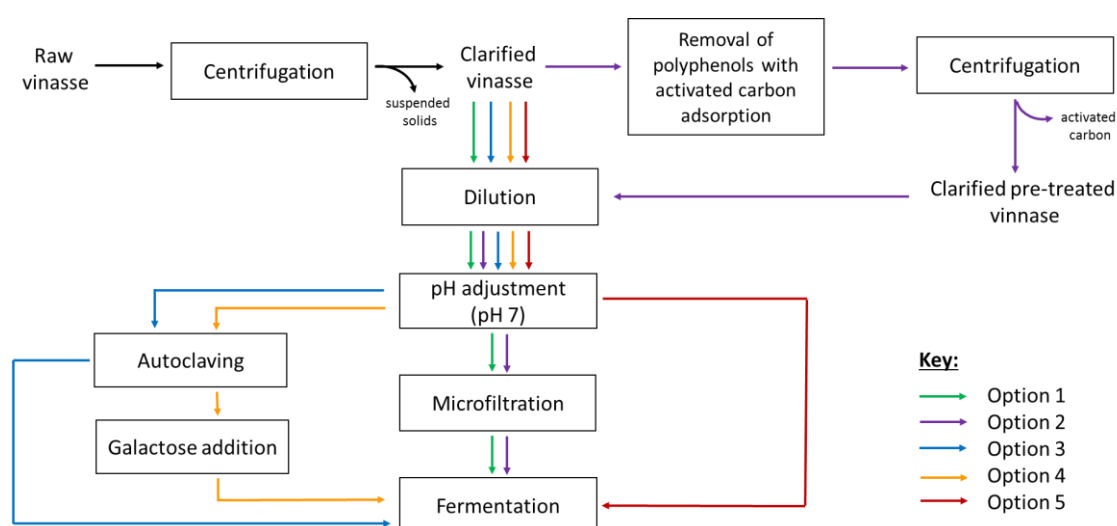
Figure 2.1. Pre-treatment options evaluated with sugar beet vinasse for use as a fermentation feedstock.

2.3.3 Agar plates

Agar plates were prepared using LB broth with agar at a working concentration of 40 g L^{-1}. Upon sterilisation, once the temperature reached approximately 40 $^{\circ}$C, kanamycin to a final concentration of 0.15 g L^{-1} was added to the agar solution and the mixture was mixed thoroughly before it was then poured aseptically into a petri dish (Fischer Scientific, UK). The agar plate was then allowed to solidify before being used for cell growth assessment.

2.4 Master stock cultures preparation

The master stock cultures for this project were prepared according to protocols by Halim (2012). Initially, the working strain was grown on an agar plate and incubated for 24 h. Following that, a single colony was picked and grown in 25 mL LB-glycerol medium supplemented with 0.15 g L^{-1} kanamycin in a 250 mL shake flask. The culture was then incubated on an orbital shaker at 250 rpm and 37 $^{\circ}$C. When the OD$_{600nm}$ of the culture reached about 0.5, the culture was withdrawn. Four hundred microliters of the culture was then pipetted aseptically into a sterilised Eppendorf tube and mixed with 200 µL of 50% (v/v) filter sterilised glycerol solution. The aliquots were then kept at -80 $^{\circ}$C for use during the course of this project.

2.5 Controlled microbioreactor system

In this work, a Micro-24 reactor (Pall Corporation, Port Washington, USA) was used as a HTP platform for parallel evaluation of microbial cell growth and biocatalyst production. The reactor allows 24 simultaneous experiments using single-use cassettes with independent control of process parameters (pH, DO and temperature) in every well within the cassette. Figure 2.2 shows the overall set-up of the Micro-24 reactor system. The Micro-24 reactor comprises of a single base unit with a closable lid. Figure 2.3 depicts the overview of the Micro-24 guard. The guard is mounted onto the orbiter at a fixed shaking diameter of 2.5 mm with the speed operates in the range 500 – 800 rpm. During shaking, the cassette was clamped on to the Micro-24 guard by an applied vacuum supported by clean dry air (CDA) provided from the compressor at 85-120 psi. The gas delivery gaskets on the guard are used for the delivery of the gas to the wells while the optic windows are for the optical sensing system. The thermistors and heaters allow the monitoring and control of temperature in each well.
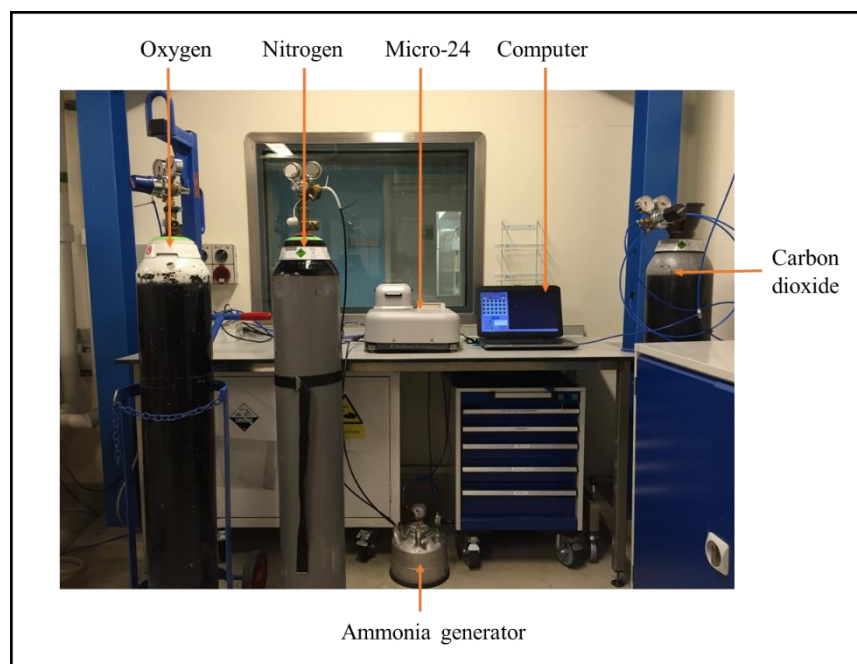
Figure 2.2. Photograph showing the overall set-up of a Micro-24 reactor. Note: the CDA line, from a centralized supply, is connected to the back of the Micro-24 machine.
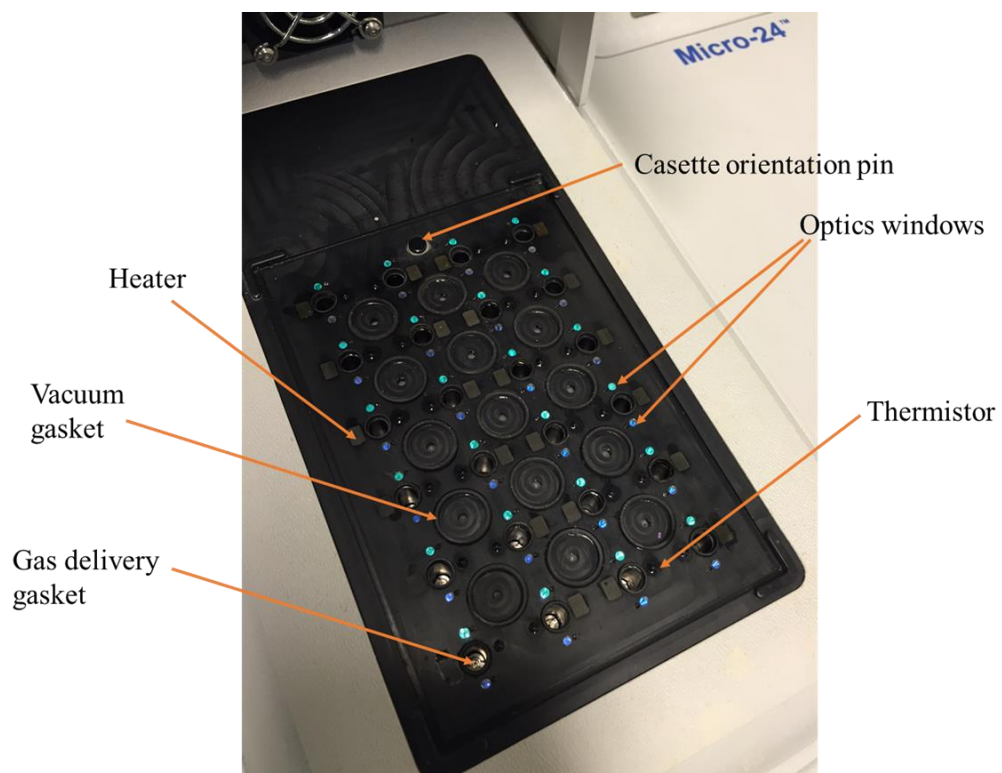
Figure 2.3. Overview of the Micro-24 guard.

Figure 2.4 shows the rear view of the Micro-24 reactor. The system allows up to three gases to be used at one time. In a microbial culture application, the pH is typically controlled by 15% (v/v) NH_3 and 50-100% (v/v) CO_2. The former gas was generated from 28% (v/v) NH_4OH that was initially diluted with RO water to 15% (v/v) before being placed in the ammonia generator (Figure 2.2). Figure 2.5 shows the gas configurations for fermentations using complex (Chapter 3) and vinasse (Chapter 4) media, respectively. The DO is normally controlled by either a pure oxygen or a blending of pure oxygen and nitrogen. The range of each gas delivered to the well is between 0.1 and 20 standard cubic centimetre per minute (sccm) and the gas addition to the well is controlled via a Proportional Integral Derivative (PID) loop control. The machine is also equipped with the heating and cooling exchanges where the incubator temperature is typically set 2 ^{o}C below the lowest temperature of the well.
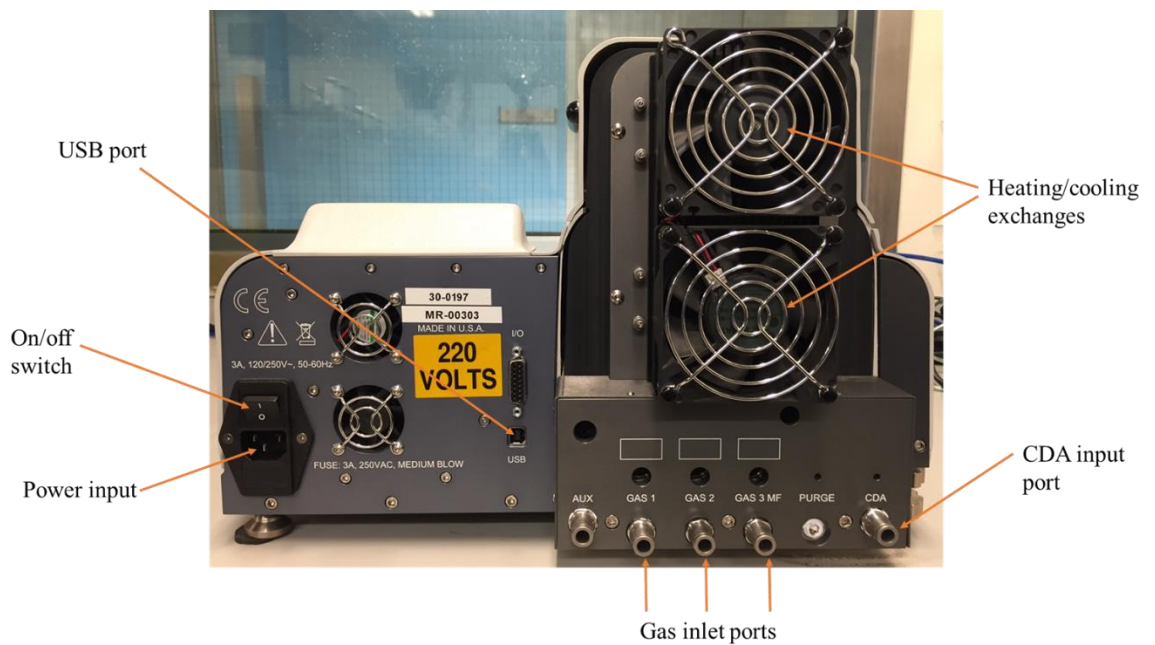
Figure 2.4. Micro-24 rear view.
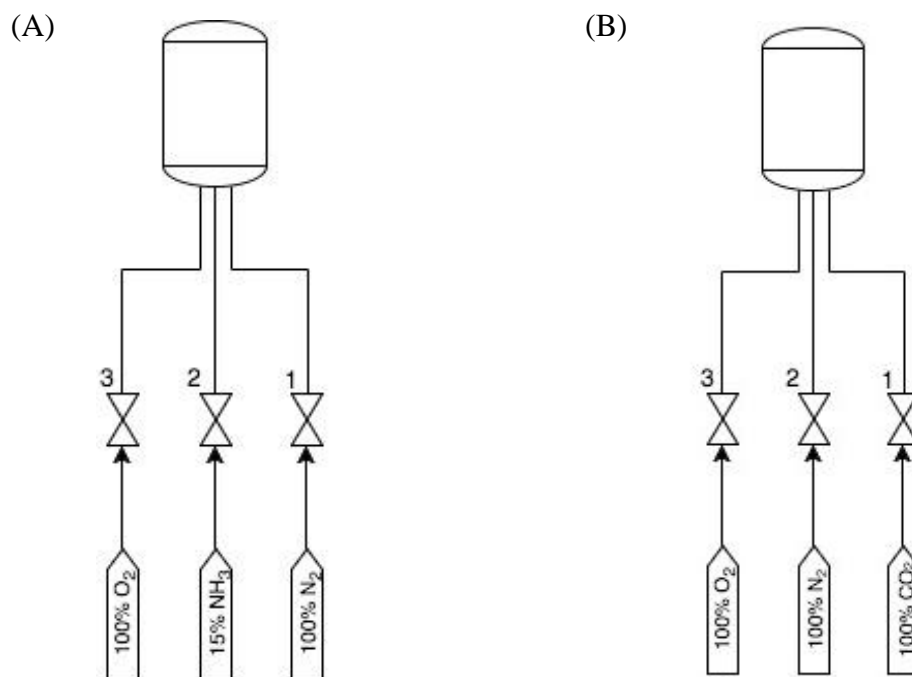
Figure 2.5. Piping and Instrumentation diagram (P&ID) showing the gas configuration during fermentations using (A) complex medium (Chapter 3) and (B) vinasse medium (Chapter 4) in the Micro-24. Numbers refer to inlet ports of Micro-24.

For each new media and sensor lot, the pH sensor offset was calibrated as it may vary with the media formulation. In contrast, the DO sensor does not vary from lot to lot and thus, a calibration may not be essential with lot changes. The protocol for the calibration of the pH sensor offset is as follows. A cassette containing the cultivation medium was incubated at the working temperature with no DO and pH control for at least 2 h. Following that, the pH of the medium withdrawn from the Micro-24 wells was measured offline using a standard pH meter (Mettler Toledo, Switzerland) and the readings were compared to the online pH values obtained from the data log provided by the operating software. The adjusted offset for the pH sensor was calculated based on Equation 2.1 where the sensor offset and slope values are provided by the manufacturer.

$$\text{Adjusted offset} = \text{sensor offset} - \left(\frac{\text{offline pH} - \text{online pH}}{\text{sensor slope}}\right) \qquad \text{(Equation 2.1)}$$

The cassette is available in regular, direct sparged (REG), baffled, direct sparged (BFL) and headspace sparged (PERC) design where the former was used in this study (Figure 2.6 (A)). Each cassette consists of 24 pre-sterilised wells that are 61 mm in height (h_w) and 14 mm in diameter (d_w) for every well. Each well has a 0.2 μm sterile sparge membrane that allows the passage of the gases. Additionally, every well is fitted with PreSens (PreSens-Precision Sensing,

GmbH, Regensburg, Germany) fluorescent pH and DO sensing patches that enable optical monitoring through light emitting diodes (LED) and detectors on the machine guard. The linear range of the pH is from 6 to 8. Meanwhile, for the DO the range and accuracy is around ±5% at 0% saturation and ±10% at 100% saturation. The temperature is controlled by a Pelletier heating element, which is equipped on the base of every well, with the range of between 18 and 45 ^{o}C. The wells are sealed using pre-sterilised closures of which in this work, Type D caps as shown in Figure 2.6 (B) were used. Both cassette and closures are supplied irradiated and intended for single use. Each cap consists of a sterilising filter in the middle that allows a two-way gas exchange with the atmosphere. Prior to using any new medium in REG and BFL cassettes, a compatibility test need to be carried out in order to determine if the medium is compatible with the sparge membranes and sensors. In this work, the following procedure was undertaken. The cassette was filled with the medium and then placed on a paper towel in an incubator at working temperature for at least two hours. Following that, the permeability of the membrane was checked by observing whether there is any leak from the well. In the case where the membrane is permeable to the medium used, the use of PERC cassette may be necessary.
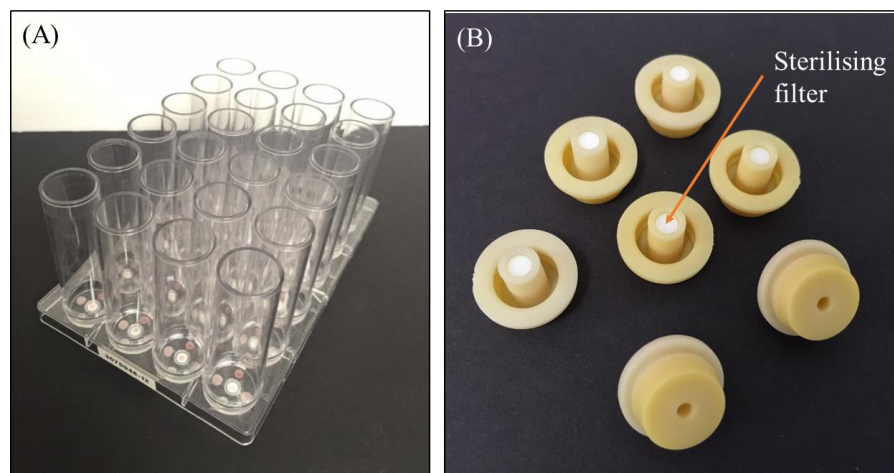
Figure 2.6. Details of the Micro-24 cassette and caps used in this work: (A) REG plate with a sparge membrane and sensor spots visible in the base of each well; (B) Type D cap incorporating a sterilising filter in the middle of the outer side.
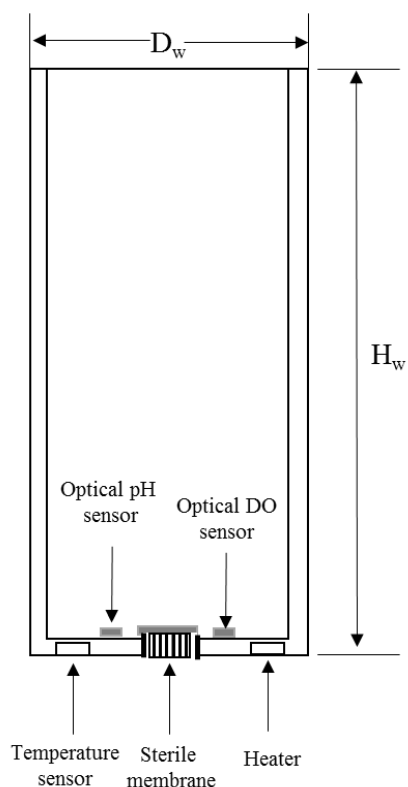
Figure 2.7. Schematic diagram of an individual well from the REG cassette showing location of sparger (sterile membrane) and optical sensors.

The process control of the Micro-24 during the incubation is monitored by a MicroReactor Control software (Pall Corporation, USA) that is pre-installed on the laptop controller, which is connected to the reactor unit by an USB connection. The control panel has several menu bar drop down options for setting up the process parameters prior to an experiment such as shaking frequency, environment temperature, well temperature, pH, DO, airflow rate and also PID values. During the operation, the control panel displays the historical and real time data of the running system as well as other information related to the reactor status. Figure 2.8 illustrates a typical example of the Micro-24 control panel screen during an operation. A graph display from a typical well showing both historical and real time data is depicted in Figure 2.9.

Reactor status selector

Well number

Status indicator

Drive meter

Current reactor reading

Current set point

Control button

Current status window
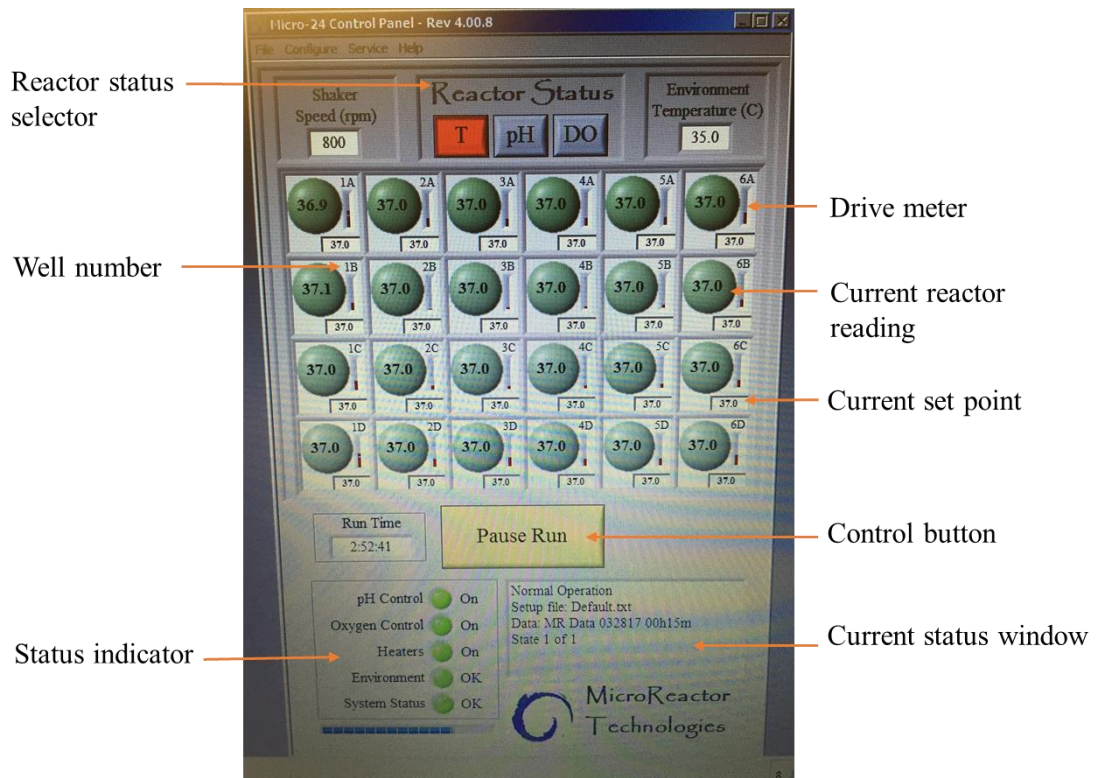
Figure 2.8. A typical example of the Micro-24 control panel screen during an operation.

Table or graph view selectors

Set point (dashed line)

Process value

Auto scaling
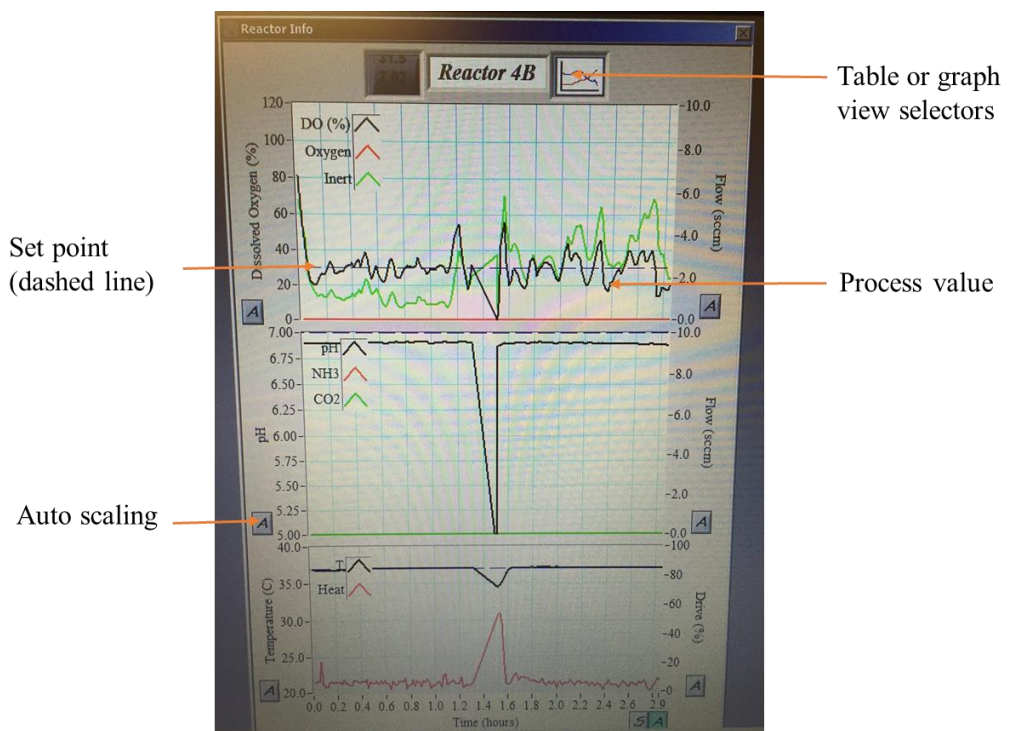
Figure 2.9. A graph display from a typical well showing both historical and real time data. The drop of DO, pH and temperature at 1.5 h is due to the removal of the cassette from the reactor for sampling.

2.6 7.5 L stirred tank reactor (STR)

Batch fermentation in a STR was performed in a 7.5 L glass reactor (BioFlo 310, New Brunswick, Hertfordshire, UK). The aspect ratio of the reactor is 1.79:1 and it consists of two, six-bladed Rushton impellers (D_i = 59 mm, D_i/D_t = 0.25) and four equally spaced baffles. The reactor is equipped with a built-in software that allows the user to interface through the touchscreen display in order to set the process parameters and monitor the progress of the operation. Figure 2.10 depicts a schematic diagram of the vessel.

The temperature was monitored by a thermocouple and controlled by the circulation of water in the external jacket of the reactor. The pH was monitored using an Ingold gel filled pH probe (Ingold Messtechnik, Urdorf, Switzerland) and controlled by the addition of 8.5% (v/v) H_3PO_4 and 28% (v/v) NH_4OH. The DO was controlled using a polarographic oxygen electrode (Ingold Messtechnik, Urdorf, Switzerland) via cascade control of air and pure oxygen at 5 L min^{-1}. Prior to sterilisation, the pH probe was calibrated using standard buffers at pH 7 and 4. The calibration for the DO probe was performed using pure nitrogen and air for the deoxygenation and oxygenation, respectively. The sparged air into the reactor was sterilised using a 0.2 μm membrane filter. Apart from the built-in software as described earlier, the reactor system is also possibly controlled from a computer via a BioCommand software (BioFlo 310, New Brunswick, Hertfordshire, UK). During the operation the historical and real time data can be accessed from this operating software. The picture of the reactor system is as shown in Figure 2.11.
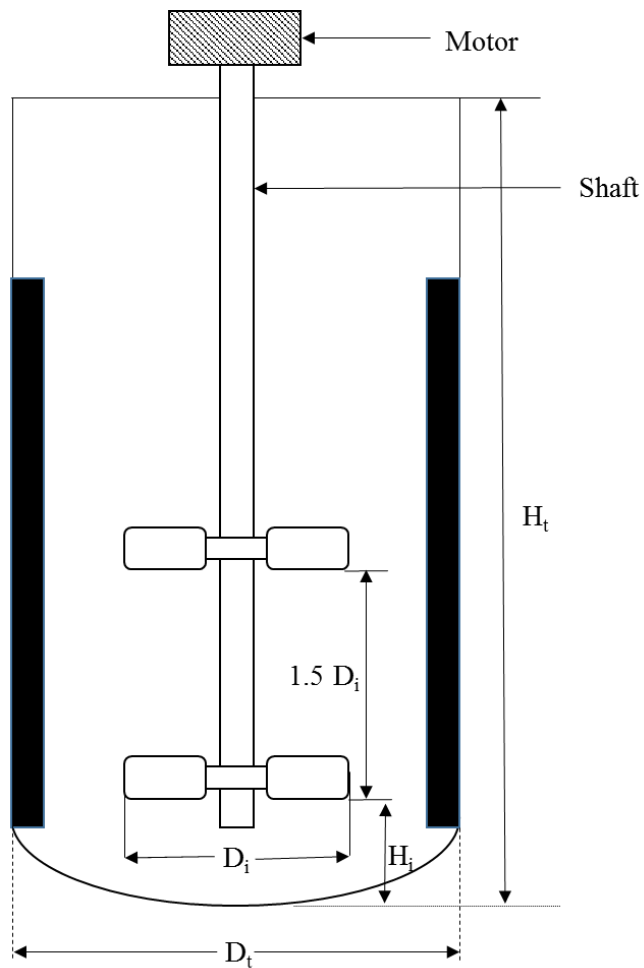
Figure 2.10. Schematic diagram showing the geometry of the 7.5 L STR (BioFlo 310, New Brunswick, Hertfordshire, UK) used in this work.
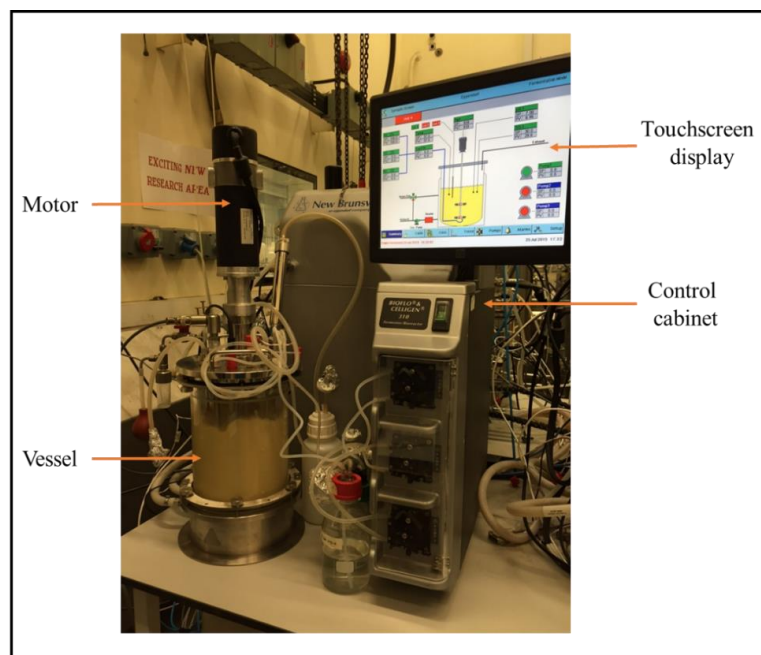
Figure 2.11. Photograph showing the 7.5 L STR (BioFlo 310, New Brunswick, Hertfordshire, UK).

2.7 Inoculum preparation

A glycerol stock vial (600 µL) of *E. coli* BL21 (DE3) (Section 2.4) was aseptically inoculated into 100 mL of sterile medium in a 1 L-baffled shake flask. In all cultivations, the medium formulation used for inoculum preparation was the same as used in the corresponding Micro-24 or 7.5 L STR fermentation. Kanamycin was added to a final concentration of 0.15 g L^{-1}. The culture was incubated on an orbital shaker (Adolf Kuhner AG, Birsfelden, Switzerland) at 250 rpm (shaking diameter 25 mm) for 12 h at 37 ^{o}C. Unless otherwise stated, the inoculum concentration was standardised at 0.1 g_{dcw} L^{-1}.

2.8 Fermentation

2.8.1 Shake flask culture

Fermentation was carried out in a 250 mL baffled shake flask with a working volume of 20 mL. Prior to inoculation, sterile kanamycin was added to the medium to a final concentration of 0.15 g L^{-1}. All cultures were shaken on an orbital shaker (Adolf Kuhner AG, Birsfelden, Switzerland) at 250 rpm at 37 ^{o}C. Sterile IPTG was added to a final concentration of 0.1 mM at mid exponential phase unless otherwise stated. All fermentations were performed in triplicate. Cell growth was followed by removing about 3 mL samples approximately every 2 h and measuring OD as described in Section 2.12.2.

2.8.2 Controlled microbioreactor culture

Fermentation was carried out in the REG plate design, fitted with Type D caps with a working volume of 6.5 mL in each well. The wells were filled aseptically with a sterile medium followed by the addition of kanamycin to a final concentration of 0.15 g L^{-1} prior to the inoculation. An autoclaved propylene glycol (PPG) was also added to each well with a working concentration of 1 mL L^{-1} and thereafter it was added as required throughout the cultivation. The culture was shaken at 800 rpm, which is the optimal speed recommended for REG cassette by the manufacturer. The DO was controlled by a blending of pure oxygen and nitrogen where the flow rate was set at 6.5 sccm for each gas. Meanwhile, the pH was controlled one sided either by using 15% (v/v) NH_3 for cultures using a synthetic medium or 100% (v/v) CO_2 in the case of vinasse medium with the flow rate of 10 sccm in either condition.

The set-points in each well were at a temperature of 37 ^{o}C and a pH and DO of 7 and 30%, respectively unless otherwise stated. The PID values of the pH and DO control used were as provided by the manufacturer. In the case of a synthetic medium, unless otherwise mentioned, the culture was induced with 0.1 mM IPTG after 6 h of inoculation. The cell growth was monitored by removing about 650 µL samples at certain time intervals where the OD was then measured as described in Section 2.12.2. Figure 2.12 illustrates a typical *E. coli* BL21 (DE3) culture grown in the Micro-24 using a complex medium after 24 h of inoculation.
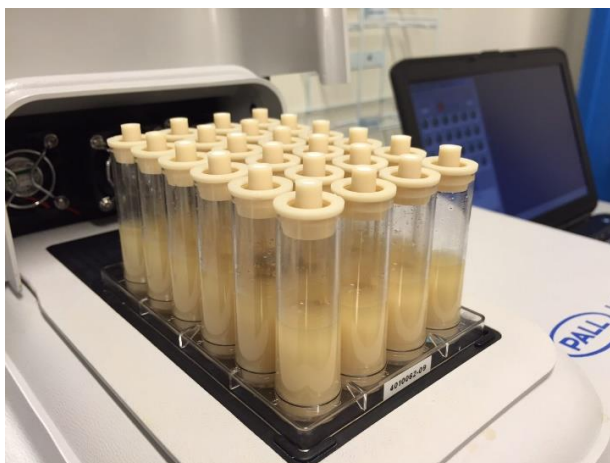
Figure 2.12. Illustration of a typical *E. coli* BL21 (DE3) culture in the Micro-24. Cells grown on a complex medium (Section 2.3.1). Photograph taken 24 hours after inoculation.

2.8.3 7.5 L STR culture

Fermentation was carried out with a working volume of 5 L. In the case of the synthetic medium, the vessel was initially filled with 4.5 L of all medium components (except KH_2PO_4 and K_2HPO_4) and was then sterilised by autoclaving. The phosphate components were sterilised separately and were aseptically added to the reactor prior to inoculation. In the case of vinasse medium, the vessel was initially filled with 4 L of water with 10 g L^{-1} yeast extract and was then sterilised at 121 ^{o}C for 20 minutes. Upon cooling to room temperature, a concentrated vinasse was then added to the vessel. In both media, filtered kanamycin with a final concentration of 0.15 g L^{-1} was aseptically added to the reactor prior to inoculation. The appropriate volume of inoculum that corresponded to a standardised initial cell concentration at 0.1 g_{dcw} L^{-1} was aseptically added to the reactor. Incubation was carried out at 37 ^{o}C. The pH was maintained at pH 7 by the controlled addition of 8.5% H_3PO_4 (v/v) and 28% NH_4OH (v/v). The DO was controlled at 30% via cascade control of airflow and oxygen. The flow rate of air/oxygen was controlled at 5 L min^{-1} (1 vvm). Sterilised antifoam PPG was added periodically as required. The culture using a synthetic medium was induced with IPTG during the exponential phase of cell growth to a final concentration of 0.1 mM. Meanwhile for cultivation using vinasse medium, no IPTG was added. Cell growth was followed by removing 5 mL samples approximately at certain time intervals and the OD was then measured as described in Section 2.12.2.

2.9 Cell recovery and lysis

For all fermentation experiments, 500 µL aliquots of the harvested broth were placed in Eppendorf tubes and centrifuged at 13 000 rpm for 40 minutes at 4 ^{o}C (Hettich Universal 320 Benchtop Centrifuge, GMI Inc, USA). The resulting supernatant was used for glycerol (Section 2.12.6), acetate (Section 2.12.6), sugar (Section 2.12.7) and sugar alcohol (Section 2.12.7) determination. The pellets were resuspended in 200 µL of 2 mM pyridoxal 5'-phosphate (PLP) in 50 mM 4-(2-hydroxyethyl)-1-piperazineethanesulfonic acid (HEPES) buffer, pH 7.4. The cells were then

disrupted using a Soniprep 150 sonicator (MSE, Sanyo, Japan) with 10 cycles of 10 seconds on and 10 seconds off at 10 µm amplitude. The disrupted cells suspension was again centrifuged and the clarified lysate recovered for protein quantification and enzyme activity analysis as described in Section 2.12.3 and 2.12.5, respectively.

2.10 Pre-treatment of vinasse

As illustrated in Figure 2.1, upon removal of the suspended solids by centrifugation, the clarified vinasse was then pre-treated using powdered AC according to a modified version of a method originally described by Pramanik *et al.* (2012). The pre-treatment process was performed in a 100 mL shake flask with a working volume of 10 mL, initial pH of 2, shaking frequency of 160 rpm and at 25 $^{\circ}$C. Different concentrations of AC (5, 10, 15 and 20 % (w/v)) and incubation time (1, 2, 3, 4, 5 and 24 h) were tested. The pre-treated vinasse was then centrifuged at 12 000 rpm for 40 minutes at 4 $^{\circ}$C. Subsequently, the pre-treated vinasse was diluted accordingly with RO water and the pH was adjusted to pH 7, using a pH meter, prior to filtration through a 0.22 µm filter (Millipore Express Plus, Merck, UK) before being used for fermentation.

2.11 Characterisation of the oxygen mass transfer coefficient (k_La)

2.11.1 Measurement of k_La in MBR

Determination of k_La was based on the dynamic gassing out method (Van't Riet, 1979). Prior to k_La measurement, the DO sensor was pre-calibrated to 0% using nitrogen and subsequently to 100% using air. The method for measuring k_La involves two stages namely deoxygenation and oxygenation. Two different configurations of the Micro-24 were required. The gasses were re-routed where house air was connected to gas inlet 3 and nitrogen to gas inlet 2. All experiments were conducted at 37 $^{\circ}$C. The cassette was filled up with 6.5 mL of fermentation medium with 1 mL L^{-1} PPG.

Figure 2.13 shows the gas configuration for k_La measurement during deoxygenation and oxygenation in the Micro-24. In the deoxygenation stage, the pH control loop was used to sparge the nitrogen. The pH set point was chosen in such a way to sparge the nitrogen to the wells until the DO readout was 0%. Following that, during the oxygenation stage, both the DO and pH control systems were turned off. The shaking frequency was set at predetermined value, between 500 – 800 rpm, while the aeration rate was varied from 1.0 to 10 sccm. The air was sparged until the DO reached saturation. The change in the measured DO profile was recorded by the MicroReactor software.
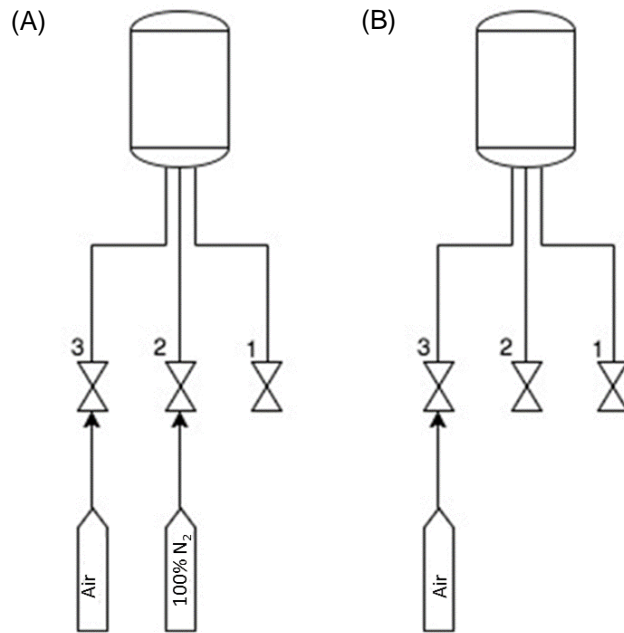
Figure 2.13. Piping and Instrumentation diagram (P & ID) showing the gas configuration for k_La measurement (dynamic gassing out method) during (A) deoxygenation and (B) oxygenation in Micro-24. Numbers refer to inlet ports of the Micro-24.

The k_La value was determined by the slope of the graph of ln (C_L^*-C_L) where C_L^* represents the equilibrium concentration of DO and C_L is the measured DO at each data point. The probe response time was determined based on the modified method by Ramirez *et al*. (2014). The measurement of probe response time was performed individually for every well and the average value of the 24 wells was then determined. Oxygenated water was prepared by sparging the air into a beaker of water. In parallel with this, the cassette was filled up with 3.25 mL of water and sparged with nitrogen until the DO readout was stabilised at 0%. A volume of 3.25 mL of oxygenated water was then added to the well. Figure 2.14 illustrates the procedure for the determination of probe response time in the MBR.
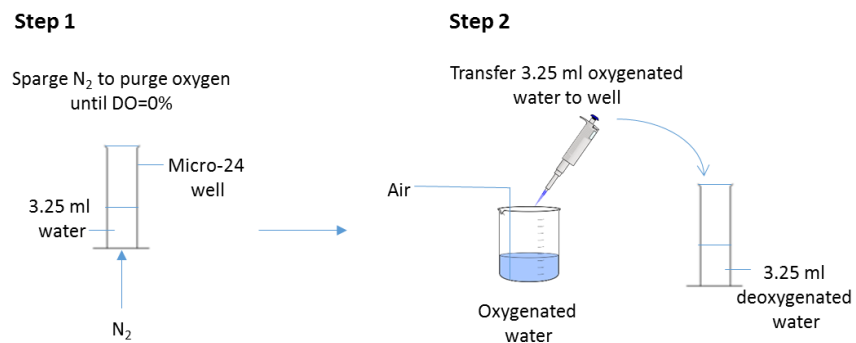
Figure 2.14. Procedure for the determination of probe response time in MBR.

Whenever the value of $1/k_La$ is less than the probe response time, then it is necessary to correct the k_La value by using Equation 2.2.

$$C_p = \frac{1}{t_m - \tau_p}\left[t_m \exp\left(\frac{-t}{t_m}\right) - \tau_p \exp\left(\frac{-t}{\tau_p}\right)\right]$$
(Equation 2.2)

Where C_p denotes the normalised DO at time t, $t_m = 1/k_La$ (s) and τ_p represents the probe response time (s).

2.11.2 Measurement of k_La in 7.5 L STR

2.11.2.1 Experimental k_La

As for the MBR, the measurement of k_La in the 7.5 L STR was based on the dynamic gassing out method. Calibration of the DO probe was carried out between 0 and 100% using nitrogen and air respectively. All experiments were performed at 37 °C with an agitation speed of 200 – 1000 rpm and airflow rate of 5 – 10 L min^{-1}. Initially, nitrogen was sparged to the reactor in order to purge the dissolved oxygen in the test medium until the DO readout was equilibrated at 0%. Following that, air was sparged and the change of DO with time was monitored and recorded by DASGIP Control 4.5 software (Eppendorf, Germany). The probe response time in the 7.5 L STR was determined by first immersing the probe in a beaker containing water that has been deoxygenated by nitrogen gas. Once the DO readout was stabilised at 0%, the probe was transferred swiftly to the reactor that was initially filled with water at 100% saturation. Likewise, whenever necessary, the effect of probe response time was incorporated in the determination of k_La values.

2.11.2.2 Calculated k_La

Calculated k_La in the 7.5 L STR was determined based on a correlation by Van't Riet (1979) that relates k_La with the process variables (Equation 2.3).

$$k_La = a(N^3 D_i^2)^b (v_s)^c$$
(Equation 2.3)

Where N is agitation speed (rpm), Di is impeller diameter (m), v_s is superficial velocity (m s^{-1}) whereas a, b and c represent coefficients. A collection of the experimental k_La values as determined in Section 2.11.2.1 were used as 'guess' k_La values to solve for the coefficients (a, b and c) by using a multiple linear regression analysis module in a MATLAB software (Matlab R14, MathWorks, USA).

2.12 Analytical Methods

2.12.1 Determination of dry cell weight

The calibration curves, as shown in Figures A1.1 (complex medium) and A1.2 (vinasse medium) were determined based on the relationship between the biomass concentration (g_{dcw} L^{-1}) and absorbance at 600 nm. Two millilitres aliquot of the cell suspension, sampled at certain time interval was pipetted into a pre-weighed Eppendorf tube and was then centrifuged at 13 000 rpm for 5 minutes (Eppendorf, AG, Germany). Following that, the supernatant was decanted and the pellet in the tube was left to dry in an oven at 90 ^{o}C until a constant weight was achieved. The biomass concentration, determined by dividing the weight of the dry pellet with the initial volume of the cell suspension added to the tube (2 mL) was then plotted over the corresponding OD value measured for every time interval.

2.12.2 Measurement of optical density (OD)

The OD of small aliquot of culture broth withdrawn at a certain time interval was determined at a wavelength of 600 nm using an Ultrospec 500 Pro spectrophotometer (Amersham Bioprocess, Amersham, UK). Whenever necessary, the aliquot was diluted with RO water such that the measured OD value was in the range 0.2 – 0.8. The OD was then translated to a dry cell weight based on the standard curve established as shown in Figure A1.1 (complex medium) and Figure A1.2 (vinasse medium).

2.12.3 Protein assay

Total protein concentration of the lysate, as obtained from Section 2.9, was determined based on the Bradford assay (Bradford, 1976). Bradford reagent was used along with bovine serum albumin (BSA) as the standard protein. Fifty microliters of diluted clarified lysate was incubated with 1 mL of Bradford reagent and the mixture was incubated at room temperature for 5 minutes. The absorbance of the reaction mixture was then measured at 595 nm using an Ultrospec 500 Pro spectrophotometer and translated into protein concentration based on the calibration curve established as shown in Figure A1.3.

2.12.4 Sodium dodecyl sulfate polyacrylamide gel electrophoresis (SDS-PAGE)

SDS-PAGE analysis was performed on a Mini -155 Protean II system (Bio-Rad Laboratories Inc., Hemel Hempstead, UK). Precast gel (10 cm x 12 wells) of SDS 10% (w/v) was run in Tris-glycine buffer system. Clarified lysate was mixed with Lamelli 4x concentrated protein sample buffer (Sigma-Aldrich, UK) and heated to 99 ^{o}C in a polymerase chain reaction (PCR) machine (Techne LTD, Cambridge, UK) for 16 min. Following that, 15-20 µg of the total protein of the clarified lysate suspension was loaded in each lane. The first lane was loaded with 3 µL of EZ-Run Prestained Rec Protein Ladder (Thermo Fisher Scientific Inc, UK) as the protein molecular weight marker. The gel was run at a power of 175 V for about 40 minutes. The gel was stained with appropriate amount of Coomassie Blue that consists of 0.1% (w/v) Coomassie Blue R-250, 40% (v/v) methanol and 10 % (v/v) acetic acid for 1-2 hour on a rocking table (Genetic Research

Instrumentation Ltd., Essex, UK). Next, the gel was de-stained overnight with de-staining buffer (10% (v/v) acetic acid, 30% (v/v) methanol and 60% (v/v) RO water). The gel was finally visualized and analysed on a Gel–Doc–it bioimaging system using Labworks 4.5 software (Bioimaging systems, Cambridge, UK).

2.12.5 CV2025 ω-TAm assay

The activity of CV2025 ω-TAm was determined based on the reaction between methylbenzylamine (MBA) and pyruvate (BDH Chemicals), yielding acetophenone (AP) and L-alanine (Casablancas *et al.*, 2013). Twenty microliter of lysate sample was mixed with 180 µL substrate buffer (50 mM phosphate buffer pH 7.4 containing substrates 11 mM MBA, 11 mM pyruvate, 1.25% (v/v) dimethyl sulfoxide (DMSO) and 0.1 mM PLP) in a 96-well, flat-bottomed microtiter plate (Radleys Discovery Technologies, Essex, UK). Throughout the reaction, the increasing absorbance of the reaction mixture was measured at 280 nm and at 30 ^{o}C, every 20 s for 2 min. The enzymatic activity was calculated according to Equation 2.4 where ΔAbs/min was determined from the slope of the linear equation for each activity measurement, d is the path of light and the extinction coefficient (cm), ε of AP 0.8477 mM^{-1} cm^{-1} was calculated from a plot of absorbance at 280 nm in the function of its concentration (Figure A1.4).

$$\frac{U}{ml} = \frac{\Delta Abs}{min} \times \frac{Vtotal}{Vsample} \times \frac{1}{\varepsilon AP} \times \frac{1}{d} \qquad \text{(Equation 2.4)}$$

One unit (U) of activity is defined as the amount of enzyme that catalyses production of 1 µ mole of AP per minute. Figure A4.1 shows typical time courses of absorbance for samples with different activity levels.

2.12.6 Determination of glycerol and acetate

Glycerol and acetate were quantified using a Dionex high performance liquid chromatography (HPLC) system consisting of an ASI-100 automated sample injector, P680 HPLC pump and STH 585 column oven. The system was fitted with an Aminex HPX-87H ion exclusion column (300 mm x 7.8 mm, Bio-Rad Labs, Rishmond, CA, USA), injection volume of 10 µL, column oven temperature of 60 ^{o}C with 5 mM H_2SO_4 as mobile phase at a flow rate of 0.6 mL min^{-1} for 30 min, monitored with a refractive index detector (RefractoMax 520 ERC) controlled by Chromeleon client 7.20 software. Retention times for glycerol and acetate were 13.3 and 14.8 min respectively. Calibration curves of peak area against solute concentration are shown in Figures A1.5 and A1.6. A chromatogram sample is shown in Figure A2.1.

2.12.7 Determination of sugars and sugar alcohols

Sugars and sugar alcohols were quantified using a Dionex ion chromatography system ICS-5000+ (Thermo Fisher Scientific Inc, Sunnyvale, USA) with AminoPac SA10 column (4×250 mm). The separation was performed at 30 °C for 30 min using gradient elution with 0.5-15 mM KOH as

the mobile phase at a flow rate of 0.25 mL min^{-1} and controlled by Chromeleon client 7.20 software. Retention times for D-xylitol, D-dulcitol, D-mannitol, D-maltitol, D-galactose and D-fructose were 2.3, 2.6, 2.8, 6.2, 12.1 and 18.7 min respectively. Calibration curves of peak height against solute concentration are shown in Figures A1.7 – A1.13. A chromatogram sample is shown in Figure A2.2.

2.12.8 Determination of polyphenols

Polyphenols was determined according to the Folin-Ciocalteu (FC) method (Cicco *et al.*, 2009). Gallic acid (GA) was used as a standard. One hundred microlitre of the test sample was mixed with 100 µL of FC reagent and equilibrated for 2 minutes prior to addition of 800 µL of 5% (v/v) sodium carbonate solution. The reaction mixture was placed in a water bath at 40 $^{\circ}$C for 20 minutes. Following that, the absorbance was read at 740 nm. 1 OD is equivalent to 0.0722 g GA. A typical calibration curve is shown in Figure A1.14.

2.12.9 Determination of viscosity

The rheology and viscosity of the culture medium were determined using a standard parallel plates method (Newton *et al.*, 2017). The measurement of viscosity of the media was carried out using a Kinexus Rheometer Lab+ (Malvern Instrument, Malvern, UK). The geometry used was PU50 (plate upper with the diameter of 50 mm) and the gap between the base and the geometry was maintained at 0.3 mm during the measurement. The measurement was carried out at 37 $^{\circ}$C. The rheometer was linked to the computer with the software interface, rSpace (Malvern Instrument, Malvern, UK) that facilitates the test set-up and exhibits the real-time profiles and data during the measurement. The shear rate range was between 100 and 1000 s^{-1} with 10 measurements made at each shear rate. An example of viscosity-shear rate curve is shown in Figure A3.1.

2.12.10 Growth inhibition assessment

The inhibitory effect of vinasse on cell growth was determined according to the cup-plate agar diffusion method (Pramanik *et al.*, 2012). About 100 µL of *E. coli* BL21 (DE3) culture was spread evenly on the LB-agar plate, which preparation as described in Section 2.3.3. A filter paper disc that had been soaked in 100% (v/v) vinasse was then placed in the middle of the plate. The plate was then incubated for 24 h at 37 $^{\circ}$C. Following that, the formation of inhibition zones was observed.

2.12.11 Growth assessment

LB agar plates supplemented with 0.15 g L^{-1} kanamycin (Section 2.3.3) were spread evenly with 48 h sample of *E. coli* BL21 (DE3) culture that was initially grown using either pasteurised or filtered dilute vinasse. Control plates were prepared by substituting the sample culture with either blank pasteurised or filtered dilute vinasse. The plates were then incubated for 24 - 72 h at 37 $^{\circ}$C, following which, the growth was then assessed.

2.13 Statistical analysis

The statistical analysis of the data was carried out by using Student's t-test. The results were considered statistically significant if the p-value <0.05.

CHAPTER 3

ESTABLISHMENT OF A SMALL SCALE FERMENTATION SYSTEM FOR PARALLEL STUDIES OF BIOCATALYST PRODUCTION

3.1 Introduction

To facilitate the early development of biocatalyst production processes, HTP cultivation systems are increasingly seen as beneficial (Section 1.4). The advantages introduced by the HTP platform has led to rapid data acquisition and in general, shortens the process development timelines. The lack of pH and DO control in conventional MWPs has limited their application in true optimisation studies to date; these are ideally conducted under controlled conditions using environmental control strategies representative of those in larger scale bioreactors. The latest microbioreactor (MBR) systems (Section 1.4.2) offer control of key process parameters at the individual well level overcoming limitations of conventional MWPs.

As discussed in Section 1.4.2, a number of studies have reported the utility of various commercial MBRs and their applications for mammalian cell culture process development. Amanullah *et al.* (2010) demonstrated the feasibility of a SimCell^{TM} MBR for a fed-batch cultivation of CHO cells. In addition, they also addressed the scalability of the process to the bench and pilot scale bioreactor. The use of an Ambr^{TM} system for mammalian cell culture as well as its comparability to a bench scale reactor has been reported by Hsu *et al.* (2012). Meanwhile, there are several publications on the characterisation of a 24-microwell bioreactor, the Micro-24 (Figure 2.2) and also its application as a scale-down tool for mammalian cell culture (Chen *et al.*, 2009; Betts *et al.*, 2014; Ramirez-Vargas *et al.*, 2014). Most recently, Sani (2016) has demonstrated the proof-of-concept of a new HTP microbioreactor system, the micro-Matrix, for CHO cell culture and its reproducibility in a lab scale reactor based on a matched mixing time.

The majority of studies on MBRs to date have focused on mammalian cell cultures. Microbial cultures, in contrast, are more challenging due to their faster growth rates, the higher cell concentrations achieved and greater oxygen requirements. A particularly important area for microbial cultures is in industrial enzyme production. In this chapter, the applicability of a controlled MBR for microbial culture will be investigated. A particular focus will be on the production of CV2025 ω-TAm (Section 1.2) by *E. coli* BL21 (DE3) given the interest in this enzyme for industrial biocatalysis. Previous works have reported the role of CV2025 ω-TAm in bioconversion processes (Kaulmann, *et al.*, 2007; Rios-Solis *et al.*, 2011; Halim *et al.*, 2013) however, optimisation of biocatalyst production has not been the focus of these studies. A good understanding of the strategies for optimising CV2025 ω-TAm production is a prerequisite for efficient and economically viable bioconversion processes.

In maximizing the expression of a recombinant protein such as CV2025 ω-TAm, establishing a high cell density culture followed by a suitable induction strategy are important considerations for maximising biocatalyst activity. The use of a controlled MBR for optimising CV2025 ω-TAm production has not previously been reported. This work will therefore provide new insights into the exploitation of controlled MBR technologies for parallel investigation of biocatalyst production.

3.2 Aim and objectives

The aim of this chapter is to establish methodologies for investigation of microbial culture and industrial enzyme production using MBR technologies. To illustrate this, a controlled MBR from Pall Corporation (Micro-24 system) will be evaluated for the production of CV2025 ω-TAm by *E. coli* BL21 (DE3). The results will provide a benchmark for further development of CV2025 ω-TAm production using renewable feedstocks (as described in Chapter 4). The experimental approach will first involve screening of suitable fermentation media for *E. coli* BL21 (DE3) in batch shake flasks followed by the development of comparable culture methods in the controlled MBR. Subsequently, the work will focus on the use of the MBR for optimisation of CV2025 ω-TAm production. The key objectives of the chapter are outlined below:

1. To establish basic culture conditions for *E. coli* BL21 (DE3) fermentation expressing CV2025 ω-TAm in batch shake flask cultures.
2. To investigate the performance of the controlled MBR for *E. coli* BL21 (DE3) culture in terms of monitoring and control of key process parameters and hence the establishment of operating strategies for reproducible culture.
3. To compare *E. coli* BL21 (DE3) culture performance between shake flask and controlled MBR cultures for CV2025 ω-TAm production.
4. To demonstrate the utility of the controlled MBR for optimisation of CV2025 ω-TAm production by investigating the influence of induction time, IPTG concentration and DO level on cell growth performance and biocatalyst titre.

3.3 Results

3.3.1 Preliminary shake flask studies (medium screening)

Initial studies focused on medium screening for *E. coli* BL21 (DE3) growth and CV2025 ω-TAm production. Cultivations were performed in a conventional, uncontrolled shake flask system as described in Section 2.8.1. The growth kinetics and specific activity data obtained will serve as a benchmark for later comparison with that obtained in the controlled MBR (Section 3.3.2.3) and those using vinasse medium (Chapter 4). Previously, CV2025 ω-TAm has been produced in cultivations employing LB-glycerol medium (Rios-Solis *et al.*, 2011; Halim *et al.*, 2013). One of the possible strategies to maximise the production of recombinant protein is by developing a

growth medium that can sustain both high cell growth rate and high protein titre (or in the case of enzymes, specific activity). In many laboratory scale studies, complex media like LB and Terrific Broth (TB) are typically adopted for growing microorganisms (Kram and Finkel, 2015) since they can generally supply adequate amounts of key nutrients. However, to achieve higher cell density and therefore a greater target protein expression level, a well-formulated medium with the optimal concentration of necessary components must be utilised.

Three different media formulations namely LB-glycerol, defined and complex media, as specified in Section 2.3.1, were evaluated as media for *E. coli* BL21 (DE3) growth and CV2025 ω-TAm production. The former medium was employed in order to reproduce the results by Rios-Solis (2012) and Halim (2012). In all formulations, glycerol was chosen as the main carbon source as this avoids excessive accumulation of acetate, which normally occurs in glucose-based cultures (Oh and Liao, 2000). Furthermore, as a by-product of biodiesel and oleochemical production, glycerol is abundantly available at a low price (Anitha *et al.*, 2016), making it an attractive carbon source in a biorefinery context.

Figure 3.1 shows the comparison of cell growth kinetics employing the three different media formulations. It was observed that the lag phase in the fermentation using a defined medium was slightly longer (4 h) in contrast to that in the complex and LB-glycerol media. This could be attributed to the presence of yeast extract in the latter two formulations. Yeast extract possesses growth factors and vitamins (Zhang *et al.*, 2003; Krause *et al.*, 2010) that are believed to accelerate the *E. coli* BL21 (DE3) growth rate. By enriching the medium with trace minerals and phosphate, as in the defined and complex media, the maximum biomass concentration was enhanced by 1.6 to 1.9-fold compared to LB-glycerol. Previous works by Rios-Solis (2012) and Halim (2012) showed that the maximum biomass concentration attained in cultivations using LB-glycerol were approximately 1.7 and 1.4 g_{dcw} L^{-1}, respectively, which are roughly comparable with the result from this study (2.0 g_{dcw} L^{-1}). The superiority of the enriched media over LB-glycerol is in agreement with other works that emphasised the significance of the additional medium components such as trace elements (García-Arrazola *et al.*, 2005; Siurkus *et al.*, 2010; Marisch *et al.*, 2013) and phopshate components (Kleman *et al.*, 1996; Paliy and Gunasekera, 2007; Soini *et al.*, 2008; Zhang *et al.*, 2013; Kram and Finkel, 2015) in achieving high cell densities.
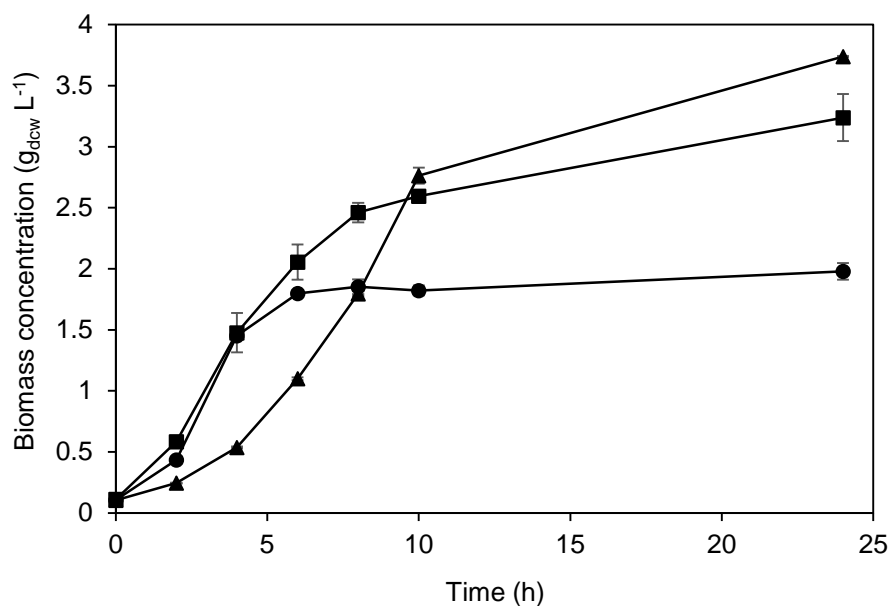
Figure 3.1. Batch fermentation kinetics of *E. coli* BL21 (DE3) cultured on various growth media in conventional shake flasks. (●) LB-glycerol, (▲) defined medium and (■) complex medium. Error bars denote one standard deviation from the mean (n=3). All fermentations were induced with 0.1 mM IPTG at 10 h for each cell growth profile. Fermentations were performed as described in Section 2.8.1. Biomass concentration was determined as described in Section 2.12.2.

The corresponding CV2025 ω-TAm activity for cell cultured in each of the different media was also quantified. The assay used for CV2025 ω-TAm activity determination (Section 2.12.5), was chosen as it is rapid, reliable and quantitative. Due to different enzyme quantification methods employed between present and previous works (Halim, 2012; Rios-Solis, 2012), a fair comparison of the enzyme activity may be challenging. Thus, in this work, the CV2025 ω-TAm activity obtained from the cultures using LB-glycerol medium will be referred to as a benchmark since the experiment was actually reproduced using similar medium as employed by Halim (2012) and Rios-Solis (2012). This is further supported by the fact that the maximum biomass attained between present and their works was roughly comparable, as discussed earlier.

Figure 3.2 shows the maximum CV2025 ω-TAm volumetric and specific activity measured in *E. coli* BL21 (DE3) fermentation using the three different media. Significant improvements, 4.6 to 8.7-fold, in volumetric activity and 1.7 to 1.9-fold, in specific activity were achieved with defined and complex media, respectively, compared to the LB-glycerol medium. Comparing the performance of the defined and complex media in terms of CV2025 ω-TAm volumetric activity, there was a significant enhancement (p-value = 0.02) shown by the use of the latter medium.

The enhancement shown in the fermentation using a complex medium may be associated with the presence of yeast extract. Yeast extract does not only promote rapid growth but also facilitates the expression of recombinant protein due to the availability of transcription enhancers like cAMP (Donovan *et al.*, 1996). This is further supported by Liu and co-workers (1999) who reported the

enhancement of recombinant protein expression by several *E. coli* BL21 (DE3) strains by the addition of yeast extract in concentrations between 0.5 - 1.5% (w/v) during induction. In summary, an enriched media formulation appears essential for the enhancement of both cell growth and CV2025 ω-TAm specific activity. Evaluation of the fermentation performance between defined and complex media will be further verified in the controlled MBR as discussed in Section 3.3.2.4.
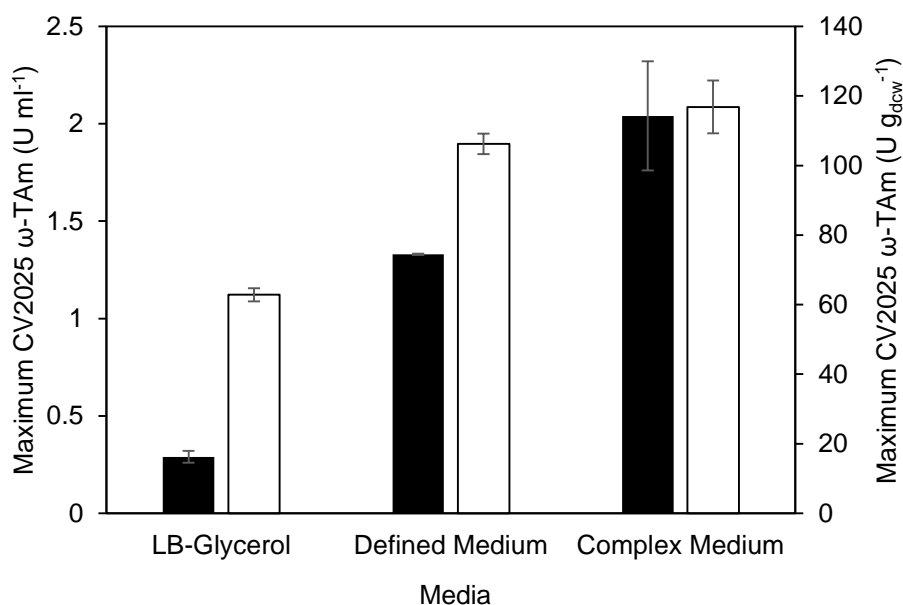
Figure 3.2. Maximum CV2025 ω-TAm (■) volumetric and (□) specific activity obtained in shake flask fermentations using different media (Figure 3.1). Error bars denote one standard deviation from the mean (n=3). The CV2025 ω-TAm activity was determined as described in Section 2.12.5.

3.3.2 Establishment of controlled MBR cultivation conditions

Following the establishment of the benchmark cultures as attained in Section 3.3.1, subsequent studies were focused on the development of cultivation conditions in the controlled MBR. Firstly, measurement and control of process parameters: temperature, pH and DO were assessed across all wells in the MBR. This will ensure the reliability of the MBR in measuring and controlling process parameters with respect to their set points as well as their consistency from well to well. Secondly, reproducibility of parallel MBR cultivations were examined with regards to cell growth, substrate consumption and biocatalyst production. The rationale behind these studies is that comparability of the cultivation performance across the MBR is essential for studies involving high throughput reactors, which reinforces the purpose of conducting parallel experiments. Subsequently, comparison of shake flask and controlled MBR culture performance was carried out whereby the output will reflect the importance of the latter platform in realizing high cell density cultures. Finally, evaluation of the fermentation media as screened in Section 3.3.1 was

performed in the controlled MBR where the findings will represent the benchmark of the cultivation performance using a synthetic medium, replacing those standards as obtained in shake flasks.

3.3.2.1 Measurement and control of process parameters

The advantage of MBR technologies over conventional shake flasks is that they enable control of key process parameters such as temperature, pH and DO. Initial batch *E. coli* BL21 (DE3) cultivations in the MBR focused on the control and reproducibility of these parameters across a single 24-well plate. Figure 3.3 illustrates the average values of temperature, pH and DO from 12 random wells during a typical fermentation process using a complex medium with standardised culture conditions as described in Section 2.8.2. The temperature profile shows a good control around the set point with a deviation of less than 0.5 ^{o}C (Figure 3.3 (A)). These results were obtained with a set point of 37 ^{o}C in all 24 wells. According to the standard operating procedure for the Micro-24, the variation of the temperature between adjacent wells must not exceed 2 ^{o}C, thus this needs to be considered in the design of any optimisation study involving variation of temperature.

One-sided pH control in Micro-24 cultures was achieved by sparging either 100% CO_2 or 15% NH_3 (Section 2.8.2). In studies involving the complex medium, as the cultures tend to acidify due to the accumulation of acetate, 15% (v/v) NH_3 was sparged into the wells in order to increase the pH back to the pH 7 set point. In cultures using sugar beet vinasse medium (Chapter 4), where the pH increases throughout the course of the fermentation, 100% (v/v) CO_2 was sparged to maintain the neutral pH.

As shown in Figure 3.3 (B), pH is controlled close to the set point (pH 7) with fluctuations generally within ± 0.2 in the complex medium. Comparative on-line and off-line pH measurements generally showed 95 – 98% agreement, indicating the comparability of pH measurement between the Micro-24 and a typical pH meter. In comparison to the pH fluctuations recorded in shake flasks the pH variation in the Micro-24 is considerably smaller.

The mean value of the DO from 12 random wells is presented in Figure 3.3 (C). The DO in each well was controlled at 30% as described in Section 2.8.2. The deviation of DO from the set point was most apparent during the first 10 h of cultivation as this mainly represents the log phase where the oxygen demand is the highest. From 10 h onwards there is a good control of pH around the set point in all wells.
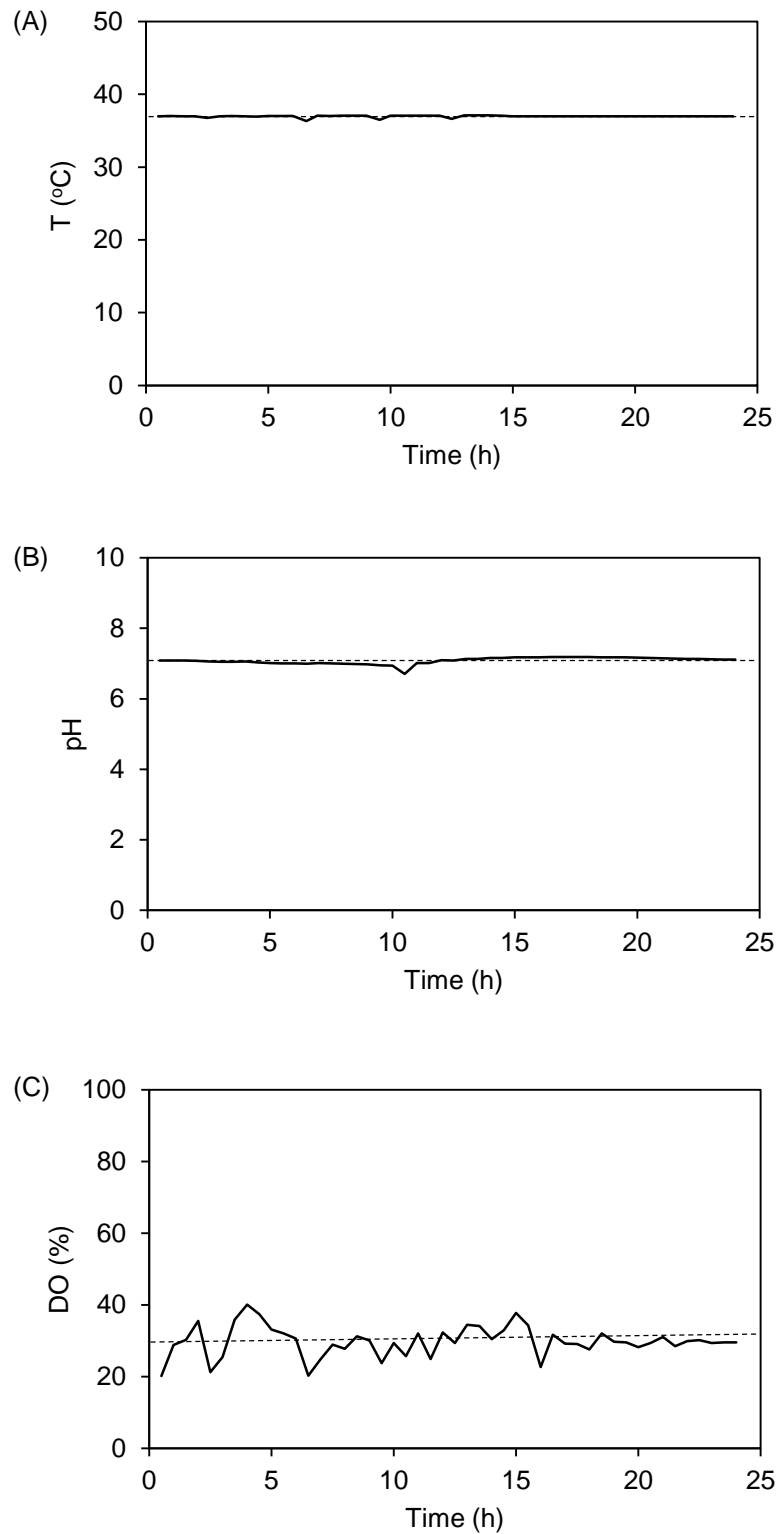
Figure 3.3. Online measurements of (A) temperature, (B) pH and (C) DO in controlled, parallel Micro-24 *E. coli* BL21 (DE3) batch fermentations. Horizontal dotted lines represent the set point for each process parameter. Figure shows mean values from 12 random wells across the cassette. Fermentations were performed using a complex medium as described in Section 2.8.2.

Overall, the results in Figure 3.3 show a good control of key fermentation parameters around their set point. In this work, the DO was controlled by blending oxygen and nitrogen, which was the same approach reported by Tang and co-workers (2006). The sparging of nitrogen was used to counterbalance the 'noise' imparted by oxygen sparging especially during the exponential phase of cell growth. This approach seems to be advantageous in terms of DO stability and the fast response towards the maintenance of DO around the set point, contrary to the one-sided control by oxygen that tends to give greater noise. However, the implementation of a two-gas DO control system will restrict pH control on the Micro-24 to be only one-sided due to the utilisation of the two out of the three available gas inlets to the reactor (Figure 2.4). Among other possible factors that might also contribute to the noise of the DO control are the PID values and the aeration rate. Although in certain circumstances tuning of PID values will be necessary, the default values provided by the manufacturer appear adequate in this case. The fine tuning of the aeration rate may also further reduce any DO fluctuations.

Overall, the results presented here show that the controlled MBR enabled direct measurement of on-line processes parameters and their control. The corresponding pH and DO variations were therefore less than in the shake flask cultures confirming the suitability of the Micro-24 bioreactor system.

3.3.2.2 Reproducibility of parallel MBR cultivations

Another essential aspect in considering the utility of any MBR platform is the well-to-well variability. Fermentation profiles and enzyme activity from cultures performed in 12 random wells across the controlled MBR plate were assessed. In all fermentations, similar culture conditions (pre-cultures, medium and induction conditions) were used as described in Section 2.8.2. The culture conditions used in these specific experiments were not optimised and hence can be improved further.

Figures 3.4 and 3.5 show the variation in biomass concentration and CV2025 ω-TAm specific activity, respectively between the wells. It is clear that there was a good reproducibility of the biomass, glycerol and acetate profiles. For biomass, the average specific growth rate recorded was 0.35 ± 0.01 h^{-1} while the average maximum biomass achieved was 12.0 ± 0.8 g$_{dcw}$ L^{-1}. The trend of the glycerol consumption in all wells was generally similar; a complete utilisation was mostly seen after 10 h of culture. The average $Y_{X/S}$ value obtained was 0.40 ± 0.03 g$_{dcw}$$^{-1}$ g^{-1}. Meanwhile, the acetate profiles across the 12 wells were comparable showing a slight accumulation during the first 10 h followed by a decrease after 24 h. Quantification of the CV2025 ω-TAm specific activity also showed a good reproducibility. The mean value of CV2025 ω-TAm specific activity recorded was 256.3 ± 21.3 U g$_{dcw}$ L^{-1}. In general, these results suggest that the environmental control that can be achieved in the Micro-24 provides consistent well-to-well performance.
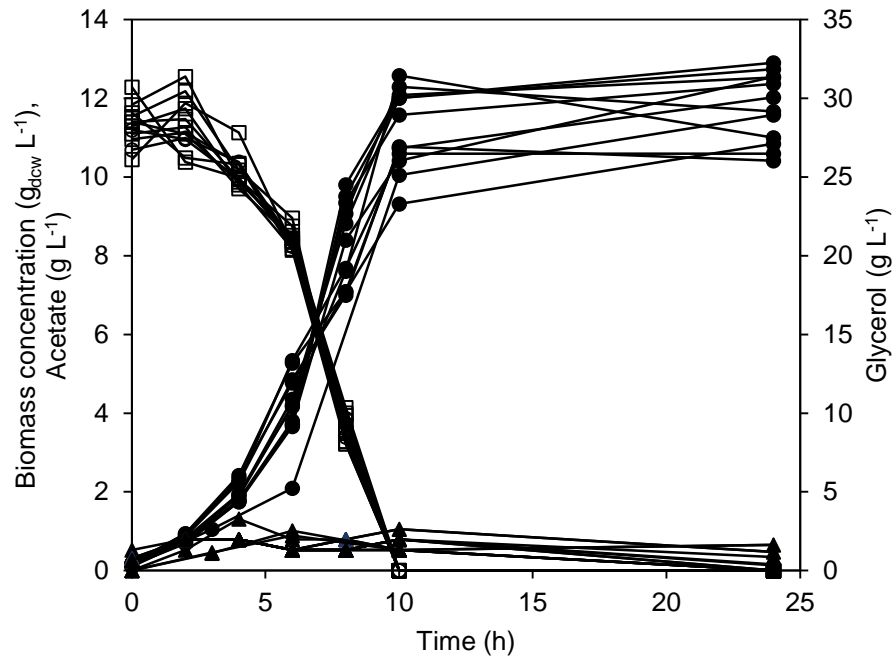
Figure 3.4. Fermentation kinetics of 12 parallel, batch *E. coli* BL21 (DE3) fermentations in the controlled MBR: (●) biomass, (□) glycerol, (▲) acetate. Fermentations were performed using a complex medium as described in Section 2.8.2. Analytical procedures were carried out as specified in Section 2.12.2 (biomass concentration) and Section 2.12.6 (glycerol and acetate).
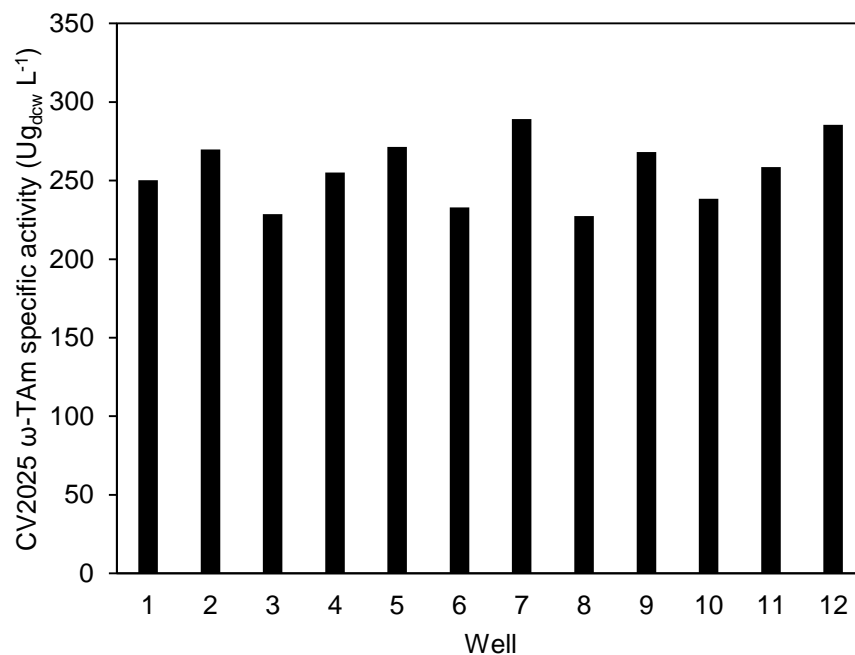
Figure 3.5. Comparison of CV2025 ω-TAm specific activity achieved at 24 h during batch *E. coli* BL21 (DE3) fermentations in 12 random wells across the controlled MBR (Figure 3.4). The CV2025 ω-TAm assay was performed as described in Section 2.12.5.

3.3.2.3 Comparison of shake flask and controlled MBR culture performance

Shake flasks have been widely used for fermentation screening owing to their simplicity and relatively low volume requirement (Buchs, 2001; Lye *et al.*, 2003). The absence of monitoring and control however, particularly for pH and DO, limits their application for more focused optimisation studies. Here, a direct comparison of the performance of shake flasks and the controlled MBR for *E. coli* BL21 (DE3) fermentation, under similar culture conditions, is demonstrated.

Figure 3.6 shows a comparison of fermentation profiles obtained in shake flasks and the controlled MBR using a complex medium. A marked enhancement in cell growth is evident in the controlled MBR with a notable increase of 3.7-fold in the biomass concentration after 24 h. MBR cultures demonstrated a close relationship between growth and glycerol consumption where rapid utilisation occurred during the exponential growth phase. The mean value of $Y_{X/S}$ in the controlled MBR cultures was 0.38 ± 0.02 g dcw per g glycerol, while that for the shake flask cultures was only 0.20 ± 0.01 g dcw per g glycerol.

The significant increase in final cell density in the controlled MBR is attributed to the DO and pH control. Since metabolism of facultative aerobes such as *E. coli* BL21 (DE3) is highly responsive to oxygen; its sufficient supply is paramount in order to ensure optimal cell growth rate and target protein production are achieved while minimising the synthesis of undesirable co-products (Marques *et al.*, 2010). As the oxygen transfer in shake flasks only depends on surface aeration aided by orbital shaking (Gupta and Rao, 2003), oxygen deficiency may become one of the bottlenecks for aerobic cultures in this cultivation platform. Although mixing may be enhanced by the use of baffled flasks and low working volume (Lotter and Buchs, 2004), the OTR is well below that which can be achieved in the oxygen sparged MBR. In baffled shake flasks, the $k_L a$ range is reported to be between 40-58 h^{-1} (Gupta and Rao, 2003) while in Micro-24 system, the $k_L a$ ranged from 8 to 90 h^{-1}, depending on several determining factors such as cassette, closure, shaking frequency and aeration rate (Ramirez-Vargas *et al.*, 2014). Quantification of oxygen mass transfer coefficients is described later in Chapter 5.
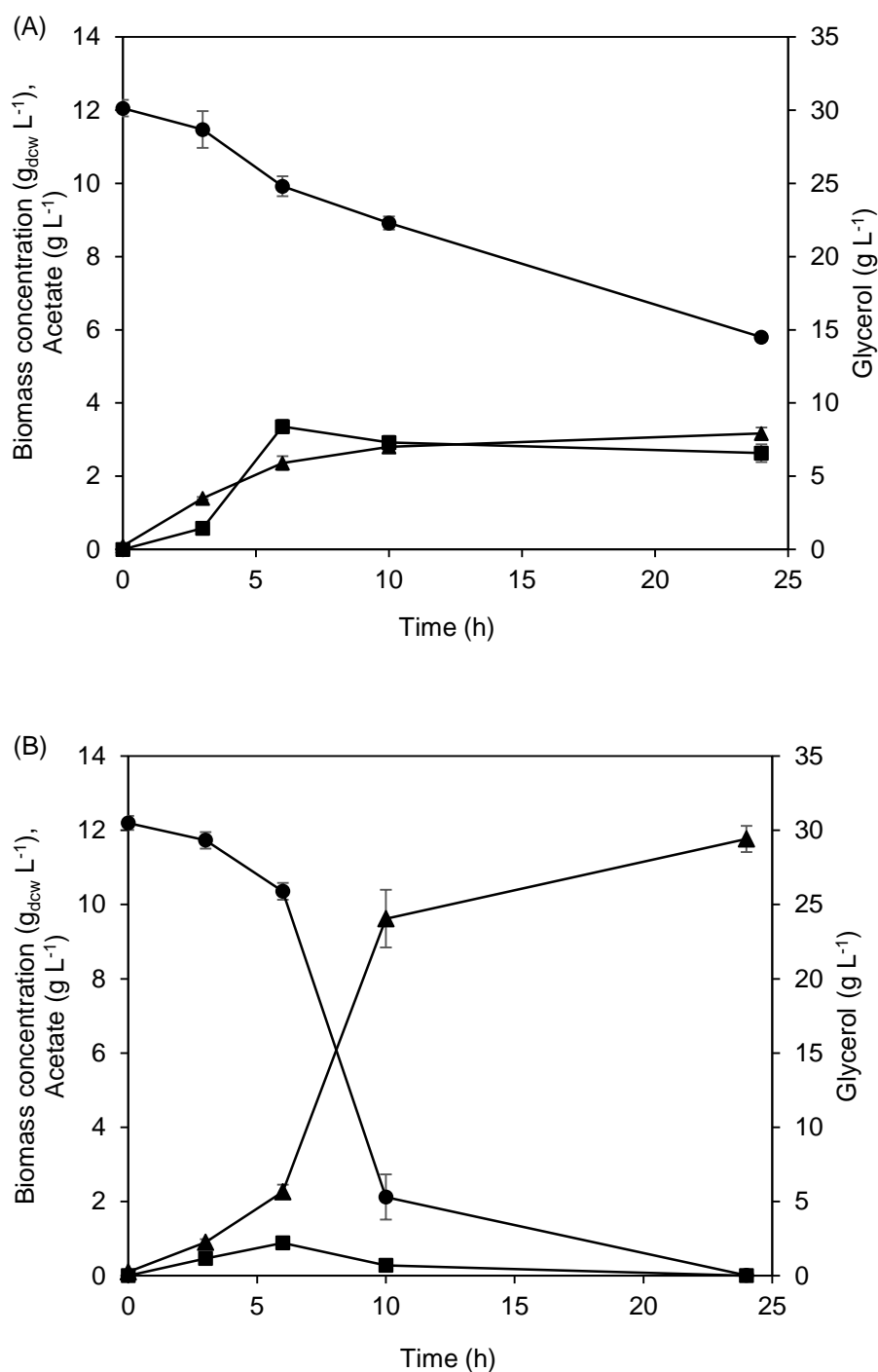
Figure 3.6. Comparison of batch *E. coli* BL21 (DE3) fermentation kinetics using a complex medium in (A) shake flask and (B) controlled MBR. (▲) biomass, (●) glycerol and (■) acetate. Error bars denote one standard deviation from the mean (n=3). Fermentations were performed as described in Section 2.8.1 (shake flask) and 2.8.2 (controlled MBR). Analytical procedures were carried out as specified in Section 2.12.2 (biomass concentration) and Section 2.12.6 (glycerol and acetate).

Accumulation of the metabolic side product acetate reaches 2.6 g L^{-1} in shake flask cultures resulting in a drop in pH from 7 to about 5.6. This has further limited the cell growth and consequently CV2025 ω-TAm production (Figure 3.6 (A)). Although there is contradictory information in the literature about acetate production in glycerol-based fermentation, the results obtained in this study are consistent with several reports (Korz *et al.*, 1995; Macaloney *et al.*, 1997; García-Arrazola *et al.*, 2005). In contrast, in the controlled MBR the acetate level remained below 1.0 g L^{-1} and the on-line data showed that the pH remained at pH 7 ± 0.2 throughout the culture.

The corresponding CV2025 ω-TAm specific activity in shake flask and controlled MBR cultures was also evaluated. Both cultures were induced with 0.1 mM IPTG at 10 h and CV2025 ω-TAm activity was determined 14 h later. The CV2025 ω-TAm volumetric and specific activity attained in the controlled MBR were 5.3 ± 0.6 U ml^{-1} and 261.7 ± 10.6 U g$_{dcw}^{-1}$ respectively, which were 2.1 and 2.2-fold higher than that attained in the shake flask cultures. The considerable improvements in cell growth and enzyme shown in the controlled MBR compared to the shake flasks confirm the benefits of introducing monitoring and control of culture parameters. This further supports the potential of the controlled MBR particularly Micro-24 as shown in this work, as a HTP platform for optimisation of biocatalyst production.

3.3.2.4 Evaluation of fermentation media in the controlled MBR

In continuation of the preliminary study using shake flask cultures described in Section 3.3.1, *E. coli* BL21 (DE3) culture on defined or complex media was further investigated in the controlled MBR. The pre-culture conditions (age and concentration) as well as induction time (10 h) (Section 2.7) and inducer concentration (0.1 mM IPTG) were standardised for both types of media.

Figure 3.7 compares the kinetics of *E. coli* BL21 (DE3) cultures in the controlled MBR using both types of media. It is clearly shown that cell growth was more rapid using a complex medium with the maximum biomass being 1.4 times greater than in the defined medium. The cell growth observed in both fermentations was found to correspond directly with their glycerol consumption profiles. Whilst a complete consumption of glycerol was seen after 24 h with the complex medium, in the defined medium, only 62% of glycerol was consumed. The depletion of glycerol in the culture employing a complex medium has resulted in the consumption of acetate, which could be seen with its reducing concentration throughout the course of the fermentation period. In contrast, in the fermentation using a defined medium, the acetate was found to accumulate to 1.2 g L^{-1} after 24 h. Similar to the results discussed in Section 3.3.1, the presence of yeast extract in the complex medium is believed to be responsible for the improved growth compared to the defined medium.
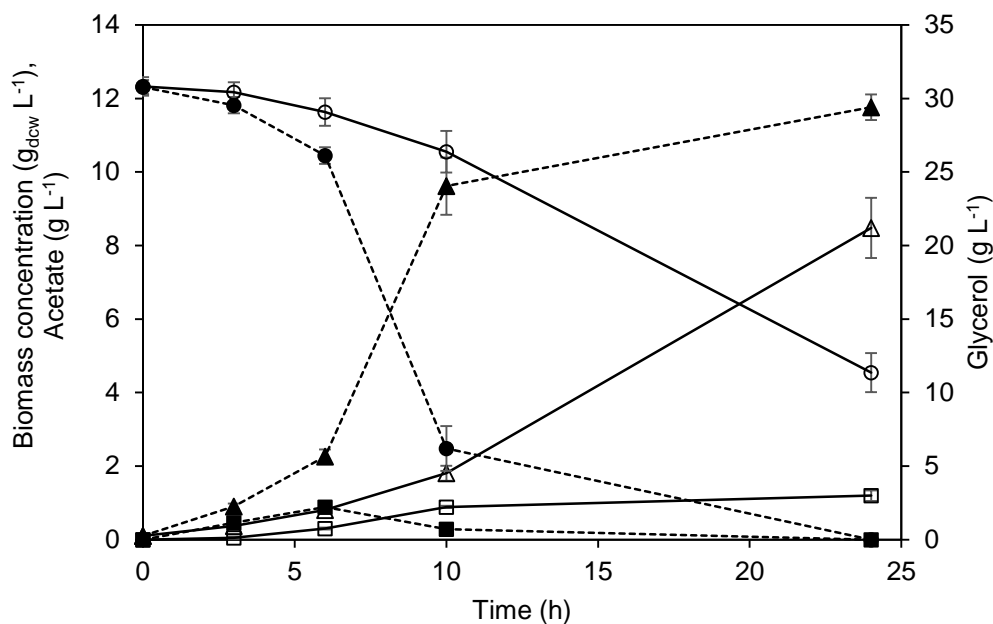
Figure 3.7. Comparison of batch *E. coli* BL21 (DE3) fermentation kinetics in the controlled MBR fermentations using defined and complex media: (△) biomass (defined medium), (▲) biomass (complex medium), (○) glycerol (defined medium), (●) glycerol (complex medium), (□) acetate (defined medium), (■) acetate (complex medium). Error bars denote one standard deviation from the mean (n=5). Fermentations were performed as described in Section 2.8.2. Analytical procedures were carried out as described in Section 2.12.2 (biomass concentration) and Section 2.12.6 (glycerol and acetate).

The corresponding CV2025 ω-TAm production from both fermentations was analysed and the biocatalyst volumetric and specific activity at 24 h are presented in Figure 3.8. The results showed that there was a significant difference (p-value = 0.01) with regards to the CV2025 ω-TAm volumetric activity obtained from fermentations using defined and complex media, with latter being the superior. Furthermore, the CV2025 ω-TAm specific activity of 252.7 U g_{dcw}^{-1} was obtained in the fermentation that employed a complex medium where this represented an enhancement of 1.2-fold over that in the cultures grown using a defined medium. These different media results obtained in the controlled MBR confirmed the advantage of using a complex medium due to its rapid and higher cell growth performance and CV2025 ω-TAm production.
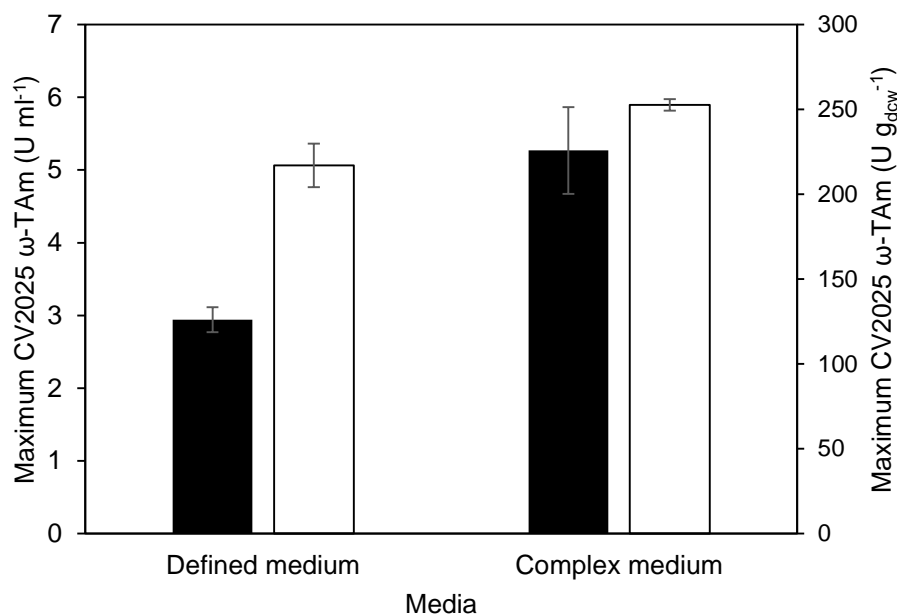
Figure 3.8. Maximum CV2025 ω-TAm (■) volumetric and (□) specific activity obtained in the controlled MBR fermentations using a defined and complex medium (Figure 3.7). Error bars denote one standard deviation from the mean (n=5). The CV2025 ω-TAm assay was performed as described in Section 2.12.5.

3.3.3 Controlled MBR fermentation optimisation studies

Following the establishment of basic culture conditions in the controlled MBR, subsequent work aimed to demonstrate the utility of the platform for fermentation optimisation studies. The effects of several parameters such as induction time, IPTG concentration and DO level on the biocatalyst production were evaluated. The rationale of these studies is that the influence of the induction time and inducer concentration on recombinant protein expression is crucial (Donovan *et al.*, 1996). Meanwhile, as the *E. coli* fermentation is an aerobic fermentation, DO level may influence the cultivation performance and thus should also be investigated. An optimal level of DO may facilitate not only the attainment of high cell density cultures but also will enhance the cost efficiency of the fermentation process.

3.3.3.1 Influence of induction time and IPTG concentration

As the *E. coli* BL21 (DE3) strain used in this work consists of an inducible T7 promoter, the addition of IPTG, which is an allolactose analogue, binds the repressor thus allowing transcription of the *lac* operon and hence protein expression. To examine the influence of induction time, induction times of 6, 8 and 10 h that represent early, middle and late exponential phase, respectively were evaluated. Two levels of IPTG concentrations, namely 0.1 and 1.0 mM, were compared. The concentration of 0.1 mM normally serves as the minimum concentration applied

in most studies involving expression of the recombinant protein in *E. coli* BL21 (DE3) including CV2025 ω-TAm (Rios-Solis, 2012). In contrast, 1.0 mM is usually referred to as the maximum level of IPTG used for induction as applied by Kaulmann and co-workers (2007) in their early works on the same biocatalyst.

Figures 3.9 and 3.10 depict cell growth, glycerol consumption and acetate concentration profiles of fermentations performed with different induction times. It was observed that there was a slight decrease of maximum biomass (7%) and specific growth rate (14%) in fermentations that were induced at 6 h when the IPTG concentration was increased from 0.1 to 1.0 mM (Table 3.1). This could be attributed to the high IPTG concentration that imparted a large metabolic burden on the cell soon after growth had actively started. The same level of IPTG did not really affect the fermentations induced during the mid and late exponential phase since at those points, the growth has already slowed down.

For fermentations that were induced during the mid and late exponential phase, the glycerol content was completely depleted after 10 h, which also denoted the point of maximum biomass and at which the growth started to cease. In all fermentations, acetate was metabolised once glycerol became deficient. The cell growth kinetics parameters were quite comparable despite the different IPTG concentrations. Generally, there was no notable difference in terms of maximum biomass, specific growth rate (μ) and biomass yield on substrate ($Y_{X/S}$) (Table 3.1).
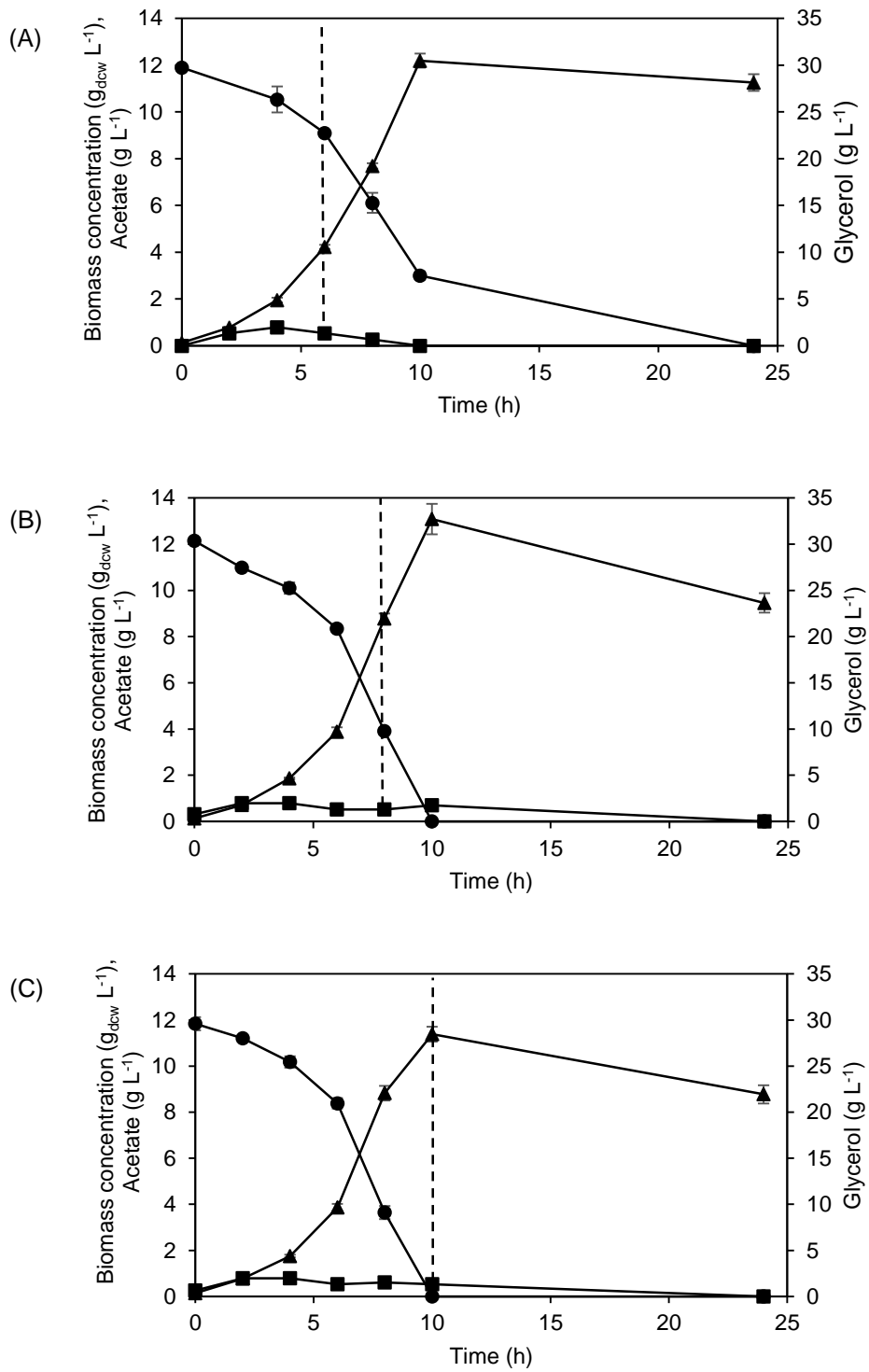
Figure 3.9. Comparison of a batch *E. coli* BL21 (DE3) fermentation kinetics in a controlled MBR induced with 0.1 mM IPTG at (A) 6 h, (B) 8 h and (C) 10 h: (▲) biomass, (●) glycerol and (■) acetate. Dotted vertical lines indicate the point of induction. Error bars denote one standard deviation from the mean (n=3). Fermentations were performed as described in Section 2.8.2. Analytical procedures were carried out as specified in Section 2.12.2 (biomass concentration) and Section 2.12.6 (glycerol and acetate).
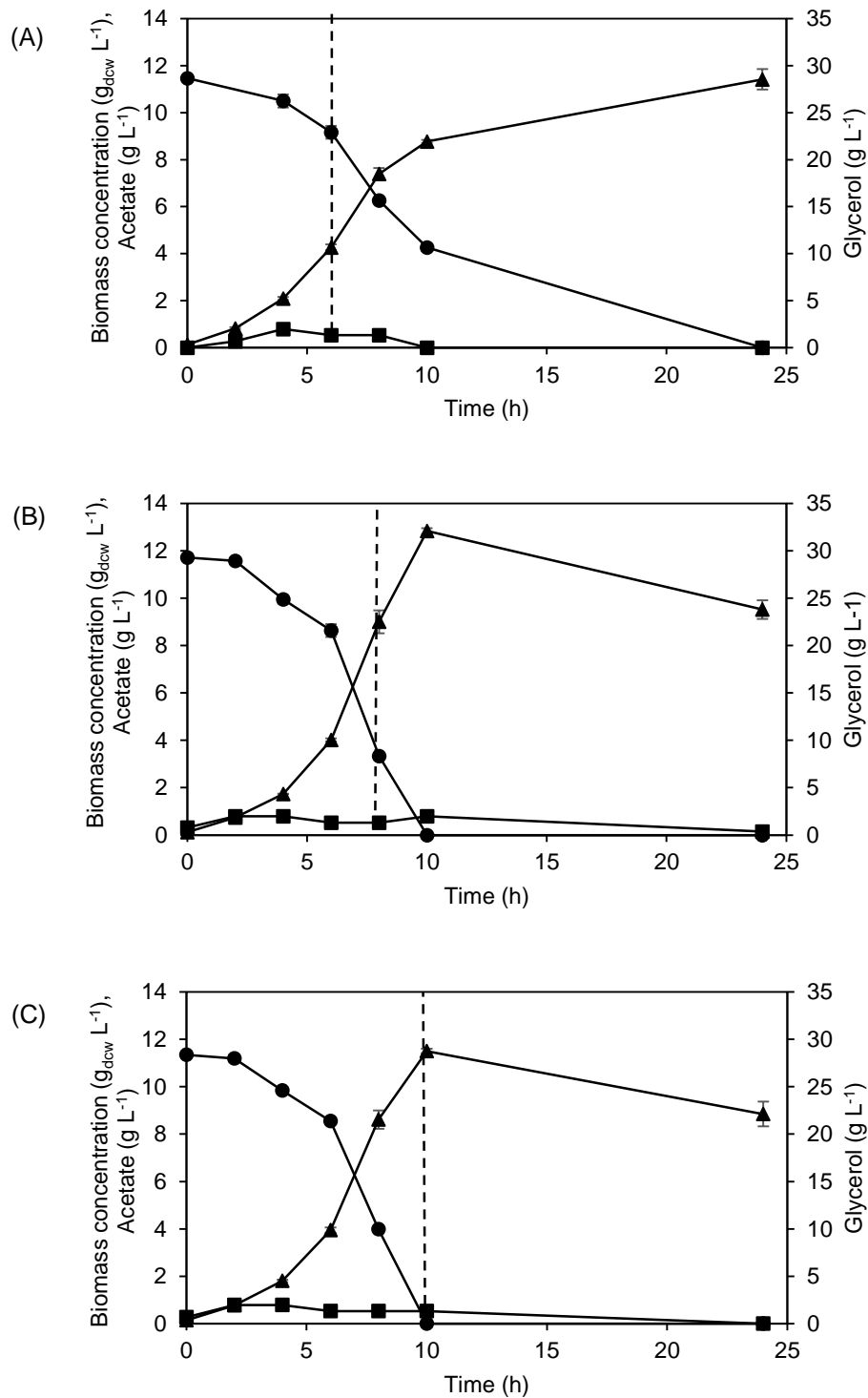
Figure 3.10. Comparison of a batch *E. coli* BL21 (DE3) fermentation kinetics in a controlled MBR induced with 1.0 mM IPTG at (A) 6 h, (B) 8 h and (C) 10 h: (▲) biomass, (●) glycerol and (■) acetate. Dotted vertical lines indicate the point of induction. Error bars denote one standard deviation from the mean (n=3). Fermentations were performed as described in Section 2.8.2. Analytical procedures were carried out as specified in Section 2.12.2 (biomass concentration) and Section 2.12.6 (glycerol and acetate).

Table 3.1. Fermentation kinetics parameters for *E. coli* BL21 (DE3) grown on a complex medium under different induction conditions. Fermentations were performed as described in Section 2.8.2. Analytical procedures were carried out as specified in Section 2.12.2 (biomass concentration) and Section 2.12.6 (glycerol).

Parameters	IPTG concentration (mM)					
	0.1			1.0		
	Induction time (h)					
	6	8	10	6	8	10
X_{max} (g_{dcw} L^{-1})	12.2 ± 0.3	13.1 ± 0.7	11.4 ± 0.3	11.4 ± 0.4	12.8 ± 0.1	11.5 ± 0.1
μ (h^{-1})	0.35 ± 0.01	0.37 ± 0.01	0.36 ± 0.01	0.30 ± 0.01	0.37 ± 0.01	0.35 ± 0.00
$Y_{x/s}$ (g g^{-1})	0.46 ± 0.04	0.46 ± 0.04	0.40 ± 0.01	0.40 ± 0.02	0.46 ± 0.03	0.42 ± 0.01

The corresponding profiles of CV2025 ω-TAm volumetric and specific activity achieved for different induction conditions are presented in Figures 3.11 and 3.12 respectively. Generally, it was observed that higher volumetric and specific enzymatic activity were achieved in fermentations that were induced at 0.1 mM IPTG compared to 1.0 mM IPTG. For instance, the difference of CV2025 ω-TAm specific activity at 24 h between fermentations induced with 0.1 mM IPTG and 1.0 mM IPTG ranged from 22 to 43%. High levels of IPTG, attempting to completely induce the *lac* operon, did not necessarily lead to an increase in the target protein expression. An excessive amount of IPTG could also result in a disproportionate metabolic burden and toxicity to the cells (Olaofe *et al.*, 2010; Marini *et al.*, 2014).

In terms of the effect of induction time, the highest CV2025 ω-TAm volumetric and specific activity were obtained when the culture was induced during the early exponential phase (6 h). As shown in Figure 3.11, there was a steady increase in CV2025 ω-TAm activities throughout the post induction period. Sufficient time for the protein expression during the exponential phase is beneficial in balancing the protein synthesis flux and therefore reducing the amount of inclusion bodies formed (Yong *et al.*, 2007). This could be the case for the induction at the early exponential phase as the longer duration supported a relatively slower rate of protein translation thus enabling the expression of the active proteins. In contrast, the time frame was reduced when the induction was performed during the mid and the late exponential phase. The CV2025 ω-TAm specific activity of cultures induced with 0.1 mM IPTG at the late exponential phase was 40% lower than the corresponding fermentation with an early induction, which may be probably associated with the decreased growth rate and substrate deficiency.
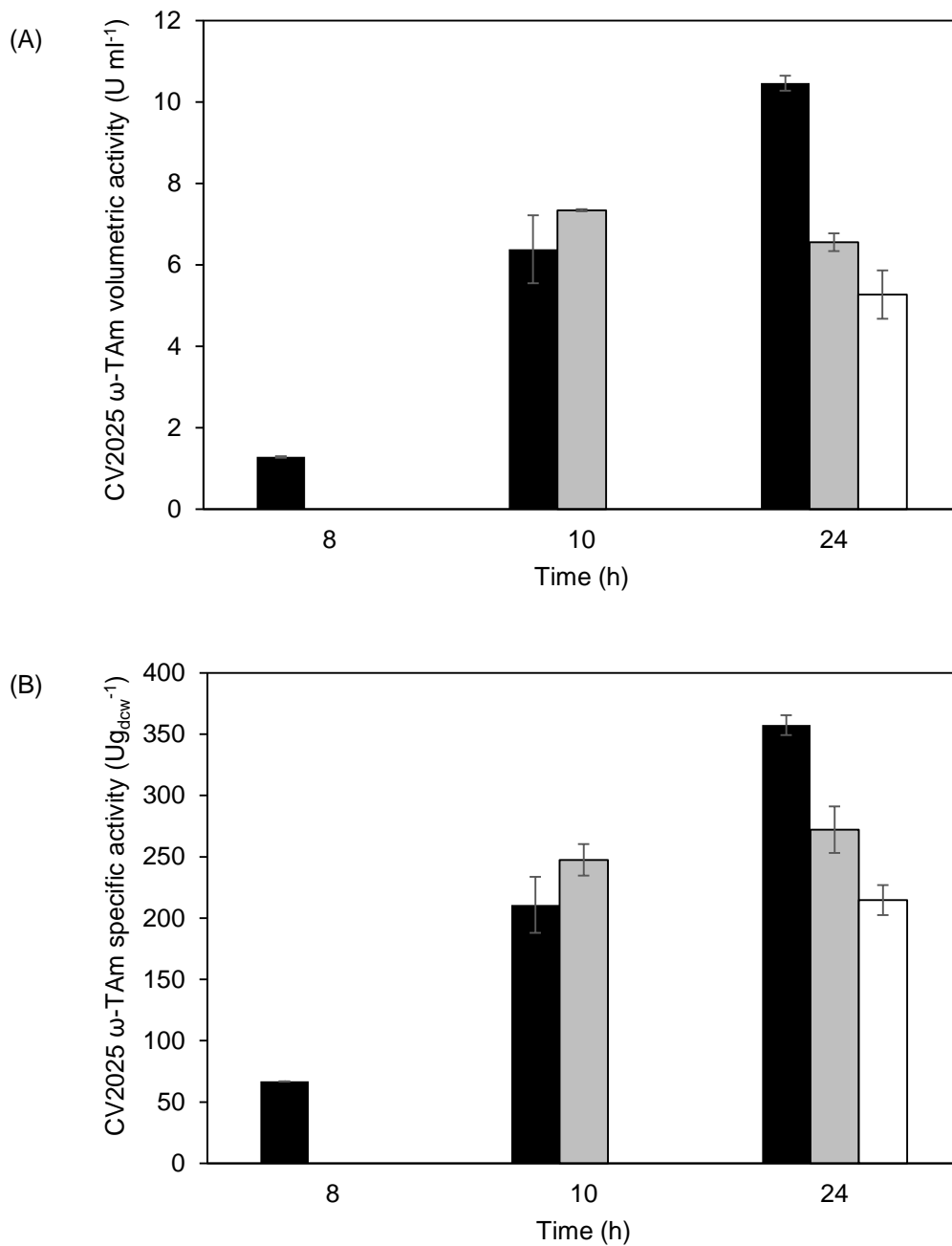
Figure 3.11. (A) Volumetric activity and (B) specific activity of CV2025 ω-TAm expressed from fermentations in a controlled MBR with (■) early, (▣) mid and (□) late exponential phase induction induced at 0.1 mM IPTG. Error bars denote one standard deviation from the mean (n=3). The CV2025 ω-TAm assay was performed as described in Section 2.12.5.
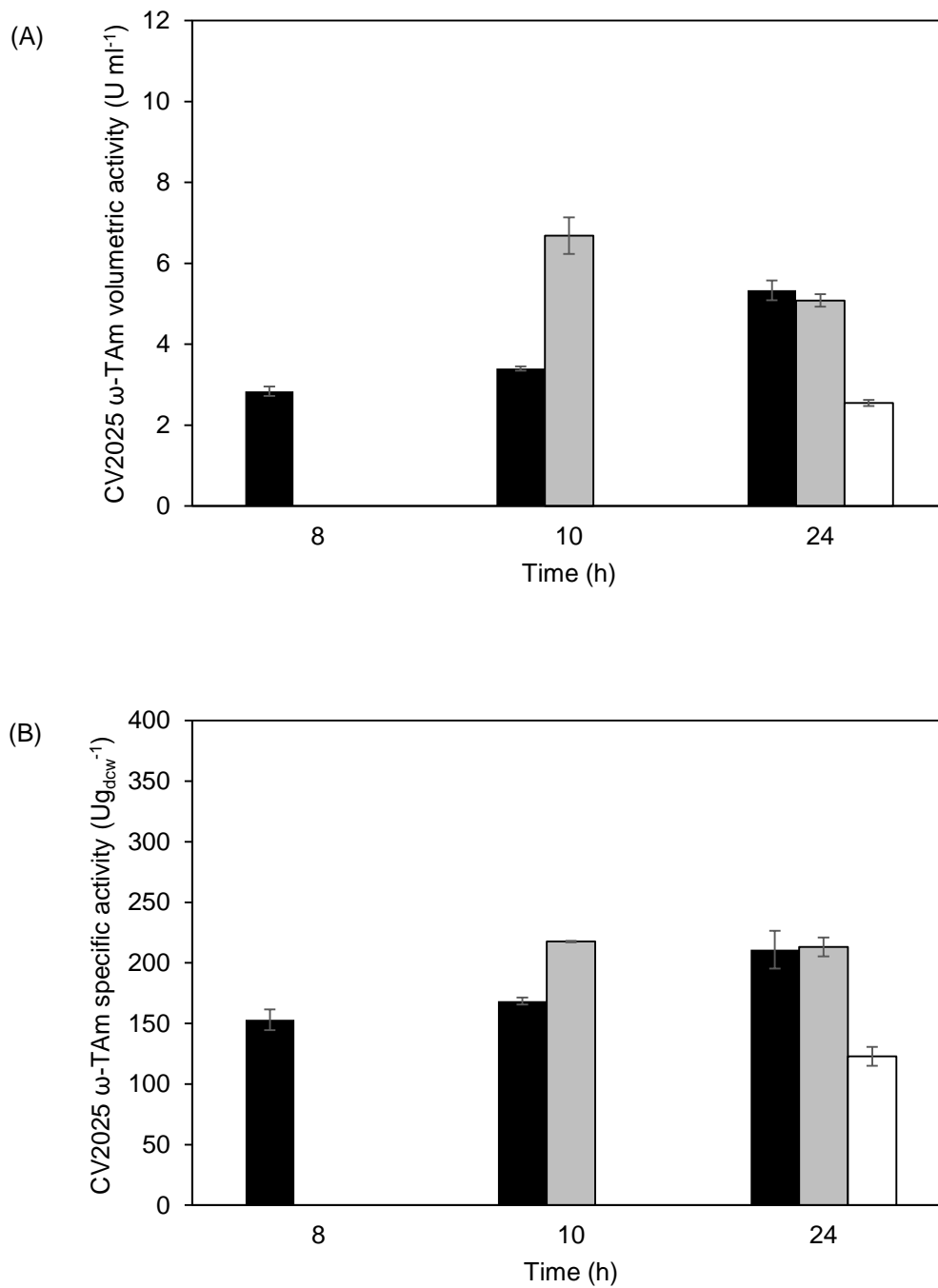
Figure 3.12. (A) Volumetric activity and (B) specific activity of CV2025 ω-TAm expressed from fermentations in a controlled MBR with (■) early, (▣) mid and (□) late exponential phase induction induced at 1.0 mM IPTG. Error bars denote one standard deviation from the mean (n=3). The CV2025 ω-TAm assay was performed as described in Section 2.12.5.

Induction of protein expression is generally ideal in the middle of the exponential phase of a cell growth where the cells still have high viability and nutrients are still abundant. The stationary phase is rarely deemed suitable for induction as the rate of the protein expression is largely dependent on the growth rate (Donovan *et al.*, 1996). The marked difference of the biocatalyst activity at different times of the exponential phase as seen in this work indicates the importance of selecting an appropriate induction time. Additionally, the biocatalyst activities obtained are even higher than reported in previous section (Figure 3.8) indicating the benefits of optimising the induction conditions.

The relationship between the maximum CV2025 ω-TAm specific activities and IPTG to biomass ratio attained in every induction condition was also studied. As shown in Figure 3.13, there was an increase in the maximum CV2025 ω-TAm specific activities as the ratio ranges between 8.8 and 23.7 µmol g_{dcw}^{-1} before it declined thereafter. The highest CV2025 ω-TAm specific activity, which was attained in the fermentation with an early induction, corresponded to IPTG to biomass ratio of 23.7 ± 0.5 µmol g_{dcw}^{-1}. The results demonstrated the reliance of the induction upon biomass hence suggesting the importance of the specific IPTG concentration on the recombinant protein expression.

Previously, Durany *et al.* (2004) reported the optimal values of the specific IPTG concentration for the production of fuculose-1-phosphate by *E. coli* to range between 33 and 70 µmol g_{dcw}^{-1}. Meanwhile, a study by Olaofe *et al.* (2010) found out that a ratio of 40 µmol IPTG per g_{dcw} enabled the attainment of a maximum amidase specific activity in *E. coli* cultivation. The variation of the specific IPTG concentration between different *E. coli* strains might be associated to the different levels of biomass achieved. In general, maintaining the optimal IPTG concentration to biomass ratio could be very useful particularly for production of recombinant protein at a higher scale or when using different fermentation strategies like a fed-batch operation where higher cell densities are attained.
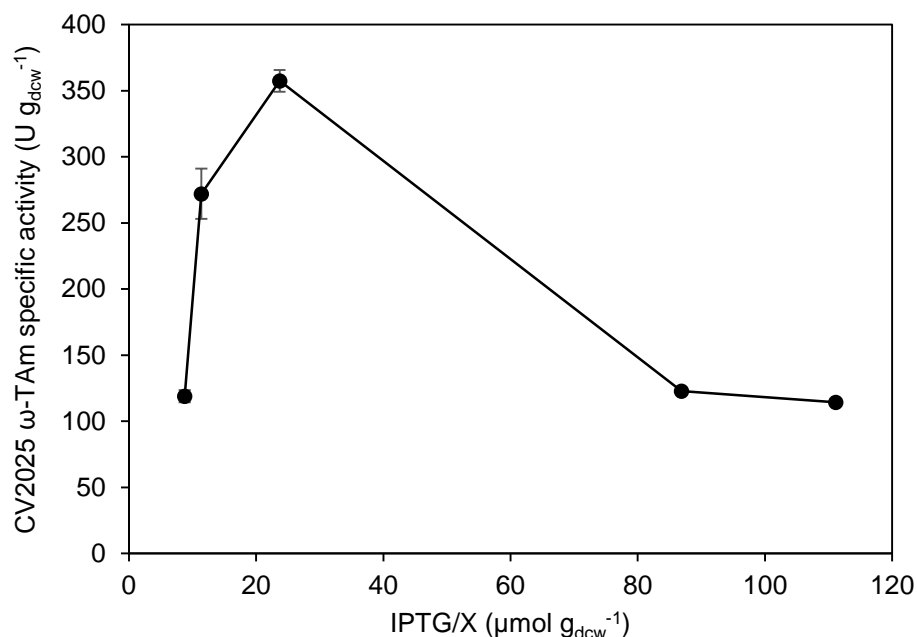
Figure 3.13. Relationship between maximum CV2025 ω-TAm specific activity and IPTG to biomass ratio. Experiments were performed as described in Figures 3.9, 3.10 and 3.11 and 3.12. Error bars denote one standard deviation from the mean (n=3).

3.3.3.2 Influence of DO level

Upon the establishment of the induction strategies for CV2025 ω-TAm production, subsequent work examined the influence of DO levels. Two levels of DO were evaluated, namely 30 and 50%. The fermentation performance was evaluated with regards to the growth kinetics and CV2025 ω-TAm activity. In all fermentations, similar pre-cultures were applied and the induction strategies were based on the optimal conditions (6 h and 0.1 mM IPTG) as specified in Section 3.3.3.1.

Table 3.2 summarizes the kinetics parameters obtained from fermentations performed at both DO values. The results showed that both cultivations yielded a comparable growth rate, maximum biomass concentration as well as product titre, suggesting that there was no apparent benefit of increasing the DO beyond 30%. It was initially hypothesized that increasing the oxygen supply might promote the development of a higher cell density but apparently, maintaining the DO above the limiting level seems to be adequate. Additionally, an excessive oxygen supply such as DO of 50% might not be favourable as it may result in toxicity to the cell. Junker (2004) revealed that the minimum DO value needed for an *E. coli* or yeast fermentation in reactor as 10% air saturation. From the results obtained here, it can be concluded that the DO of 30% was relevant for the *E. coli* BL21 (DE3) fermentation expressing CV2025 ω-TAm in Micro-24, where this process condition will be applied in the subsequent studies.

Table 3.2. Comparison of growth kinetics parameters and enzyme activity from fermentations performed at DO of 30 and 50%. Fermentations were performed as described in Section 2.8.2. Analytical procedures were carried out as specified in Section 2.12.2 (biomass concentration) and Section 2.12.6 (glycerol and acetate).

Parameters	Dissolved oxygen (%)	
	30	50
μ (h^{-1})	0.36 ± 0.01	0.36 ± 0.01
X_{max} (g$_{dcw}$ L^{-1})	12.4 ± 0.5	12.9 ± 0.4
$Y_{X/S}$ (g$_{dcw}$ g^{-1})	0.45 ± 0.03	0.42 ± 0.02
CV2025 ω-TAm specific activity (U g$_{dcw}$$^{-1}$)	370.0 ± 11.4	377.4 ± 8.4
CV2025 ω-TAm volumetric activity (U mL^{-1})	9.6 ± 0.3	9.8 ± 0.2

3.4 Summary

In this chapter, a HTP controlled MBR cultivation platform for microbial culture is demonstrated for the production of CV2025 ω-TAm by *E. coli* BL21 (DE3). Additionally, important strategies for enhancing the cell growth and production of CV2025 ω-TAm have been highlighted. Preliminary work on the evaluation of the fermentation medium for CV2025 ω-TAm production (Section 3.3.1) has showed that an enriched medium has significantly increased the maximum biomass concentration as well as the biocatalyst titre in comparison with the typically used LB-glycerol (Figures 3.1 and 3.2). Furthermore, the establishment of *E. coli* BL21 (DE3) cultivations expressing CV2025 ω-TAm in a controlled MBR has been demonstrated (Section 3.3.2). Good process monitoring and control was observed (Figure 3.3) and the well-to-well cultivation performance across the reactor was found to be reproducible (Figures 3.4 and 3.5). In addition, a significant enhancement of the cultivation performance was observed in a controlled MBR in comparison with the basic shake flask culture while representing a 31-fold volumetric reduction (Figure 3.6). Further comparison of the cultivation performance between defined and complex media in the controlled MBR has confirmed the superiority of the latter medium for optimal production of CV2025 ω-TAm (Figure 3.7).

The utility of the controlled MBR as an optimisation platform for CV2025 ω-TAm production was demonstrated by investigating several factors such as induction time, inducer concentration and DO level (Section 3.3.3). The results showed that an early induction (6 h), 0.1 mM IPTG and 0.024 mmol IPTG g$_{dcw}$$^{-1}$ yielded a maximal attainment of CV2025 ω-TAm expression in a batch culture (Figure 3.11). Evaluation of the DO level between 30 and 50 % oxygen saturation suggested little impact on fermentation performance and CV2025 ω-TAm titre obtained (Table 3.2).

Overall, the results confirm the suitability of the controlled MBR as a HTP platform for parallel studies of microbial fermentation and enzyme production in early stage of process development. As the controlled MBR is amenable to further intensifications such as automation and also integration of a liquid handling system, current limitations of the platform that are associated with the manual feeding and sampling may be solved. The optimal levels of CV2025 ω-TAm production obtained in this chapter provide a baseline for subsequent work where the exploitation of a renewable feedstock for biocatalyst production is examined. This will be discussed in the following chapter.

CHAPTER 4

EVALUATION OF SUGAR BEET VINASSE AS A BIOREFINERY FEEDSTOCK FOR BIOCATALYST PRODUCTION

4.1 Introduction

In the development of any bioprocess the expense of the feedstock is a major contributor to the overall cost (Stanbury *et al.*, 1999). As discussed in Section 1.6, there is growing interest in the exploitation of renewable feedstocks as media suitable for fermentation. Among the many potential renewable feedstocks for the production of value-added products are waste streams generated from biorefineries. Integration of the new process streams with the existing ones may potentially increase the overall profitability of biorefinery operation.

One potentially useful biorefinery waste stream is sugar beet vinasse. This is the stillage generated after the distillation process during bioethanol production (Section 1.6.1). In spite of the ecological hazards that vinasse poses, due to its high organic content, the stillage consists of several useful components particularly glycerol (Espana-Gamboa *et al.*, 2011). Glycerol can be exploited as a carbon source to support microbial growth and consequently the production of recombinant proteins (Section 1.3.1.1). The abundant on-site supply of vinasse will ensure sustainability of an integrated biorefinery process. As discussed in detail in Section 1.6.1, previous studies have reported the use of vinasse for production of an array of value-added products such as polyhydroxyalkanoates (Bhattacharyya *et al.*, 2012; Pramanik *et al.*, 2012) biohydrogen and volatile fatty acids (Sydney, 2013) xylitol (Salgado *et al.*, 2010). Nevertheless, there is an ongoing need to explore the feasibility of vinasse utilisation in specific applications. To date, there has been no report on exploitation of vinasse for *E. coli* fermentation in the literature.

In the context of an integrated sugar beet biorefinery, as discussed in Section 1.7, on-site production of enzyme used for the valorisation of sugar beet breakdown products would be beneficial. One of the industrially relevant biocatalysts being investigated in this regard is CV2025 ω-TAm (Section 1.2). For example, L-arabinose that can be derived from sugar beet pectin (Ward *et al.*, 2015) may serve as potential substrate for CV2025 ω-TAm yielding a spectrum of useful intermediates for various applications. Exploration of sugar beet vinasse as a potential feedstock for the production of CV2025 ω-TAm by *E. coli* BL21 (DE3) is therefore of interest. Fermentation process optimisation often requires a large number of experiments (Panda *et al.*, 2007). In this work the controlled MBR (Micro-24) methods established in Chapter 3 will be used to help evaluate CV2025 ω-TAm production from *E. coli* BL21 (DE3) cultured on vinasse with addition of various nutrients supplements.

4.2 Aim and objectives

Given the wider context of this project (Section 1.6) the aim of this chapter is to explore the feasibility of using sugar beet vinasse as a feedstock for the production of industrial biocatalysts. The work will utilise the HTP fermentation platform established in Chapter 3. The focus will again be on production of CV2025 ω-TAm by *E. coli* BL21 (DE3) with the previous growth and activity data obtained with a complex medium being used as a benchmark for comparison (Section 3.3.3). The specific objectives of this chapter are outlined below.

1. To characterise the composition of sugar beet vinasse with a view to its utilisation as a renewable fermentation feedstock.
2. To demonstrate the utility of vinasse as a feedstock for *E. coli* BL21 (DE3) growth and CV2025 ω-TAm production and to assess the stability and variability of vinasse from different batches on cell growth and biocatalyst titre.
3. To establish methods for the pre-treatment of vinasse, e.g. polyphenols removal, and to subsequently evaluate the impact of pre-treatment on fermentation performance.
4. To optimise CV2025 ω-TAm production from sugar beet vinasse, using the controlled MBR established in Chapter 3, by evaluating the influence of medium supplements on cell growth and biocatalyst titre.
5. To establish a fundamental understanding of *E. coli* BL21 (DE3) metabolism and nutrient uptake when grown in vinasse medium.

4.3 Results

4.3.1 Characterisation of sugar beet vinasse

Before using sugar beet vinasse for fermentations, it is of importance to evaluate its composition especially in recognising potential fermentable components. The significance is that identification of the key fermentable components will facilitate successive studies such as pre-treatment options, optimisation and metabolic understanding of vinasse utilisation.

Sugar beet vinasse, supplied from the AB Sugar biorefinery at Wissington, UK, was first characterised in terms of its physical properties and composition. It is a heterogenous mixture consisting of suspended solids, made up of mostly dead yeast cells, and a blackish liquid fraction. Figure 4.1 shows vinasse before and after the removal of the suspended solids by centrifugation. Unlike previous reports in the literature that focused more on environmental aspects (Espana-Gamboa *et al.*, 2011; Pramanik *et al.*, 2012), vinasse characterisation in this study focused on the composition of fermentable sugars and related compounds. Table 4.1 outlines the composition of vinasse obtained from two different batches.
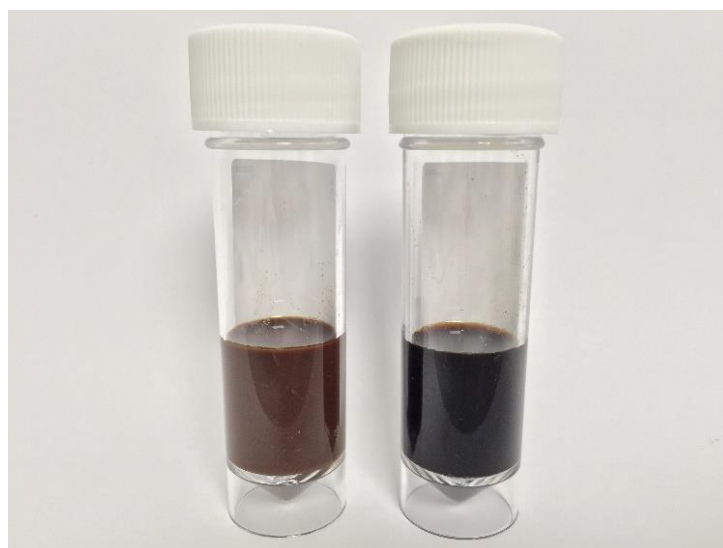
Figure 4.1. Raw vinasse before (left) and after (right) suspended solids separation. Suspended solids removal by centrifugation as described in Section 2.3.2.

Table 4.1. Characterisation of vinasse composition from two separate batches provided by AB Sugar (Wissington biorefinery, UK). The analytical procedures were performed as specified in Section 2.12.6 (glycerol and acetate) Section 2.12.7 (sugars and sugar alcohols), Section 2.12.3 (total protein) and Section 2.12.8 (polyphenols). Errors represent one standard deviation about the mean (n=3).

Parameters	Batch 1	Batch 2
pH	4.9	5.4
Glycerol (g L^{-1})	187.6 ± 2.8	183.6 ± 2.3
D-mannitol (g L^{-1})	8.0 ± 0.0	5.3 ± 0.1
D-galactose (g L^{-1})	5.5 ± 0.0	10.2 ± 0.1
D-xylitol (g L^{-1})	5.4 ± 0.1	6.5 ± 0.1
D-fructose (g L^{-1})	2.0 ± 0.0	2.1 ± 0.1
D-dulcitol (g L^{-1})	2.0 ± 0.0	1.5 ± 0.0
Acetate (g L^{-1})	1.7 ± 0.0	7.2 ± 0.1
Total Protein (g L^{-1})	5.1 ± 0.1	11.5 ± 0.2
Polyphenols (g$_{eq}$ L^{-1})	6.0 ± 0.0	7.1 ± 0.2

As shown in Table 4.1, sugar beet vinasse has an acidic pH in the range 4.9 and 5.4. This is in agreement with the values reported in the literature (Caqueret *et al.*, 2008; Parnaudeau *et al.*, 2008; Salgado *et al.*, 2010; Pramanik *et al.*, 2012; Ryznar-Luty *et al.*, 2015). The acidic pH of vinasse can be associated with organic acids that are probably formed during the yeast fermentation. As vinasse is formed from ethanol fermentation, its composition is closely influenced by the metabolism of the ethanol-producing microorganism. The concentration of glycerol in vinasse in this study was found to range from 184 to 188 g L^{-1}. A study by Lutoslawski *et al.* (2011) reported a much lower concentration of glycerol (3.33 g L^{-1}) in sugar beet vinasse obtained from Wloclawek, Poland. The resulting concentration of glycerol in vinasse is thought to be proportional to the initial concentration of molasses employed for the ethanol fermentation process. As detailed in Section 1.6.2, glycerol has been revealed as a potential carbon source for the production of fuels and chemicals as it is inexpensive, abundantly available and possesses a relatively high degree of reduction (Murarka *et al.*, 2008).

The analysis in Table 4.1 also shows that vinasse contains several sugars such as D-fructose and D-galactose. These sugars are believed to originate from D-raffinose, a trisaccharide composed of D-galactose, D-glucose and D-fructose, which is also found in the sugar beet (Haagenson *et al.*, 2008). There was no D-glucose and D-raffinose detected in vinasse in this study. Additionally, sugar alcohols including D-mannitol, D-xylitol and D-dulcitol were also identified with concentrations of less than 10 g L^{-1}. The presence of sugar alcohols as by-products of ethanol producing yeasts has been discussed in the literature (Spencer *et al.*, 1957; Onishi and Sizuki, 1968). The type of sugar alcohols and their amounts produced vary with different yeast strains (Peterson *et al.*, 1958).

Apart from potential fermentation carbon sources, vinasse also possesses cell growth inhibitors such as acetate and polyphenols (Table 4.1). The acetate concentration ranged from 1.7 to 7.2 g L^{-1}, which was is in agreement with Cibis *et al.* (2011). In contrast, the acetate concentration reported by Ryznar-Luty *et al.* (2008) was higher (12.1 g L^{-1}) than the results here. On the other hand, it was observed that sugar beet vinasse also comprised of polyphenols, ranged between 6.6 and 7.1 g L^{-1} (expressed as gallic acid). Previous works reported the concentration of polyphenols in vinasse in the range between 1.9 and 2.5 g L^{-1} (Salgado *et al.*, 2010) or in a much lower amount (< 1 g L^{-1}) (Martín Santos *et al.*, 2003; Bhattacharyya *et al.*, 2012).

Literature also indicates that the variation of the physico-chemical characteristics of vinasse can be attributed to the type of crop that it originated from, as well as variation in the ethanol fermentation and distillation processes (Espana Gamboa *et al.*, 2011). In general, the characterisation results obtained here suggest that vinasse has potential for use as a fermentation feedstock. This will be explored in the following section.

4.3.2 Preliminary studies on vinasse as a fermentation feedstock

Following the characterisation of sugar beet vinasse, an evaluation of the basic culture conditions needed for CV2025 ω-TAm production by *E. coli* BL21 (DE3) is necessary. These include assessments of suitable concentration of vinasse for fermentations, basic trends of recombinant protein expression in *E. coli* BL21 (DE3) when grown on vinasse as well as the stability of vinasse with regards to different batches. Assessment of these conditions will create an understanding on the basic culture requirements so as to facilitate further steps to improve the cultivation performance.

4.3.2.1 Influence of vinasse concentration and IPTG induction on *E. coli* BL21 (DE3) growth

Preliminary studies on the evaluation of vinasse as a fermentation medium for CV2025 ω-TAm production by *E. coli* BL21 (DE3) were carried out in batch shake flasks. The initial aim was to study the influence of vinasse concentration and IPTG induction on cell growth and CV2025 ω-TAm activity. Different concentrations of vinasse (17, 25, 50 and 100% (v/v)) were prepared using RO water as a diluent. The detailed pre-processing procedure is described as Option 1 in Figure 2.1 (Section 2.3.2). Figure 4.2 depicts the cell growth kinetics using vinasse and a complex fermentation medium (Section 2.3.1) as a control. It was observed that in both non-induced and IPTG-induced cases, the vinasse concentration of 50 and 100% (v/v) exerted an inhibitory effect on the *E. coli* BL21 (DE3) growth. The inhibitory effect might be possibly caused by polyphenols in vinasse. On the other hand, the influence of acetate on cell growth might not be pronounced since its concentration in vinasse from Batch 1, which is used in this preliminary study, is 1.7 g L^{-1}. This is much lower than the inhibitory level for *E. coli* that is about 5 g L^{-1} (Lee, 1996).

In fermentations using 17 and 25% (v/v) vinasse, comparable cell growth profiles were observed in both non-induced and induced cultures. The maximum biomass concentration obtained in non-induced cultures using 17 and 25% (v/v) vinasse was about 70 - 80% of that using the complex medium. For the induced cultures it was 60 - 63%. The good cell growth obtained in these cultures suggested a tolerance against the lower concentrations of polyphenols. Previous literature reports have suggested the feasibility of sugar cane / sugar beet vinasse as growth media for several microorganisms such as *Chlorella vulgaris* (Marques *et al.*, 2013), *Haloarcula marismortui* (Pramanik *et al.*, 2012), *Spirulina maxima* (Barrocal *et al.*, 2010) and *Debaryomyces hansenii* (Salgado *et al.*, 2010) but there has been no study reported for *E. coli* thus far.
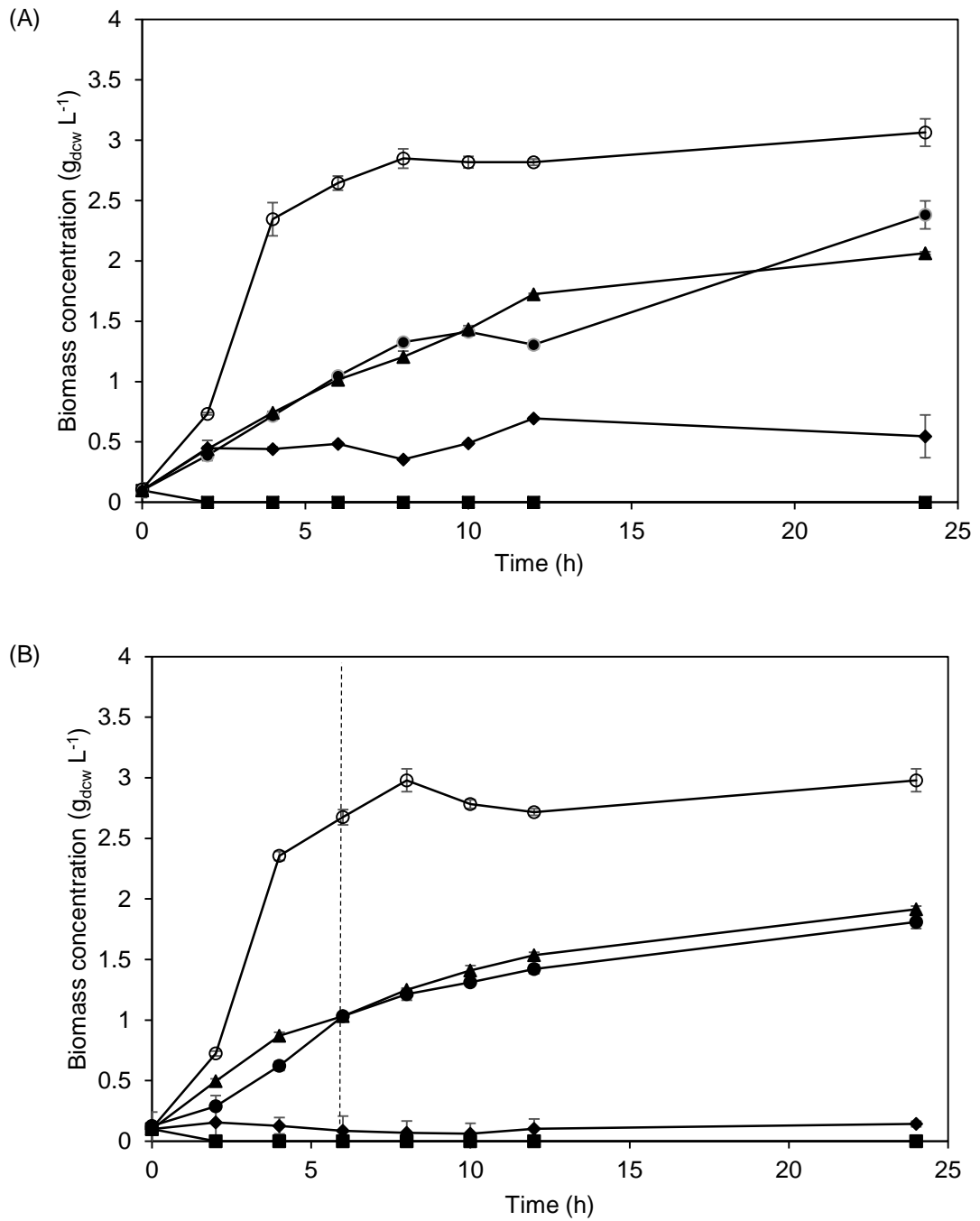
Figure 4.2. Comparison of batch fermentation kinetics of *E. coli* BL21 (DE3) cultured in shake flasks with (A) no IPTG induction, and (B) IPTG induction using complex and vinasse media: (○) complex medium; (▲) 17% (v/v) vinasse; (●) 25% (v/v) vinasse; (♦) 50% (v/v) vinasse; (■) 100% (v/v) vinasse. Vertical dotted line indicates the point of IPTG induction. Error bars denote one standard deviation about the mean (n=3). Fermentations were performed as described in Section 2.8.1. Biomass concentration was determined as described in Section 2.12.2.

The corresponding CV2025 ω-TAm titres from the fermentations using 17 and 25% (v/v) vinasse were also determined. Figure 4.3 shows the comparison of the CV2025 ω-TAm volumetric and specific activity obtained from the non-induced and IPTG-induced fermentations using vinasse and a standard complex medium. In induced cultures, the results showed that the maximum CV2025 ω-TAm volumetric and specific activity achieved at 24 h using both vinasse media were comparable (p-values of 0.24 and 0.66, respectively) and consistent with the similar levels of cell growth. The maximum specific activity attained in vinasse medium was about 70 - 72% of that in the complex medium.

Interestingly, it was also observed that there was CV2025 ω-TAm expression in non-induced fermentations employing both vinasse media. Comparable attainments of maximum CV2025 ω-TAm volumetric and specific activity in fermentations using 17 and 25% (v/v) vinasse were achieved with p-values of 0.12 and 0.69, respectively. The maximum CV2025 ω-TAm specific activities achieved in 17 and 25% (v/v) vinasse medium were 90 and 89 U g_{dcw} L^{-1}, respectively; this is 2.6-fold higher than that obtained in the non-induced complex medium fermentations and between 79 – 80% of the maximum value attained in the complex medium cultures with IPTG induction. This is an important finding since the cost of IPTG for enzyme induction would represent a significant contribution to the overall Cost of Goods at large scale.

The SDS-PAGE analysis of the soluble intracellular protein obtained from each fermentation, is shown in Figure 4.4. This confirms the expression of CV2025 ω-TAm in both non-induced and induced cultures employing vinasse medium. CV2025 ω-TAm expression in the non-induced cultures is most likely due to the presence of significant concentrations of D-galactose in vinasse (Table 4.1), which can act as an inducer of enzyme expression with *lac* promoter due to the similarity in structure to IPTG and lactose (Xu *et al.*, 2012). This phenomenon is termed auto-induction, that is the expression of a recombinant protein due to the presence of a natural inducer in the medium (Xu *et al.*, 2012). Elucidation of the role of D-galactose as an inducer will be discussed in detail in Section 4.3.2.2.
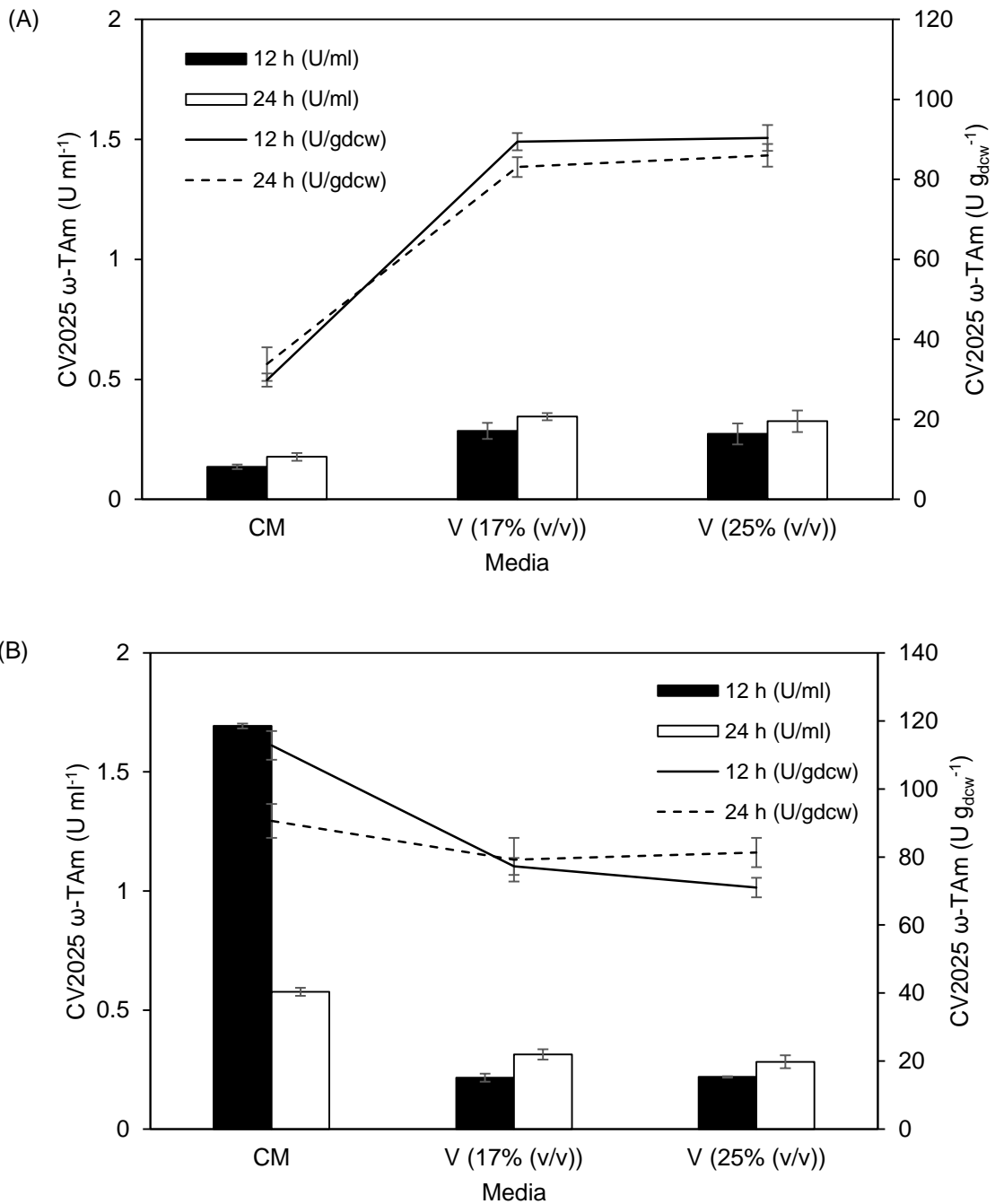
Figure 4.3. Volumetric and specific activity of CV2025 ω-TAm at 12 and 24 h from fermentations with (A) no IPTG induction, and (B) IPTG induction. Data shown for fermentations from Figure 4.2 using complex medium (CM), 17% (v/v) and 25% (v/v) vinasse (V). Error bars denote one standard deviation about the mean (n=3). The CV2025 ω-TAm assay was performed as described in Section 2.12.5.
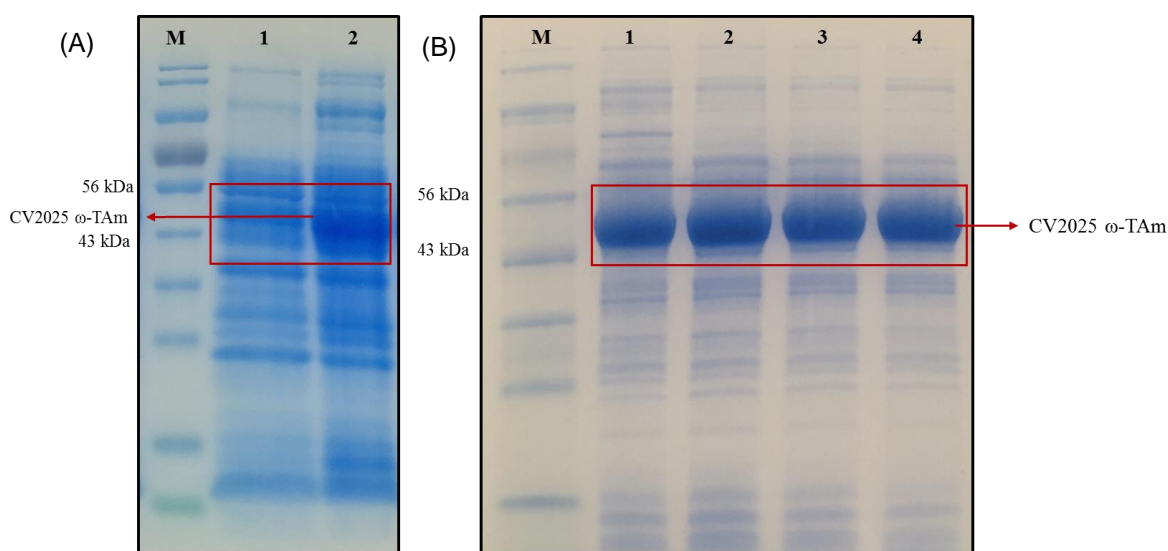
Figure 4.4. SDS-PAGE analysis of the soluble cellular extract obtained from *E. coli* BL21 (DE3) fermentations at 12 h (Figure 4.2) using (A) complex medium; lane 1: non-induced, lane 2: IPTG induced (B) vinasse medium; lane 1: 25% (v/v) vinasse, non-induced, lane 2: 17% (v/v) vinasse, non-induced, lane 3: 25% (v/v) vinasse, IPTG-induced, lane 4: 17% (v/v) vinasse, IPTG-induced. Fifteen microgram of protein were applied per lane. M represents marker. Molecular weight of CV2025 ω-TAm is 51 kDa (Rios-Solis, 2012). SDS-PAGE analysis was performed as described in Section 2.12.4.

4.3.2.2 Confirmation of auto-induction by D-galactose

To confirm that the auto-induction of CV2025 ω-TAm was due to the presence of D-galactose in the sugar beet vinasse, a separate experiment was carried out, incorporating addition of D-galactose to the standard complex medium. A D-galactose concentration of 5.1 mM, which is similar to that in 17% (v/v) vinasse, was added to the complex medium either at 0 or 6 h. Figure 4.5 shows the time course of cell growth and CV2025 ω-TAm expression from fermentations using a complex medium in the absence and presence of D-galactose. Whilst no noticeable variation was seen in cell growth, there was a significant difference in CV2025 ω-TAm expression between the fermentations. In cultures that were supplemented with D-galactose at 0 and 6 h, the CV2025 ω-TAm specific activity reached a maximum of 279 and 98 U g_{dcw}^{-1} respectively, whereas in the non-supplemented culture, the titre only represented the basal expression level from the *lac* operon.

The expression of CV2025 ω-TAm in the clarified lysates obtained from each fermentation in this study was confirmed by SDS-PAGE results as illustrated in Figure 4.6. Since the gel was loaded with similar total protein concentration, the CV2025 ω-TAm in the culture induced with D-galactose at 0 h (lane B) is expressed at a higher level than the host cell protein and hence is more pure and has higher specific activity. Overall, these results suggest that the D-galactose worked well in inducing the *lac* operon of *E. coli* BL21 (DE3) strain used in this study, yielding a considerable level of CV2025 ω-TAm expression overcoming the requirement for IPTG induction.
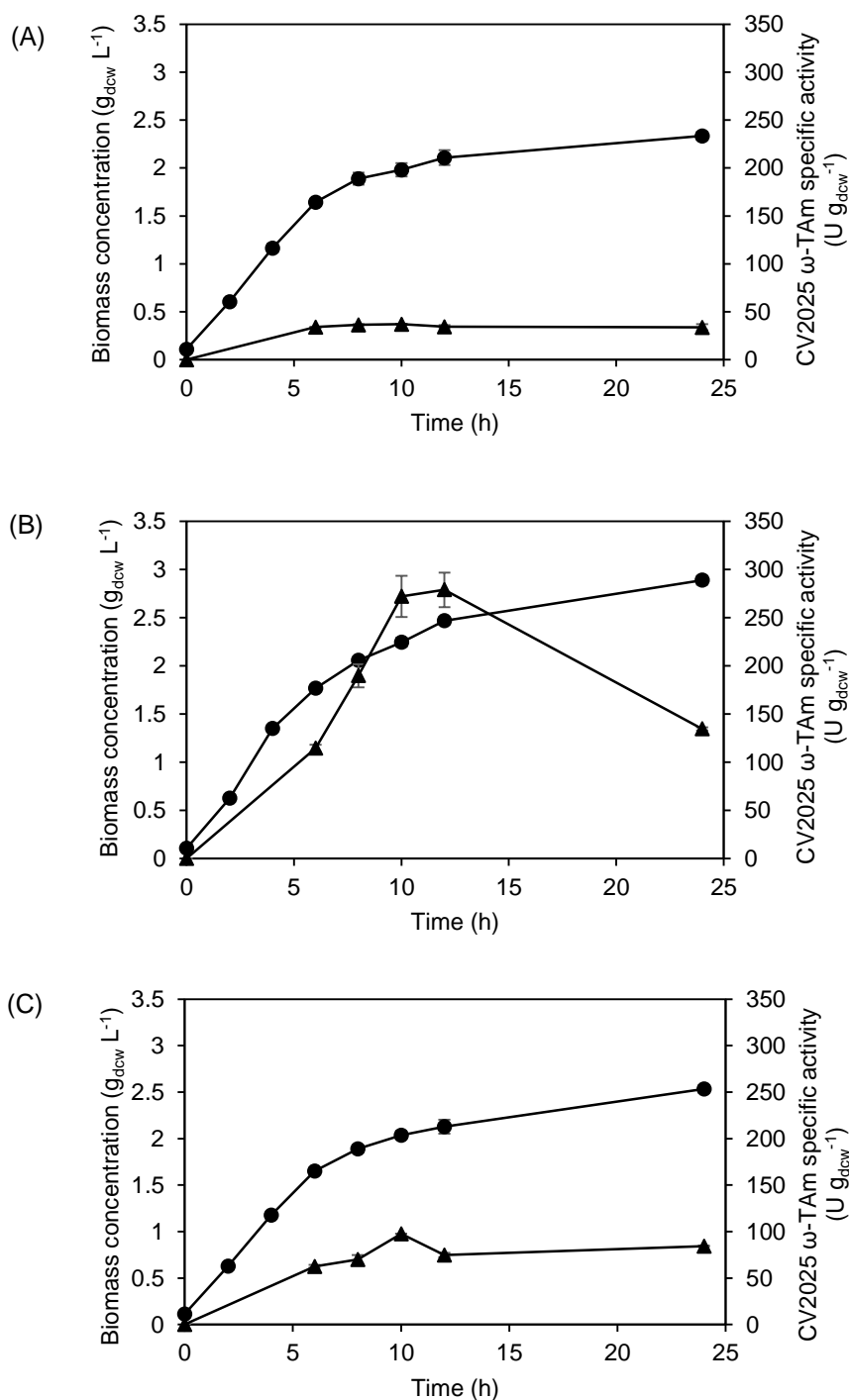
Figure 4.5. Comparison of batch *E. coli* BL21 (DE3) fermentation kinetics and CV2025 ω-TAm specific activity cultured on (A) complex medium (B) complex medium supplemented with 5.1 mM D-galactose at 0 h and (C) complex medium supplemented with 5.1 mM D-galactose at 6 h: (●) biomass concentration (▲) CV2025 ω-TAm specific activity. Error bars denote one standard deviation about the mean (n=3). Fermentations were performed as described in Section 2.8.1. The analytical procedures were performed as described in Section 2.12.2 (biomass concentration) and Section 2.12.5 (CV2025 ω-TAm assay).
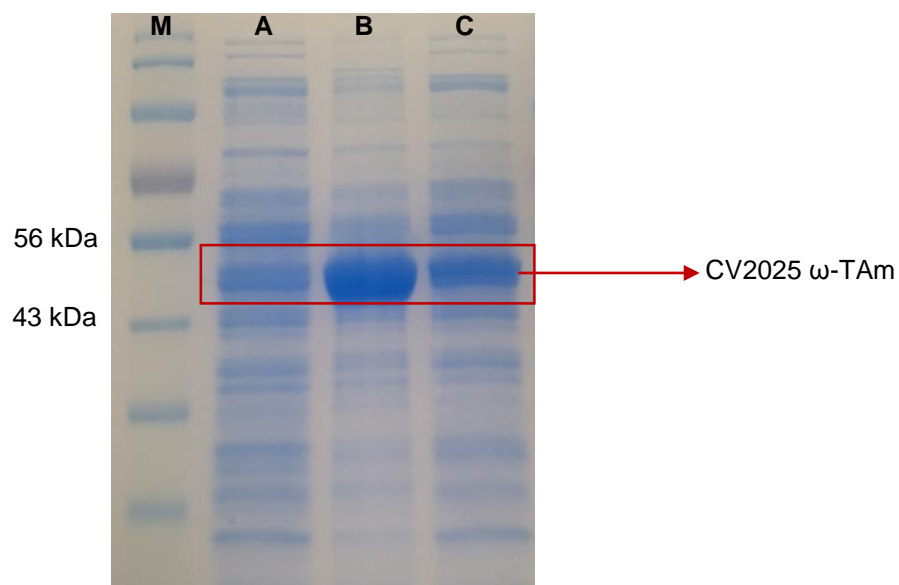
Figure 4.6. SDS-PAGE of the soluble cellular extract obtained from the cultivations of *E. coli* BL21 (DE3) expressing CV2025 ω-TAm at 12 h (Figure 4.5): (A) no D-galactose, (B) D-galactose supplemented at 0 h, (C) D-galactose supplemented at 6 h. Fifteen microgram of protein were applied per lane. M represents marker. SDS-PAGE analysis was performed as specified in Section 2.12.4.

Additionally, the difference in the CV2025 ω-TAm specific activity obtained from the D-galactose-induced cultures clearly indicated that the induction time is a significant factor for the biocatalyst production. In contrast to IPTG addition, that may retard cell growth upon induction, addition of D-galactose from the beginning of the fermentation did not retard the cell growth and appeared to be more beneficial than the induction during the logarithmic phase. The addition of D-galactose at 0 h mostly mimicked the vinasse medium, which originally had D-galactose at a comparable concentration. These results confirm that D-galactose in the vinasse medium can cause an auto-induction for recombinant protein production.

The occurrence of auto-induction by D-galactose has been discussed in several published works. Xu *et al.* (2012) reported auto-induction in the production of therapeutic proteins in *E. coli* BL21 (DE3) using both T7 and *tac* promoters, where the modified LB medium used comprised of soy peptone that had D-galactose added. They also observed that the minimum concentration of D-galactose that can trigger the induction of the *E. coli* promoter was 0.4 mM, which is below the levels used here in 17 and 25% (v/v) vinasse that were 5.1 and 7.6 mM, respectively. In another study, León *et al.* (2003) reported that 2.8 mM D-galactose was sufficient to cause an induction of the *lac* promoter in a recombinant *E. coli* for the production of the enzyme penicillin acylase. These results suggest that if D-galactose is to be used as an alternative to IPTG for induction then, an in-depth study on the D-galactose concentration for an optimal enzyme expression is necessary.

Auto-induction in fermentation processes employing sugar beet molasses as a feedstock was reported by Calik and Levent (2009) for the production of benzaldehyde lyase in *E. coli* BL21 (DE3). In contrast to sugar beet vinasse, sugar beet molasses is the non-crystallised syrup resulting after the extraction process during the sugar production (Finkenstadt, 2014). Calik and Levent (2009) inferred that the auto-induction of the *lac* promoter was linked to the presence of galactose, released from raffinose that is present in sugar beet molasses. The efficiency of the galactose-mediated induction is influenced by the type of strain used in the fermentation (De Leon *et al.*, 2003). The transport of galactose towards the *lac* operon was assumed to be facilitated by the inactivation of the galactose kinase gene (*galK*) in the mutant strain, which eventually enabled the induction of the recombinant protein (Wu and Kalckar, 1966; Wu, 1967).

An auto-induction of the *lac* promoter in *E. coli* BL21 (DE3) in vinasse medium, as found here, has not been described in the literature to date. It is expected that other types of waste residues or streams, especially those from sugar-based industries that contain D-galactose, might also exhibit an auto-induction phenomenon if utilised as fermentation media for a recombinant protein production. Although the advantages of this auto-induction may be significant for expression of a single heterologous protein, it might be more challenging in the case of multiple protein expression in a single host system as there may be a need to separately regulate protein expression from different plasmids. However, since IPTG is expensive, toxic and requires intensive studies on optimum induction conditions, elimination of its use in the fermentation may give another potential benefit of vinasse as a feedstock for enzyme production within an integrated sugar beet biorefinery.

4.3.2.3 Evaluation of batch to batch stability

The studies discussed so far were carried out using vinasse from Batch 1 whereas in later work, the vinasse used was from another batch (Batch 2). Thus, it was necessary to evaluate the reproducibility of CV2025 ω-TAm production between different batches even if their overall composition was similar (Table 4.1). Batch 2 contained similar concentrations of glycerol and polyphenols, by nearly twice as much galactose and 4.2-fold acetate. The preparation of the vinasse medium from each batch was described as Option 1 in Figure 2.1 (Section 2.3.2) and fermentations were performed in batch shake flasks using 17% (v/v) vinasse with no IPTG induction.

Figure 4.7 shows the time course of cell growth obtained from fermentations using vinasse medium prepared from both batches. Despite a small variation (<25%) in biomass concentration throughout the period of fermentation, the cell growth trends exhibited were seen to be similar. Moreover, a good agreement was found between the two cultivations in terms of the specific growth rate and maximum biomass concentration obtained: 0.19 and 0.19 h^{-1} and 2.3 and 2.2 g_{dcw} L^{-1}, respectively. Although there were some variations in vinasse composition, such as in D-

mannitol, D-galactose, acetate and total protein, between the two batches (Table 4.1), those components might not have a profound influence on the cell growth. The impact of the high concentration of acetate in Batch 2 was alleviated by the 6-fold dilution (17% (v/v) vinasse) that may reduce the concentration of acetate to below the inhibitory level for *E. coli* BL21 (DE3) growth.
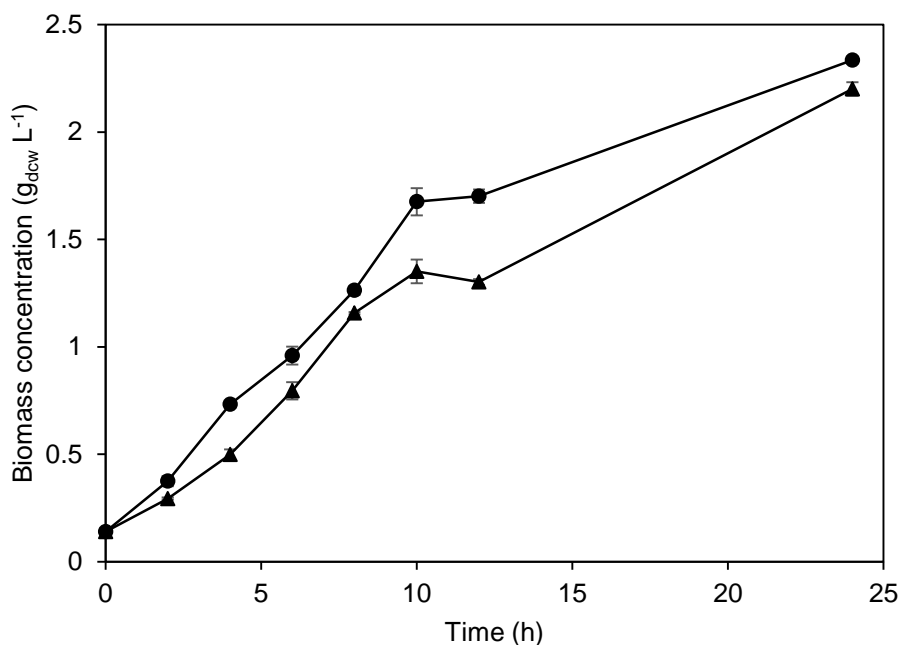
Figure 4.7. Comparison of batch *E. coli* BL21 (DE3) fermentation kinetics cultured on diluted vinasse medium prepared from (●) Batch 1 and (▲) Batch 2 (see Table 4.1 for compositions). Error bars denote one standard deviation about the mean (n=3). Fermentations were performed in shaken flasks as described in Section 2.8.1. Biomass concentration was determined as described in Section 2.12.2.

The corresponding production of CV2025 ω-TAm from the fermentations was also examined. The volumetric and specific activity of the enzyme in the two fermentations as a function of time is presented in Figure 4.8. In both cases, the CV2025 ω-TAm volumetric and specific activity reached a maximum of around 0.5-0.6 U ml^{-1} and 110 U g_{dcw}^{-1}, respectively between 12 and 24 h of cultivation. As with the cell growth profile, the maximum CV2025 ω-TAm volumetric and specific activity at 12 h showed insignificant statistical variations with p-values of 0.54 and 0.95, respectively between the two batches, suggesting the reproducibility of the feedstock with regards to the impact on cell growth and enzyme activity. The variation of D-galactose levels between the two batches seems not to be significant, suggesting that the concentration of D-galactose in the dilute vinasse from either batch is higher than the minimum concentration of D-galactose needed to cause an auto-induction. Overall, it is concluded that there was good reproducibility in cell growth and enzyme expression using the two batches of vinasse confirming the reliability of the results produced.
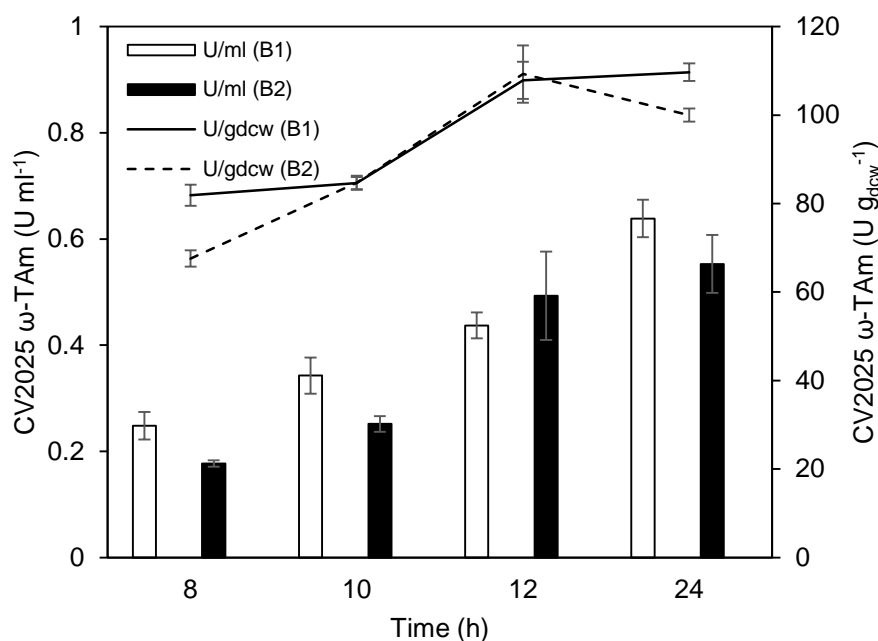
Figure 4.8. Comparison of CV2025 ω-TAm volumetric and specific activity obtained at different time points during the shake flask fermentations shown in Figure 4.7 using vinasse medium from Batch 1 (B1) and Batch 2 (B2). Error bars denote one standard deviation about the mean (n=3). The CV2025 ω-TAm assay was performed as described in Section 2.12.5.

4.3.3 Vinasse pre-treatment options

Along with the establishment of the basic culture conditions for CV2025 ω-TAm production in *E. coli* BL21 (DE3) as discussed above, development of an efficient pre-treatment strategy is also an important concern. An effective pre-treatment strategy will facilitate the exploitation of the useful components as well as elimination of inhibitory compounds in the feedstock, which in turn can support an optimal production of the target protein during the fermentation.

As shown in Figure 2.1, a number of options for pre-treatment of the sugar beet vinasse before fermentation utilisation could be considered (Section 2.3.2). Initially, two potential options were evaluated, illustrated as Option 1 and 2 (Figure 2.1). In both cases, only the liquid fraction was considered for the fermentation and the suspended solids were firstly removed in the early stage of the preparation. This was considered necessary due to the high level of minerals in those suspended solids that can result in the cessation of cell growth (Salgado *et al.*, 2010). In the subsequent step of Option 1, vinasse was diluted to the optimal concentration (17% (v/v)), as described in Section 4.3.2.1 and sterilisation of the medium was performed by microfiltration (Section 2.3.2).

In Option 2, the vinasse was pre-treated by AC adsorption (Pramanik *et al.*, 2012). This aimed to remove the polyphenolic compounds in vinasse that might be inhibitory to cell growth. The quantification of polyphenols was based on GA (Section 2.12.8). Initially, a growth inhibition

assessment was performed whereby the effect of vinasse on *E. coli* BL21 (DE3) growth on an agar plate was examined. Figure 4.9 shows the inhibition zone around a filter paper disc that had been soaked in vinasse. It was evident that cell growth was inhibited in the vicinity of the disc resulting in an inhibition zone toward the centre of the plate. As the vinasse concentration decreased towards the edge of the plate, the inhibition zone became less apparent and the cell growth was more visible.

These results are in line with those obtained in Section 4.3.2.1, confirming inhibition of *E. coli* BL21 (DE3) growth at high concentration of vinasse that might be caused by the presence of polyphenols that are known to inhibit cell growth (Pramanik *et al.*, 2012). Hence, in pre-treatment of vinasse via Option 2, AC adsorption for polyphenols removal was examined prior to fermentation. It is revealed that adsorption process using AC or other adsorbent materials serves as among the best options for the removal of polyphenolic compounds from natural feedstocks (Garcia-Araya *et al.*, 2003; Figaro *et al.*, 2006; Caqueret *et al.*, 2008). AC has previously been shown to exhibit excellent capacities for adsorbing organic matter such as polyphenolic compounds (Caqueret *et al.*, 2008).
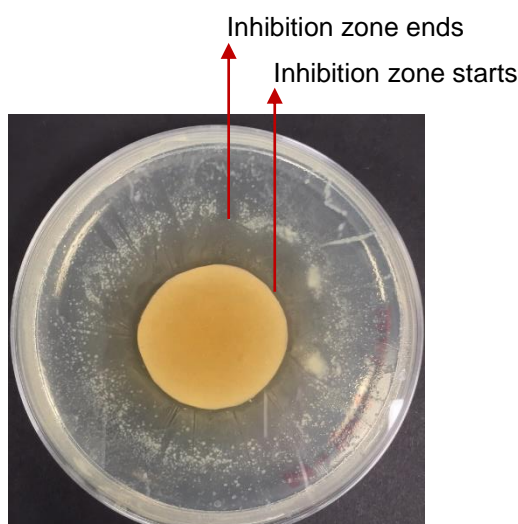
Figure 4.9. Inhibition zone on an *E. coli* BL21 (DE3) agar plate after 24 h of incubation. The agar plate was initially swabbed with an *E. coli* BL21 (DE3) culture before being incubated with a disc containing concentrated vinasse. Experiment was performed as described in Section 2.12.10.

4.3.3.1 Pre-treatment of vinasse by activated carbon (AC)

In this pre-treatment study, the influence of AC concentration and incubation time on polyphenols removal was investigated. Prior to pre-treatment, the pH of the vinasse was first adjusted to pH 2. An acidic pH is favourable for efficient adsorption (Caqueret *et al.*, 2008). This is because at acidic pH, protonation of AC acidic functional groups facilitates the adsorption of hydrophobic polyphenolic compounds (Qi *et al.*, 2004).

Figure 4.10 shows the change in polyphenols concentration in vinasse using different pre-treatment conditions. The profiles are also compared to a control case that has no AC added. The amount of polyphenols reduction was found to be proportional to the concentration of AC used. Pre-treatment of vinasse with 15 and 20% (w/v) AC led to a maximum removal of polyphenols of 85 - 89%, which is comparable with the findings by Pramanik and co-workers (2012). Overall, a rapid decrease of the polyphenols concentration was observed whereby the adsorption process reached a steady concentration after 1 h of incubation.
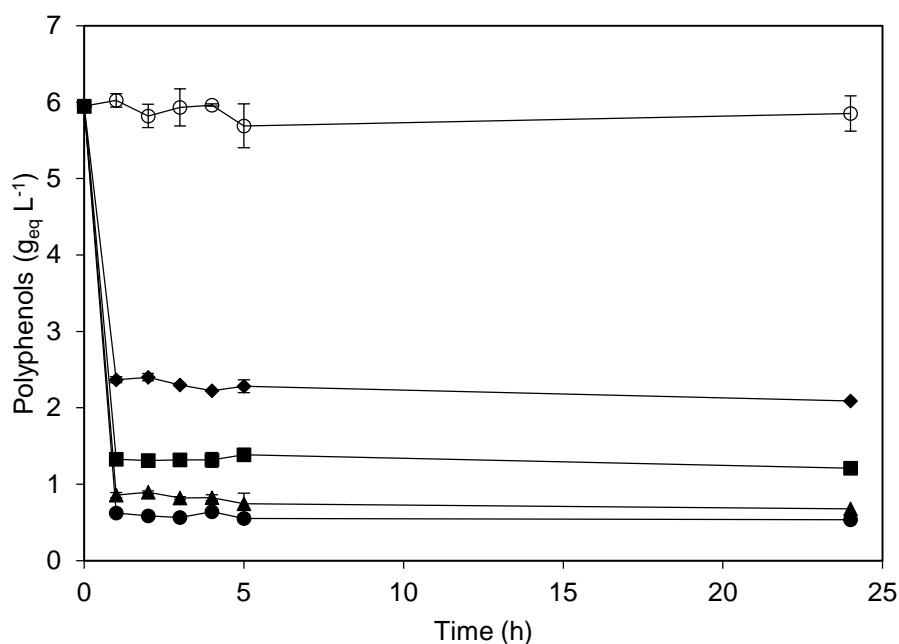
Figure 4.10. Kinetics of polyphenols removal in untreated (control) and AC pre-treated vinasse using different concentrations of AC: (♦) 5% (w/v); (■) 10% (w/v); (▲) 15% (w/v); (●) 20% (w/v) and (○) control. Error bars denote one standard deviation about the mean (n=3). AC pre-treatment of vinasse was performed as described in Section 2.10. The polyphenols concentration was determined as described in Section 2.12.8.

Figure 4.11 compares the physical appearance of the untreated and pre-treated vinasse using different AC concentrations. As clearly seen, decolourisation was achieved in the pre-treated vinasse. The intensity of the brown colour was proportional to the concentration of polyphenols remaining in the pre-treated vinasse. This clearly suggests that the brown colour of vinasse is associated with the presence of the polyphenolic compounds. Evaluation of the AC pre-treated vinasse as a fermentation medium will be discussed in the subsequent section.
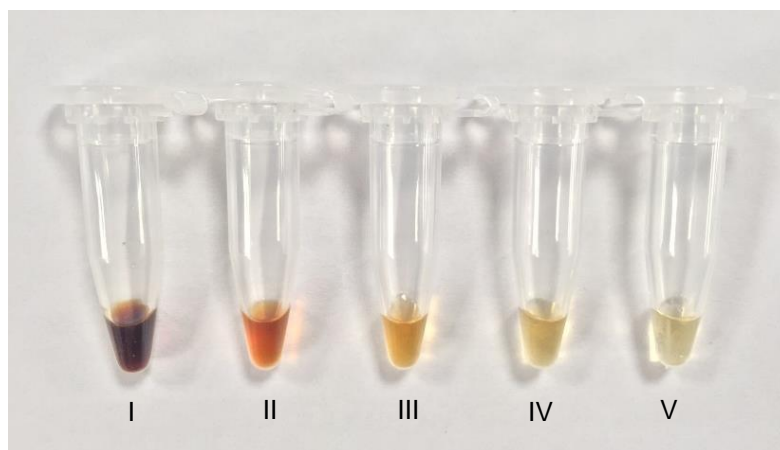
Figure 4.11. Appearance of the untreated and AC pre-treated vinasse from the experiments shown in Figure 4.10. I: untreated vinasse; II: pre-treated vinasse 5% AC (w/v); III: pre-treated vinasse 10% AC (w/v); IV: pre-treated vinasse 15% AC (w/v); V: pre-treated vinasse 20% AC (w/v). Samples taken and photographed after 24 h of incubation.

4.3.3.2 Impact of vinasse pre-treatment options on *E. coli* BL21 (DE3) fermentations

The impact of untreated and AC pre-treated vinasse on *E. coli* BL21 (DE3) fermentations and CV2025 ω-TAm production was next investigated. All of the AC pre-treated vinasse media were diluted with RO water to 17% (v/v); as found to be optimal in Section 4.3.2.1. The media were further prepared as described in Section 2.3.2. The pre-treated vinasse using 20% (w/v) AC was not included in this study since it exhibited a comparable level of residual polyphenols as that prepared using 15% (w/v) AC. All fermentations were carried out in batch shake flasks.

Figure 4.12 shows the time course of cell growth using the dilute untreated and pre-treated vinasse media. Generally, all profiles followed a similar trend with regards to cell growth whereby a stationary phase was reached after about 12 h of incubation. The specific growth rate observed in all fermentations using the pre-treated vinasse media ranged between 0.21 and 0.25 h^{-1}, which were higher than in the culture using untreated vinasse (0.17 h^{-1}). The maximum biomass concentrations obtained from cultures using both untreated and pre-treated vinasse were comparable and in the range 1.8 to 2.3 g_{dcw} L^{-1}, indicating that AC pre-treatment has limited further impact on cell growth after vinasse dilution.
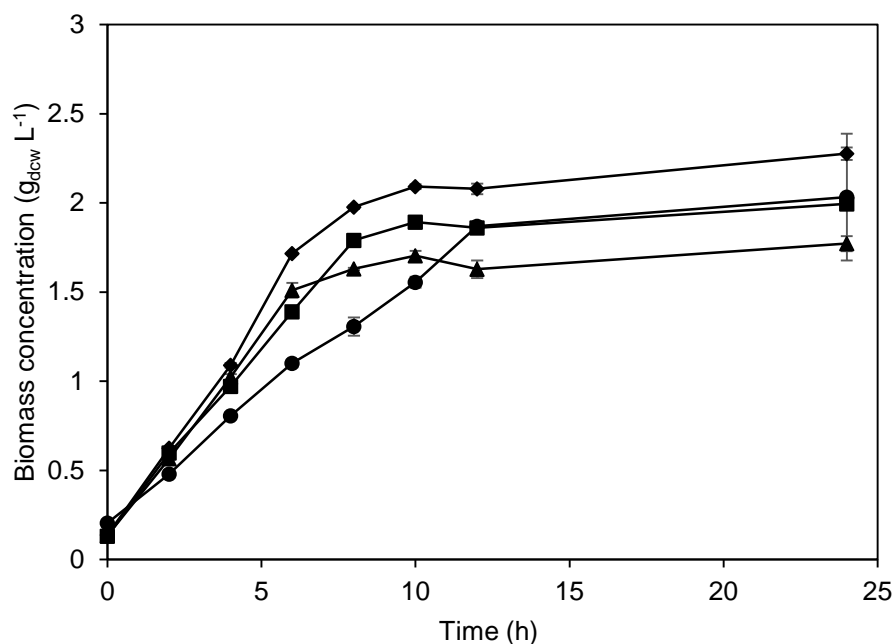
Figure 4.12. Comparison of batch fermentation kinetics of *E. coli* BL21 (DE3) cultured in shake flasks using diluted vinasse, untreated and pre-treated with different AC concentrations: (♦) 5% (w/v); (■)10% (w/v), (▲)15% (w/v) and (●) no AC. Error bars denote one standard deviation about the mean (n=3). Pre-treatment was performed as described in Section 2.10. Fermentations were performed as described in Section 2.8.1. Biomass concentration was determined as described in Section 2.12.2.

The corresponding CV2025 ω-TAm expression from fermentations employing the dilute untreated and pre-treated vinasse was also evaluated. Figure 4.13 depicts the CV2025 ω-TAm volumetric and specific activity attained in all cultures at 24 h. The results showed that both volumetric and specific activity of CV2025 ω-TAm attained in cultures employing pre-treated vinasse were found to be much lower than that achieved using the dilute untreated vinasse. Comparing this performance with the results obtained in Section 4.3.2.1, it can be strongly suggested that the polyphenols concentration in 17 and 25% (v/v) vinasse media, which was approximately 1.0 and 1.5 g_{eq} L^{-1}, respectively, did not impart significant inhibitory effect on both cell growth and biocatalyst production. It can be inferred here that the removal of polyphenols in vinasse may not necessarily be a prerequisite for an enhanced fermentation performance as long as the minimum inhibitory concentration of the compound on the cell growth is not exceeded. This finding suggests the pre-processing procedure of vinasse is likely to be less laborious and thus offers another advantage of its application along with other benefits. The preparation of vinasse medium for the subsequent works in this chapter will be based on the methodology outlined in Option 1 unless otherwise stated.
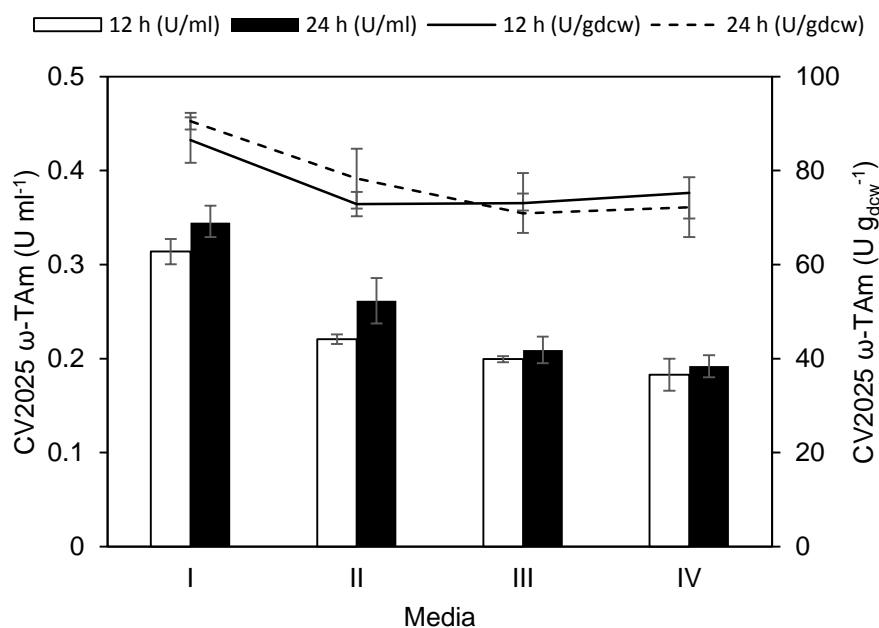
Figure 4.13. Volumetric and specific activity of CV2025 ω-TAm from *E. coli* BL21 (DE3) fermentations at 12 h and 24 h using dilute untreated vinasse (I) and dilute pre-treated vinasse with 5% (w/v) AC (II), 10% (w/v) AC (III) and 15% (w/v) AC (IV). Biomass growth as shown in Figure 4.12. Error bars denote one standard deviation about the mean (n=3). The CV2025 ω-TAm assay was performed as described in Section 2.12.5.

4.3.4 Optimisation of CV2025 ω-TAm expression using vinasse medium

Following the establishment of a suitable method for vinasse preparation (Section 4.3.3), subsequent work aimed to further enhance biocatalyst production using the vinasse medium. The use of the HTP controlled MBR established in Section 3.3.2 would be explored for this purpose. One of the major challenges noted thus far with vinasse was the low cell growth rate, which was about 1.9-fold lower than that achieved using a complex medium (Figure 4.2). Therefore, the influence of vinasse medium supplementation with trace elements (Section 2.3.1) and nitrogen-containing substrates namely yeast extract, NH_4Cl and $(NH_4)_2SO_4$ on cell growth and biocatalyst production was investigated. The rationale behind these medium supplementation experiment is to replace any nutrients in the vinasse that have either been used during yeast fermentation or degraded during distillation. Figure 4.14 shows the comparison of the batch *E. coli* BL21 (DE3) fermentation kinetics cultured on complex medium and various vinasse-based media and the growth kinetic parameters are outlined in Table 4.2. The corresponding maximum CV2025 ω-TAm volumetric and specific activity are shown in Figure 4.15.
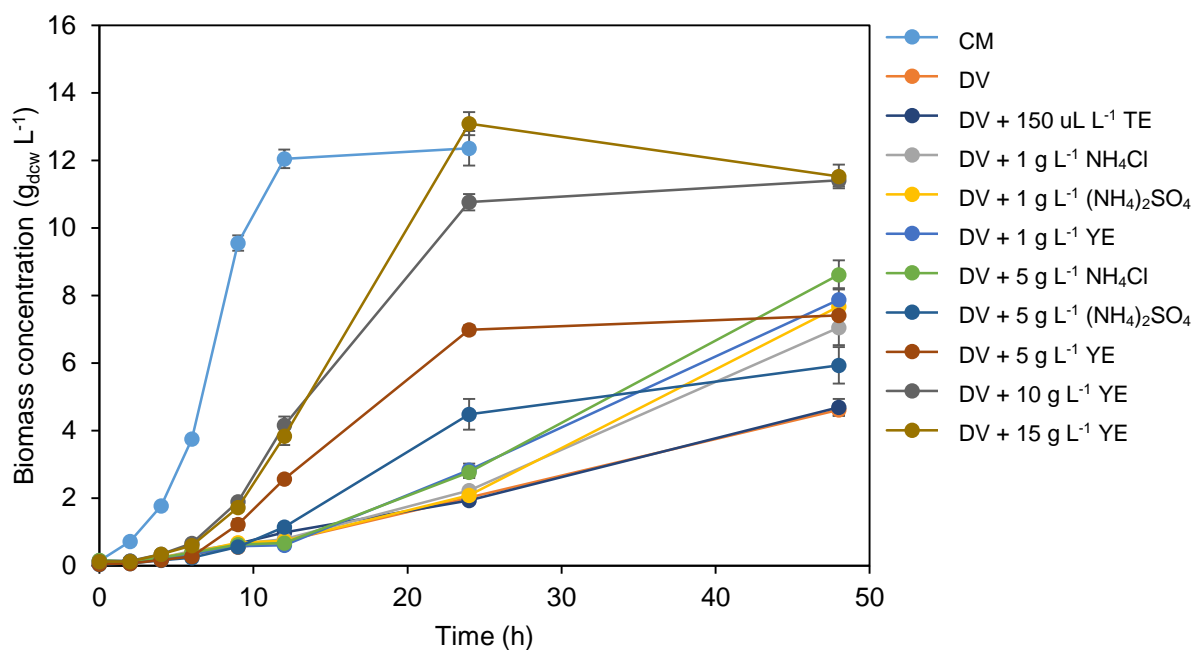
Figure 4.14. Comparison of batch *E. coli* BL21 (DE3) fermentation kinetics cultured on complex medium and various vinasse-based media. Error bars denote one standard deviation about the mean (n=3). Fermentations were performed in a controlled MBR as described in Section 2.8.2. Biomass determination was performed as described in Section 2.12.2. CM: complex medium; DV: dilute vinasse; TE: trace element; YE: yeast extract.

Table 4.2. Fermentation kinetic parameters for *E. coli* BL21 (DE3) grown on complex and various vinasse-based media. Biomass growth as shown in Figure 4.14. DV: dilute vinasse; TE: trace elements; YE: yeast extract.

Medium	Specific growth rate, μ (h^{-1})	Maximum biomass concentration, X_{max} (g_{dcw} L^{-1})
Complex medium	0.36 ± 0.01	11.5 ± 0.6
DV only	0.13 ± 0.00	4.5 ± 0.2
DV + 150 uL L^{-1} TE	0.12 ± 0.01	4.7 ± 0.3
DV + 1 g L^{-1} NH_4Cl	0.27 ± 0.01	6.8 ± 0.1
DV + 1 g L^{-1} $(NH_4)_2SO_4$	0.26 ± 0.02	7.7 ± 0.1
DV + 1 g L^{-1} YE	0.34 ± 0.02	6.1 ± 0.3
DV + 5 g L^{-1} NH_4Cl	0.22 ± 0.01	7.9 ± 0.1
DV + 5 g L^{-1} $(NH_4)_2SO_4$	0.23 ± 0.01	8.4 ± 0.2
DV + 5 g L^{-1} YE	0.35 ± 0.03	7.7 ± 0.5
DV + 10 g L^{-1} YE	0.36 ± 0.02	11.4 ± 0.2
DV + 15 g L^{-1} YE	0.38 ± 0.01	13.1 ± 0.3
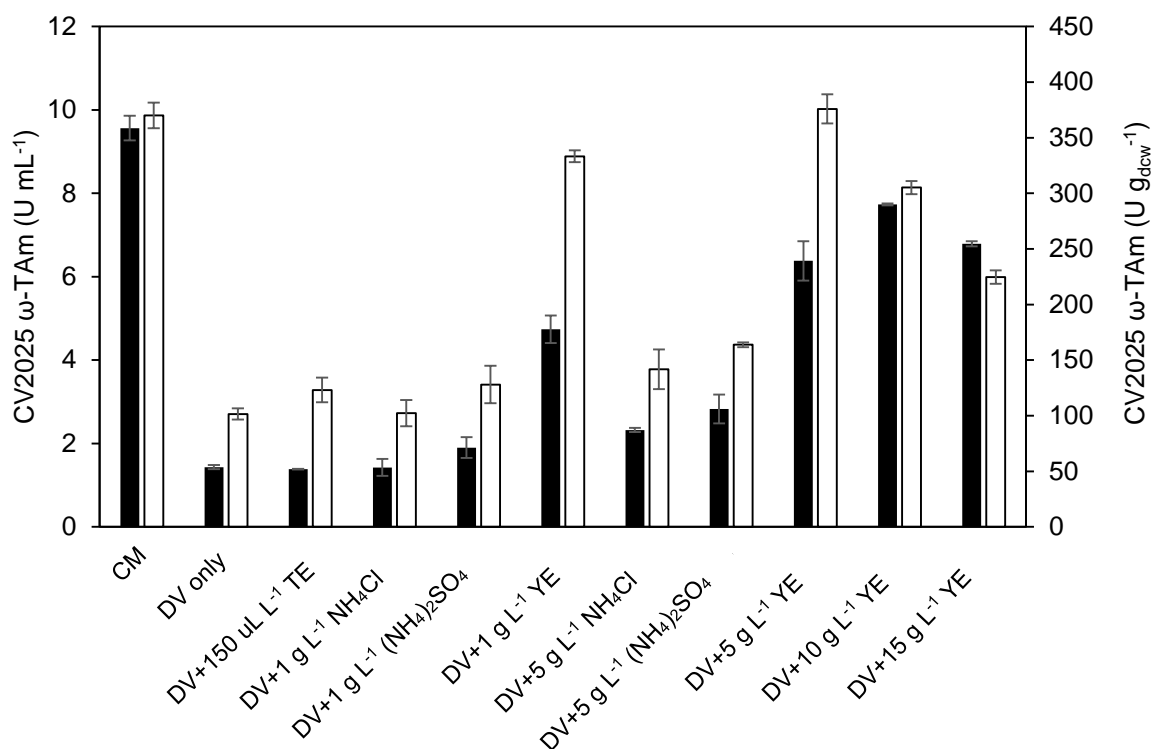
Figure 4.15. Maximum (■) volumetric and (□) specific activity of CV2025 ω-TAm from *E. coli* BL21 (DE3) fermentations using complex medium and various vinasse-based media. Biomass growth as shown in Figure 4.14. Error bars denote one standard deviation about the mean (n=3). The CV2025 ω-TAm assay was performed as described in Section 2.12.5. CM: complex medium; DV: dilute vinasse; TE: trace elements; YE: yeast extract.

Initial assessment of the effect of trace elements on biocatalyst production showed that there was no significant effect of cell growth rate or the maximum biomass concentration. The negligible impact could be because trace elements might not be at limiting concentration for *E. coli* BL21 (DE3) growth. Even if they had been partly utilised in the bioethanol fermentation any remaining nutrients would have been concentrated during the distillation step. Whilst an increase in CV2025 ω-TAm specific activity by 21% was observed in the supplemented cultures, the volumetric activity was comparable to that in the base vinasse medium.

Evaluation of nitrogen source addition to the vinasse, in the concentration range of 1 - 5 g L^{-1} had a more notable impact. The maximum biomass concentration and specific growth rate were found to increase by 1.4 - 1.9-fold and 1.7 - 2.7-fold, respectively (Table 4.2). In particular, it was observed that the addition of yeast extract increased CV2025 ω-TAm production in comparison with the other nitrogenous substrates evaluated in this study. For example, addition of 1 g L^{-1} of $(NH_4)_2SO_4$ to the dilute vinasse promoted a 1.4-fold increase in CV2025 ω-TAm volumetric activity whereas in the fermentation supplemented with 1 g L^{-1} of yeast extract, the titre increased 3.4-fold. Supplementation of vinasse with yeast extract at 5 g L^{-1} showed the greatest improvement in maximum biomass concentration and CV2025 ω-TAm specific activity by 1.7 and 3.7-fold, respectively compared to the non-supplemented culture. The presence of transcription enhancers

such as cyclic adenosine monophosphate (cAMP) in the yeast extract (Donovan *et al*, 1996; Grossman *et al*., 1998) may also facilitate recombinant protein expression as has been discussed widely in the literature (Liu *et al*., 1999; Fu *et al*., 2006; Nair *et al*., 2009; Jia *et al*., 2011).

The study on the yeast extract supplementation was subsequently extended by investigating the effect of higher concentration from 10 to 15 g L^{-1}. It was found that the maximum biomass concentration increased proportionately with the increasing concentration of yeast extract. In terms of the cell growth rate, the cultures supplemented with 10 to 15 g L^{-1} yeast extract yielded an enhancement of about 2.8 to 2.9 times higher than the non-supplemented culture. This was again expected since yeast extract also contains other growth factors and vitamins (Zhang *et al*., 2003; Krause *et al*., 2010).

Increasing the yeast extract concentration up to 10 g L^{-1} had a positive effect on the CV2025 ω-TAm production. With regards to enzyme titre (U ml^{-1}), the culture supplemented with 10 g L^{-1} yeast extract was found to achieve the highest CV2025 ω-TAm activity being approximately 5.4-fold greater than the non-supplemented culture. Moreover, the titre obtained in this optimal vinasse medium represented 81% of that attained using the complex medium. As this medium formulation gave a suitable compromise between availability and cost, it will be used in the scale-up studies described later in Chapter 5.

Within the context of the sugar beet biorefinery (Section 1.7) it is noted that commercial yeast extract is typically manufactured from *S. cerevisae,* which is the same strain used for bioethanol production. There is thus the potential to integrate lysis of the yeast recovered post fermentation, into the existing biorefinery. The on-site production of yeast extract, from another waste stream, to supplement the vinasse medium could remove the need to purchase yeast extract from other commercial sources. The idea of incorporating an autolysis process between the ethanol fermentation and distillation process was discussed by Moon *et al*. (2013) whereby they reported the feasibility of the vinasse produced from autolysed yeast to enhance the production of lactic acid by 27%. Another potential route of producing yeast extract is by exploiting the used yeast cells directly after the ethanol fermentation. Chae *et al*. (2001) reported the utilisation of brewer's yeast cells for the production of yeast extract by an enzymatic hydrolysis. In either case, the on-site production of yeast extract may eliminate the dependence on external sources and may help minimise the overall cost of production.

4.3.5 Understanding *E. coli* BL21 (DE3) metabolism in vinasse medium

Having shown the utility of vinasse as a fermentation medium it is of fundamental interest to understand *E. coli* BL21 (DE3) metabolism when grown on vinasse and more specifically the utilisation of the different fermentable carbon sources present. As discussed in Section 4.3.1, besides glycerol as the main component, vinasse also consists of several sugars and sugar alcohols. To enable consideration of carbon source utilisation the kinetics of different substrate

consumption were determined for a fermentation using diluted vinasse supplemented with 10 g L^{-1} yeast extract. Figure 4.16 shows the time course of cell growth and substrates consumption throughout the fermentation.

As indicated in Figure 4.16, the initial phase of cell growth was accompanied by a decrease in D-mannitol concentration. It was also observed that during this initial phase of D-mannitol consumption, the concentration of all the other sugars and sugar alcohols remained largely unchanged. A decrease of glycerol concentration was then observed which only began once the D-mannitol had been fully depleted. This occurred in what appears to be the mid exponential phase of cell growth. Additionally, it was seen that the reduction of glycerol was also followed by a simultaneous drop in D-xylitol and D-dulcitol concentrations as well as acetate. Acetate was found to be generated particularly during the period of D-mannitol metabolism where a concentration of up to 6 g L^{-1} was produced during exponential growth. Nonetheless, the capability of the *E. coli* BL21 (DE3) strain to co-utilise the acetate along with glycerol, D-xylitol and D-dulcitol appears to eliminate the inhibitory effect of acetate on cell growth. Throughout the fermentation the concentrations of D-fructose and D-maltitol remained constant indicating that they were not utilised during the *E. coli* BL21 (DE3) growth in the vinasse medium.
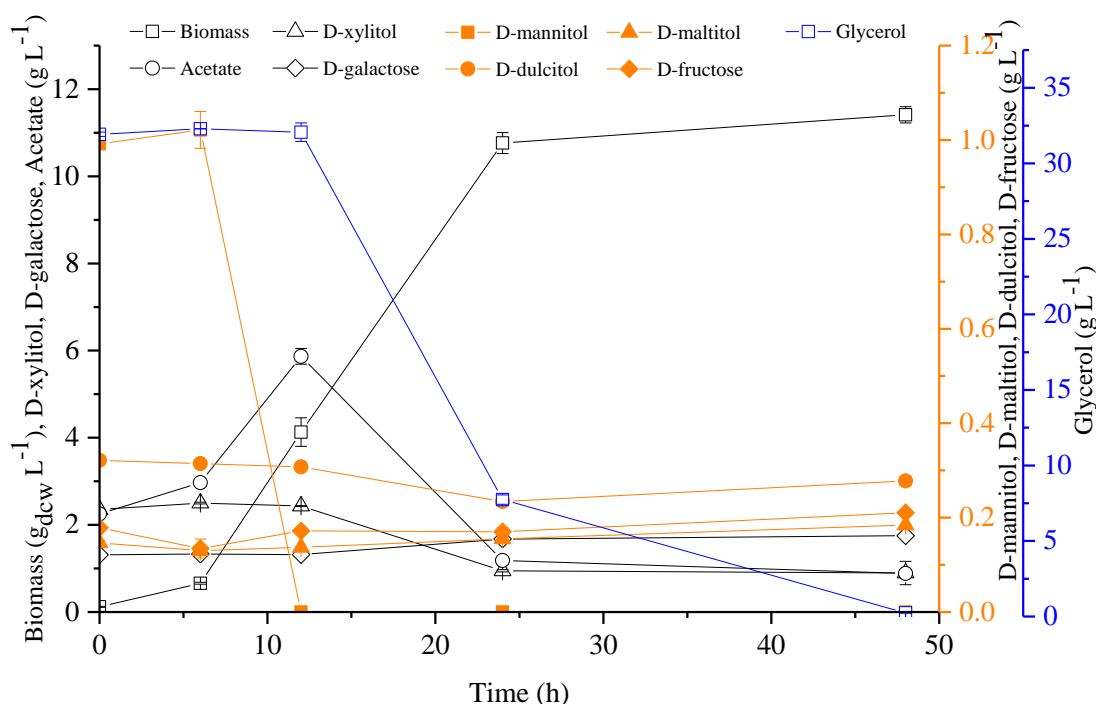
Figure 4.16. Carbon source utilisation, cell growth and acetate formation during batch fermentation of *E. coli* BL21 (DE3) cultured on dilute vinasse medium supplemented with 10 g L^{-1} yeast extract. Error bars denote one standard deviation about the mean (n=3). Fermentations were performed in the controlled MBR as described in Section 2.8.2. The analytical procedures were carried out as described in Section 2.12.2 (biomass), Section 2.12.6 (glycerol and acetate) and Section 2.12.7 (sugars and sugar alcohols).

The above results suggest that D-mannitol was the favoured carbon and energy source during the initial stage of *E. coli* BL21 (DE3) growth in the vinasse medium followed by glycerol. This may be attributed to the phenomenon of carbon catabolite repression (CCR), a mechanism that represses the secretion of enzymes responsible for the metabolism of the secondary substrate when the preferred carbon and energy source is present (Gorke and Stulke, 2008). CCR serves as an important regulatory mechanism for the microorganism to thrive in a natural environment that comprises many complex nutrients (Aidelberg *et al.*, 2014). Among examples of CCR phenomena in *E. coli* include a repression of lactose metabolism in the presence of glucose (Monod, 1942) and a consumption of arabinose over xylose (Kang *et al.*, 1998; Desai and Rao, 2010). On the other hand, D-mannitol was also reported to exert strong catabolite repression on the glucitol and galactitol operons (Lengeler and Lin, 1972). To date, the occurrence of CCR between D-mannitol and glycerol has not been reported in the literature.

As discussed previously in the characterisation study (Section 4.3.1), there was no D-glucose detected in the vinasse. Glucose is known as the preferred substrate for many microorganisms including *E. coli* (Gorke and Stulke, 2008). The phenomenon of diauxic growth in *E. coli* BL21 (DE3) between glucose, as the primary substrate and other sugars such as sorbitol, rhamnose, xylose, arabinose and galactose (Monod, 1942) and glycerol (Martínez-Gómez *et al.*, 2012) has previously been reported. To further elucidate the principles of *E. coli* BL21 (DE3) metabolism when grown on vinasse medium and D-glucose, cultures were carried out in the presence of added D-glucose. In this experiment, D-glucose was added to the vinasse medium at a concentration of 3 g L^{-1}. A low concentration of D-glucose was chosen here to facilitate its rapid consumption during the fermentation.

Figure 4.17 illustrates the time course of cell growth and carbon source consumption in the fermentation using the vinasse medium supplemented with 3 g L^{-1} D-glucose. It was observed that D-glucose was metabolised first with a rapid decrease in its concentration between 4 and 12 h; this corresponded to a reciprocal increase in biomass concentration from 0.09 to 1.58 g L^{-1}. The consumption of D-mannitol up to 12 h was minimal with only about 26% being used. Subsequently, a significant utilisation of D-mannitol was observed between 12 and 24 h when the D-glucose concentration became limiting. This suggests that although D-glucose and D-mannitol were found to be utilised simultaneously, *E. coli* BL21 (DE3) metabolism appeared to favour D-glucose over D-mannitol. In an early report by Lengeler and Lin (1972) on D-mannitol metabolism in *E. coli*, it is revealed that when the wild-type *E. coli* cells were grown in the presence of D-glucose and D-mannitol, the metabolic pathway of the latter is not hampered by the presence of the former. In this experiment, the switch to a third carbon source after D-mannitol consumption was not observed since cell growth was retarded due to the accumulation of acetate that reached nearly 10 g L^{-1} after 24 h of incubation. As a consequence, the maximum biomass concentration only reached 2.2 g L^{-1} compared to 11.4 g L^{-1} when cultured on the basic, yeast extract supplemented vinasse medium (Figure 4.16). This significant increase in acetate, not seen in the base-case vinasse fermentation (Section 4.3.4) was believed to be caused by D-glucose metabolism, which generates approximately 4.6 moles of acetate per mole of D-glucose

consumed (Figure 4.17). Moreover, in base-case vinasse fermentation (Figure 4.16), the acetate was co-utilised during the glycerol consumption, resulting in the decrease of its concentration to about 1 g L^{-1} after 48 h of incubation. The key finding obtained in this supplementary study is that, between D-glucose and D-mannitol, the former remains the favoured carbon source by *E. coli* BL21 (DE3). Moreover, the absence of D-glucose in vinasse has given an advantage in the exploitation of glycerol, which constitutes as the main carbon source of the feedstock.
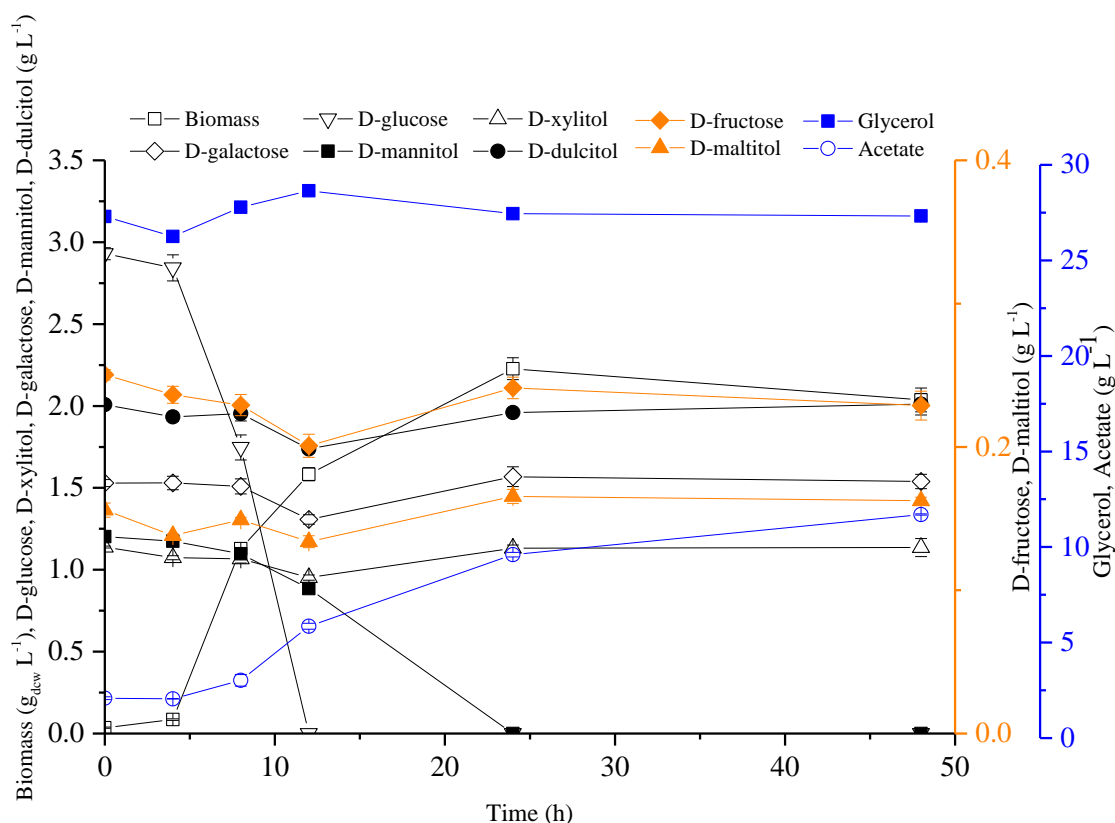
Figure 4.17. Carbon source utilisation, cell growth and acetate formation during batch fermentation of *E. coli* BL21 (DE3) cultured on dilute vinasse medium supplemented with 10 g L^{-1} yeast extract and 3 g L^{-1} D-glucose. Error bars denote one standard deviation about the mean (n=3). Fermentations were performed in the controlled MBR as described in Section 2.8.2. The analytical procedures were carried out as described in Section 2.12.2 (biomass), Section 2.12.6 (glycerol and acetate) and Section 2.12.7 (sugars and sugar alcohols).

Overall, the hierarchy of the carbon source utilisation by *E. coli* BL21 (DE3) when cultured in the yeast extract supplemented vinasse medium is proposed to be:

D-mannitol > Glycerol > D-xylitol, D-dulcitol

An understanding of this hierarchy is important since industrial production of CV2025 ω-TAm within an integrated biorefinery would most likely occur by fed-batch fermentation. In developing a fed-batch process this preferential utilisation must be taken into account. In this case, glycerol

might serve as the best feeding option since it appears to be the limiting substrate for cell growth (after D-mannitol) and is, itself a relatively cheap by-product of the biofuel industry (Li *et al.*, 2013).

4.4 Summary

This chapter has demonstrated the successful exploitation of sugar beet vinasse as a biorefinery feedstock for industrial biocatalyst production. The initial work on the characterisation of vinasse showed that the feedstock contains several potential components suitable for *E. coli* BL21 (DE3) fermentation such as glycerol, sugars and sugar alcohols (Table 4.1). Preliminary studies in batch shake flask cultures showed the feasibility of this feedstock at concentrations in the range of 17 - 25 % (v/v) for *E. coli* BL21 (DE3) growth and expression CV2025 ω-TAm (Section 4.3.2). It has also been demonstrated that vinasse can be utilised with minimal pre-treatment (Section 4.3.3). Simple dilution with water by a factor of 6 results in a reduction in the concentration of glycerol to fermentable levels as well as a reduction in polyphenols concentration to below inhibitory levels (Section 4.3.3.2). Removal of the residual polyphenols concentration by AC adsorption to levels below 1 g L^{-1} did not lead to any remarkable improvements in *E. coli* BL21 (DE3) growth (Figure 4.12) and expression CV2025 ω-TAm (Figure 4.13). Moreover, evaluation of batch to batch variation of vinasse indicated little change in composition or concentration of key nutrients (Table 4.1) and hence comparable fermentation performance in terms of cell growth and CV2025 ω-TAm titre (Figures 4.7 and 4.8).

Interestingly, the vinasse medium demonstrated an auto-induction phenomenon whereby the CV2025 ω-TAm titre in non-induced cultures was found to be comparable with that obtained in standard IPTG-induced cultures (Figures 4.3 and 4.4). Auto-induction was associated with the presence of D-galactose in the vinasse that previous literature has shown to be a weak inducer of the *lac* operon (Xu *et al.*, 2012). In a biorefinery context, this eliminates the need for IPTG induction, which can be expensive at large scale.

Further optimisation of the fermentation performance in the controlled MBR showed that, by supplementing the dilute vinasse medium with 10 g L^{-1} yeast extract, an enhancement of 2.8 and 2.5-fold was achieved in terms of the specific growth rate and maximum biomass concentration, respectively (Figure 4.14 and Table 4.2). Moreover, the CV2025 ω-TAm volumetric and specific activity showed increases of 5.4 and 3 times, respectively compared to the non-supplemented culture (Figure 4.15). Finally, the metabolic preference of *E. coli* BL21 (DE3) in the presence of the various carbon sources in vinasse was also elucidated showing that D-mannitol and glycerol were the favoured sources (Figure 4.16).

In the following chapter, scale-up of CV2025 ω-TAm production from MBR to a larger scale (7.5 L) STR will be addressed.

CHAPTER 5

SCALE TRANSLATION BETWEEN MINIATURE AND LABORATORY SCALE BIOREACTORS

"Scale-up strategies tend to be 'mixed bags' engendering art, empiricism, conventional wisdom and (frequently) wishful thinking." – Marvin Charles

5.1 Introduction

In the previous chapters the controlled MBR was established as a platform for rapid fermentation process development and biocatalyst production. Its application was shown for a standard complex medium (Section 3.3.3) and for a vinasse medium within the context of a sugar beet biorefinery (Section 4.3.4). For both cases it is necessary to evaluate the reproducibility of the processes developed at a larger scale. This will validate the utility of the controlled MBR as a small scale optimisation platform. Various strategies for scaling up fermentations were described previously in Section 1.5.1 that may be potentially employed depending on the details of specific cultures and reactors.

Based on the few early studies involving the scalability of fermentations from Micro-24 to conventional STR scale (Section 1.4.2), there is still lack of definition around the engineering basis employed. For example, Isett *et al.* (2007) reported a direct comparison between the Micro-24 and a 20 L reactor for *S. cerevisae* and *E. coli* cultures based on offline metabolite and cell growth profiles. However, no engineering scale-up basis was highlighted in either cultivation. Likewise, the application of Micro-24 as a scale-down model for CHO cell culture has also been reported by Chen and co-workers (2009), nevertheless, there is limited description about the scale-up strategy used. In another work, the feasibility of the Micro-24-derived models for cultivating *P. pastoris* in a 7 L STR has been demonstrated (Holmes *et al.*, 2009). Whilst good scalability of the model was achieved in the latter platform, little is known on the basis of the scale-up. In contrast, the feasibility of using matched mixing time as a scale-up basis for CHO cell culture between the Micro-24 and a 1.5 L STR has been reported by Betts (2014). This is probably the only work that provides a clearly defined engineering basis for scale-up of Micro-24 cultures although its application is limited to mammalian cell cultures where oxygen transfer is not rate limiting.

An engineering basis for scale-up of aerobic fermentations, such as *E. coli* cultures, between controlled MBRs and laboratory scale STRs remains to be established and validated. One of the most effective approaches for scaling up aerobic fermentations in general, is based on matched k_La values (Section 1.5.1.1). The use of this approach has been reported widely for conventional MWPs (Islam *et al.*, 2008; Baboo *et al.*, 2012; Marques *et al.*, 2012). The advantage of using k_La as a basis for scale-up of aerobic cultures is that it directly links the oxygen transfer performance of the specific culture conditions with the uptake rate of a growth-limiting nutrient i.e. oxygen. The

ability to monitor and control DO in the Micro-24 provides an additional refinement over conventional MWPs.

5.2 Aim and objectives

The aim of this chapter is therefore to establish k_La as an engineering basis for scale-up of *E. coli* BL21 (DE3) growth and enzyme production between the controlled MBR and a conventional 7.5 L STR. Based on work in the previous chapters the approach will be validated for production of CV2025 ω-TAm in *E. coli* BL21 (DE3). The general applicability of the approach will be established by scaling up optimal culture conditions established for both the complex (Section 3.3.3) and vinasse media (Section 4.3.4). In fermentations using a complex medium, optimal induction conditions (Section 3.3.3.1) will also be reproduced. The specific objectives of this chapter are outlined below.

1. To quantify k_La values in the controlled MBR and 7.5 L STR as a function of operating conditions and to establish suitable engineering correlations.
2. To demonstrate the use of matched k_La values as a scale-up strategy for *E. coli* BL21 (DE3) fermentations for CV2025 ω-TAm production between MBR and 7.5 L STR scales.
3. To develop an effective pre-processing procedure for vinasse preparation for larger scale fermentations.
4. To demonstrate the scalability of *E. coli* BL21 (DE3) fermentation for CV2025 ω-TAm production between the controlled MBR and 7.5 L STR based on matched k_La values using complex and vinasse media.
5. To intensify the CV2025 ω-TAm production in the 7.5 L STR at higher k_La values using complex and vinasse media.

5.3 Results

5.3.1 Quantification of k_La values in the controlled MBR and a 7.5 L STR

Prior to any scale-up studies, it is necessary to quantify the scaling parameter and characterise its variation as a function of bioreactor operating conditions. The rationale is that such studies will provide an understanding on the fundamental behaviours of the scaling parameter with respect to bioreactor operation. This in turn will ease decision making in the scale-up work through the identification of a matched condition between two platforms, such as similar k_La, as well as development of mathematical models that can be used to predict how the scaling parameter varies under different operating conditions at the two scales.

In this work, the k_La was first characterised in both the controlled MBR and a STR using three types of media: water, complex medium and vinasse medium. The dynamic gassing-out method was used in all experimental runs (Section 2.11). Unless otherwise stated, all of the process parameters during the k_La characterisation studies were standardised as in fermentations (Section 2.8.2 and 2.8.3) in order to mimic the culture environment. The probe response times for the controlled MBR (fluorescence-based optical sensor) and 7.5 L STR (standard polarographic oxygen electrode probe) were determined as 16.3 and 13 s, respectively (Section 2.11). Whenever necessary, the influence of the probe response time was incorporated in the k_La determination by applying Equation 2.2 (Section 2.11.1).

Figure 5.1 illustrates typical DO profiles obtained during the deoxygenation and oxygenation stages in the controlled MBR and 7.5 L STR, respectively. In both reactors the DO is seen to fall to zero during nitrogen sparging and then increases rapidly upon the switch to sparging with air. In the case of the controlled MBR the variation in DO as a function of low (36 h^{-1}), medium (47 h^{-1}) and high (77 h^{-1}) k_La values is shown in Figure A4.1. As expected the rate of DO increases with increasing k_La values with DO ultimately reaching the 100% level in all three cases. This data confirms the sensitivity of k_La quantification in the MBR using the fluorescence-based optical sensors.
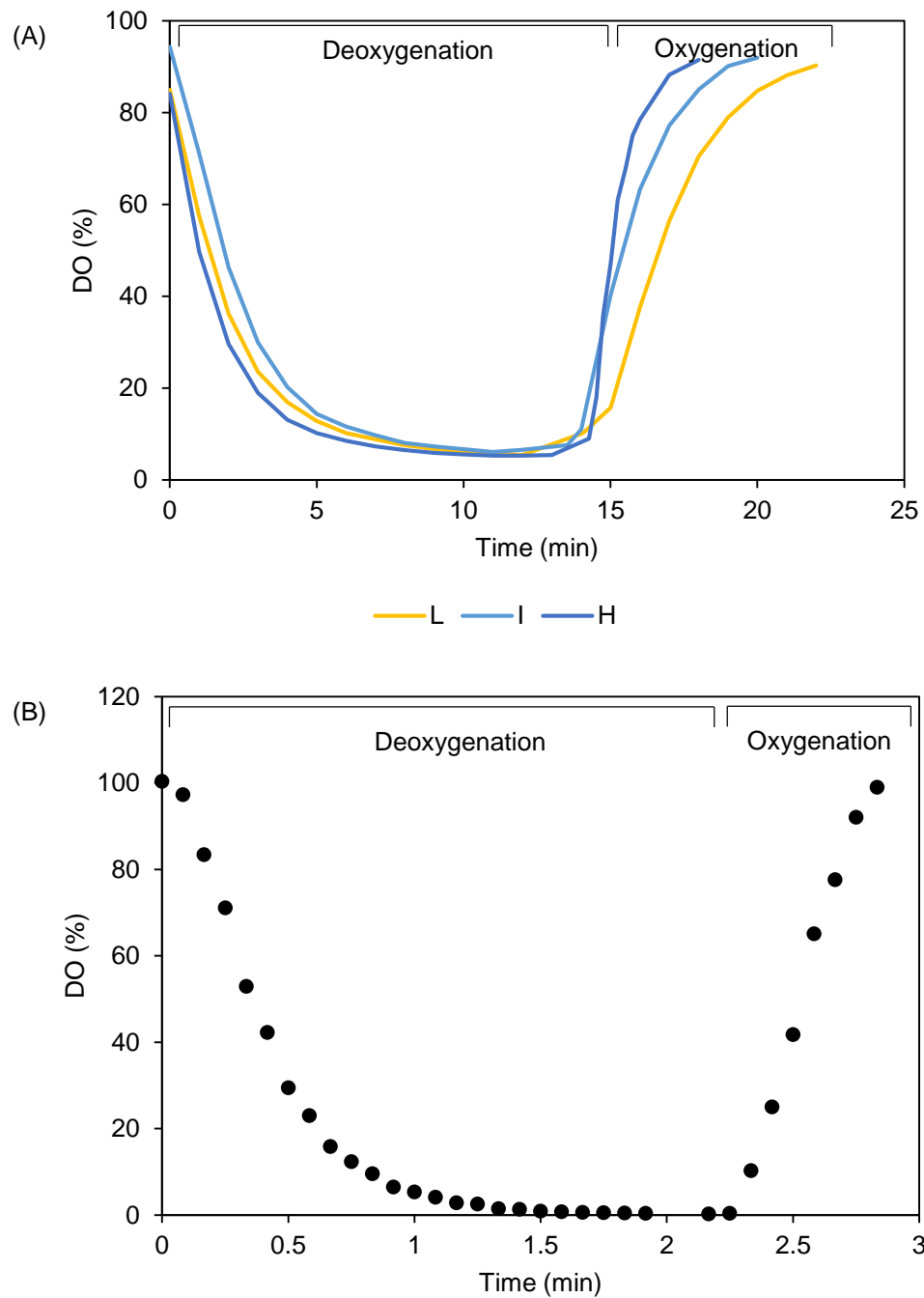
Figure 5.1. Typical examples of DO profiles during deoxygenation and oxygenation stages of k_La measurement in the (A) controlled MBR at different k_La designated as low (L), intermediate (I) and high (H) values and (B) 7.5 L STR. Experiments were performed as described in Section 2.11.1 (controlled MBR) and Section 2.11.2 (7.5 L STR).

5.3.1.1 Variation of k_La values in the controlled MBR

Figure 5.2 shows the profiles of k_La in the controlled MBR using water, complex and vinasse media at different shaking frequencies and aeration rates. Overall, the k_La values obtained in water, which ranged from 33 - 143 h^{-1}, were much higher than in the other two media. This is expected since water has a much lower viscosity than the other two fluids as shown in Appendix 3 (Figure A3.1) and oxygen transfer is known to be inversely proportional to viscosity.

Comparing the k_La values obtained between the complex and vinasse media, generally, higher profiles were attained in the former case with maximum k_La of 77 h^{-1} in contrast to 67 h^{-1} in the latter case. The addition of antifoam to both media may also impact the OTR by increasing bubble coalescence that consequently reduces the specific surface area and thus lowers the k_La (Al-Masry, 1999). Figure 5.2 also shows that increasing the shaking frequency and aeration rate leads to an increase in the k_La values with a greater dependency on the former. The increase in the shaking frequency results an increase in the displaced liquid height in the well, which in turn enhances the gas liquid interfacial area, a and hence k_La (Betts *et al.*, 2014).
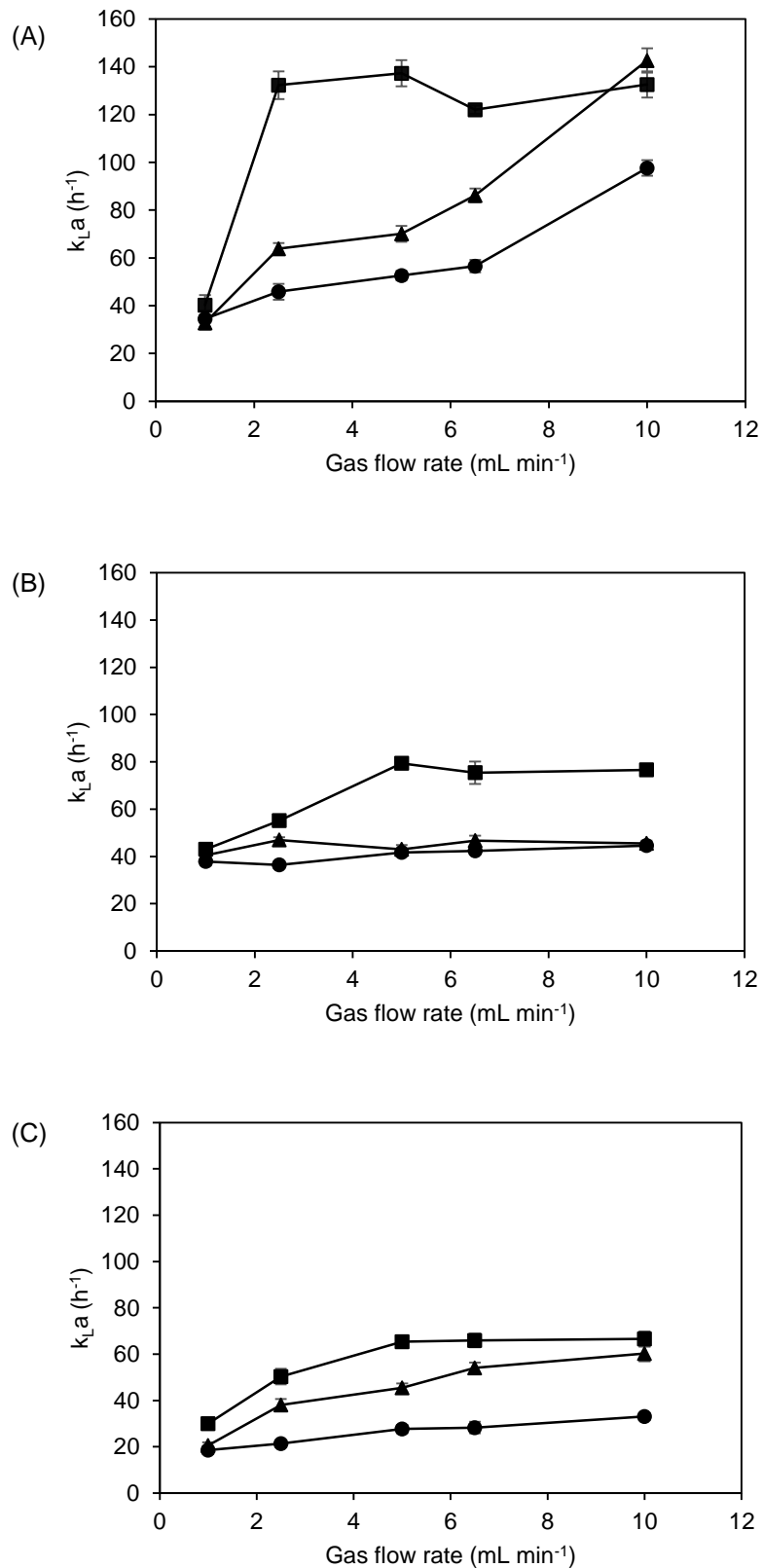
Figure 5.2. k_La variation in the controlled MBR at different shaking frequencies and aeration rates using (A) water (B) complex medium with 1 mL L^{-1} PPG and (C) vinasse medium with 1 mL L^{-1} PPG; (●) 650 rpm, (▲) 750 rpm, (■) 800 rpm. Error bars denote one standard deviation about the mean (n=3). Experiments were performed as described in Section 2.11.1.

Table 5.1 summarizes and compares the k_La values obtained in the present work and those reported in the literature for the Micro-24. Whilst there is order of magnitude agreement between the values, differences between the various studies are likely due to the different media, cassettes and caps used. Different media might have different rheological properties that may influence the mixing behaviour and k_La values. Likewise, the presence of a single baffle and the central draft tube in the BFL and PERC cassettes, respectively, may also create different hydrodynamic behaviours in comparison to the REG cassette, which may also lead to variation in the measured oxygen transfer rate. Additionally, the type of caps fitted to each well may also have an impact on the k_La behaviour (Ramirez-Vargas *et al.*, 2014).

Table 5.1. Comparison of k_La values in Micro-24 between the present work and literature data. For the present work data, k_La values were determined as described in Section 2.11.1.

k_La (h^{-1})	Cassette	Medium	Reference
46 – 143	REG	Water	Present work
38 – 77		Complex medium with 1 mL L^{-1} PPG	
21 – 67		Vinasse medium with 1 mL L^{-1} PPG	
4 – 53	REG	Proprietary CHO growth medium	Betts *et al.*
4 – 46		Water with 0.5 g L^{-1} Pluronic solution	(2014)
4 – 22	PERC	Proprietary CHO growth medium	
4 – 44		Water with 0.5 g L^{-1} Pluronic solution	
8 – 90	BFL and PERC	Water	Ramirez-Vargas *et al.* (2014)
33 – 56 (non-sparged)	REG	Galactose-limited, leucine-free defined medium	Isett *et al.* (2007)

5.3.1.2 Variation of k_La values in the 7.5 L STR

Comparable experiments were performed in the 7.5 L STR. Figure 5.3 depicts the k_La profiles obtained using water, complex and vinasse media in the 7.5 L STR at different agitation speeds and aeration rates. Overall, a similar trend as in the controlled MBR was observed whereby the k_La values increased as the agitation speed and aeration rate were increased. In all three media, the impact of airflow rate on the measured k_La values was small which is in the agreement with the findings of Gill *et al.* (2008). For example, increasing the agitation rate by two-fold in water resulted in an enhancement in k_La of 3.2-fold while increasing the aeration rate from 1 - 2 vvm only gave an increase in k_La of approximately 1.3-fold. In the case of the STR an increase in the agitation speed will lead to an increase in energy dissipation throughout the vessel. This, in turn, facilitates the bubble breakage into smaller sizes and hence an increase in gas-liquid surface area, OTR and hence k_La.

The highest k_La values were determined in water at 2 vvm, which ranged between 57 and 474 h^{-1}. In complex and vinasse media, the range of k_La values was comparable although the absolute values were slightly lower i.e. 43 – 378 and 41 – 322 h^{-1}, respectively. The similar impact of culture medium on k_La values as seen in the controlled MBR emphasizes the important role of the rheological factor in resulting the variation of the k_La profiles between the test fluids. It is observed that in any medium, the k_La range obtained in the 7.5 L STR spans over those achieved in the controlled MBR (Section 5.3.1.1), indicating the possibility of matching the k_La between the two scales for the scale-up purposes. This will be highlighted further in Section 5.3.3.
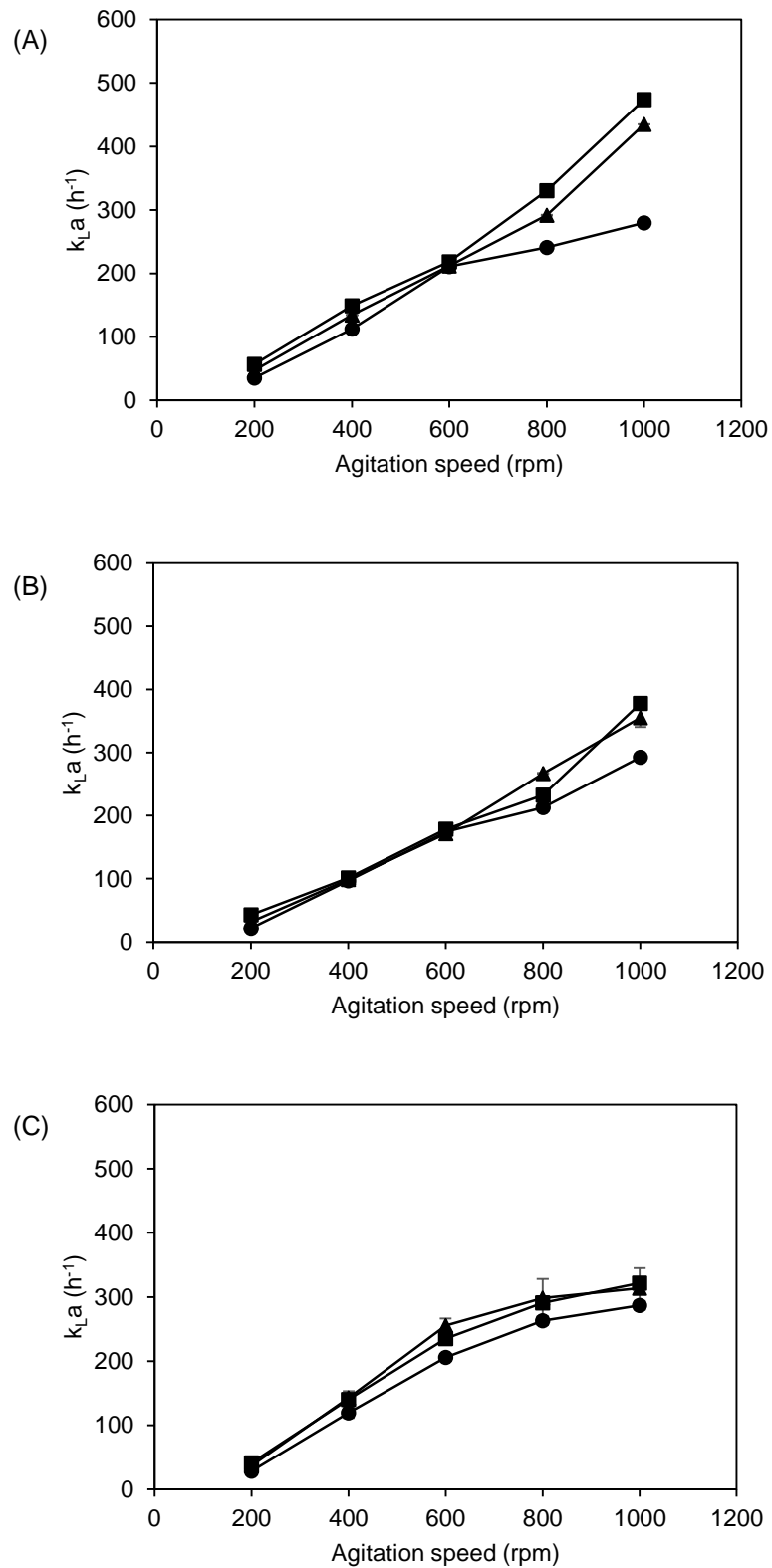
Figure 5.3. k_La variation in a 7.5 L STR at different agitation speeds and aeration rates using (A) water (B) complex medium with 1 mL L^{-1} PPG and (C) vinasse medium with 1 mL L^{-1} PPG; (●) 1 vvm, (▲) 1.5 vvm, (■) 2 vvm. Error bars denote one standard deviation about the mean (n=3). Experiments were performed as described in Section 2.11.2.

The k_La variation in water and complex medium exhibited a linear relationship which is in agreement with previous studies (Islam, 2008; Baboo, 2012). On the other hand, the k_La profile for the vinasse medium showed two distinct phases: a linear increase in k_La was observed between 200 and 800 rpm whereas further increasing the speed from 800 to 1000 rpm resulted in a slight increase in the k_La values. Table 5.2 outlines the linear relationship between k_La and agitation speed developed for each medium at different airflow rates. The regression coefficient, R^2 values determined for all equations were all greater than 0.9, indicating a good degree of linearity between k_La and agitation speed over the specified ranges.

Table 5.2. Linear relationship between k_La and agitation speed (N) developed for each medium at different airflow rates.

Medium	Airflow rate (vvm)	Equation	R^2
Water	1	$k_La=0.31N - 9.15$	0.95
	1.5	$k_La=0.47N - 55.69$	0.98
	2	$k_La=0.51N - 58.54$	0.98
Complex medium with 1 mL L^{-1} PPG	1	$k_La=0.33N - 37.92$	0.99
	1.5	$k_La=0.41N - 59.90$	0.99
	2	$k_La=0.40N - 53.97$	0.96
Vinasse medium with 1 mL L^{-1} PPG	1	$k_La=0.33N - 17.40$	0.96
	1.5	$k_La=0.35N - 3.12$	0.91
	2	$k_La=0.39N - 7.66$	0.96

Figure 5.4 shows the comparison between the experimental and calculated k_La values of which the latter were determined using the equations as outlined in Table 5.2 for each medium. As shown, there is good agreement between the experimental and predicted k_La values for all three media. Furthermore, the k_La data obtained from this work generally showed good consistency with those reported in the literature as outlined in Table 5.3. Any discrepancy may be associated with the difference in medium and bioreactor operating conditions applied in each work.
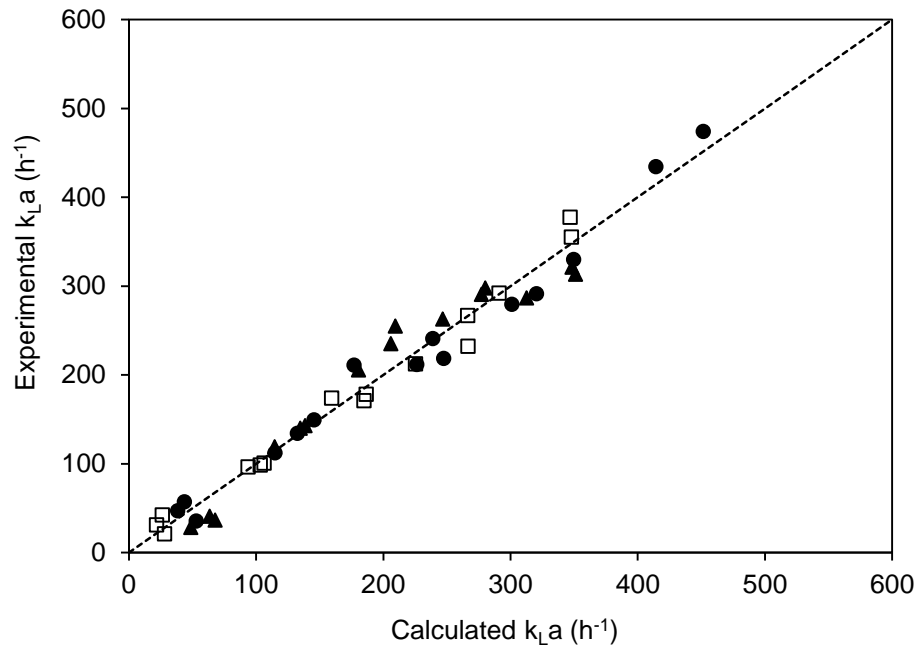
Figure 5.4. Comparison between experimental and calculated k_La values in the 7.5 L STR using (●) water, (□) complex medium and (▲) vinasse medium. Dotted lines represent parity plot (x=y). Experimental k_La values were determined based on procedures described in Section 2.11.2.1. Calculated k_La were determined based on equations as outlined in Table 5.2.

Table 5.3. Comparison of k_La values in a 7.5 L STR between present and literature data. For present work data, k_La determination was described as in Section 2.11.2.1.

k_La (h^{-1})	Medium	Agitation speed (rpm)	Specific aeration rate (vvm)	Reference
36 – 474	Water	200 – 1000	1 – 2	Present work
21 – 378	Complex medium			
29 – 322	Vinasse medium			
160 – 275	TB	200 – 800	1	Islam (2008)
~40 – 225	TB	400 – 800	1	Baboo (2012)

To be able to relate k_La values to bioreactor operating conditions i.e. power input and gas velocity, it is useful to establish k_La correlations based on Van't Riet (1979) correlation (Equation 2.3) (Section 2.11.2.2). The N^3D^2 term is associated with the agitation speed (N) and impeller diameter (D_i) while superficial velocity (v_s) is linked to the aeration rate. Although k_La is widely represented by the power per unit volume (P/V_L) term, measurement of an accurate power input to the reactor might be a challenge. Alternatively, the $N^3D_i^2$ term may be used to replace P/V_L term and this has been highlighted in several works (Yagi and Yoshida, 1975; Ozbek and Gayik, 2001). Equations 5.1, 5.2 and 5.3 represent the correlations developed here for water, complex and vinasse media,

respectively over the full range of agitation and aeration rates studied. These correlations were obtained by fitting the models to the full experimental data sets as described in Section 2.11.2.2.

$$k_L a = 0.0256 (N^3 D_i^2)^{0.43} (v_s)^{0.52} \qquad \text{(Equation 5.1)}$$

$$k_L a = 0.0086 (N^3 D_i^2)^{0.44} (v_s)^{0.12} \qquad \text{(Equation 5.2)}$$

$$k_L a = 0.0104 (N^3 D_i^2)^{0.46} (v_s)^{0.27} \qquad \text{(Equation 5.3)}$$

A comparison of the values of the constants and exponent values obtained for the correlations developed in this study with those reported in the literature are summarised in Table 5.4. Generally good agreement was observed between the results reported here and the literature data. Any slight discrepancy is again thought to be due to variation in the media compositions and bioreactor designs used.

Table 5.4. Comparison of k_La correlation coefficient values obtained from this study and literature data. For the present work, the coefficient values were determined as described in Section 2.11.2.2.

Medium	Coefficient value				Reference
	a	**b^1**	**b^2**	**c**	
Water	0.0256	0.43	-	0.52	Present work
Complex medium + PPG	0.0086	0.44	-	0.12	
Vinasse medium + PPG	0.0104	0.46	-	0.27	
Water	n.a.	0.42	-	0.62	Ozbek and Gayik (2001)
Water	n.a.	0.16 -0.37	0.4 – 1.0	0.3 – 0.48	Aksak (1990)
Water	n.a.	0.43 – 0.68	n.a.	n.a.	Yoshida *et al.* (1960)
Water + glycerol + millet jelly	n.a.	0.74	n.a.	n.a.	Yagi and Yoshida (1975)
Coalescing medium	0.026	-	0.4	0.5	Van't Riet (1979)
Non-coalescing medium	0.002	-	0.7	0.2	Van't Riet (1979)
TB	0.002	-	0.7	0.2	Islam *et al.* (2008)
Water-ions	0.22	-	0.35	0.52	Gill *et al.* (2008)
Water	0.01	-	0.48	0.40	Smith *et al.* (1977)
Water	0.0068	-	0.94	0.65	Vilaca *et al.* (2000)
Water	0.01	-	0.7	0.58	Linek *et al.* (2004)

Key: '-' – not applicable; n.a. – data not available; a – refers to correlation constant; b^1 – refers to coefficient of $N^3D_i^2$; b^2 – refers to coefficient of P/V_L (where applicable); c – refers to coefficient of v_s.

The experimental k_La values for the STRs, as discussed in Section 5.3.1.2 were further compared to the k_La values calculated from the developed correlations (Equations 5.1 - 5.3). The comparison between the experimental and calculated k_La data for each medium is presented in Figure 5.5. Generally, in water and complex medium, there is good agreement between the experimental and calculated k_La values with R^2 values of 0.97 and 0.98, respectively. Meanwhile, for the vinasse medium, good comparability was observed up to 800 rpm, above which the model correlation seems to overpredict the experimental k_La values.

Although the correlation (Equation 2.3) that relates the $N^3D_i^2$ term may not be widely referred to in the literature, it is shown here that it does demonstrate a reasonable fit to the data as the more commonly used P/V_L term.
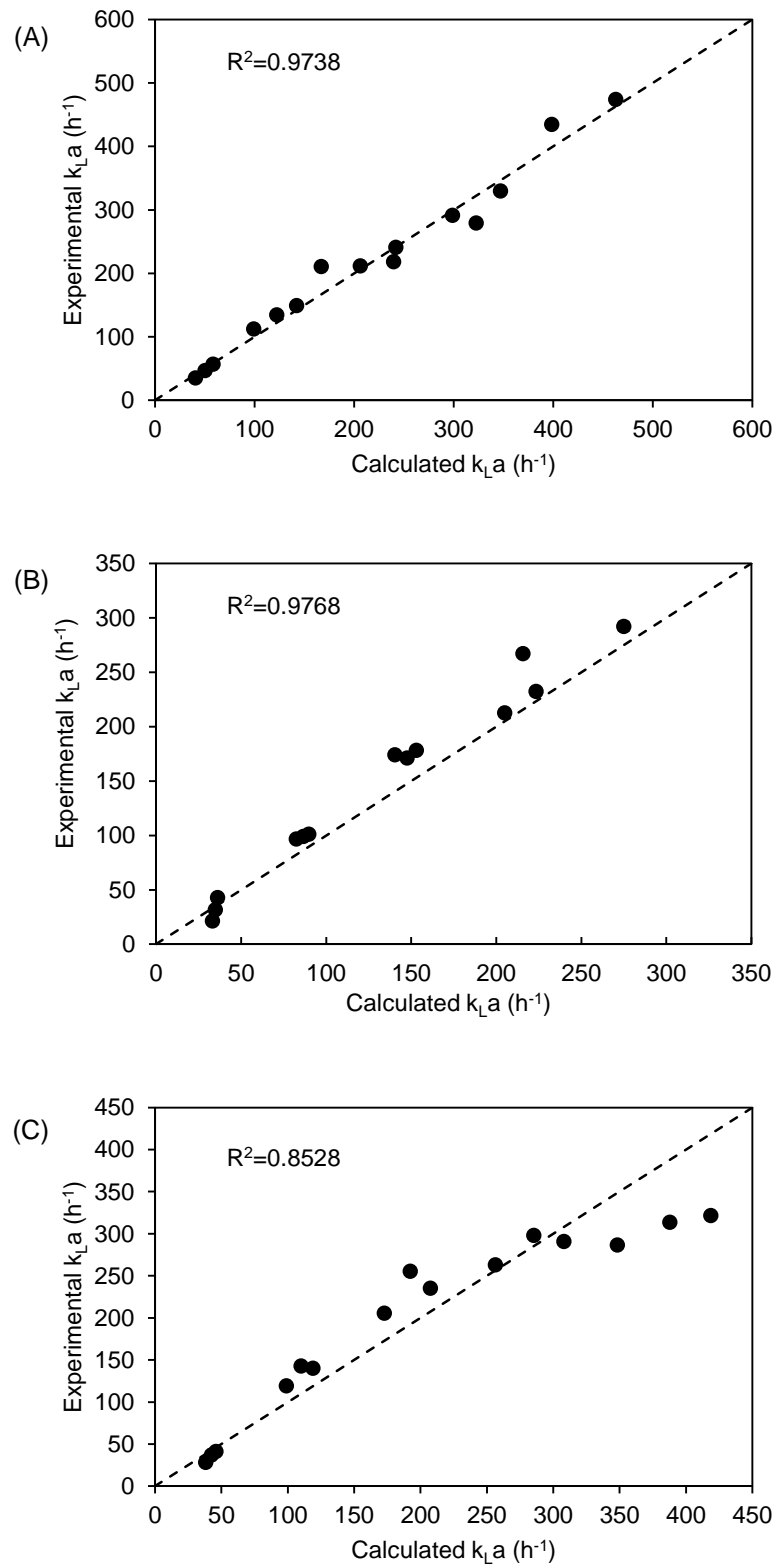
Figure 5.5. Comparison between experimental and calculated k_La values in the 7.5 L STR using (A) water, (B) complex medium and (C) vinasse medium. Dotted lines represent parity plot (x=y). Experimental k_La values were determined based on procedures described in Section 2.11.2.1. Calculated k_La were determined based on Equations 5.1 - 5.3.

5.3.2 Evaluation of options for large scale vinasse preparation

As discussed in Section 4.3.3, two options for vinasse preparation prior to fermentation were proposed. Option 1, which included filtration as the sterilisation technique, was used for the small scale optimisation studies described in Section 4.3.4. Considering larger scale applications, filtration may not be ideal as it is costly (membrane surface area required) and time consuming (low permeate fluxes with complex media). Therefore, a more efficient and cost effective procedure needs to be developed. On the other hand, evaluation of Option 2 (Figure 2.1) has been discussed in Section 4.3.3.2 whereby the results showed that the AC pre-treatment has insignificant impact on cell growth and CV2025 ω-TAm production. Thus, in this section, several other pre-processing options for vinasse suitable for large scale applications (designated as Options 3-5 in Figure 2.1) will be evaluated in terms of cell growth performance and CV2025 ω-TAm production. Option 1 will be referred to as a benchmark. This study was carried out in the controlled MBR with the experimental procedure as described in Section 2.8.2.

As outlined in Figure 2.1, in both Options 3 and 4, autoclaving was used as the sterilisation technique for vinasse. In Option 3, the autoclaved vinasse was used directly for fermentation while in Option 4, the autoclaved vinasse medium was supplemented with filter sterilised D-galactose at two different concentrations (0.7 and 1.7 g L^{-1}). The former concentration represents the diminished concentration of D-galactose determined after autoclaving raw vinasse while the latter is equivalent to that in 17% (v/v) diluted vinasse. Finally, in Option 5, no sterilisation step was performed after pH adjustment. The vinasse medium prepared from Option 5 is hereafter referred to as pasteurised dilute vinasse. In all fermentations, the diluted vinasse medium (17% v/v) was supplemented with 10 g L^{-1} yeast extract and 0.15 g L^{-1} kanamycin.

Figure 5.5 shows the time course of fermentations using vinasse media prepared via different options 1 and 3 - 5. It is clear that the same overall cell growth trends can be observed across all cultures. Apparently, in cultures employing autoclaved vinasse, no inhibition of cell growth was observed although Maillard reactions during heating might be expected to have an impact. The Maillard reaction occurs between a carbonyl group from a reducing sugar and an amino acid group from a nitrogenous substrate (Maillard, 1912). Rufian-Henares *et al.* (2006) and Hauser *et al.* (2014) observed the inhibitory impact of Maillard reaction products on *E. coli* cell growth. The extent of Maillard reactions may be influenced by several factors such as temperature and duration of the heating step, which in turn may determine the yield and composition of the resulting Maillard reaction products (Mu *et al.*, 2016).

It can be inferred from the data shown in Figure 5.6 that the extent of the Maillard reactions that occur following autoclaving of the vinasse medium does not result in reaction products that inhibit the cell growth. It is also interesting to note the comparable cell growth performance obtained in fermentations employing pasteurised vinasse as found when using filtered vinasse. This further suggests the promising application of the pasteurised vinasse directly for a fermentation.
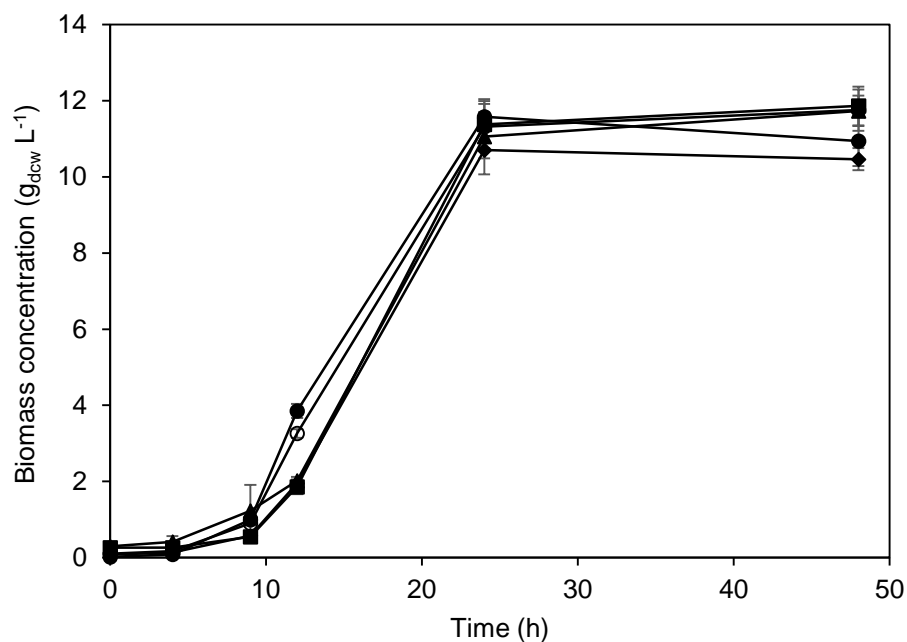
Figure 5.6. Comparison of batch fermentation kinetics of *E. coli* BL21 (DE3) cultured in the controlled MBR using (●) filtered dilute vinasse medium, (▲) autoclaved vinasse medium without D-galactose, (■) autoclaved vinasse medium with 0.7 g L^{-1} D-galactose, (♦) autoclaved vinasse medium with 1.7 g L^{-1} D-galactose and (○) pasteurized diluted vinasse medium. Error bars denote one standard deviation about the mean (n=3). Fermentations were performed as described in Section 2.8.2. Biomass concentration was determined as described in Section 2.12.2.

A growth assessment was carried out in order to examine the growth of *E. coli* BL21 (DE3) on agar plates using pasteurised and filtered dilute vinasse as fermentation media (Section 2.12.11). Figure 5.7 compares the results obtained using pasteurised and filtered dilute vinasse media, respectively. It was observed that after 72 hours of incubation, there was no visible growth of microorganisms in the control experiments that contained either pasteurized dilute vinasse (Figure 5.7 (A)) or filtered dilute vinasse (Figure 5.7 (C)). Meanwhile, roughly comparable growth is seen after 24 h of incubation when 48 h samples from the *E. coli* BL21 (DE3) cultures, initially grown using either pasteurized or filtered dilute vinasse, was applied on the agar plates, as shown in Figures 5.7 (B) and 5.7 (D), respectively. The presence of kanamycin, which is the CV2025 ω-TAm selection marker used in this study also facilitates the culture of *E. coli* BL21 (DE3) pQR801 during the early stage of the culture post inoculation.
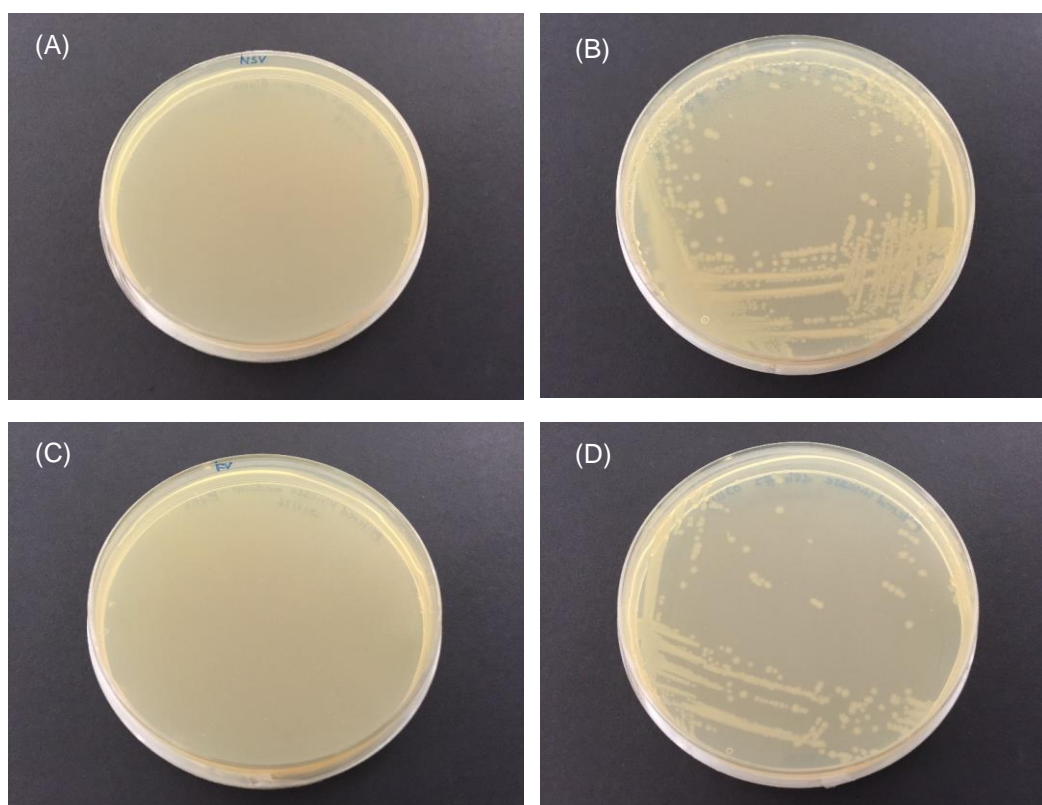
Figure 5.7. LB-agar plates spread with (A) blank pasteurised dilute vinasse medium, after 72 h of incubation and (B) 48 h sample of *E. coli* BL21 (DE3) culture grown using pasteurised dilute vinasse medium, after 24 h of incubation. (C) blank filtered dilute vinasse medium after 72 h of incubation and (D) 48 h sample of *E. coli* BL21 (DE3) culture grown using filtered dilute vinasse medium, after 24 h of incubation. Preparation of LB-agar plates as described in Section 2.3.3. Growth assessment was performed as described in Section 2.12.11.

The corresponding CV2025 ω-TAm production from the cultures grown using different types of vinasse media was also evaluated. Figure 5.8 compares the CV2025 ω-TAm volumetric and specific activity obtained at several time points during the different cultures. In the culture where filtered dilute vinasse was used, the highest volumetric and specific activity of CV2025 ω-TAm attained after 48 h were 6.4 U ml^{-1} and 286.8 U g$_{dcw}$$^{-1}$, respectively. Meanwhile, the maximum volumetric and specific activity attained in cultures using dilute autoclaved vinasse medium only reached 4.4 U ml^{-1} and 160.3 U g$_{dcw}$$^{-1}$, respectively. It was initially expected that the decrease of the biocatalyst titre may be associated with the reduction of D-galactose by about 46% after autoclaving. As discussed in Chapter 4, D-galactose in vinasse was identified as acting as an inducer to the *lac* operon, resulting in expression of CV2025 ω-TAm in *E. coli* BL21 (DE3). Nevertheless, supplementing the dilute autoclaved vinasse medium with synthetic D-galactose, as shown by the performances of cultures using autoclaved vinasse (AV) II and AV III, was not able to match the CV2025 ω-TAm specific activity attained in fermentations using dilute filtered vinasse medium (although an enhancement of about 14 - 17% was observed with D-galactose supplementation). The maximum CV2025 ω-TAm volumetric and specific activity achieved using dilute pasteurized vinasse medium were 6.4 U ml^{-1} and 246.5 U g$_{dcw}$$^{-1}$, respectively, which were

approximately 30% and 35% higher than the maximum obtained using dilute autoclaved vinasse medium. This further supports the use of the pasteurised vinasse for larger scale fermentations.
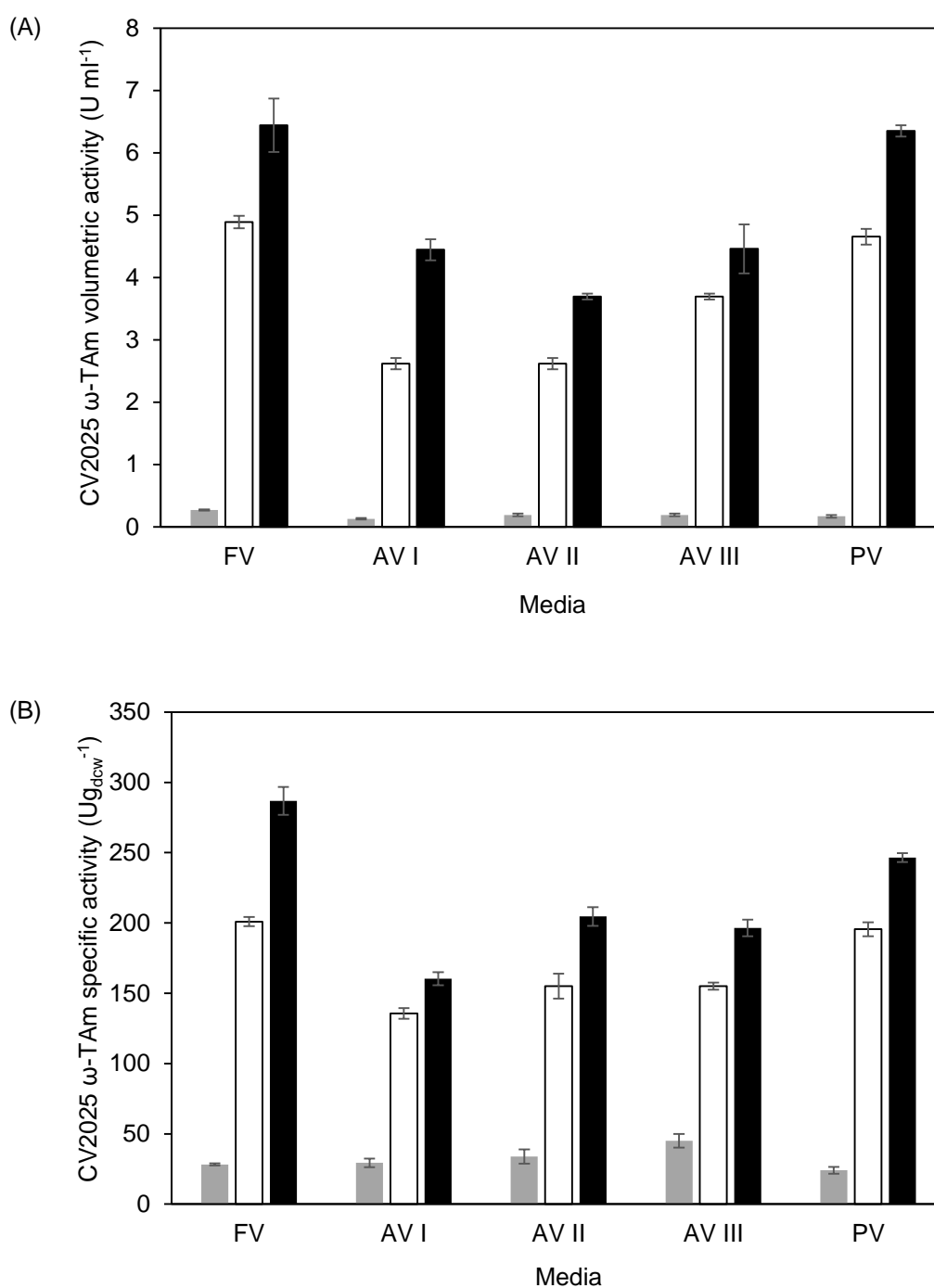
Figure 5.8. (A) Volumetric activity and (B) specific activity of CV2025 ω-TAm from *E. coli* BL21 (DE3) fermentations samples at (▨) 12 h, (▢) 24 h and (▪) 48 h using dilute filtered vinasse (FV), dilute autoclaved vinasse (AV I), dilute autoclaved vinasse with 0.7 g L^{-1} D-galactose (AV II), dilute autoclaved vinasse with 1.7 g L^{-1} D-galactose (AV III) and dilute pasteurized vinasse (PV). Biomass growth as shown in Figure 5.7. Error bars denote one standard deviation about the mean (n=3). The CV2025 ω-TAm assay was performed as described in Section 2.12.5.

The complexity of the vinasse composition has made it challenging to fully understand the interaction of various components during processing. As discussed in Section 4.3.1, vinasse consists of several compounds including reducing sugars and nitrogenous substrates (Table 4.1). The existence of these two compounds in vinasse poses a challenge regarding heat sterilisation in that the high temperature may lead to Maillard reaction products. Whilst no apparent inhibition was observed on the cell growth, the decrease of the biocatalyst titre despite the D-galactose supplementation is not fully understood. It is hypothesised that an unknown inhibitory pathway might have been formed upon autoclaving that in turn might impact the induction of the *lac* operon and hence production of CV2025 ω-TAm.

The feasibility of using dilute pasteurised vinasse directly for fermentations offers an additional benefit for vinasse valorisation. Vinasse has already been exposed to a high temperature during distillation where the microbial load will already have been reduced. Owing to the other potential benefits such as low cost, no requirement for IPTG induction (Section 4.3.2.1) and simple pre-processing steps (Section 4.3.3.2), direct use of pasteurised vinasse offers practical and economic fermentation feedstock. Subsequent work will be focusing on using pasteurised vinasse as a fermentation medium.

5.3.3 Fermentation scale-up at matched $k_L a$ and specific aeration rate

5.3.3.1 Scale-up with complex medium

Previous works have suggested the use of $k_L a$ as a basis for scale-up of aerobic fermentations between shaken microwells and laboratory stirred tank bioreactors (Section 1.5.2). The selection of a matched $k_L a$ value between the two reactors in this study was restricted to the value attained at 800 rpm in the controlled MBR, the optimal speed recommended by the supplier for the REG cassette, and also to 1 vvm, the standardised specific aeration rate for the fermentations in both reactors. Figure 5.9 shows the comparison of $k_L a$ profile at 1 vvm in the controlled MBR and 7.5 L STR using a complex medium. The matched $k_L a$ value selected was 75 h^{-1}. Based on Equation 5.2, the agitation speed in the 7.5 L STR determined at 75 h^{-1} and 1 vvm was 374 rpm. The shaking frequency and agitation speed in the controlled MBR and 7.5 L STR were maintained throughout the fermentation so as to provide an approximately uniform level of oxygen transfer rate. The same inoculum, which was prepared in shake flasks (Section 2.7), was used for both reactors in order to eliminate any possible variation arising from the seed culture. The optimal IPTG induction conditions as established in Section 3.3.3.1 were applied in both systems. Table 5.5 outlines the process parameters of both reactors for fermentations at 75 h^{-1}.
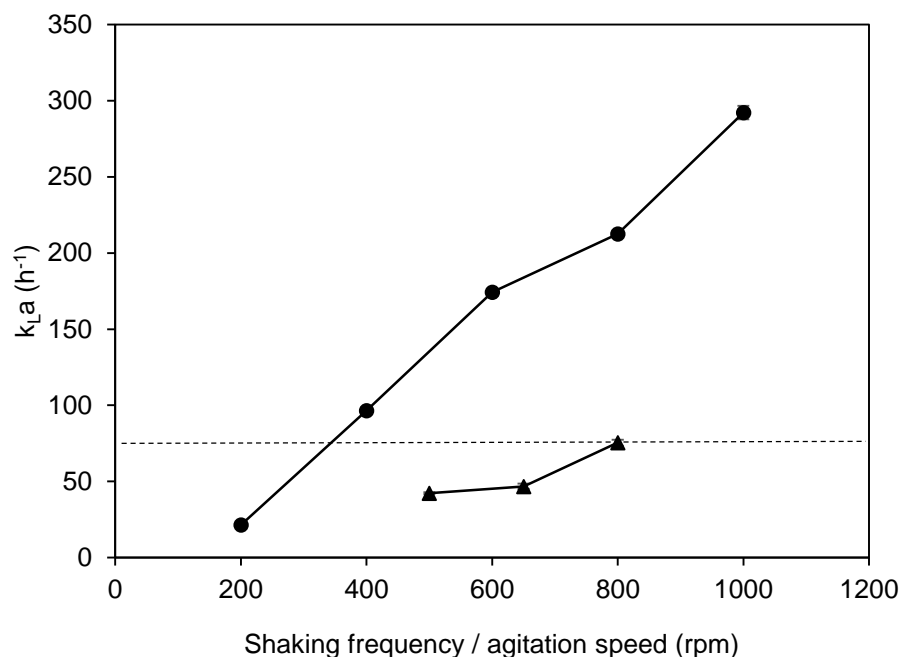
Figure 5.9. Comparison of k_La profile in (▲) the controlled MBR and (●) a 7.5 L STR using a complex medium with 1 mL L^{-1} PPG aerated at 1 vvm as a function of shaking frequency or agitation speed respectively. Horizontal dotted line indicates the matched k_La value between the two reactors. Error bars denote one standard deviation about the mean (n=3). Experiments were performed as described in Section 2.11.1 (controlled MBR) and Section 2.11.2 (7.5 L STR).

Table 5.5. Process parameters in the controlled MBR and 7.5 L STR during scale-up using the complex medium at a matched k_La of 75 h^{-1}. Fermentations were performed as described in Section 2.8.2 (controlled MBR) and Section 2.8.3 (7.5 L STR).

Parameter	Controlled MBR	7.5 L STR
Total reactor volume	10 mL	7.5 L
Working volume	6.5 mL	5 L
Shaking frequency / agitation speed	800 rpm	374 rpm
Orbital shaking diameter	2.5 mm	Not applicable
Specific aeration rate	1 vvm	1 vvm
k_La	75 h^{-1}	75 h^{-1}
DOT	30%	30%
pH	7	7
Temperature	37 ºC	37 ºC

Figures 5.10 and 5.11 show the fermentation kinetic profiles achieved in the controlled MBR and 7.5 L STR, respectively. A comparable trend of cell growth was observed between the cultures grown in both reactors whereby a stationary phase was achieved after 12 h of incubation, accompanied by the reciprocal decrease of the glycerol concentrations. In both cases, complete utilisation of glycerol was achieved after 24 hours. Additionally, the maximum specific growth rates attained in the controlled MBR (0.36 h^{-1}) and 7.5 L STR (0.38 h^{-1}) were also comparable.

Whilst there was direct gas sparging in both the controlled MBR and 7.5 L STR, the difference of DO profiles observed between both systems as depicted in Figures 5.10 (B) and 5.11 (B), was likely due to dissimilar levels of gas bubble break-up and dispersion and dissimilar control mechanisms. In the MBR, the DO was controlled by blending oxygen and nitrogen that resulted in an instantaneous regulation around the set point throughout the course of the fermentation. In contrast, in the 7.5 L STR, the DO was controlled by blending air and oxygen. Initially the DO profile shows a gradual decrease with increasing biomass concentration until the set point was reached. Thereafter, the DO was maintained around the set point until the point the oxygen demand decreased, which led to an increase in DO towards the end of the cultivation. In general, the DO in both reactors was successfully maintained above the critical level for *E. coli* BL21 (DE3) growth, which is about 10% (Junker, 2004).
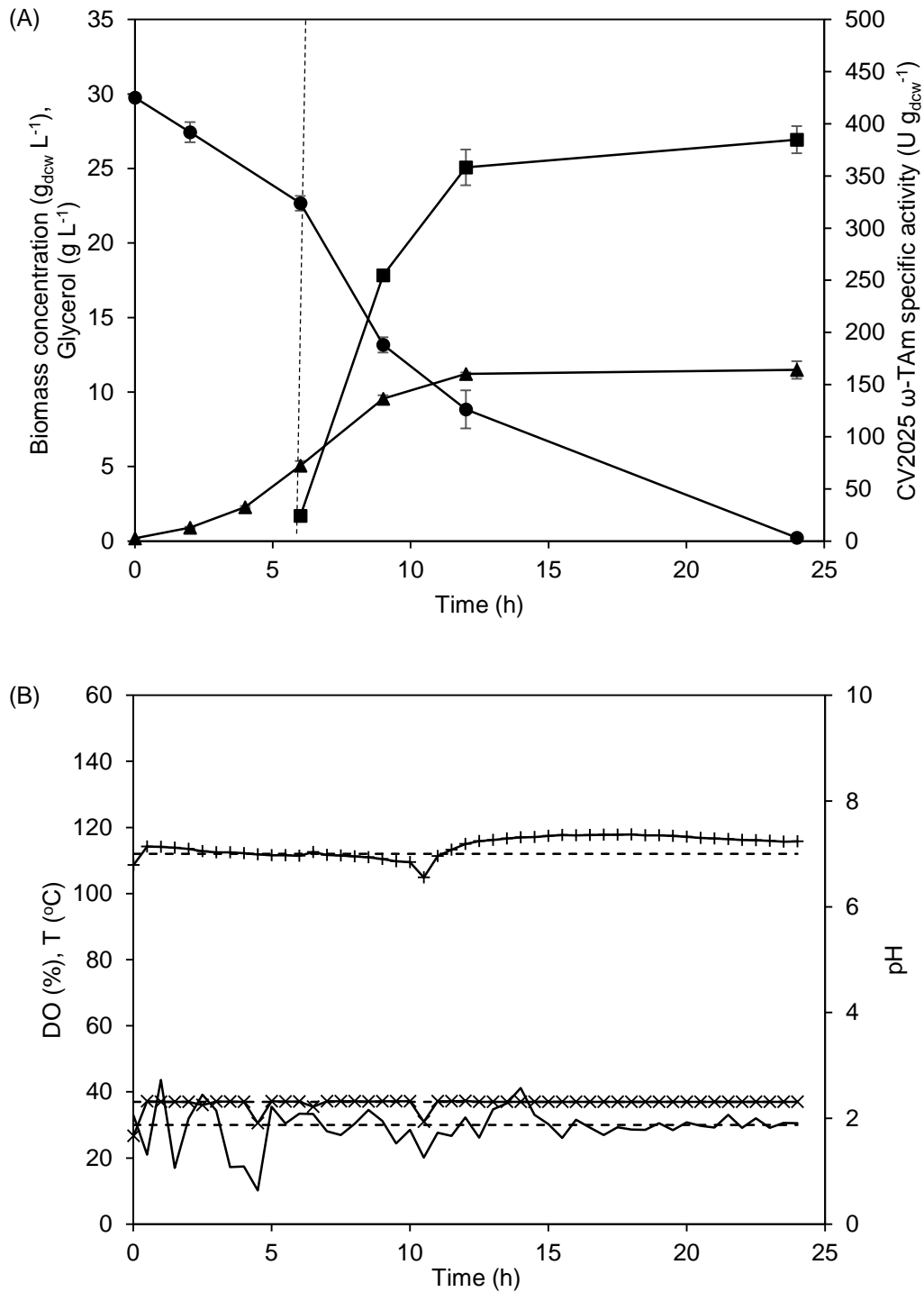
Figure 5.10. (A) *E. coli* BL21 (DE3) fermentation kinetics in the controlled MBR at a k_La of 75 h^{-1}: (▲) biomass concentration, (●) glycerol, (■) CV2025 ω-TAm specific activity. (B) Online data showing (-) DO, (✶) temperature and (+) pH profiles obtained in the controlled MBR. Dotted vertical line indicates the point of IPTG induction. Dotted horizontal lines indicate the set point for each process parameter. Error bars denote one standard deviation about the mean (n=3). Fermentations were performed as described in Section 2.8.2. Analytical procedures were performed as described in Section 2.12.2 (biomass concentration), Section 2.12.5 (CV2025 ω-TAm assay) and Section 2.12.6 (glycerol).
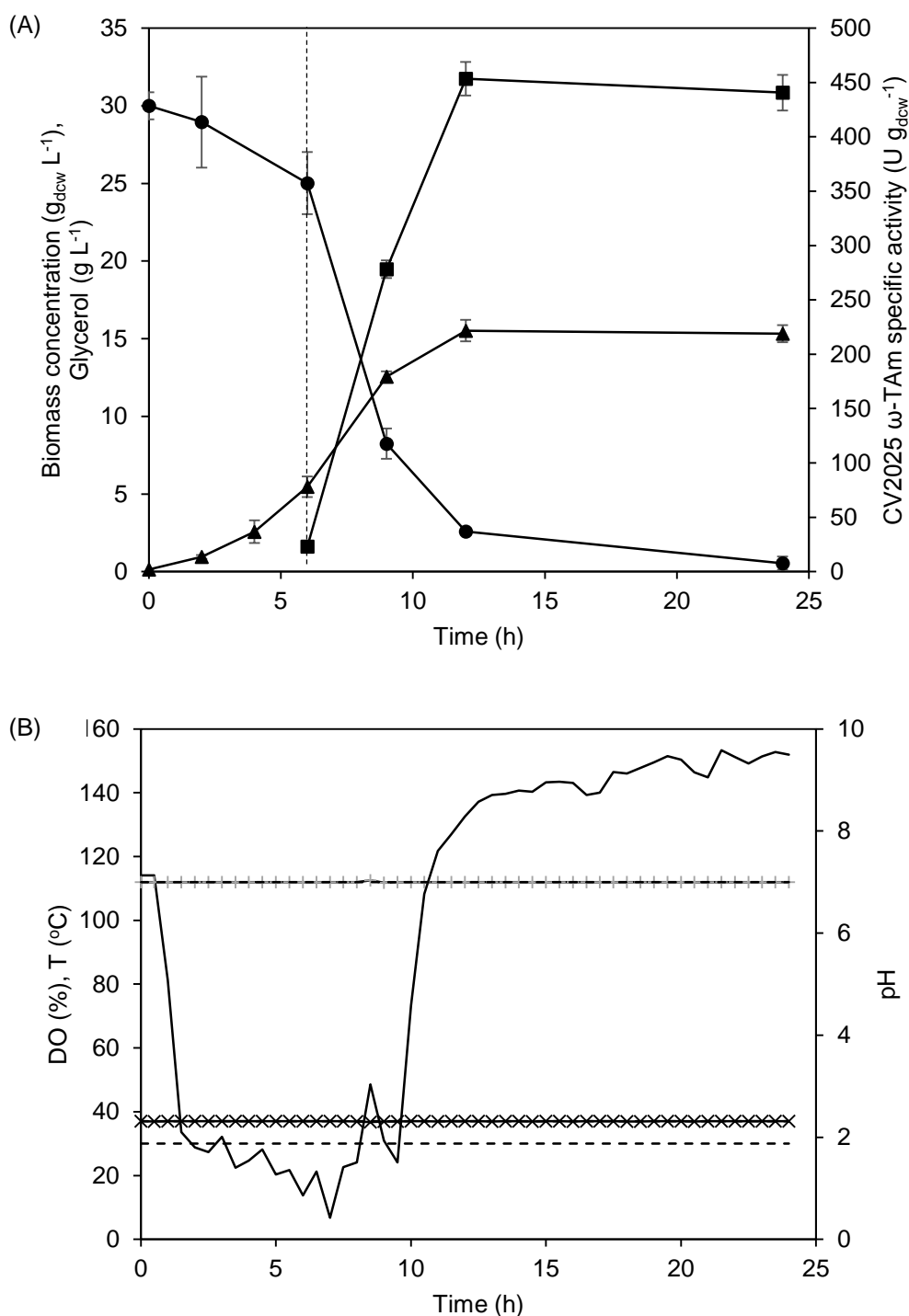
Figure 5.11. (A) *E. coli* BL21 (DE3) fermentation kinetics in the 7.5 L STR at a k_La of 75 h^{-1}: (▲) biomass concentration, (●) glycerol, (■) CV2025 ω-TAm specific activity. (B) Online data showing (-) DO, (✻) temperature and (+) pH profiles obtained in the 7.5 L STR. Dotted vertical line indicates the point of IPTG induction. Dotted horizontal lines indicate the set point for each process parameter. Error bars denote one standard deviation about the mean (n=3). Fermentations were performed as described in Section 2.8.3. Analytical procedures were performed as described in Section 2.12.2 (biomass concentration) and Section 2.12.6 (glycerol).

Figure 5.12 depicts the CV2025 ω-TAm volumetric and specific activity attained at different time points in the controlled MBR and 7.5 L STR. Although the CV2025 ω-TAm volumetric activity between the two platforms were statistically different at a significance level of 0.05, particularly from 9 to 24 h, a similar trend was observed in both cultivations whereby the highest titres were achieved at 12 h. In addition, the CV2025 ω-TAm specific activity achieved in both platforms at every time interval were found to be statistically similar. A good comparability of the biocatalyst specific activity is crucial in order to show that there is no loss of process efficiency during the scale translation. A summary of the fermentation kinetics parameters obtained in both controlled MBR and 7.5 L STR at 75 h^{-1} is outlined in Table 5.6.
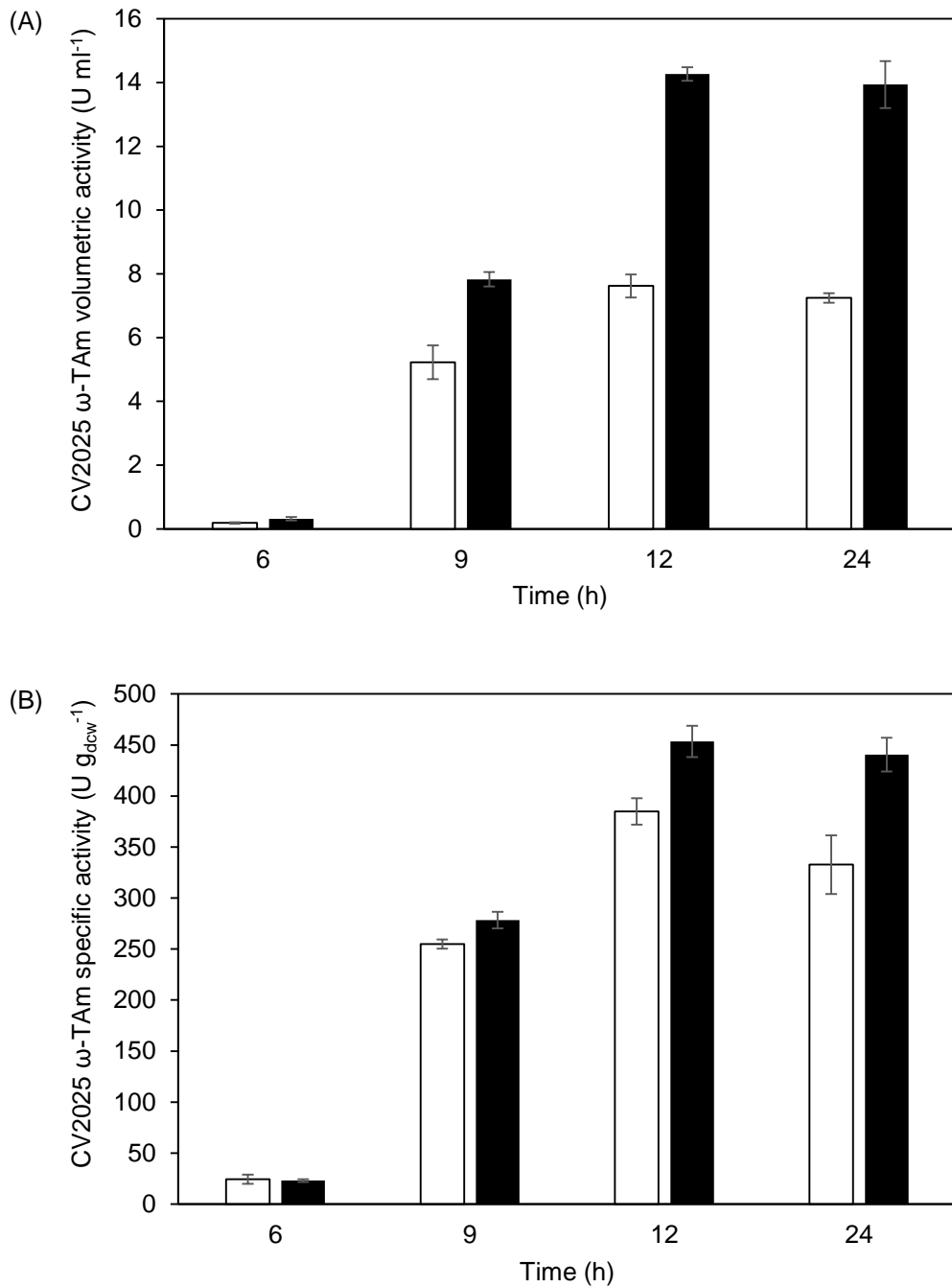
Figure 5.12. (A) Volumetric and (B) specific activity of CV2025 ω-TAm from *E. coli* BL21 (DE3) fermentations performed at a matched k_La of 75 h^{-1} at different time points in (□) controlled MBR and (■) 7.5 L STR cultures. Biomass growth as shown in Figure 5.10 (controlled MBR) and Figure 5.11 (7.5 L STR). Error bars denote one standard deviation about the mean (n=3). The CV2025 ω-TAm assay was performed as described in Section 2.12.5.

Table 5.6. Comparison of fermentation kinetics parameters between the controlled MBR and 7.5 L STR at a matched k_La value of 75 h^{-1}. Fermentation kinetics as shown in Figure 5.10 (controlled MBR) and Figure 5.11 (7.5 L STR). Analytical procedures were performed as described in Section 2.12.2 (biomass concentration), Section 2.12.5 (CV2025 ω-TAm assay) and Section 2.12.6 (glycerol).

Parameter	Controlled MBR	7.5 L STR	p-value
			Controlled MBR vs. 7.5 L STR
X_{max} (g_{dcw} L^{-1})	11.5 ± 0.6	15.5 ± 0.7	0.05
μ (h^{-1})	0.36 ± 0.01	0.38 ± 0.01	0.29
Maximum CV2025 ω-TAm specific activity (U g_{dcw}^{-1})	385 ± 13	454 ± 15	0.07
Maximum CV2025 ω-TAm volumetric activity (U ml^{-1})	7.6 ± 0.4	14.3 ± 0.2	0.01
$Y_{X/S}$ (g g^{-1})	0.42 ± 0.00	0.51 ± 0.00	0.01

Parity plots of biomass concentration, glycerol consumption and CV2025 ω-TAm volumetric and specific activity between the two scales are shown in Figure 5.13. Except for CV2025 ω-TAm volumetric activity, in general, plots show good similarity with the points lying mostly near to the parity lines. These results demonstrate the promising feasibility of a 769-fold volumetric scale-up between the two platforms using a matched k_La value and specific aeration rate as the scaling parameters.

(A)

$R^2=0.9917$

7.5 L STR [Biomass concentration] $(g_{dcw}$ $L^{-1})$

Controlled MBR [Biomass concentration] $(g_{dcw}$ $L^{-1})$

(B)

$R^2=0.9724$

7.5 L STR [CV2025 ω-TAm volumetric activity] (U ml^{-1})

Controlled MBR [CV2025 ω-TAm volumetric activity] (U ml^{-1})

(C)

$R^2=0.9862$

7.5 L STR [CV2025 ω-TAm specific activity] (U g_{dcw}^{-1})

Controlled MBR [CV2025 ω-TAm specific activity] (U g_{dcw}^{-1})

(D)
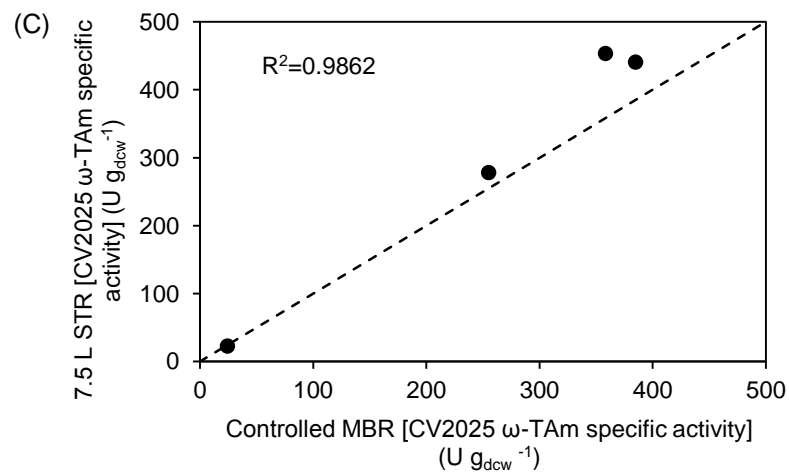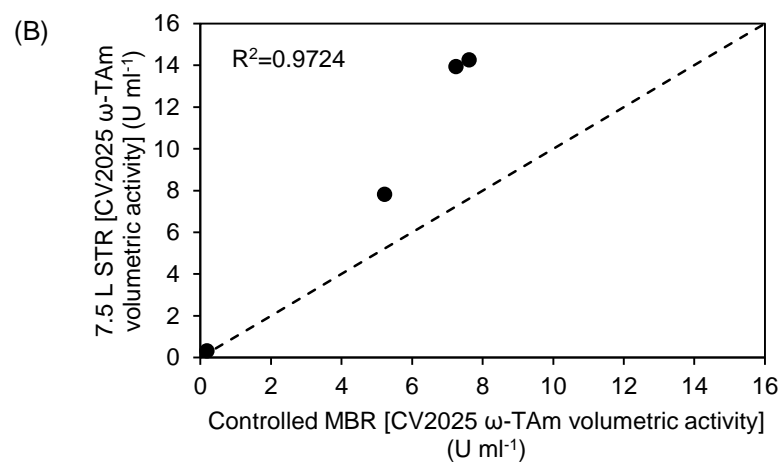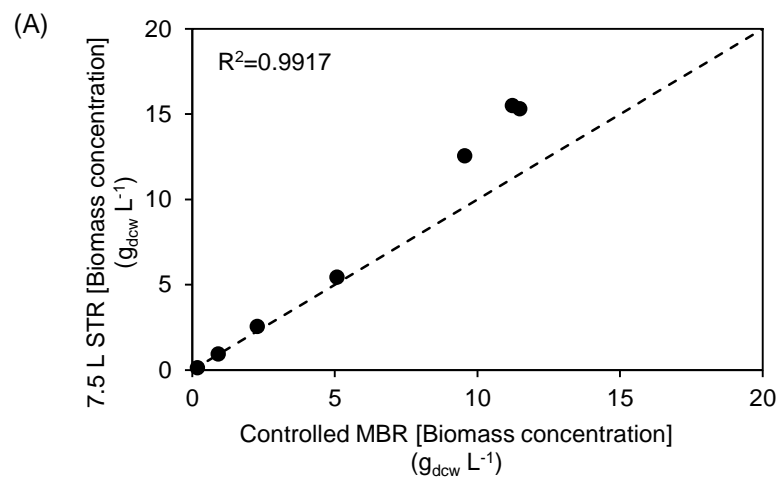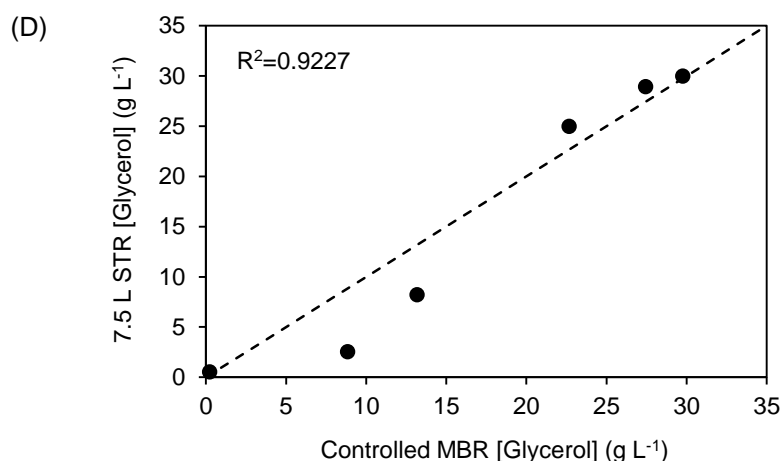
Figure 5.13. Parity plots of (A) biomass concentration, (B) CV2025 ω-TAm volumetric activity, (C) CV2025 ω-TAm specific activity and (D) glycerol concentration in the controlled MBR and 7.5 L STR. Fermentation kinetics were shown in Figure 5.10 (controlled MBR) and Figure 5.11 (7.5 L STR). Dotted lines represent parity lines (x=y).

5.3.3.2 Scale-up with vinasse medium

As decided in Section 5.3.2, a pasteurised dilute vinasse medium represents a potential biorefinery fermentation feedstock. In this case, the same scale-up procedure as in Section 5.3.3.1 was applied whereby matched k_La values and specific aeration rates were used as the scaling parameters. The comparison of the k_La profile at 1 vvm in the controlled MBR and 7.5 L STR is shown in Figure 5.14 where the matched k_La value selected was 66 h^{-1}. Equation 5.3 was used to determine the corresponding agitation speed in the 7.5 L STR at 66 h^{-1} and 1 vvm, which was found to be 298 rpm. The shaking frequency and agitation speed in the controlled MBR and 7.5 L STR were maintained at 800 and 298 rpm, respectively throughout the fermentation. Table 5.7 outlines the process parameters used for both reactors for fermentations at 66 h^{-1}. A similar seed culture was applied in fermentations in both systems (Section 2.7).
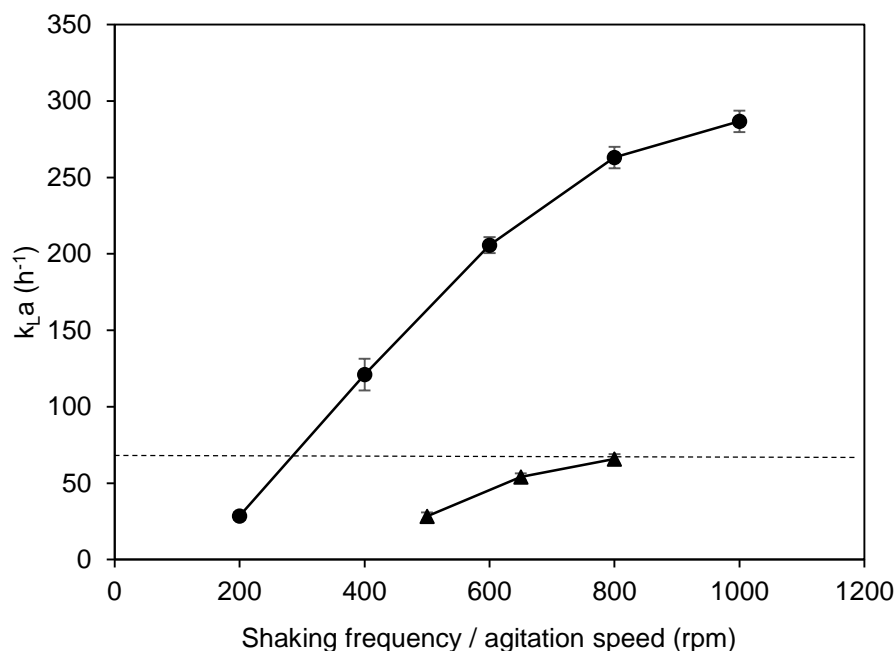
Figure 5.14. Comparison of k_La profile in (▲) the controlled MBR and (●) a 7.5 L STR using vinasse medium with 1 mL L^{-1} PPG aerated at 1 vvm as a function of shaking frequency or agitation speed, respectively. Horizontal dotted line indicates the matched k_La value between the two reactors. Error bars denote one standard deviation about the mean (n=3). Experiments were performed as described in Section 2.11.1 (controlled MBR) and Section 2.11.2 (7.5 L STR).

Table 5.7. Process parameters in the controlled MBR and 7.5 L STR during scale-up using the vinasse medium at a matched k_La of 66 h^{-1}. Fermentations were performed as described in Section 2.8.2 (controlled MBR) and Section 2.8.3 (7.5 L STR).

Parameter	Controlled MBR	7.5 L STR
Total reactor volume	10 mL	7.5 L
Working volume	6.5 mL	5 L
Shaking frequency / agitation speed	800 rpm	298 rpm
Orbital shaking diameter	2.5 mm	Not applicable
Specific aeration rate	1 vvm	1 vvm
k_La	66 h^{-1}	66 h^{-1}
DOT	30%	30%
pH	7	7
Temperature	37 °C	37 °C

Figures 5.15 and 5.16 represent the fermentation profiles in the controlled MBR and 7.5 L STR at 66 h^{-1}, respectively. The results showed good comparability of cell growth kinetics between the two platforms. The same trend for substrate consumption is also exhibited in both reactors whereby D-mannitol was the primary substrate followed by a simultaneous consumption of glycerol, D-xylitol and D-dulcitol.
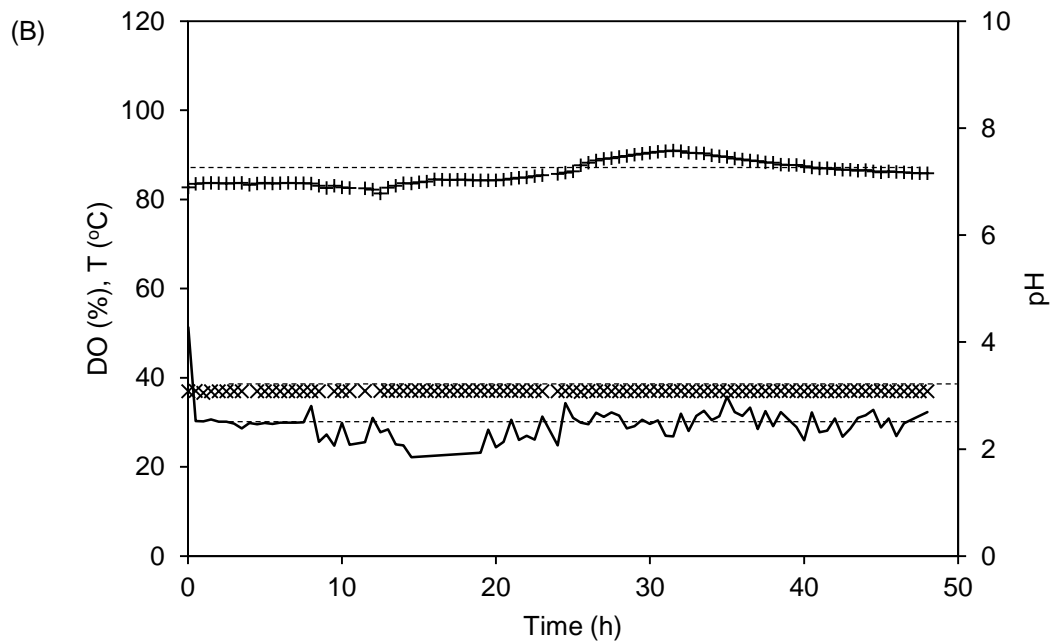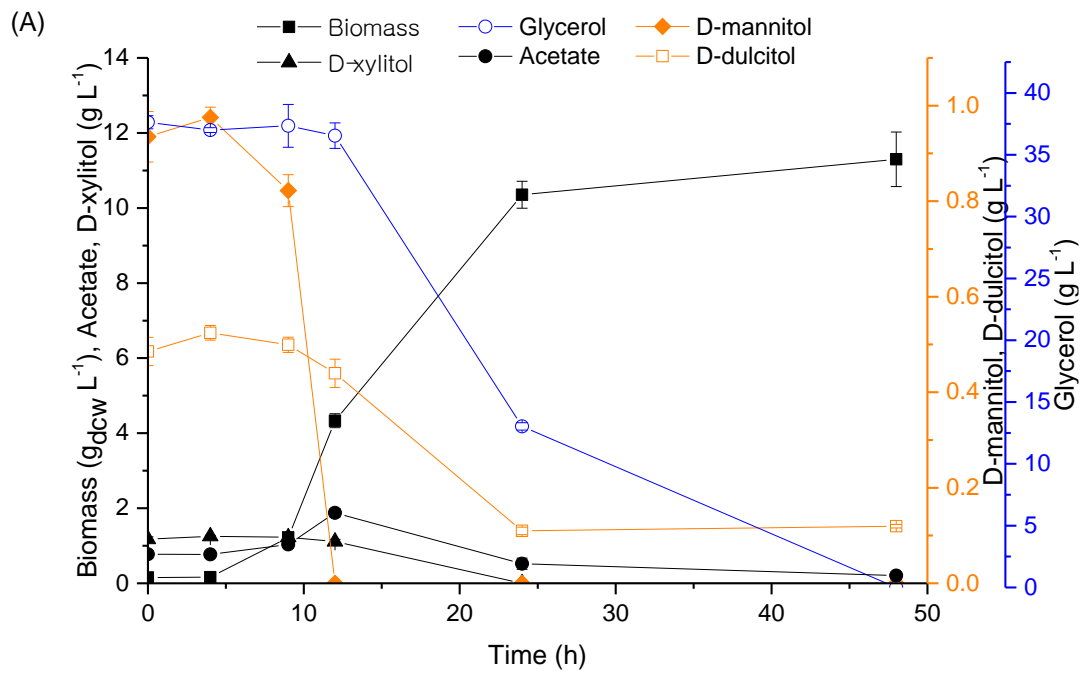
Figure 5.15. (A) *E. coli* BL21 (DE3) fermentation performance in the controlled MBR at a k_La of 66 h^{-1} (B) Online data showing (-) DO, (x) temperature and (+) pH profiles obtained in in the controlled MBR throughout the fermentation course. Dotted horizontal lines indicate the set point for each process parameter. Error bars denote one standard deviation about the mean (n=3). Fermentations were performed as described in Section 2.8.2. Analytical procedures were performed as described in Section 2.12.2 (biomass concentration), Section 2.12.6 (glycerol and acetate) and Section 2.12.7 (sugars and sugar alcohols).
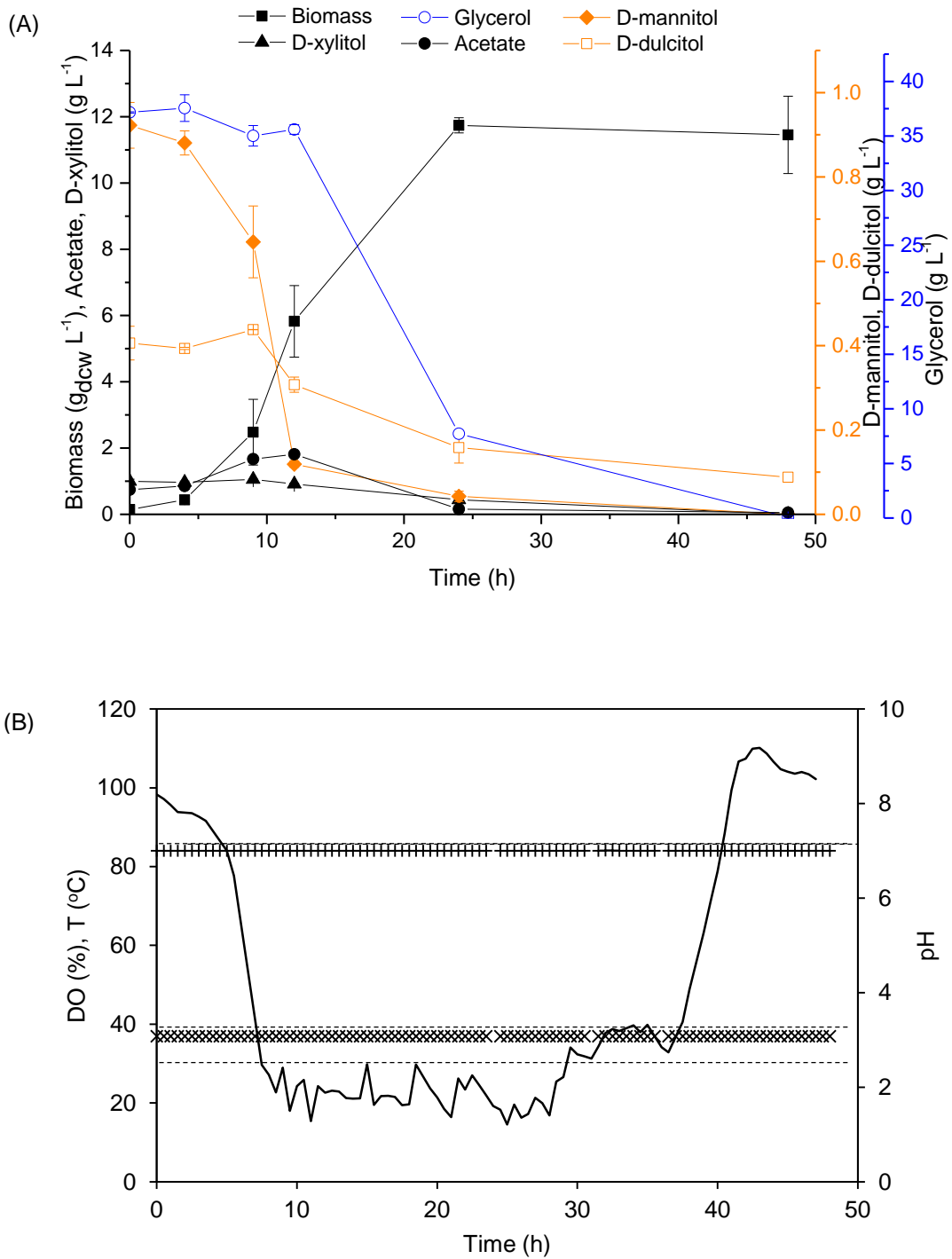
Figure 5.16. (A) *E. coli* BL21 (DE3) fermentation kinetics in the 7.5 L STR at a k_La of 66 h⁻¹ (B) Online data showing (-) DO, (x) temperature and (+) pH profiles obtained in 7.5 L STR throughout the fermentation course. Dotted horizontal lines indicate the set point for each process parameter. Error bars denote one standard deviation about the mean (n=3). Fermentations were performed as described in Section 2.8.3. Analytical procedures were performed as described in Section 2.12.2 (biomass concentration), Section 2.12.6 (glycerol and acetate) and Section 2.12.7 (sugars and sugar alcohols).

Figure 5.17 depicts the CV2025 ω-TAm volumetric and specific activity attained at different time intervals in the two platforms. The highest CV2025 ω-TAm volumetric and specific activity in both cultivations were achieved at 48 h. Generally, the CV2025 ω-TAm volumetric and specific activity obtained from fermentations in both reactors at every time interval were found to be statistically equivalent with respect to a significance level of 0.05. The summary of the fermentation kinetics parameters between the controlled MBR and 7.5 L STR at 66 h^{-1} is summarised in Table 5.8.
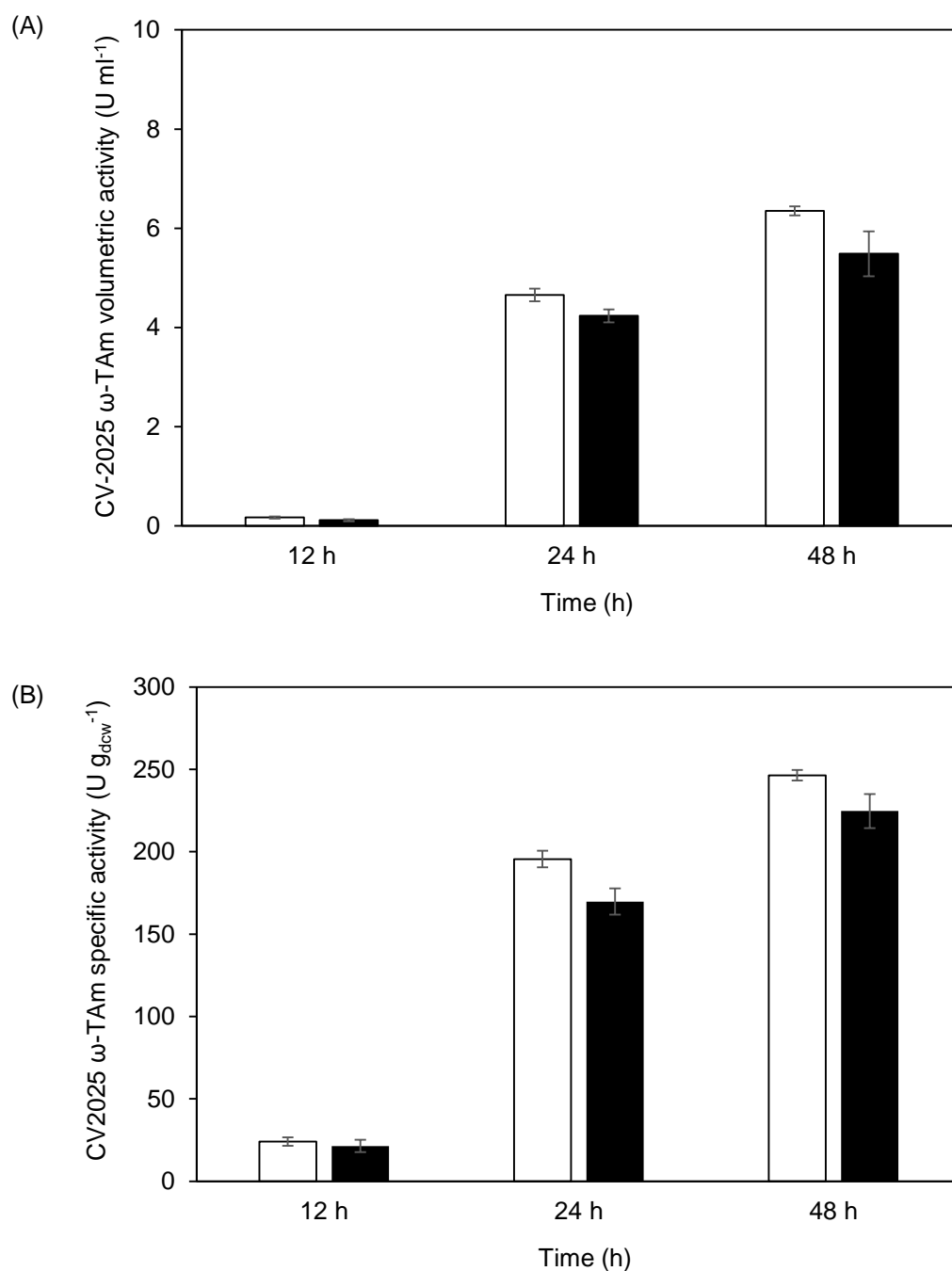
Figure 5.17. (A) Volumetric activity and (B) specific activity of CV2025 ω-TAm from *E. coli* BL21 (DE3) fermentations performed at a matched k$_L$a of 66 h^{-1} in (□) controlled MBR and (■) 7.5 L STR cultures. Biomass growth as shown in Figure 5.15 (controlled MBR) and Figure 5.16 (7.5 L STR). Error bars denote one standard deviation about the mean (n=3). The CV2025 ω-TAm assay was performed as described in Section 2.12.5.

Table 5.8. Comparison of fermentation kinetics parameters between the controlled MBR and 7.5 L STR at a matched k_La value of 66 h^{-1}. Fermentation kinetics as shown in Figure 5.15 (controlled MBR) and Figure 5.16 (7.5 L STR). Analytical procedures were performed as described in Section 2.12.2 (biomass concentration), Section 2.12.5 (CV2025 ω-TAm assay) and Section 2.12.6 (glycerol and acetate).

Parameter	Controlled MBR	7.5 L STR	p-value Controlled MBR vs. 7.5 L STR
X_{max} (g_{dcw} L^{-1})	11.3 ± 0.7	11.7 ± 0.2	0.67
μ (h^{-1})	0.35 ± 0.01	0.35 ± 0.02	1.0
Maximum CV2025 ω-TAm specific activity (U g_{dcw}^{-1})	246.5 ± 3.2	224.7 ± 10.4	0.17
Maximum CV2025 ω-TAm volumetric activity (U ml^{-1})	6.4 ± 0.1	5.5 ± 0.5	0.07

Figure 5.18 illustrates parity plots of biomass concentration, substrate utilisation and product formation obtained in the two different scale bioreactors. Although some disparities were observed for D-dulcitol (Figure 5.18 (F)) and D-xylitol (Figure 5.18 (G)) consumption profiles, the R^2 values recorded for the main factors such as biomass concentration (Figure 5.18 (A)), CV2025 ω-TAm volumetric activity (Figure 5.18 (B)), CV2025 ω-TAm specific activity (Figure 5.18 (C)), D-mannitol (Figure 5.18 (D)), and glycerol (Figure 5.18 (E)) were greater than 0.95, indicating good reproducibility between the two scales. In general, along with the results discussed in Section 5.3.3.1, the results here further confirmed the reproducibility of the CV2025 ω-TAm production between the two reactors using vinasse medium. This gives an initial insight into the potential of biocatalyst production using a renewable feedstock on a larger scale.

(A)

R²=0.9743

7.5 L STR [Biomass concentration] (g_{dcw} L^{-1})

Controlled MBR [Biomass concentration] (g_{dcw} L^{-1})

(B)

R²=0.998

7.5 L STR [CV2025 ω-TAm volumetric activity] (U ml^{-1})

Controlled MBR [CV2025 ω-TAm volumetric activity] (U ml^{-1})

(C)

R²=0.9980

7.5 L STR [CV2025 ω-TAm specific activity] (U g_{dcw}^{-1})

Controlled MBR [CV2025 ω-TAm specific activity] (U g_{dcw}^{-1})

(D)

R²=0.9660

(E)

R²=0.9799

(F)

R²=0.9092

164
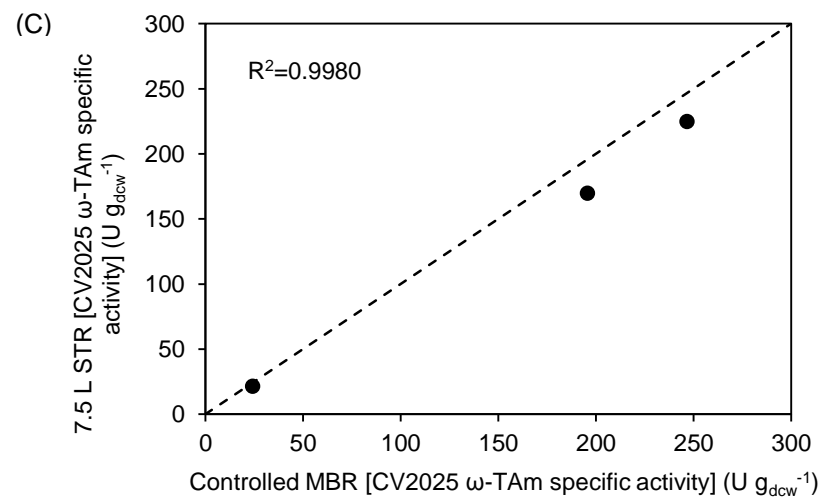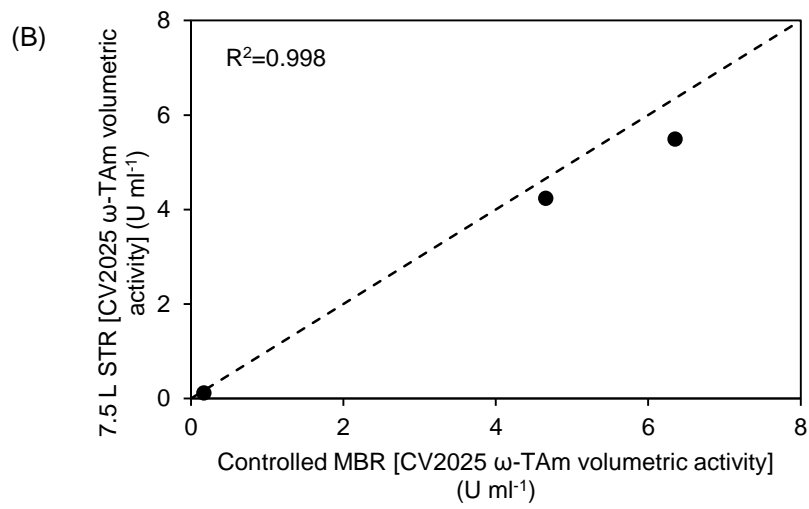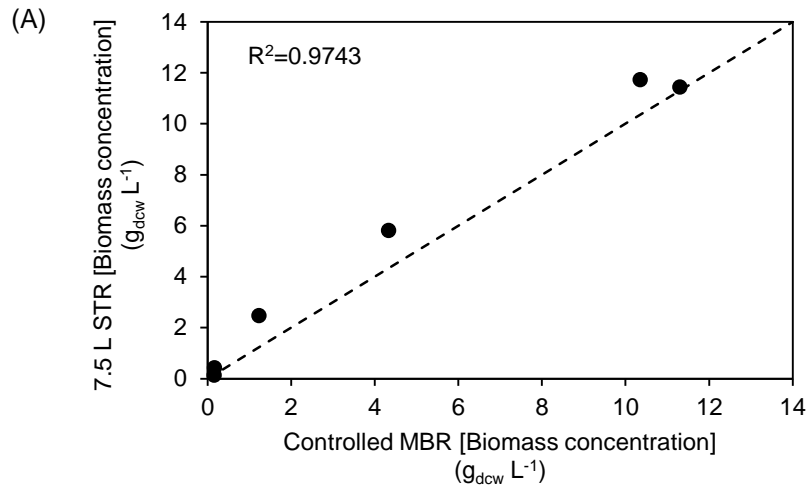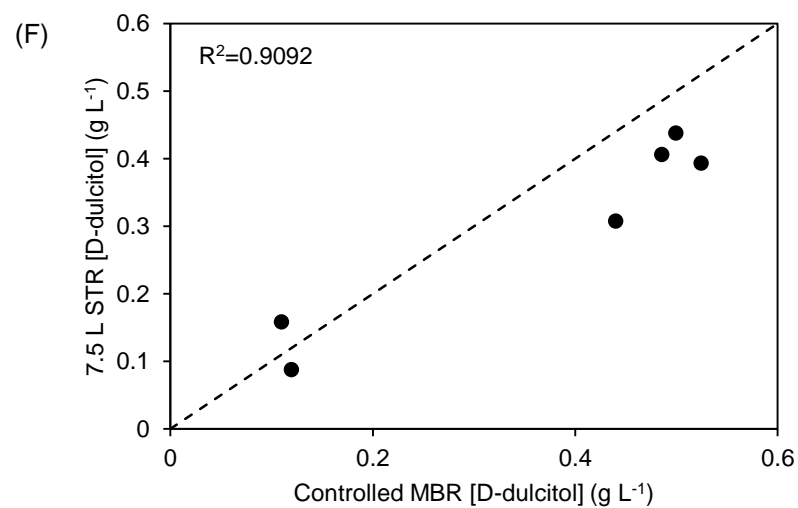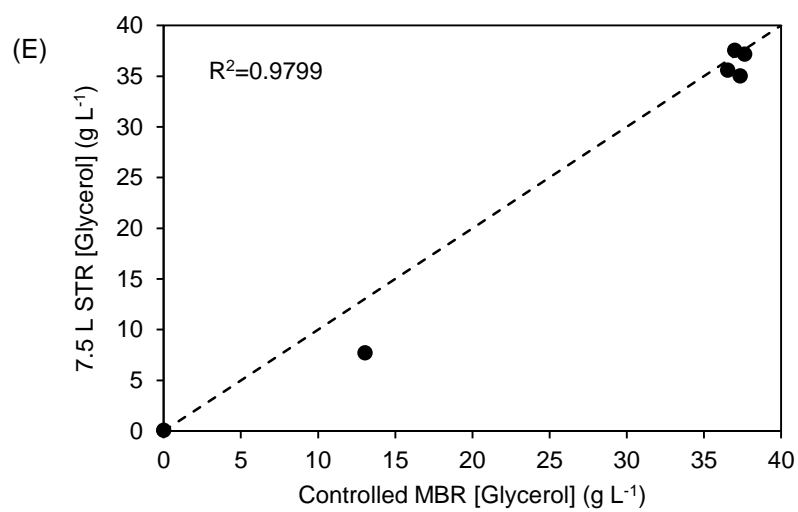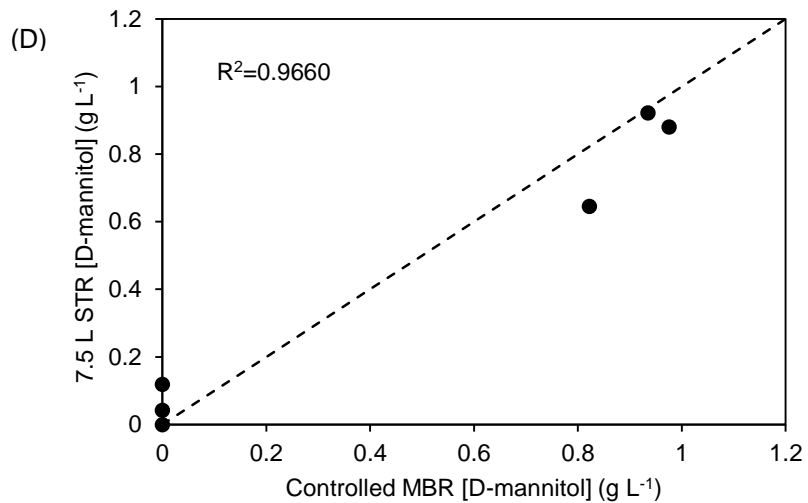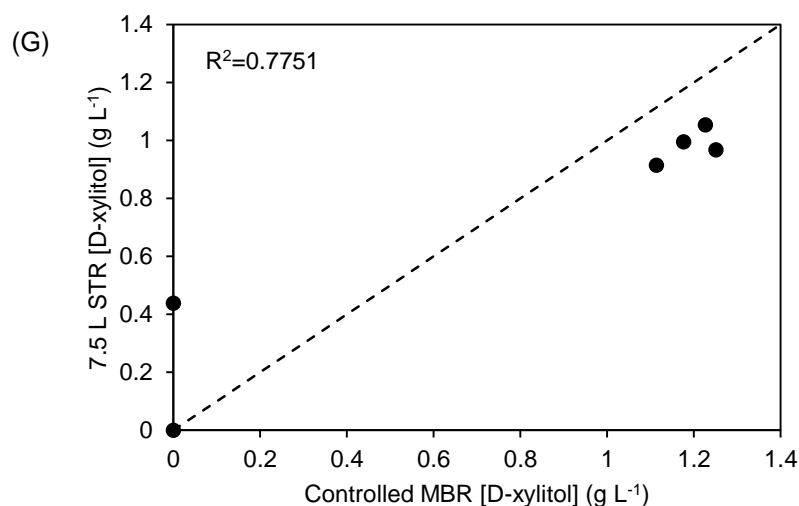
**Figure 5.18.** Parity plots of (A) biomass concentration, (B) CV2025 ω-TAm volumetric activity (C) CV2025 ω-TAm specific activity, (D) D-mannitol, (E) glycerol, (F) D-dulcitol and (G) D-xylitol consumption in the controlled MBR and 7.5 L STR. Fermentation kinetics were shown in Figure 5.15 (controlled MBR) and Figure 5.16 (7.5 L STR), respectively. Dotted lines represent parity lines (x=y).

5.3.3.3 Opportunities and challenges of scale translation between the controlled MBR and STR

In comparison to conventional MWP technologies (Section 1.4.1), one of the benefits of scaling up using a controlled MBR system is the potential for pH and DO control. Most previous studies that reported on scale-up between MWP and STR did not have pH and DO control at the microwell scale (Ferreira-Torres *et al.*, 2005; Islam *et al.*, 2008; Kensy *et al.*, 2009a; Baboo *et al.*, 2012). As discussed in Section 3.2.2, accumulation of organic acid such as acetate during fermentation in shake flasks with no pH control leads to a severe drop in pH from 7 to about 5.6, thus resulting in inhibition of cell growth and consequently a reduction in product titre. Moreover, the lack of direct gas sparging and DO control may also cause oxygen-limitation. This will retard the growth of aerobic microorganisms and consequently hinder the optimal production of protein of interest while may also trigger the synthesis of the undesirable side products (Marques *et al.*, 2010). Therefore, the availability of pH and DO control during the scale translation between the controlled MBR and STR as demonstrated in this work, will enable better defined and more predictive scale-up than in the earlier MWP studies.

One limitation, however, is the small window in which k_La values overlap between the controlled MBR and 7.5 L STR and the lower values found in the controlled MBR (Section 5.3.1). Whilst the mixing in the controlled MBR can be considered ideal at 800 rpm, nonetheless, the k_La value attained at that particular speed in the 7.5 L STR was lower than matched k_La values used in previous works which ranged between 115 and 277 h^{-1} (Michelleti *et al.*, 2006; Islam *et al.*, 2008;

Baboo *et al.*, 2012). Further intensification of biocatalyst production in STR may be thereof be expected by enhancing k_La and oxygen transfer rate.

In general, the scale-up approach based on similar k_La values and specific aeration rates as demonstrated in this study was found adequate to support the scale translation between the controlled MBR and STR for both media. This confirms the reliability of the former platform as a small scale system that can support rapid and parallel studies of biocatalyst production as discussed in Section 3.3.3 (complex medium) and Section 4.3.4 (vinasse medium). In the subsequent section, opportunities for further intensification of CV2025 ω-TAm production in the 7.5 L STR at higher k_La values will be explored.

5.3.4 Enhancement of STR biocatalyst productivity at higher k_La values

Having established a feasible basis for scale-up, the feasibility of further enhancing CV2025 ω-TAm production in the 7.5 L STR using both media was explored. The k_La during fermentation was increased by 4-fold resulting in agitation speeds of 1073 and 818 rpm in complex and vinasse media, respectively. The increased k_La values in both media were chosen so as to yield agitation speeds that lie within the normal range operated for a 7.5 L STR, which is approximately between 600 and 1000 rpm. Figures 5.19 and 5.20 show the fermentation kinetic profiles achieved in the 7.5 L STR at the abovementioned agitation speeds using complex and vinasse media, respectively.

In fermentations using a complex medium (Figure 5.19 (A)), increasing the k_La by 4-fold led to an increase in maximum biomass concentration and volumetric CV2025 ω-TAm activity by about 1.2 and 1.4-fold, respectively. Meanwhile, in vinasse medium (Figure 5.20 (A)), it was found that the maximum biomass concentration increased by 1.4-fold whereas the volumetric CV2025 ω-TAm activity rose by 1.9 fold. These results show that there is some potential to further improve fermentation performance by increasing k_La once the initial scale-up has been verified. As also shown in Figures 5.19 (A) and 5.20 (A) the carbon source utilisation follows the same trends as shown previously (Figures 5.11 and 5.16) only they occur slightly more rapidly due to the increased cell growth and CV2025 ω-TAm synthesis. Table 5.9 summarises the kinetic parameters obtained from fermentations performed using both media.
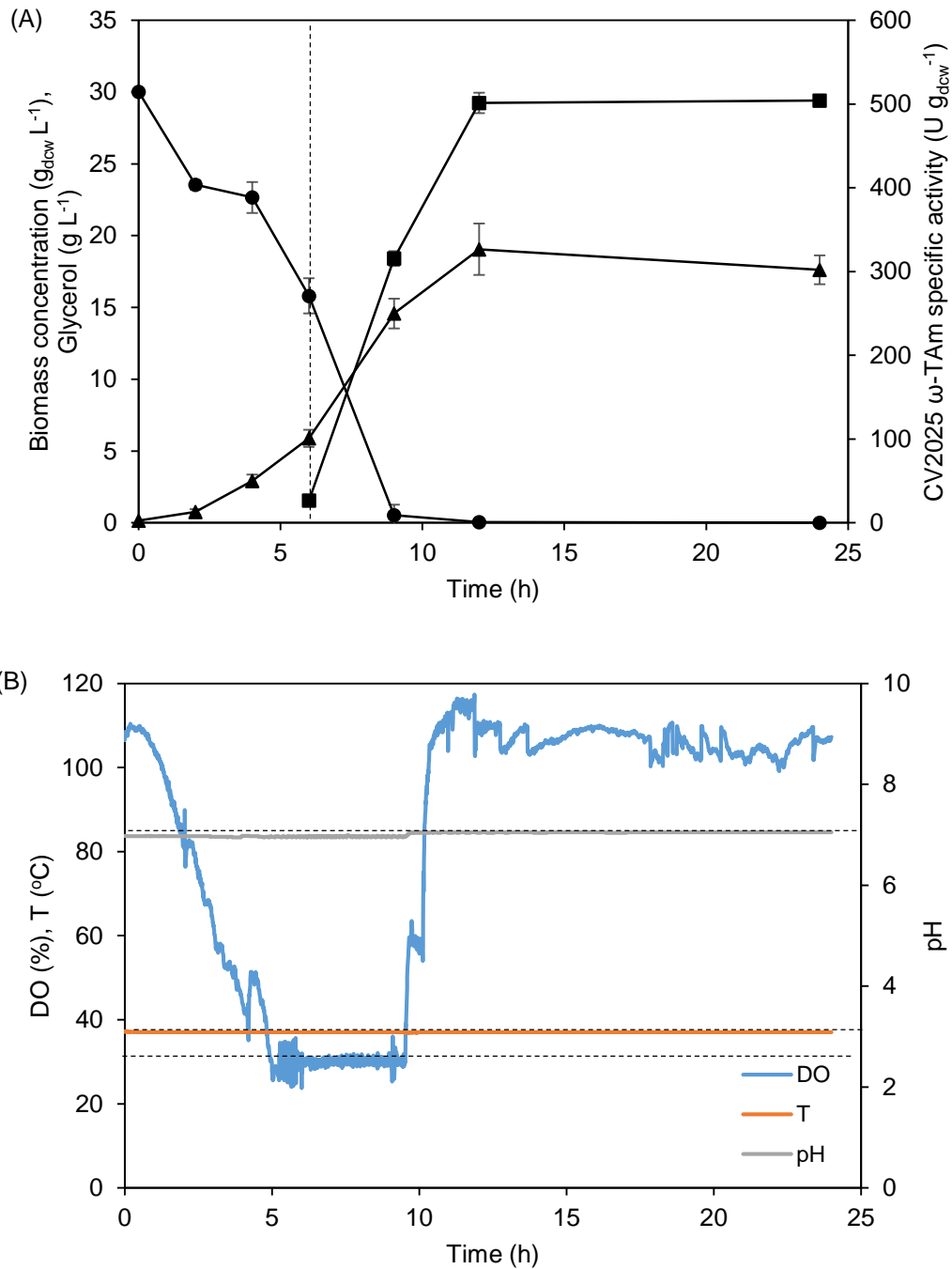
Figure 5.19. (A) *E. coli* BL21 (DE3) fermentation kinetics in the 7.5 L STR using complex medium at a $k_L a$ of 302 h^{-1}. Dotted vertical line indicates the point of IPTG induction: (▲) biomass concentration, (●) glycerol, (■) CV2025 ω-TAm specific activity. (B) Online data showing DO, temperature and pH profiles obtained in the 7.5 L STR throughout the fermentation course. Dotted vertical line indicates the point of IPTG induction. Dotted horizontal lines indicate the set point for each process parameter. Error bars denote one standard deviation about the mean (n=3). Fermentations were performed as described in Section 2.8.3. Analytical procedures were performed as described in Section 2.12.2 (biomass concentration), Section 2.12.5 (CV2025 ω-TAm assay) and Section 2.12.6 (glycerol).
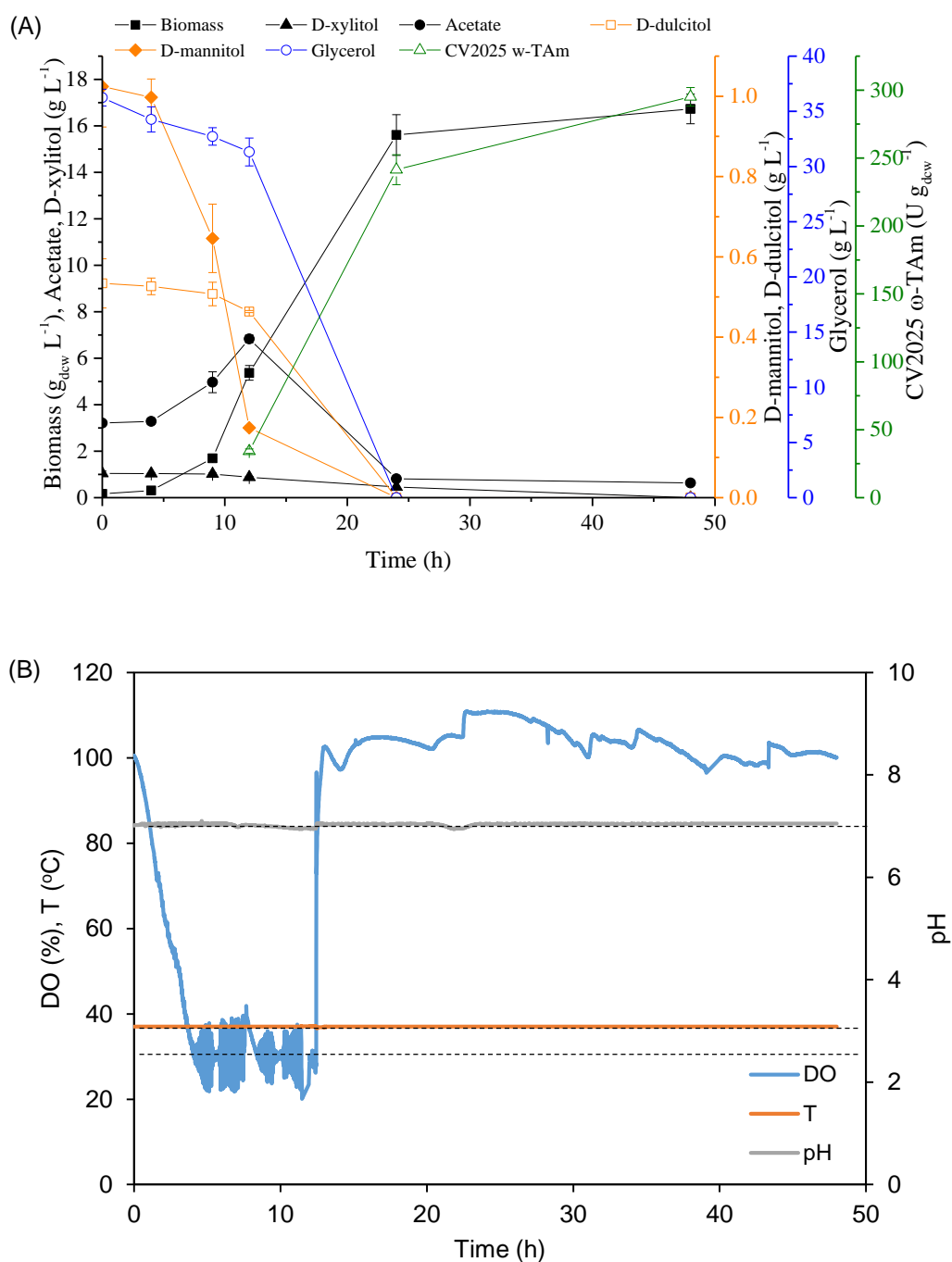
Figure 5.20. (A) *E. coli* BL21 (DE3) fermentation kinetics in the 7.5 L STR using vinasse medium at a k_La of 264 h^{-1} (B) Online data showing DO, temperature and pH profiles obtained in the 7.5 L STR throughout the fermentation course. Dotted horizontal lines indicate the set point for each process parameter. Error bars denote one standard deviation about the mean (n=3). Fermentations were performed as described in Section 2.8.3. Analytical procedures were performed as described in Section 2.12.2 (biomass concentration), Section 2.12.5 (CV2025 ω-TAm assay), Section 2.12.6 (glycerol and acetate) and Section 2.12.7 (sugars and sugar alcohols).

Table 5.9. Comparison of fermentation kinetic parameters in the 7.5 L STR using complex and vinasse media at initial scale-up k_La values and 4-fold increased k_La values. Fermentation kinetics were shown in Figure 5.19 (A) (complex medium) and Figure 5.20 (A) (vinasse medium). Fermentations were performed as described in Section 2.8.3. Analytical procedures were performed as described in Section 2.12.2 (biomass concentration), Section 2.12.5 (CV2025 ω-TAm assay).

Medium	k_La (h^{-1})	μ (h^{-1})	X_{max} (g$_{dcw}$ L^{-1})	Maximum CV2025 ω-TAm specific activity (U g$_{dcw}$$^{-1}$)	Maximum CV2025 ω-TAm volumetric activity (U mL^{-1})
Complex medium	75	0.38 ± 0.01	15.5 ± 0.7	453.5 ± 15.0	14.3 ± 0.2
	302	0.43 ± 0.04	19.1 ± 1.8	504.2 ± 4.0	20.5 ± 0.8
Vinasse medium	66	0.35 ± 0.02	11.7 ± 0.2	224.7 ± 10.4	5.5 ± 0.5
	264	0.35 ± 0.03	16.7 ± 0.6	295.1 ± 6.9	10.6 ± 0.1

Finally since DO could be adequately controlled in the fermentations with both media, developments could focus on fed-batch operation to increase biomass and CV2025 ω-TAm yields further. In this case, other scale-up bases might need to be considered such as matched mixing time that has been reported to be relevant for high cell density cultivation of yeast and *E. coli* fed-batch cultures (Junker, 2004).

5.4 Summary

The overall aim of this chapter of establishing a suitable basis for scale-up of controlled MBR fermentations to a stirred laboratory scale reactor has been achieved. Initially, characterisation of k_La in both reactors was performed (Section 5.3.1). This provided an understanding of how oxygen transfer capability varied as a function of bioreactor operating conditions (Figures 5.2 and 5.3). The overlap in k_La values at the two scales suggested the feasibility of using matched k_La as a suitable basis for *E. coli* cultivations from the controlled MBR to a 7.5 L STR (Section 5.3.3) for both complex (Figures 5.10, 5.11 and 5.12) and vinasse media (Figures 5.15, 5.16 and 5.17).

In the case of the vinasse medium, a suitable pre-processing procedure particularly for large scale fermentations has been proposed (Section 5.3.2). The feasibility of using pasteurised dilute vinasse directly for fermentations has further enhanced the viability of this feedstock for use within an integrated sugar beet biorefinery (Figures 5.6 and 5.8). The minimal pre-processing required with no additional sterilisation after ethanol distillation offers an economic advantage in terms of time and energy saving. Furthermore, the use of pasteurised dilute vinasse has been proven to

be feasible for a laboratory scale fermentation as demonstrated in the 7.5 L STR (Sections 5.3.3 and 5.3.4).

The scale-up comparisons with both complex and vinasse media showed good comparability in terms of the trends in cell growth, substrate consumption and product formation (Section 5.3.3). Although further improvement could be made in order to increase the comparability of maximum biomass concentration and CV2025 ω-TAm volumetric activity for fermentations using a complex medium (Figures 5.10 – 5.12), the results shown in vinasse medium were nonetheless promising with little significant difference between the two scales (Figures 5.15 – 5.17). Overall, the feasibility of a 769-fold scale-up between the two reactors has confirmed the promising role of the controlled MBR as a HTP platform for early process development studies. Further enhancement of the biocatalyst production at higher $k_L a$ values (Section 5.3.4) indicated the potential of further improving fermentation performance at STR scale (Table 5.9). In the following chapter, general conclusions from these studies and recommendations for future work will be discussed.

CHAPTER 6

GENERAL CONCLUSIONS AND FUTURE WORK

6.1 General conclusions

The emerging need for cost effective and sustainable productions of industrial biocatalysts has spurred on the creation of new technologies to speed their development and optimise their manufacture. This work has established HTP methodologies for characterisation and optimisation of industrial biocatalysts for use within a biorefinery context in line with the main aim of this thesis as stated in Section 1.9. The research undertaken has demonstrated a novel concept for on-site production of CV2025 ω-TAm within the framework of an integrated sugar beet biorefinery. This has been achieved by exploitation of one of the biorefinery waste streams, sugar beet vinasse as a cheap and renewable fermentation feedstock. Several key findings and their significance will be discussed in detail in the following sub sections.

6.1.1 Controlled MBR

As mentioned in Chapter 3, the primary objective was to establish a parallel cultivation platform using a 24-well, controlled MBR system (Micro-24) to characterise biocatalyst production (Figure 2.2). Initially, the basic culture conditions for CV2025 ω-TAm production were established whereby a suitable synthetic-based medium that favoured maximum biomass concentration and biocatalyst titre was selected (Section 3.3.1). In particular, the results indicated superior performance with a complex medium (Figures 3.1 and 3.2). Establishment of a standard culture using a pre-defined medium in shake flasks served as a first benchmark in this study for later comparison with the results obtained using the controlled MBR and also vinasse medium. Subsequently, the utility of the controlled MBR was first evaluated in terms of measurement and control of key process parameters like temperature, pH and DO (Figure 3.3) as well as the culture reproducibility (Figures 3.4 and 3.5). Good measurement and control of the process parameters were observed and this has validated the functionality of the MBR in providing a controlled environment throughout the cultivation. Furthermore, the reproducibility of the culture performance throughout the MBR has confirmed the suitability of the platform for parallel studies. Following that, an *E. coli* BL21 (DE3) fermentation expressing CV2025 ω-TAm was successfully developed in the controlled MBR system (Section 3.3.2), demonstrating enhancements of 3.7, 2.1 and 2.2-fold of maximum biomass concentration (Figure 3.6), CV2025 ω-TAm volumetric and specific activity respectively, over the conventional shake flask culture. This has further confirmed the advantages offered by the MBR as a result of the provision of a controlled environment during cultivations.

6.1.2 Optimisation of biocatalyst production

The utility of the controlled MBR was further demonstrated by optimising CV2025 ω-TAm production using both complex and vinasse media. In the former case, the influence of several factors such as induction time, inducer concentration and DO level on the fermentation performance were investigated in parallel (Section 3.3.3). While a DO of 30% was found adequate to support the *E. coli* BL21 (DE3) fermentation expressing CV2025 ω-TAm in the controlled MBR system (Table 3.2), the best induction strategies involved induction during the early logarithmic growth phase (6 h) with volumetric and specific IPTG concentrations of 0.1 mM (Figures 3.9 (A) and 3.11) and 23.7 μmol g_{dcw}^{-1} (Figure 3.13), respectively. An enhancement of 2 and 1.4-fold of maximum CV2025 ω-TAm volumetric and specific activity respectively, were achieved in comparison with the non-optimised performance. The fermentation performance achieved using a pre-defined medium here served as a benchmark for comparison with the cultivations using vinasse medium.

Optimisation of CV2025 ω-TAm using vinasse medium was carried out in the controlled MBR by investigating the influence of supplementation of the medium with several media components (i.e. trace elements and nitrogenous substrates). The results showed that nitrogenous substrates had a positive impact on the fermentation performance (Section 4.3.4). In comparison with the non-supplemented case, the results showed that supplementation of dilute vinasse with 10 g L^{-1} yeast extract resulted in enhancements in specific growth rate and maximum biomass concentration by about 2.8 and 2.5-fold, respectively (Figure 4.14 and Table 4.2). Meanwhile, the intensification of the CV2025 ω-TAm volumetric and specific activity were 5.5 and 3 times, respectively higher than that obtained using the non-supplemented culture (Figure 4.15). Generally, it has been shown that the utility of the controlled MBR mimics a conventional STR. For the optimisation studies using both complex and vinasse media it has been demonstrated that an optimal titre of CV2025 ω-TAm was successfully achieved.

6.1.3 Scalability of controlled MBR results

Following establishment of optimal CV2025 ω-TAm production conditions using both complex and vinasse media in the controlled MBR, another objective was to scale-up the optimised production yields to a larger scale reactor (Section 1.9). These results are discussed in Chapter 5. The scale-up methodology used was based on matched k_La values and specific aeration rates between the two reactors. Initially, the k_La was characterised in the controlled MBR system (Figure 5.2) and 7.5 L STR (Figure 5.3) using water, complex and vinasse media. Suitable k_La correlations were developed for the case of the 7.5 L STR (Equations 5.1 – 5.3). In general, the results showed a linear relationship shown in water (Figure 5.4 (A)) and complex medium (Figure 5.4 (B)) was found to be in a good agreement with R^2 values greater than 0.90. For vinasse medium, prior to the scale-up work, several possible options for pre-processing were investigated (Section 5.3.2). The results suggested that the use of pasteurised dilute vinasse was the most relevant

considering both practicability and feasibility. Having a nearly comparable fermentation performance with that obtained using the filtered dilute vinasse in terms of cell growth (Figure 5.6) and biocatalyst titre (Figure 5.8), the option offers another economic advantage in terms of time and energy saving since no additional sterilisation is required after the ethanol distillation and pasteurisation.

As discussed in Section 5.3.3, it was shown that the scale-up strategy based on matched k_La values and specific aeration rates was suitable to achieve reproducible batch fermentation performance using both media between the controlled MBR and laboratory scale reactor. Although notable discrepancies were seen in the utilisation of certain substrates (Figures 5.13 (D), 5.18 (F) and 5.18 (G)), a good reproducibility in terms of biomass concentration (Figures 5.13 (A), 5.18 (A)) and CV2025 ω-TAm production (Figures 5.13 (C), 5.18 (B) and 5.18 (C)) was observed between the two scales for both media with the R^2 values attained of more than 0.95. Generally, the consistency of the fermentation performance and biocatalyst titre achieved using both media has confirmed the feasibility of a 769-fold scale translation between the two reactors. This further validates the significant role of the controlled MBR as a HTP platform to support early process development studies for industrial biocatalysts production.

Eventually, further enhancement of biocatalyst activity in the 7.5 L STR using both complex and vinasse media was performed by increasing the k_La by 4-fold (Section 5.3.4). An increase of about 1.2-fold of the maximum biomass concentration and 1.5-fold of the maximum volumetric CV2025 ω-TAm activity were achieved in the complex medium system while in the vinasse medium, the further enhancements were 1.4 and 1.9-fold, respectively (Table 5.9). In both cases, the results suggested that by increasing the OTR in the STR, the fermentation performance can be enhanced, indicating the potential of further process intensification upon. In conclusion, the key findings in Chapter 5 included the predictive methodologies for scaling up the optimal CV2025 ω-TAm production from the controlled MBR to a 7.5 L STR using both complex and vinasse media. The feasibility of the scale translation between the two platforms is crucial in ensuring the relevance of the process developed in the controlled MBR to industrial applications.

6.1.4 Vinasse as a fermentation feedstock

The need for the production of industrial biocatalysts such as CV2025 ω-TAm as demonstrated in this study, has stemmed from the future demand for integrated biorefinery designs, which can realize the effective exploitation of monosaccharides derived from SBP such as L-arabinose and D-galacturonic acid (Cardenas *et al.*, 2017). Sugar beet vinasse appears to be an interesting fermentation feedstock for biocatalyst production due to its abundant availability and high concentration of glycerol.

As discussed in Chapter 4, exploitation of sugar beet vinasse as a fermentation feedstock for CV2025 ω-TAm production led to the discovery of several significant insights. The

characterisation studies confirmed the presence of several useful compounds in vinasse with the major component being glycerol (Table 4.1). Assessment on the batch to batch stability of vinasse showed the comparability of the feedstock with respect to the fermentation performance (Figure 4.7) and enzyme activity (Figure 4.8). It was observed that cell growth and CV2025 ω-TAm production were feasible at vinasse concentration between 17 and 25% (v/v), while higher concentrations (50 and 100% (v/v)) were found to be inhibitory (Figure 4.2).

Evaluation of the impact of induction using IPTG showed that comparable expression of CV2025 ω-TAm was achieved in both non-induced and induced fermentations (Figures 4.3 and 4.4). This was confirmed to be due to an auto-induction phenomenon promoted by the presence of D-galactose in vinasse (Figures 4.5 and 4.6). The auto-induction in vinasse has contributed another potential benefit of the feedstock removing the need for IPTG as an inducer, which is expensive and can be cytotoxic. An assessment on the pre-processing options of vinasse for a fermentation (Section 4.3.3) showed that dilution with water was sufficient to reduce the glycerol concentration to a fermentable level as well as inhibitory polyphenols. This eliminates the need for laborious pre-treatment steps to remove the latter compound (Figures 4.12 and 4.13). Upon the optimisation of the vinasse medium (Figure 4.15), the optimal titre of CV2025 ω-TAm was found to represent 81% of the performance achieved using a complex medium. This has further confirmed the promising performance of the vinasse medium in comparison with the standard pre-defined medium.

This part of the thesis also demonstrated the metabolic preference of *E. coli* BL21 (DE3) in the presence of multiple carbon sources in vinasse (Section 4.3.5). The findings suggested that sequential metabolism occurred between D-mannitol and glycerol with the former being the primary carbon source (Figure 4.16). The occurrence of CCR between D-mannitol and glycerol was predicted, which has not been reported previously in the literature. An additional study to further understand *E. coli* BL21 (DE3) metabolic preferences in the presence of D-glucose and vinasse medium showed that the former sugar was favoured over D-mannitol during the fermentation (Figure 4.17). The knowledge gained here could facilitate better understanding on the metabolism of *E. coli* BL21 (DE3) when grown on multiple carbon sources. In addition, this could aid the decision for the feeding substrate during fed-batch fermentations using vinasse medium in future.

Overall, the results achieved here have confirmed the feasibility and potential benefits of vinasse as a fermentation feedstock, which further provides novel insights into the potential for on-site industrial biocatalyst production within an integrated sugar beet biorefinery. Whilst the focus of this study was on the production of CV2025 ω-TAm in *E. coli* BL21 (DE3), the same approach may be undertaken for production of other valuable bioproducts in other microorganisms. Utilisation of an inexpensive fermentation feedstock such as vinasse will help to increase the sustainability of an integrated biorefinery industry in future.

6.2 Future work

Future work comprises studies to clarify and extend some of the findings reported here and also to explore the broader context of the work. These are discussed in detail below:

- A more in-depth study to further increase the enzyme titre using either synthetic or vinasse-based media could be undertaken. Here the application of DoE methods to evaluate more factors and investigating the interactions between factors could be beneficial.

- Detailed studies on the mechanism of auto-induction by D-galactose in vinasse medium is considered essential. Furthermore, the auto-induction strategy could be optimised further by addition of more D-galactose and investigation of induction time and temperature.

- Development of a HTP microreactor with a feeding system will be an advantage in developing fed-batch approaches for biocatalyst production in order to further enhance the cell growth and enzyme titre.

- A comparative bioconversion study using CV2025 ω-TAm produced from vinasse with that produced from a synthetic medium is required in order to assess the utility of the biocatalysts produced. The studies should consider various aspects including comparison of the biocatalytic performance between whole cell, lysate and pure enzyme, substrate screening and also strategies to enhance the biocatalytic activity. Evaluation of the monomers derived from SBP such as L-arabinose and D-galacturonic acid as the substrates may also be attractive. If the use of pure enzyme is considered beneficial for the bioconversion then, future studies should also consider the purification of the CV2025 ω-TAm.

- The possibility of integrating fermentation and bioconversion using whole cell biocatalyst into a single-pot process could also be explored. Optimisation of the bioconversion will be necessary in order to enhance the viability of the whole process.

- The proof-of-concept of vinasse as a fermentation feedstock can be further extended to other processes involving different microorganisms and target enzymes. This could expand the utility and flexibility of the feedstock especially when its production is expected to increase with the growing demand for bioethanol in the near future. Moreover, this can also contribute an economic advantage to the biorefinery industry.

- As discussed in Section 4.3.4, whilst the supplementation of vinasse medium with yeast extract has intensified the biocatalyst titre significantly, the additional cost associated with the yeast extract must also be taken into account, especially for large scale operation.

Further biorefinery integration could be explored such as by generating yeast extract on-site from the *S. cerevisae* biomass waste stream obtained after the bioethanol fermentation. This will require development of an autolysis process using either dried or wet yeast cells. The development of an on-site autolysis process will not just benefit the supplementation of vinasse for a bioproduction but it may also contribute another potential product stream to the biorefinery. Following that, studies of the autolysis itself such as process optimisation, characterisation and evaluation of the resulting yeast extract should be performed.

- In gaining a fundamental insight into the *E. coli* BL21 (DE3) metabolism when grown in media with multiple carbon sources such as vinasse, an assessment on genes and enzymes involved in the metabolic pathway is necessary. Additionally, studies involving measurement of the promoter activity coupled with the cell growth assessment might also be beneficial to optimise utilisation of all carbohydrates present in the vinasse.

- Building on development of a microreactor suitable for fed-batch operation, different feeding strategies may also be investigated. In the case of vinasse medium, variability of the feeding materials whether fresh dilute vinasse or glycerol should be determined.

- Different scale-up options involving other parameters and their combination should be investigated in translating the optimal production of the biocatalyst from microreactors to even larger scale reactors. This may facilitate an effective scale-up of fed-batch operations in future.

- Finally, it would be beneficial to perform a comparative economic analysis of the costs and constraints regarding biocatalyst production from synthetic and vinasse media. This will provide a definitive picture on the feasibility of using vinasse to produce industrial enzymes within an integrated sugar beet biorefinery.

REFERENCES

Adler, J., Epstein, W. (1974). Phosphotransferase-system enzymes as chemoreceptors for certain sugars in *Escherichia coli* chemotaxis. *Proceedings of the National Academy of Sciences of the United States of America*, 71 (7), 2895–2899.

Adnan, N. A. A., Suhaimi, S.N., Abd-Aziz, S., Hassan, M. A., Phang, L. Y. (2014). Optimization of bioethanol production from glycerol by *Escherichia coli* SS1, *Renewable Energy*, 66, 625–633.

Aidelberg, G., Towbin, B. D., Rothschild, D., Dekel, E., Bren, A., Alon, U. (2014). Hierarchy of non-glucose sugars in *Escherichia coli. BMC Systems Biology*, 8, 133.

Akoh, C. C., Chang, S. W., Lee, G. C., Shaw, J. F. (2008). Biocatalysis for the production of industrial products and functional foods from rice and other agricultural produce. *Journal of Agricultural and Food Chemistry*, 56, 10445–10451.

Allison, N., Richards, J. (2013). Current status and future trends for disposable technology in the biopharmaceutical industry. *Journal of Chemical Technology and Biotechnology*, 89 (9), 1283-1287.

Amanullah, A., Otero, J. M., Mikola, M., Hsu, A., Zhang, J., Aunins, J., Schreyer, H. B., Hope, J. A., Russo, A. P. (2010). Novel micro-bioreactor high throughput technology for cell culture process development: Reproducibility and scalability assessment of fed-batch CHO cultures. *Biotechnology and Bioengineering*, 106, 57–67.

Anitha, M., Kamarudin, S. K., Kofli, N. T. (2016). The potential of glycerol as a value-added commodity. *Chemical Engineering Journal*, 295, 119-130.

Ascanio, G. (2015). Mixing time in stirred vessels: A review of experimental techniques. *Chinese Journal of Chemical Engineering*, 23, 1065-1076.

Baboo, J. Z., Galman, J. L., Lye, G. J., Ward, J. M., Hailes, H. C., Micheletti, M. (2012). An automated microscale platform for evaluation and optimization of oxidative bioconversion processes. *Biotechnology Progress*, 28 (2), 392–405.

Back, A., Rossignol, T., Krier, F., Nicaud, J. M., Dhulster, P. (2016). High-throughput fermentation screening for the yeast *Yarrowia lipolytica* with real-time monitoring of biomass and lipid production. *Microbial Cell Factories*, 15, 147.

Bareither, R., Pollard, D. (2011). A review of the advanced small scale parallel bioreactor technology for accelerated process development. *Biotechnology Progress*, 27 (1), 2–14.

Barrett, T. A., Wu, A., Zhang, H., Levy, M. S., Lye, G. J. (2010). Microwell engineering characterization for mammalian cell culture process development. *Biotechnology and Bioengineering,* 105, 260–75.

Barrocal, V. M., Garcia-Cubero, M. T., Gonzalez-Benito, G., Coca, M. (2010). Production of biomass by *Spirulina maxima* using sugar beet vinasse in growth media. *New Biotechnology*, 27 (6), 851–856.

Bech Jensen, E. and Carlsen, S. (1990). Production of recombinant human growth hormone in *Escherichia coli*: Expression of different precursors and physiological effects of glucose, acetate and salts. *Biotechnology and Bioengineering,* 36, 1-11.

Beltran, J., Dominguez, J., Partido, E. (2005). Physico-chemical treatment for the depuration of wine distillery wastewaters (vinasses). *Water Science and Technology*, 51, 159–166.

Benitez, F., Real, F., Acero, J., Garcia, J. Sanchez, M. (2003). Kinetics of ozonation and aerobic biodegradation of wine vinasses in discontinuous and continuous processes. *Journal of Hazardous Materials*, 101, 203–218.

Betts, J. P. J. (2014). Incorporation of developability into cell line selection. EngD Thesis, University College London.

Betts, J. P. J., Warr, S. R. C., Finka, G. B., Uden, M., Town, M., Janda, J. M., Baganz, F., Lye, G. J. (2014). Impact of aeration strategies on fed-batch cell culture kinetics in a single-use 24-well miniature bioreactor. *Biochemical Engineering Journal*, 82, 105–116.

Bhaskar, G. (2004). A short stereoselective synthesis chloroamphenicol and (+) thiamphenicol. *Tetrahedron: Asymmetry*, 15, 1279-1283.

Bhattacharyya, A., Pramanik, A., Maji, S. K., Haldar, S., Mukhopadhyay, U. K., Mukherjee, J. (2012). Utilisation of vinasse for production of poly-3-(hydroxybutyrate-co-hydroxyvalerate) by *Haloferax mediterranei*. *AMB Express*, 2 (1), 34.

Bohon, M. D., Metzger, B. A., Linak, W. P., King, C.J., Roberts, W.L. (2011). Glycerol combustion and emissions. *Proceedings of the Combustion Institute, 33*, 2717–2724.

Borges, M.R., Balaban, R. D. C. (2014). L-Arabinose (pyranose and furanose rings)-branched poly(vinyl alcohol): enzymatic synthesis of the sugar esters followed by free radical polymerization. *Journal of Biotechnology*, 192, 42–49.

Borgnia, M. J., Agre, P. (2001). Reconstitution and functional comparison of purified GlpF and AqpZ, the glycerol and water channels from *Escherichia coli*. *Proceedings of the National Academy of Sciences of the United States of America*, 98 (5), 2888–93.

Boruwa, J., Borah, J. C., Gogoi, S. and Barua, N. C. (2005). A short asymmetric total synthesis of chloramphenicol using a selectively protected 1,2-diol. *Tetrahedron Letters*. 46, 1743-1746.

Bradford, M. M. (1976). A rapid and sensitive method for the quantitation of microgram quantities of protein utilizing the principle of protein-dye binding. *Analytical Biochemistry*, 72, 248–54.

British Sugar, Personal Communication (2017).

Brunhuber, N. M., Blanchard, J. S. (1994). The biochemistry and enzymology of amino acid dehydrogenases. *Critical Reviews in Biochemistry and Molecular Biology*, 29, 415–467.

Buchholz, K., Kasche, V., Bornscheuer, U. T. (2005). Biocatalysts and enzyme technology, WILEY-VCH Verlag GmbH & Co. KGaA, Weinheim (Introduction to Enzyme Technology).

Buchs J. (2001). Introduction to advantages and problems of shaken cultures. *Biochemical Engineering Journal,* 7, 1–98.

Buchs, J., Maier, U., Milbradt, C., Zoels, B. (2000a). Power consumption in shaking flasks on rotary shaking machines: I. power consumption measurement in unbaffled flasks at low liquid viscosity. *Biotechnology and Bioengineering,* 68, 589–593.

Buchs, J., Maier, U., Milbradt, C., Zoels B. (2000b). Power consumption in shaking flasks on rotary shaking machines: II. non-dimensional description of specific power consumption and flow regimes in unbaffled flasks at elevated liquid viscosity. *Biotechnology and Bioengineering,* 68, 594–601.

Buckland, B. C. (1984). The translation of scale in fermentation processes: the impact of computer process control. *Bio/Technology*, 2, 875–883.

Bunch, A. W. (1994). High cell density growth of micro-organisms. *Biotechnology and Genetic Engineering Reviews*, 12, 535-561.

Burke, F. (2008). Scale up and scale down of fermentation processes, in Practical Fermentation Technology (eds B. McNeil and L. M. Harvey), John Wiley & Sons, Ltd, Chichester, UK.

Çalik, P., Levent, H. (2009). Effects of pretreated beet molasses on benzaldehyde lyase production by recombinant *Escherichia coli* BL21(DE3)pLySs. *Journal of Applied Microbiology*, 107 (5), 1536–1541.

Caner, H., Groner, E., Levy, L. (2004). Trends in the development of chiral drugs. *Drug Discovery Today*, 9 (3), 105-110.

Caqueret, V., Bostyn, S., Cagnon, B., Fauduet, H. (2008). Purification of sugar beet vinasse - Adsorption of polyphenolic and dark colored compounds on different commercial activated carbons. *Bioresource Technology*, 99, 5814–5821.

Cárdenas-Fernández, M., Bawn, M., Bennett, C. E. M., Bharat, P. K. V., Subrizi, F., Suhaili, N., Ward, D. P., Bourdin, S., Dalby, P. A., Hailes, H. C., Hewitson, P., Ignatova, S., Kontoravdi, C., Leak, D. J., Shah, N., Sheppard, T. D., Ward, J. M., Lye, G. J. (2017). An integrated biorefinery concept for conversion of sugar beet pulp into value-added chemicals and pharmaceutical intermediates. *Faraday Discussions*, 202, 415-431.

Casablancas, A., Cárdenas-Fernández, M., Álvaro, G., Benaiges, M. D., Carminal, G., De Mas, C., Gonzalez, G., Lopez, C., López-Santín, J. (2013). New ammonia lyases and amine transaminases: Standardization of production process and preparation of immobilized biocatalysts. *Electronic Journal of Biotechnology*, 16 (3).

Cavalheiro, J. M. B. T., De Almeida, M., Grandfils, C., Da Fonseca, M. (2009). Poly (3-hydroxybutyrate) production by *Cupriavidus necato* using waste glycerol. *Process Biochemistry*, 44, 509-515.

Chae, H. J., Joo H., In, M. J. (2001). Utilisation of brewer's yeast cells for the production of food-grade yeast extract . Part 1 : effects of different enzymatic treatments on solid and protein recovery and flavor characteristics. *Bioresource Technology*, 76, 253–258.

Chatzifragkou, A., Papanikolaou, S., Dietz, D., Doulgeraki, A. I., Nychas, G. J. E, Zeng, A. P. (2011). Production of 1, 3-propanediol by *Clostridium butyricu* growing on biodiesel-derived crude glycerol through a non-sterilized fermentation process. *Applied Microbiology and Biotechnology*, 91, 101-112.

Chauhan, V., Singh, A., Waheed, S. M., Singh, S., Bhatnagar, R. (2001). Constitutive expression of protective antigen gene of Bacillus anthracis in *Escherichia coli*. *Biochemical and Biophysical Research Communications*, 283, 308–315.

Chen, A., Chitta, R., Chang, D., Amanullah, A. (2009). Twenty-four well plate miniature bioreactor system as a scale-down model for cell culture process development. *Biotechnology and Bioengineering*, 102 (1), 148–60.

Choi, J. H., Keum, K. C., Lee, S. Y. (2006). Production of recombinant proteins by high cell density culture of *Escherichia coli*. *Chemical Engineering Science*, 61, 876-885.

Choi, J. H., Lee, S. J., Lee, S. Y. (2003). Enhanced production of insulin-like growth factor I fusion protein in *Escherichia coli* by coexpression of the down-regulated genes identified by transcriptome profiling. *Applied and Environmental Microbiology*, 69, 4737–4742.

Choi, J. H., Lee, S.Y. (2004). Secretory and extracellular production of recombinant proteins using *Escherichia coli*. *Applied Microbiology and Biotechnology,* 64, 625–635.

Choi, J. M., Han, S. S., Kim, H. S. (2015). Industrial applications of enzyme biocatalysis: Current status and future aspects. *Biotechnology Advances*, 33, 1443-1454.

Choi, W. J., Hartono, M. R., Chan, W. H., Yeo, S.S. (2011). Ethanol production from biodiesel-derived crude glycerol by newly isolated *Kluyvera cryocrescen*. *Applied Microbiology and Biotechnology*, 89, 1255-1264.

Christen, P., Metzler, D.E. (1985). Transaminases, NY: Wiley, New York.

Christofoletti, C.A., Escher, J.P., Correia, J.E., Marinho, J.F.U., Fontanetti, C.S. (2013). Sugarcane vinasse: environmental implications of its use. *Waste Management.* 33, 2752–2761.

Cibis, E., Ryznar-Luty, A., Krzywonos, M., Lutoslawski, K., Miskiewicz, T. (2011). Betaine removal during thermo- and mesophilic aerobic batch biodegradation of beet molasses vinasse: Influence of temperature and pH on the progress and efficiency of the process. *Journal of Environmental Management*, 92 (7), 1733–1739.

Cicco, N., Lanorte, M. T., Paraggio, M., Viggiano, M., Lattanzio, V. (2009). A reproducible, rapid and inexpensive Folin-Ciocalteu micro-method in determining phenolics of plant methanol extracts. *Microchemical Journal*, 91 (1), 107–110.

Coca, M., Pena, M., Gonzalez, G. (2006). Chemical oxidation processes for decolorization of brown-colored molasses wastewater. *Ozone: Science and Engineering*, 27, 365 - 369.

Cooper, C. M., Fernstorm, G.A., Miller, S.A. (1944). Performance of agitated gas–liquid contactors. *Industrial and Engineering Chemistry*, 36, 504–509.

Cserjan-Puschmann, M., Grabheer, R., Striedner, G., Clememtschitsch, F., Bayer, K. (2002). Optimizing recombinant microbial fermentation processes: An integrated approach. *Biopharm*, 15, 26–34.

Cui, Y., Cui, W., Liu, Z., Zhou, L., Kobayashi, M., Zhou, Z. (2014). Improvement of stability of nitrile hydratase via protein fragment swapping. *Biochemical and Biophysical Research Communications*, 450 (1), 401–408.

Danckwerts, P. V., Gillham, A. J. (1966). The design of gas absorbers: I. — Methods for predicting rates of absorption with chemical reaction in packed columns, and tests with 11/2in. Raschig rings. *Transactions of the Institution of Chemical Engineers*, 44, T42–54.

de Carvalho, C. C. C. R. (2010). Enzymatic and whole cell catalysis: Finding new strategies for old processes. *Biotechnology Advances*, 29, 75-83.

de Carvalho, C. C. C. R., da Fonseca M. M. R. (2007). Bacterial whole cell biotransformations: in vivo reactions under in vitro conditions. *Dynamic Biochemistry, Process Biotechnology and Molecular Biology*, 1, 32–39.

De Leon, A., Breceda, G. B., de la Rosa, A. P. B., Jimenez-Bremont, J. F., Lopez, Revilla, R. (2003). Galactose induces the expression of penicillin acylase under control of the las promoter in recombinant *Escherichia coli. Biotechnology Letters*, 25, 1397 - 1402.

De Oliveira, B.G., Carvalho, J.L.N., Cerri, C.E.P., Cerri, C.C., Feigl, B.J. (2013). Soil greenhouse gas fluxes from vinasse application in Brazilian sugarcane areas. *Geoderma*, 200, 77-84.

De Roode, B. M., Van Beek, J., Van Der Padt, A., Franssen, M.C.R., Boom, R.M. (2001). The integrated enzymatic production and downstream processing of hexyl glucoside, *Enzyme and Microbial Technology*, 29, 513-520.

Desai, A. A. (2011). Sitagliptin manufacture: a compelling tale of green chemistry, process intensification, and industrial asymmetric catalysis. *Angewandte Chemie*, 50, 1974–1976.

Desai, T. A., Rao, C. V. (2010). Regulation of arabinose and xylose metabolism in *Escherichia* coli. *Applied and Environmental Microbiology*, 76, 1524 - 1532.

Deshpande, R. R., Wittmann, C., Heinzle, E. (2004). Microplates with integrated oxygen sensing for medium optimization in animal cell culture. *Cytotechnology,* 46 (1), 1-8.

Diaz, B., Gomes, A., Freitas, M., Fernandes, E., Nogueira, D. R., Gonzalez, J., Moure, A., Levoso, A., Vinardell, M. P., Mitjans, M., Dominguez, H, Parajo, J. C. (2012). Valuable polyphenolic antioxidants from wine vinasses. *Food and Bioprocess Technology*, 5 (7), 2708–2716.

Dincer, A., Telefoncu, A. (2007). Improving the stability of cellulase by immobilization on modified polyvinyl alcohol coated chitosan beads. *Journal of Molecular Catalysis B: Enzymatic*, 45, 10–14.

Donovan, R. S., Robinson, C. W., Glick, B. R. (1996). Review: optimizing inducer and culture conditions for expression of foreign proteins under the control of the lac promoter. *Journal of Industrial Microbiology*, 16 (3), 145–54.

Doran, P. M. (1995). Bioprocess engineering principles. GB: Academic Press.

Duan, X. G., Chen, S., Chen, J., Wu, J. (2013). Enhancing the cyclodextrin production by synchronous utilisation of isoamylase and alpha-CGTase. *Applied Microbiology Biotechnology*, 97, 3467–3474.

Duetz, W.A., Ruedi, L., Hermann, R., O'Connor, K., Buchs, J., Witholt, B. (2000). Methods for intense aeration, growth, storage, and replication of bacterial strains in microtiter plates. *Applied and Environment Microbiology*, 66, 2641–2646.

Durany, O., Caminal, G., de Mas, C., Lopez-Santin, J. (2004). Studies on the expression of recombinant fuculose-1-phosphate aldolase in *E. coli. Process Biochemistry*, 39, 1677-1684.

Effio, C. L., Baumann, P., Weigel, C., Vormittag, P. (2016). High-throughput process development of an alternative platform for the production of virus-like particles in *Escherichia coli. Journal of Biotechnology,* 219, 7-19.

Einarsson, H., Snygg, B. G., Eriksson, C. (1983). Inhibition of bacterial growth by Maillard reaction products, *Journal of Agriculture and Food Chemistry,* 31, 1043-1047.

Elmahdi, I., Baganz, F., Dixon, K., Harrop, T., Sugden, D., Lye, G. J. (2003). pH control in microwell fermentations of *S. erythraea* CA340: influence on biomass growth kinetics and erythromycin biosynthesis. *Biochemical Engineering Journal*, 16, 299-310.

Espana-Gamboa, E., Mijangos-Cortes, J., Barahona-Perez, L., Dominguez-Maldonado, J., Hernandez-Zarate, G., Alzate-Gaviria, L. (2011). Vinasses: characterization and treatments. *Waste Management and Research*, 29, 1235–1250.

Fadel, M., Zohri, A. A., Makawy, M., Hsona, M. S., Abdel-Aziz, A. M. (2014). Recycling of vinasse in ethanol fermentation and application in Egyptian distillery factories. *African Journal of Biotechnology*, 13 (47), 4390-4398.

Fang, S., Li, J., Liu, L., Du, G., Chen, J. (2011). Overproduction of alkaline polygalacturonate lyase in recombinant *Escherichia coli* by a two-stage glycerol feeding approach. *Bioresource Technology*, 102 (22), 10671–10678.

Fernandes, P. (2010). Miniaturization in biocatalysis, *International Journal of Molecular Sciences,* 11, 858-879.

Fernando, S., Adhikari, S., Chandrapal, C., Murali, N. (2006). Biorefineries: current status, challenges, and future direction. *Energy Fuels*, 20, 1727–1737.

Ferreira-Torres, C., Micheletti, M., Lye, G. J. (2005). Microscale process evaluation of recombinant biocatalyst libraries: application to Baeyer-Villiger monooxygenase catalysed lactone synthesis. *Bioprocess and Biosystems Engineering*, 28, 83-93.

Figaro, S., Louisy-Louis, S., Lambert, J., Ehrhardt, J. J., Ouensanga, A., Gaspard, S. (2006). Adsorption studies of recalcitrant compounds of molasses spentwash on activated carbons. *Water Research,* 40, 3456 - 3466.

Finkenstadt, V. L. (2014). A review on the complete utilisation of the sugarbeet. *Sugar Technology*, 16 (4), 339-346.

Fitzgibbon, F., Nigam, P., Singh, D., Archant, R. (1995). Biological treatment of distillery waste for pollution-remediation. *Journal of Basic Microbiology*, 35, 293-301.

Fu, X., Wei, D., Tong, W. (2006). Effect of yeast extract on the expression of thioredoxin – human parathyroid hormone from recombinant *Escherichia coli. Journal of Chemical Technology and Biotechnology*, 81, 1866–1871.

Gao, Y., Allison, N. (2015). Extractables and leachables issues with the application of single use technology in the biopharmaceutical industry. *Journal of Chemical Technology and Biotechnology,* 91, 289-295.

Garcia-Araya, J. F., Beltran, F. J., Alvarez, P., Massa, F. J. (2003). Activated carbon adsorption of some phenolic compounds present in agroindustrial wastewater. *Adsorption*, 9, 107 - 115.

García-Arrazola, R., Siu, S. C., Chan, G., Buchanan, I., Doyle, B., Titchener-Hooker, N., Baganz, F. (2005). Evaluation of a pH-stat feeding strategy on the production and recovery of Fab' fragments from *E. coli. Biochemical Engineering Journal*, 23 (3), 221–230.

Garcia-Ochoa, F., Gomez, E. (1998). Mass transfer coefficient in stirrer tank reactors for xanthan solutions. *Biochemical Engineering Journal,* 1, 1–10.

Garcia-Ochoa, F., Gomez, E. (2009). Bioreactor scale-up and oxygen transfer rate in microbial processes: An overview. *Biotechnology Advances*, 27 (2), 153–176.

Gavit, P., Better, M. (2000). Production of antifungal recombinant peptides in *Escherichia coli*. *Journal of Biotechnology*, 79, 127–136.

Ghislieri, D., Turner, N. J. (2013). Biocatalytic approaches to the synthesis of enantiomerically pure chiral amines. *Topics in Catalysis*, 57, 284–300.

Gill, N. K., Appleton, M., Baganz, F., Lye, G. J. (2008). Design and characterisation of a miniature stirred bioreactor system for parallel microbial fermentations. *Biochemical Engineering Journal*, 39 (1), 164–176.

Ginovart, M., Prats, C., Portell, X., Silbert, M. (2011). Exploring the lag phase and growth initiation of a yeast culture by means of an individual-based model. *Food Microbiology*, 28 (4), 810–817.

Giomarelli, B., Schumacher, K. M., Taylor, T. E., Sowder, R. C., Hartley, J. L., McMahon, J. B., Mori, T. (2006). Recombinant production of anti-HIV protein, griffithsin, by auto-induction in a fermentor culture. *Protein Expression and Purification*, 47, 194–202.

Girard, P., Jordan, M., Tsao, M., Wurm, F. M. (2001). Small-scale bioreactor system for process development and optimization. *Biochemical Engineering Journal*, 7, 117–119.

Gogate, P. R., Beenackers, A.A.C.M and Pandit, A. B. (2000) Multiple-impeller systems with a special emphasis on bioreactors: a critical review. *Biochemical Engineering Journal,* 6, 109–144.

Gordon, E., Horsefield, R., Swarts, H. G. P., de Pont, J. J. H. H. M., Neutze, R., Snijder, A. (2008). Effective high-throughput overproduction of membrane proteins in *Escherichia coli. Protein Expression and Purification*, 62, 1–8.

Gorke, B, Stulke, J. (2008). Carbon catabolite repression in bacteria: many ways to make the most out of nutrients, *Nature Reviews,* 6, 613-624.

Grossman, T. H., Kawasaki, E. S., Punreddy, S. R., Osburne, M. S. (1998). Spontaneous cAMP-dependent derepression of gene expression in stationary phase plays a role in recombinant expression instability. *Gene*, 209 (1-2), 95–103.

Gupta, A., Rao, G. (2003). A study of oxygen transfer in shake flasks using a non-invasive oxygen sensor. *Biotechnology and Bioengineering*, 84 (3), 351-358.

Gustavsson, M., Muraleedharan, M. N., Larsson, G. (2014). Surface expression of ω-transaminase in *Escherichia coli*. *Applied and Environmental Microbiology*, 80 (7), 2293–8.

Haagenson, D. M., Klotz, K. L., Campbell, L. (2008). Impact of storage temperature, storage duration, and harvest date on sugarbeet raffinose metabolism. *Postharvest Biology and Technology*, 49 (2), 221-228.

Haddadin, F. T., Harcum, S. W. (2005). Transcriptome profiles for high-cell-density recombinant and wild-type *Escherichia coli. Biotechnology and Bioengineering*, 90, 127–153.

Halim, M. (2012). Microscale approaches to the design and optimisation of equilibrium controlled bioconversions. PhD Thesis, University College London.

Halim, M., Rios-Solis, L., Micheletti, M., Ward, J. M., Lye, G. J. (2013). Microscale methods to rapidly evaluate bioprocess options for increasing bioconversion yields: application to the ω-transaminase synthesis of chiral amines. *Bioprocess and Biosystems Engineering*, 37 (5), 931-941.

Hang, H., Mu, W. M., Jiang, B., Zhao, M., Zhou, L. L., Zhang, T., Miao, M. (2011). Recent advances on biological difructose anhydride III production using inulase II from inulin. *Applied Microbiology Biotechnology*, 92, 457–465.

Hansen, C. F., Hernandez, A., Mullan, B. P., Moore, K., Trezona-Murray, M., King, R. H., Pluske, J. R. (2009). A chemical analysis of samples of crude glycerol from the production of biodiesel in Australia, and the effects of feeding crude glycerol to growing-finishing pigs on performance, plasma metabolites and meat quality at slaughter. *Animal Production Science*, 49, 154-161.

Hauser C., Müller U., Sauer T., Augner K., Pischetsrieder, M. (2014). Maillard reaction products as antimicrobial components for packaging films. *Food Chemistry,* 145, 608-613.

Hegde, S., Pant, T., Pradhan, K., Badiger, M., and Gadgil, M. (2012). Controlled release of nutrients to mammalian cells cultured in shake flasks. *Biotechnology Progress,* 28 (1), 188-195.

Heiss, S., Hormann, A., Tauer, C., Sonnleitner, M., Egger, E., Grabherr, R., Heinl, S. (2016). Evaluation of novel inducible promoter / repressor systems for recombinant protein expression in *Lactobacillus plantarum. Microbial Cell Factories*, 15, 50.

Hilterhaus, L., Thum, O., Liese, A. (2008). Reactor concept for lipase-catalyzed solvent-free conversion of highly viscous reactants forming two-phase systems. *Organic Process Research and Development*, 12, 618–625.

Hiremath, A., Kannabiran, M., Rangaswamy, V. (2011). 1, 3-Propanediol production from crude glycerol from jatropha biodiesel process. *New Biotechnology*, 28, 19-23.

Holmes, W. J., Darby, R. A. J., Wilks, M. D. B., Smith, R., Bill, R. M. (2009). Developing a scalable model of recombinant protein yield from *Pichia pastoris*: the influence of culture conditions, biomass and induction regime. *Microbial Cell Factories*, 8, 35.

Hortsch, R., Weuster-Botz, D. (2011). Growth and recombinant protein expression with *Escherichia coli* in different batch cultivation media. *Applied Microbiology and Biotechnology*, 90 (1), 69–76.

Hsu, W. T., Aulakh, R. P. S., Traul, D. L., Yuk, I. H. (2012). Advanced microscale bioreactor system: A representative scale-down model for bench-top bioreactors. *Cytotechnology*, 64 (6), 667–678.

Huber, R., Ritter, D., Hering, T., Hillmer, A. K., Kensy, F., Muller, C., Wang, L., Buchs, J. (2009). Robo-Lector - a novel platform for automated high-throughput cultivations in microtiter plates with high information content. *Microbial Cell Factories*, 8, 42.

Hughmark, G. A. (1980). Power requirements and interfacial area in gas–liquid turbine agitated systems. *Industrial and Engineering Chemistry Process Design and Development,* 19, 638–641.

Huisman, G. W., Collier, S. J. (2013). On the development of new biocatalytic processes for practical pharmaceutical synthesis. *Current Opinion in Chemical Biology*, 17, 284–292.

Huisman, G. W., Liang, J., Krebber, A. (2010). Practical chiral alcohol manufacture using ketoreductases. *Current Opinion in Chemical Biology*, 14, 122–129.

Hynes, J., Floyd, S., Soini, A.E., O'Connor, R., Papkovsky, D.B. (2003). Fluorescence-based cell viability screening assays using water soluble O_2 probes. *Journal of Biomolecular Screening,* 8, 264–272.

Hyun, Y. L., Davidson, V. L. (1995). Mechanistic studies of aromatic amine dehydrogenase, a tryptophan tryptophylquinone enzyme. *Biochemistry*, 34, 816–823.

Ibrahim, M. H. A., Steinbüchel, A. (2009). Poly (3-Hydroxybutyrate) production from glycerol by *Zobellella denitrifican* MW1 via high-cell-density fed-batch fermentation and simplified solvent extraction*. Applied Environmental Microbiology*, 75, 6222-6231.

Ingram, C. U., Bommer, M., Smith, M.E.B., Dalby, P.A. Ward, J.M., Hailes, H.C., Lye, G.J. (2007). One-pot synthesis of amino-alcohols using a de-novo transketolase and alanine:pyruvate transaminase pathway in *Escherichia coli*. *Biotechnology and Bioengineering*, 96, 559–569.

Isett, K., George, H., Herber, W., Amanullah, A. (2007). Twenty-four-well plate miniature bioreactor high-throughput system : assessment for microbial cultivations, *Biotechnology and Bioengineering*, 98 (5), 1017–1028.

Islam, R. S. (2007). Novel engineering tools to aid drug discovery processes. PhD Thesis, University of London.

Islam, R. S., Tisi, D., Levy, M. S., Lye, G. J. (2008). Scale-up of *Escherichia coli* growth and recombinant protein expression conditions from microwell to laboratory and pilot scale based on matched k La. *Biotechnology and Bioengineering*, 99 (5), 1128–1139.

Jackson, N. B., Liddell, J. M., Lye, G. J. (2006). An automated microscale technique for the quantitative and parallel analysis of microfiltration operations. *Journal of Membrane Science*, 276, 31–41.

Jager, G., Wulfhorst, H., Zeithammel, E. U., Elinidou, E., Spiess, A. C., Buchs, J. (2011). Screening of cellulases for biofuel production: Online monitoring of the enzymatic hydrolysis of insoluble cellulose using high-throughput scattered light detection. *Biotechnology Journal*, 6, 74-85.

Janakiraman, V., Kwiatkowski, C. (2015). Application of high-throughput mini-bioreactor system for systematic scale-down modeling, process characterization, and control strategy development. *Biotechnology Progress*, 31 (6), 1623-1632.

Janke, L., Leite, A. F., Batista, K., Silva, W., Nikolausz, M., Nelles, M., Stinner, W. (2016). Enhancing biogas production from vinasse in sugarcane biorefineries: Effects of urea and trace elements supplementation on process performance and stability. *Bioresource Technology*, 217, 10-20.

Jeong, S., Hwang, B. Y., Kim, J., Kim, B. G. (2000). Lipase-catalysed reaction in the packed bed reactor with continuous extraction column to overcome a product inhibition, *Journal of Molecular Catalysis B: Enzymatic*, 10, 597-604.

Jia, L., Cheng, H., Wang, H. (2011). From shake flasks to bioreactors : survival of *E. coli* cells harboring pGST – hPTH through auto-induction by controlling initial content of yeast extract. *Applied Microbiology and Biotechnology*, 90 (4), 1419–1428.

Jin, H. X., Hu, Z. C., Zheng, Y. G. (2012). Enantioselective hydrolysis of epichlorohydrin using whole *Aspergillus niger* ZJB-09173 cells in organic solvents. *Journal of Biosciences*, 37, 695–702.

John, G. T., Heinzle, E. (2001). Quantitative screening method for hydrolases in microplates

using pH indicators: determination of kinetic parameters by dynamic pH monitoring. *Biotechnology and Bioengineering*, 72, 620–627.

Johnson, D.T., Taconi, K.A. (2007). The glycerin glut: Options for the value-added conversion of crude glycerol resulting from biodiesel production. *Environmental Progress,* 26, 338–348.

Ju, L. K., Chase, G.G. (1992). Improved scale-up strategies of bioreactors. *Bioprocess Engineering*, 8, 49–53.

Junker, B. H. (2004). Scale-up methodologies for *Escherichia coli* and yeast fermentation processes. *Journal of Bioscience and Bioengineering*, 97 (6), 347–364.

Kamm, B., Gruber, P. R., Kamm, M. (2006). Biorefineries - industrial processes and products. Weinheim: Wiley-VCH, Michigan, USA.

Kamm, B., Kamm, M. (2004a). Biorefinery systems. *Chemical and Biochemical Engineering Quarterly*, 18 (1), 1–6.

Kamm, B., Kamm, M. (2004b). Principles of biorefineries. *Applied Microbiology and Biotechnology*, 64, 137–145.

Kang, H. Y., Song, S., Park, C. (1998). Priority of pentose utilisation at the level of transcription: arabinose, xylose, and ribose operons. *Molecules and Cells*, 8, 318–323.

Kang, M. S., Han, S. S., Kim, M. Y., Kim, B.Y., Huh, J. P., Kim, H.S., Lee, J. H. (2014). High-level expression in *Corynebacterium glutamicum* of nitrile hydratase from *Rhodococcus rhodochrous* for acrylamide production. *Applied Microbiology Biotechnology*, 98, 4379–87.

Kao, W.C., Lin, D.S., Cheng, C.L., Chen, B.Y., Lin, C.Y., Chang, J.S. (2013). Enhancing butanol production with *Clostridium pasteurianum* CH4 using sequential glucose-glycerol addition and simultaneous dual-substrate cultivation strategies, *Bioresource Technology*, 135, 324–330.

Kaulmann, U., Smithies, K., Smith, M. E. B., Hailes, H. C., Ward, J. M. (2007). Substrate spectrum of ω-transaminase from *Chromobacterium violaceum* DSM30191 and its potential for biocatalysis. *Enzyme and Microbial Technology*, 41 (5), 628–637.

Kensy, F., Engelbrecht, C., Büchs, J. (2009a). Scale-up from microtiter plate to laboratory fermenter: evaluation by online monitoring techniques of growth and protein expression in *Escherichia coli* and *Hansenula polymorpha* fermentations. *Microbial Cell Factories*, 8, 68.

Kensy, F., Zang, E., Faulhammer, C., Tan, R. K., Buchs, J. (2009b). Validation of a high-throughput fermentation system based on online monitoring of biomass and fluorescence in continuosly shaken microtiter plates. *Microbial Cell Factories*, 8, 31.

Kleman, G. L., Horken, K. M., Tabita, F. R., Strohl, W. R. (1996). Overproduction of recombinant ribulose 1 , 5-bisphosphate carboxylase / oxygenase from Synechococcus sp. Strain PCC6301 in glucose-controlled high-cell-density fermentations by *Escherichia coli* K-12.

Applied and Environmental Microbiology, 62 (9), 3502-3507.

Korz, D.J., Rinas, U., Hellmuth, K., Sanders, E.A. Deckwer, W. D. (1995). Simple fed-batch technique for high cell density cultivation of *Escherichia coli. Journal of Biotechnology*, 39, 59–65.

Koszelewski, D., Lavandera, I., Clay, D., Rozzell, D., Kroutil, W. (2008). Asymmetric (9), synthesis of optically pure pharmacologically relevant amines employing ω-Transaminases. *Advanced Synthesis and Catalysis*, 350, 2761–2766.

Kram, K. E., Finkel, S. E. (2015). Rich medium composition affects *Escherichia coli* survival, glycation and mutation frequency during long-term batch culture. *Applied and Environmental Microbiology*, 81 (13), 4442-4450.

Krause, M., Ukkonen, K., Haataja, T., Ruottinen, M., Glumoff, T., Neubauer, A., Neubauer, P., Vasala, A. (2010). A novel fed-batch based cultivation method provides high cell-density and improves yield of soluble recombinant proteins in shaken cultures. *Microbial Cell Factories*, 9, 11.

Krenkova, J., Foret, F. (2004). Immobilized microfluidic enzymatic reactors. *Electrophoresis*, 25, 3550–3563.

Kwon, S. J., Ko, S.Y. (2002). Synthesis of statine employing a general syn-amino alcohol building block, *Tetrahedron: Letters*, 43, 639-641.

Lara, A. R., Galindo, E., Ramrez, O. T., Palomares, L.A. (2006). Living with heterogeneities in bioreactors: understanding the effects of environmental gradients on cells. *Molecular Biotechnology*, 34 (3), 355–381.

Lavery, M., Nienow, A.W. (1987). Oxygen transfer in animal cell culture. *Biotechnology and Bioengineering*, 30, 368–373.

Lee, C. A., Jacobsont, G. R., Saier, M. H. (1981). Plasmid-directed synthesis of enzymes required for D-mannitol transport and utilisation in *Escherichia coli. Biochemistry*, 78 (12), 7336–7340.

Lee, S. J., Kim, S. B., Kang, S. W., Han, S. O., Park, C., Kim, S. W. (2012). Effect of crude glycerolderived inhibitors on ethanol production by *Enterobacter aerogenes. Bioprocess and Biosystems Engineering*, 35, 85-92.

Lee, S. Y. (1996).High cell-density culture of *Escherichia coli. Trends in Biotechnology*, 14 (3), 98-105.

Lengeler, J., Biologie, F., Regensburg, D. U. (1975). Nature and properties of hexitol transport systems in *Escherichia coli. Journal of Bacteriology,* 124 (1), 39–47.

Lengeler, J., Lin, E. C. C. (1972). Reversal of the mannitol-sorbitol diauxie in *Escherichia coli*, *Journal of Bacteriology*, 112 (2), 840–848.

León, A. De, Breceda, G. B., Barba, A. P., Rosa, D., Jiménez-bremont, J. F., López-revilla, R. (2003). Galactose induces the expression of penicillin acylase under control of the lac promoter in recombinant *Escherichia coli. Biotechnology Letters*, 17, 1397–1402.

Li, C., Lesnik, K. L., Liu, H. (2013). Microbial conversion of waste glycerol from biodiesel production into value-added products. *Energies*, 6, 4739-4768.

Li, J., Jaitzig, J., Lu, P., Sussmuth, R. D., Neubauer, P. (2015). Scale-up bioprocess development for production of the antibiotic valinomycin in *Escherichia coli* based on consistent fed-batch cultivations. *Microbial Cell Factories*, 14, 83.

Li, T., Liang, J., Ambrogelly, A., Brennan, T., Gloor, G., Huisman, G., Lalonde, J., Lekhal, A., Mijts, B., Muley, S., Newman, L., Tobin, M., Wong, G., Zaks, A., Zhang, X. (2012). Efficient,

chemoenzymatic process for manufacture of the boceprevir bicyclic [3.1.0] proline intermediate based on amine oxidase-catalyzed desymmetrization. *Journal of American Chemical Society*, 134, 6467–6472.

Liang, Y. N., Sarkany, N., Cui, Y., Blackburn, J. W. (2010). Batch stage study of lipid production from crude glycerol derived from yellow grease or animal fats through microalgal fermentation. *Bioresource Technology*, 101, 6745-6750.

Lin, E.C.C. (1976). Glycerol dissmilation and its regulation in bacteria. *Annual Review of Microbiology,* 30, 535–578.

Liu, Y. C., Chang, W. M., Lee, C. Y. (1999). Effect of oxygen enrichment aeration on penicillin G acylase production in high cell density culture of recombinant *E. coli*. *Bioprocess Engineering*, 21 (3), 227–230.

Liu, Y. S, Wu, J. Y., Ho, K. P. (2006). Characterization of oxygen transfer conditions and their effects on *Phaffia rhodozyma* growth and carotenoid production in shake-flask cultures. *Biochemical Engineering Journal,* 27, 331–335.

Long, Q., Liu, X., Yang, Y., Li, L., Harvey, L., McNeil, B., Bai, Z. (2014). The development and application of high throughput cultivation technology in bioprocess development. *Journal of Biotechnology*, 192, 323-338.

Losen, M., Frolich, B., Pohl, M., Buchs, J. (2004). Effect of oxygen limitation and medium composition on *Escherichia coli* fermentation in shake flask cultures. *Biotechnology Progress*, 20, 1062-1068.

Lotter, S., Buchs, J. (2004). Utilisation of specific power input measurements for optimization of culture conditions in shaking flasks. *Biochemical Engineering Journal*, 17, 195-203.

Lutoslawski, K., Ryznar-Luty, A., Cibis, E., Krzywonos, M., Miskiewicz, T. (2011). Biodegradation of beet molasses vinasse by a mixed culture of microorganisms: Effect of aeration conditions and pH control. *Journal of Environmental Sciences*, 23 (11), 1823 - 1830.

Lye, G. J., Ayazi-Shamlou, P., Baganz, F., Dalby, P.A., Woodley, J. M. (2003). Accelerated design of bioconversion processes using automated microscale processing techniques. *TRENDS in Biotechnology*, 21 (1), 29-37.

Lye, G. J., Woodley, J. M. (1999). Application of *in-situ* product removal techniques to biocatalytic processes. *TRENDS in Biotechnology*, 17, 395–402.

Macaloney, G., Draper, I., Preston, J. (1996). At-Line Control and Fault Analysis in an industrial high cell density *Escherichia Coli* fermentation, using NIR spectroscopy. *Food and Bioproducts Processing,* 74 (4), 212-220.

Macaloney, G., Hall, J. W., Rollins, M. J., Draper, I., Anderson, K.B., Preston, J., Thompson, B.G., McNeil, B. (1997).The utility and performance of near-infra red spectroscopy in simultaneous monitoring of multiple components in a high cell density recombinant *Escherichia coli* production process, *Bioprocess Engineering*, 17, 157–167.

Macedo, N., Brigham, C. J. (2014). From beverages to biofuels: The journeys of ethanol-producing microorganisms. *International Journal of Biotechnology for Wellness Industries,* 3*,* 79-87.

Maijala, P., Kleen, M., Westin, C., Poppius-Levlin, K., Herranen, K., Lehto, J. H., Reponen, P., Maentausta, O., Mettala, A., Hatakka, A. (2008). Biomechanical pulping of softwood with enzymes and white-rot fungus *Physisporinus rivulosus. Enzyme and Microbial Technology*, 43, 169–177.

Maillard, L.C. (1912). Action des acides amines sur les sucres: formation des melanoidines

par voie methodique. *Comptes Rendus Hebdomadaires des Seances de l'Academie des sciences*, 154, 66-68.

Maity, S. K. (2014). Opportunities, recent trends and challenges of integrated biorefinery: Part I. *Renewable and Sustainable Energy Reviews*, 43, 1427 - 1445.

Makrides, S. C. (1996). Strategies for achieving high-level expression of genes in *Escherichia coli. Microbiological Review*, 60, 512–538.

Malik, M. S., Park, E. S., Shin, J. S. (2012). Features and technical applications of ω-transaminases. *Applied Microbiology and Biotechnology*, 94, 1163-1171.

Marchlis, L. (1957). Factors affecting the lag phase of growth of filamentous fungus, *Allomyces mycrogynus. American Journal of Botany*, 44 (2), 113–119.

Marini, G., Luchese, M. D., Argondizzo, A. P. C., de Góes, A. C. M. A., Galler, R., Alves, T. L., Medeiros, M. A., Larentis, A. L. (2014). Experimental design approach in recombinant protein expression: determining medium composition and induction conditions for expression of pneumolysin from *Streptococcus pneumoniae* in *Escherichia coli* and preliminary purification process. *BMC Biotechnology*, 14, 1.

Marisch, K., Bayer, K., Scharl, T., Mairhofer, J., Krempl, P. M., Hummel, K., Razzazi-Fazeli, E., Striedner, G. (2013). A comparative analysis of industrial *Escherichia coli* K-12 and B strains in high-glucose batch cultivations on process, transcriptome and proteome level. *PloS One*, 8(8), e70516.

Marques, M. P. C., Cabral, J. M. S., Fernandes, P. (2010). Bioprocess scale-up: Quest for the parameters to be used as criterion to move from microreactors to lab-scale. *Journal of Chemical Technology and Biotechnology*, 85 (9), 1184–1198.

Marques, M. P. C., Walshe, K., Doyle, S., Fernandes, P., De Carvalho, C. C. C. R. (2012). Anchoring high-throughput screening methods to scale-up bioproduction of siderophores. *Process Biochemistry*, 47 (3), 416–421.

Marques, S. S. I., Nascimento, I. A., De Almeida, P. F., Chinalia, F. A. (2013). Growth of *Chlorella vulgaris* on sugarcane vinasse: The effect of anaerobic digestion pretreatment. *Applied Biochemistry and Biotechnology*, 171 (8), 1933–1943.

Martín Santos, M. A., Fernández Bocanegra, J. L., Martín Martín, A., García García, I. (2003). Ozonation of vinasse in acid and alkaline media. *Journal of Chemical Technology and Biotechnology*, 78, 1121–1127.

Martínez-Gómez, K., Flores, N., Castañeda, H. M., Martínez-Batallar, G., Hernández-Chávez, G., Ramírez, O. T., Gosset, G., Encarnacion, S., Bolivar, F. (2012). New insights into *Escherichia coli* metabolism: carbon scavenging, acetate metabolism and carbon recycling responses during growth on glycerol. *Microbial Cell Factories*, 11, 46.

Matosevic, S., Szita, N., Baganz, F. (2011). Fundamentals and applications of immobilised microfluidic enzymatic reactors. *Journal of Chemical Technology and Biotechnol*ogy, 86, 325–334.

Matsumoto, T., Katsura, D., Kondo, A., Fukuda, H. (2002). Efficient secretory overexpression of *Bacillus subtilis* pectate lyase in *Escherichia coli* and single-step purification. *Biochemical Engineering Journal*, 12, 175-179.

Mattanovich, D., Kramer, W., Lüttich, C., Weik, R., Bayer, K., Katinger, H. (1998). Rational design of an improved induction scheme for recombinant *Escherichia coli. Biotechnology and Bioengineering*, 58, 296–298.

Mazumdar, S., Clomburg, J. M., Gonzalez, R. (2010). *Escherichia coli* strains engineered for homofermentative production of D-lactic acid from glycerol. *Applied Environmental Microbiology,* 76, 4327–4336.

Mehta, P. K., Hale, T. I., Christen, P. (1993). Aminotransferases: demonstration of homology and division into evolutionary subgroups. *European Journal of Biochemistry / FEBS*, 214, 549–561.

Menzella, H. G., Gramajo, H. C. (2004). Recombinant protein production in high cell density cultures of *Escherichia coli* with galactose as a gratuitous inducer. *Biotechnology Progress*, 20 (4), 1263-1266.

Micard, V., Renard, C. M. G. C., Thibault, J. F. (1996). Enzymatic saccharification of sugar-beet pulp, *Enzyme and Microbial Technology*, 19, 162–170.

Michel, B. J., Miller, S. (1962). Power requirements of gas-liquid agitated systems. *AIChE Journal,* 8 (2), 262-266.

Michelleti, M., Barrett, T., Doig, S. D., Baganz, F., Levy, M. S., Woodley, J. M., Lye, G. J. (2006). Fluid mixing in shaken bioreactors: Implications for scale-up predictions from microlitre-scale microbial and mammalian cell cultures. *Chemical Engineering Science*, 61, 2939 - 2949.

Minas, W., Bailey, J.E., Duetz, W. (2000). Streptomycetes in micro-cultures: growth, production of secondary metabolites, and storage and retrieval in the 96–well format. *Antonie Van Leeuwenhoek*, 78, 297–305.

Monache, G. D., Zappia, G. (1999). A stereocontrolled synthesis of (-)-detoxinine from L -ascorbic acid. *Tetrahedron: Asymmetry*, 10, 2961-2973.

Monod, J. (1942). Recherches Sur La Croissance Des Cultures Bacttriennes. Paris: Hermann and Cie.

Monod, J. (1949). The growth of microbial culture. *Annual Review of Microbiology*, 3, 371-394.

Montes, F. J., Catal´an, J., Gal´an, M. A. (1999). Prediction of k_La in yeast broths. *Process Biochemistry,* 34, 549–555.

Moon, S. K., Lee, J., Song, H, Cho, J. H, Choi, G. W., Seung, D. (2013). Characterization of ethanol fermentation waste and its application to lactic acid production by *Lactobacillus paracasei*, *Bioprocess and Biosystems Engineering,* 36, 547–554.

Murarka, A., Dharmadi, Y., Yazdani, S. S., Gonzalez, R. (2008). Fermentative utilisation of glycerol by *Escherichia coli* and its implications for the production of fuels and chemicals. *Applied and Environmental Microbiology*, 74 (4), 1124-1135.

Nair, R., Salvi, P., Banerjee, S., Raiker, V. A., Bandyopadhyay, S., Soorapaneni, S., Kotwal, P., Padmanabhan, S. (2009). Yeast extract mediated autoinduction of lacUV5 promoter : an insight. *New Biotechnology*, 26 (6), 282–288.

Najafpour, G. D. (2007). *Biochemical Engineering and Biotechnology*. Elsevier Science, Amsterdam, The Netherlands.

Nakagawa, S., Oda, H., Anazawa, H. (1995). High cell density cultivation and high recombinant protein production of *Escherichia coli* strain expressing uricase. *Bioscience, Biotechnology and Biochemistry*, 59 (12), 2263-2267.

Nakamura, C. E., Whited, G. M. (2003). Metabolic engineering for the microbial production of 1,3-propanediol. *Current Opinion in Biotechnology*, 14, 454–459.

Nancib, N., Mosrati, R., Boudrant, J. (1993). Modelling of batch fermentation of a recombinant Escherichia coli producing glyceraldehyde-3-phosphate dehydrogenase on a complex selective medium. *The Chemical Engineering Journal*, 52, B35-B48.

Navarro, A. R., Sepulveda, M. D. C., Rubio, M. C. (2000). Bio-concentration of vinasse from the alcoholic fermentation of sugar cane molasses. *Waste Management*, 20, 581-585.

Nealon, A. J., O'Kennedy, R. D., Titchener-Hooker, N. J., Lye, G. J. (2006). Quantification and prediction of jet macro-mixing times in static microwell plates. *Chemical Engineering Science,* 61, 4860–4870.

Neijssel, O. M., Hueting, S., Crabbendam, K. J., Tempest, D.W. (1975). Dual pathways of glycerol assimilation in *Klebsiella aerogenes* NCIB 418. *Archives of Microbiology,* 104, 83–87.

Newton, J. M., Vlahopoulou, J., Zhou, Y. (2017). Investigating and modelling the effects of cell lysis on the rheologial properties of fermentation broths. *Biochemical Engineering Journal*, 121, 38-48.

Nienow, A. W., Rielly, C. D., Brosnan, K., Bargh, N., Lee, K., Coopman, K., Hewitt, C. J. (2013). The physical characterisation of a microscale parallel bioreactor platform with an industrial CHO cell line expressing an IgG4. *Biochemical Engineering Journal*, 76, 25-36.

Nishi, K., Kim, I. H., Ma, S. J. (2010). Expression of the human soluble epoxide hydrolase in Escherichia coli by auto-induction for the study of high-throughput inhibition assays. *Protein Expression and Purification*, 69, 34–38.

Oh, B. R., Seo, J. W., Heo, S. Y., Hong, W. K., Luo, L. H., Joe, M., Park, D. H., Kim, C. H. (2011). Efficient production of ethanol from crude glycerol by a *Klebsiella pneumonia* mutant strain. *Bioresource Technology*, 102, 3918-3922.

Oh, M. K., Liao, J. C. (2000). Gene expression profiling by DNA microarrays and metabolic fluxes in *Escherichia coli. Biotechnology Progress*, 16, 278–86.

Ohara, H. (2003). Biorefinery. *Applied Microbiology and Biotechnology*, 62, 474–477.

Ojo, E. O. (2016). Photobioreactor technologies for high-throughput microalgae cultivation. PhD Thesis, University College London.

Olaofe, O. A., Burton, S. G., Cowan, D. A., Harrison, S. T. L. (2010). Improving the production of a thermostable amidase through optimising IPTG induction in a highly dense culture of recombinant *Escherichia coli. Biochemical Engineering Journal*, 52 (1), 19–24.

Onishi, H., Sizuki, T. (1968). Production of D-mannitol and glycerol by yeasts. *Applied Microbiology*, 16 (12), 3–8.

Ouellette, T., Destrau, S., Ouellette, T., Zhu, J., Roach, J. M., Coffman, J. D., Hecht, T., Lynch, J. E., Giardina, S. L. (2003). Production and purification of refolded recombinant human IL-7 from inclusion bodies. *Protein Expression and Purification*, 30, 156–166.

Ozturk, S. S. (1996). Engineering challenges in high density cell culture systems. *Cyotechnology*, 22 (1-3), 3-16.

O'Grady, J., Morgan, J.A. (2011). Heterotrophic growth and lipid production of *Chlorella protothecoide* on glycerol. *Bioprocess Biosystem Engineering*, 34, 121-125.

O'Riordan, T. C, Buckley, D., Ogurtsov, V., O'Connor, R., Papkovsky, D. B. (2000). A cell viability assay based on monitoring respiration by optical O_2 sensing. *Analytical Biochemistry*, 278, 221–227.

Pachapur, V. L., Sarma, S. J., Brar, S. K., Le Bihan, Y., Buelna, G., Soccol, C. R. (2015). Evidence of metabolic shift on hydrogen, ethanol and 1,3-propanediol production from crude glycerol by nitrogen sparging under micro-aerobic conditions using co-culture of *Enterobacter aerogenes* and *Clostridium butyricum. International Journal of Hydrogen Energy*, 40, 8669–8676.

Paliy, O., Gunasekera, T. S. (2007). Growth of *E. coli* BL21 in minimal media with different gluconeogenic carbon sources and salt contents. *Applied Microbiology and Biotechnology*, 73, 1169–1172.

Panda, B. P., Ali, M., Javed, S. (2007). Fermentation process optimization. *Research Journal of Microbiology*, 2 (3), 201 - 208.

Panova, A., Mersingera, L. I., Liu, Q., Foo, T., Roe, D. C., Spillan, W. L., Sigmund, A. E., Ben-Basset, A., Wagner, L. W., O'Keefe, D. P., Wu, S., Petrillo, K. L., Payne, M. S., Breske, S. T., Gallagher, F. G., Dicosimo, R. (2007). Chemoenzymatic synthesis of glycolic acid. *Advanced Synthesis and Catalysis*, 349, 1462-1474.

Park, E. S., Shin, J. S. (2013). ω-Transaminase from *Ochrobactrum anthropi* is devoid of substrate and product inhibitions. *Applied and Environmental Microbiology*,79(13), 4141–4.

Parnaudeau, V., Condom, N., Oliver, R., Cazevieille, P., Recous, S. (2008). Vinasse organic matter quality and mineralization potential, as influenced by raw material, fermentation and concentration processes. *Bioresource Technology*, 99, 1553–1562.

Patrick, K. (2004). Enzyme technology improves efficiency, cost, safety of stickies removal program. *Paper Age*, 120, 22–25.

Persidis, A. (1998). High throughput screening. *Nature Biotechnology*. 16, 488–489.

Peterson, W. H., Hendershot, W. F., Hajny, G. J. (1958). Factors affecting production of glycerol and D-arabitol by representative yeasts of the genus *Zygosaccharomyces*. *Applied Microbiology*, 6, 349-357.

Pettigrew, D. W., Yu, G. J., Liu, Y. (1990). Nucleotide regulation of *Escherichia coli* glycerol kinase: Initial-velocity and substrate binding studies. *Biochemistry*, 29 (37), 8620–8627.

Piubelli, L., Campa, M., Temporini, C.,Binda, E., Mangione, F., Amicosante, M., Terreni, M., Marinelli, F., Pollegioni, L. (2013). Optimizing *Escherichia coli* as a protein expression platform to produce *Mycobacterium tuberculosis* immunogenic proteins. *Microbial Cell Factories*, 12, 115.

Pollard, D. J., Woodley, J. M. (2006). Biocatalysis for pharmaceutical intermediates: the future is now. *Trends in Biotechnology*, 25 (2), 66-73.

Poo, H., Song, J. J., Hong, S. P., Choi, Y. H., Yun, S. W., Kim, J. H., Lee, S. C., Lee, S. G., Sung, M. H. (2002). Novel high-level constitutive expresion system, pHCE vector, for a convenient and cost-effective soluble production of human tumor necrosis factor-α. (2002). *Biotechnology Letters*, 24, 1185-1189.

Pramanik, A., Mitra, A., Arumugam, M., Bhattacharyya, A., Sadhukhan, S., Ray, A., Haldar, S., Mukhopadhyay, U. K., Mukherjee, J. (2012). Utilisation of vinasse for the production of polyhydroxybutyrate by *Haloarcula marismortui*. *Folia Microbiologica*, 57, 71–79.

Qi, J., Li, Z., Guo, Y., Xu, H. (2004). Adsorption of phenolic compounds micro- and mesoporous rice husk-based active carbons. *Materials Chemistry and Physics*, 87, 96–101.

Quicker, G., Schumpe A., Konig, B., Deckwer, W. D. (1981). Comparison of measured and calculated oxygen solubilities in fermentation media. *Biotechnology and Bioengineering*, 23, 635–650

Rameez, S., Mostafa, S. S., Miller, C., Shukla, A. A. (2014). High-throughput miniaturized bioreactors for cell culture process development: reproducibility, scalability, and control. *Biotechnology Progress*, 30 (3), 718-727.

Ramirez-Vargas, R., Vital-Jacome, M., Camacho-Perez, E., Hubbard, L., Thalasso, F. (2014). Characterization of oxygen transfer in a 24-well microbioreactor system and potential respirometric applications. *Journal of Biotechnology*, 186, 58–65.

Rao, D. G. (2010). Introduction to Biochemical Engineering Second Edition. Tata McGraw Hill, New Delhi, India.

Rayat, A. C. M. E., Micheletti, M., Lye, G. J. (2010). Evaluation of cell disruption effects on primary recovery of antibody fragments using microscale bioprocessing techniques. *Biotechnology Progress*, 26, 1312–1321.

Richards, J. W. (1961). Studies in aeration and agitation. *Progress in Industrial Microbiology*, 3, 143–72.

Rieckenberg, F., Ardao, I., Rujananon, R., Zeng, A. P. (2014). Cell-free synthesis of 1,3-propanediol from glycerol with a high yield. *Engineering Life Sciences*, 14, 380–386.

Riesenberg, D. (1991). High-cell-density cultivation of *Escherichia coli. Current Opinion in Biotechnology*, 380, 380–384.

Rios-Solis, L. (2012). Microscale evaluation of de novo engineered whole cell biocatalysts, Phd Thesis, University College London.

Rios-Solis, L., Halim, M., Cázares, a., Morris, P., Ward, J. M., Hailes, H. C., Dalby, P. A., Baganz, F., Lye, G. J. (2011). A toolbox approach for the rapid evaluation of multi-step enzymatic syntheses comprising a "mix and match" *E. coli* expression system with microscale experimentation. *Biocatalysis and Biotransformation*, 29 (5), 192–203.

Rios-Solis, L., Morris, P., Grant, C., Odeleye, A. O. O., Hailes, H. C., Ward, J. M., Dalby, P. A., Baganz, F., Lye, G. J. (2015). Modelling and optimisation of the one-pot, multi-enzymatic synthesis of chiral amino-alcohols based on microscale kinetic parameter determination. *Chemical Engineering Science*, 122, 360–372.

Roberts, S. M., Turner, N. J., Willetts, A. J., Turner, M. K. (1995). Introduction to biocatalysis using enzymes and microorganisms. 1st ed. Cambridge: Cambridge University Press.

Rodriguez, G., Anderlei, T., Micheletti, M., Yianneskis, M., Ducci, A. (2014). On the measurement and scaling of mixing time in orbitally shaken bioreactors. *Biochemical Engineering Journal*, 82, 10 - 21.

Rodriguez-Colinas, B., de Abreu, M. A., Fernandez-Arrojo, L., de Beer, R., Poveda, A., Jimenez-Barbero, J., Haltrich, D., Ballesteros Olmo, A. O., Fernandez-Lobato, M., Plou, F. J. (2011). Production of galacto-oligosaccharides by the beta-galactosidase from *Kluyveromyces lactis*: comparative analysis of permeabilized cells versus soluble enzyme. *Journal of Agricultural and Food Chemistry*, 59, 10477–10484.

Rohe, P., Venkanna, D., Kleine, B., Freudl, R., Oldiges, M. (2012). An automated workflow for enhancing microbial bioprocess optimization on a novel microbioreactor platform. *Microbial Cell Factories*, 11, 144.

Rozwadoska, M. D. (1993). An efficient synthesis of S-(+)- amphetamine. *Tetrahedron: Asymmetry*, 4, 1619-1624.

Rufián-Henares, J. A., Morales, F. J. (2006). A new application of a commercial microtiter plate-based assay for assessing the antimicrobial activity of Maillard reaction products. *Food Research International,* 39, 33-39.

Rushton, J. H., Costich, E. W., Everett, H. J. (1950a). Power characteristics of mixing impellers: part I. *Chemical Engineering Progress*, 46, 395 - 404.

Rushton, J. H., Costich, E. W., Everett, H. J. (1950b). Power characteristics of mixing impellers: part II. *Chemical Engineering Progress*, 46, 467 - 476.

Rymowicz, W., Rywińska, A., Marcinkiewicz, M. (2009). High-yield production of erythritol from raw glycerol in fed-batch cultures of *Yarrowia lipolytic. Biotechnology Letter*, 31, 377-380.

Rywińska, A, Rymowicz, W, Żlarowska, B. (2009). Biosynthesis of citric acid from glycerol by acetate mutants of *Yarrowia lipolytic* in fed-batch fermentation. *Food Technology and Biotechnology*, 47, 1-6.

Ryznar-Luty, A., Cibis, E., Krzywonos, M., Miskiewicz, T. (2015). Efficiency of aerobic biodegradation of beet molasses vinasse under non-controlled pH: conditions for betaine removal. *Archives of Environmental Protection*, 41 (1), 3-14.

Ryznar-Luty, A., Krzywonos, M., Cibis, E., Miśkiewicz, T. (2008). Aerobic biodegradation of vinasse by a mixed culture of bacteria of the genus Bacillus: Optimization of temperature, pH and oxygenation state. *Polish Journal of Environmental Studies*, 17 (1), 101–112.

Sabra, W., Dietz, D., Tjahjasari, D., Zeng, A. P. (2010). Biosystems analysis and engineering of microbial consortia for industrial biotechnology. *Engineering Life Sciences*, 10, 407–21.

Salgado, J. M., Carballo, E. M., Max, B., Dominguez, J. M. (2010). Characterization of vinasses from five certified brands of origin (CBO) and use as economic nutrient for the xylitol production by *Debaryomyces hansenii. Bioresource Technology*, 101 (7), 2379–2388.

Sanchez, S., Demain, A. L. (2011). Enzymes and bioconversions of industrial, pharmaceutical, and biotechnological significance. *Organic Process Research and Development,* 15, 224–230.

Sani, M. H. (2016). Evaluation of microwell based systems and miniature bioreactors for rapid cell culture bioprocess development and scale-up. PhD Thesis, University College London.

Sarris, D., Papanikolaou, S. (2016). Biotechnological production of ethanol: Biochemistry, processes and technologies. *Engineering in Life Sciences*, 16, 307-329.

Sayer, C., Isupov, M. N., Littlechild, J. A. (2007). Crystallization and preliminary X-ray diffraction analysis of omega-amino acid:pyruvate transaminase from *Chromobacterium violaceum. Acta Crystallographica. Section F, Structural Biology and Crystallization Communications*, 63, 117–119.

Schmidt, F. R. (2005). Optimization and scale up of industrial fermentation processes. *Applied Microbiology and Biotechnology*, 68, 425-435.

Schmidt, M., Babu, K. R., Khanna, N., Marten, S., Rinas, U. (1999). Temperature-induced production of recombinant human insulin in high-cell density cultures of recombinant *Escherichia coli. Journal of Biotechnology*, 68 (1), 71–83.

Scholten, E., Renz, T., Thomas, J. (2009). Continuous cultivation approach for fermentative succinic acid production from crude glycerol by *Basfia succiniciproducens* DD1. *Biotechnology Letter*, 31, 1947-1951.

Serrato, J. A., Palomares, L. A., Meneses-Acosta, A., Ramirez, O. T. (2004). Heterogeneous conditions in dissolved oxygen affect N-glycosylation but not productivity of a monoclonal antibody in hybridoma cultures. *Biotechnology and Bioengineering*, 88 (2), 176-188.

Shen, Y. L., Zhang, Y., Sun, A. Y., Xia, X. X., Wei, D. Z., Yang, S. L. (2004). High-level production of soluble tumor necrosis factor-related apoptosis-inducing ligand (Apo2L/TRAIL) in high-density cultivation of recombinant *Escherichia coli* using a combined feeding strategy. *Biotechnology Letters*, 26, 981-984.

Shiloach, J., Bauer, S. (1975). High-yield growth of *E. coli* at different temperatures in a bench scale fermentor. *Biotechnology and Bioengineering*, XVII, 227–239.

Shiloach, J., Fass, R. (2005). Growing *E. coli* to high cell density - A historical perspective on method development. *Biotechnology Advances*, 23, 345-357.

Shin, J. S., Kim, B. G. (2001). Comparison of the omega-transaminases from different microorganisms and application to production of chiral amines. *Bioscience, Biotechnology and Biochemistry*, 65, 1782–1788.

Siles, J. A., Martín, M.A., Chica, A.F., Martín, A. (2010). Anaerobic co-digestion of glycerol and wastewater derived from biodiesel manufacturing. *Bioresource Technology,* 101, 6315–6321.

Silk, N. J., Denby, S., Lewis, G., Kuiper, M., Hatton, D., Field, R., Baganz, F., Lye, G. J. (2010). Fed-batch operation of an industrial cell culture process in shaken microwells. *Biotechnology Letters,* 32 (1), 73-78.

Silva, C. J. S. M., Prabaharan, M., Gubitz, G., Cavaco-Paulo, A. (2005). Treatment of wool fibres with subtilisin and subtilisin-PEG. *Enzyme and Microbial Technology*, 36, 917–922.

Siurkus, J., Panula-Perälä, J., Horn, U., Kraft, M., Rimseliene, R., Neubauer, P. (2010). Novel approach of high cell density recombinant bioprocess development: optimisation and scale-up from microliter to pilot scales while maintaining the fed-batch cultivation mode of *E. coli* cultures. *Microbial Cell Factories*, 9, 35.

Sivakesava, S., Xu, Z. N., Chen, Y. H., Hackett, J., Huang, R. C., Lam, E., Lam, T. L., Siu, K. L., Wong, R. S. C., Wong, W. K. R. (1999). Production of excreted human epidermal growth factor (hEGF) by an efficient recombinant *Escherichia coli* system. *Process Biochemistry*, 34, 893-900.

Smith, M. E. B. Chen, B. H., Hibbert, E. G., Kaulmann, U., Smithies, K., Galman, J. L., Baganz, F., Dalby, P.A., Hailes, H.C., Lye, G.J., Ward, J.M., Woodley, J.M., Micheletti, M. (2010). A multidisciplinary approach toward the rapid and preparative-scale biocatalyticsynthesis of chiral amino alcohols: a concise transketolase/transaminase-mediated synthesis of (25,35)-2-aminopentane-1,3-diol. *Organic Process Research and Development*, 14, 99–107.

Soini, J., Ukkonen, K., Neubauer, P. (2008). High cell density media for *Escherichia coli* are generally designed for aerobic cultivations - consequences for large-scale bioprocesses and shake flask cultures. *Microbial Cell Factories*, 7, 26.

Solomon, E., Lin, E. C. (1972). Mutations affecting the dissimilation of mannitol by Escherichia coli K-12. *Journal of Bacteriology*, 111 (2), 566–574.

Spencer, J. F. T., Shu, P. (1957). Polyhydric alcohol production by osmophilic yeasts: effect of oxygen tension and inorganic phosphate concentration. *Canadian Journal of Microbiology*, 3, 559 - 567.

Stahl, S. R., Greasham, O., Chartrain, M. (2000). Implementation of a rapid microbial screening procedure for biotransformation activities. *Journal of Bioscience and Bioengineering*, 89, 367–371.

Stanbury, P. F., Whitaker, A., Hall, S. J. (1999). Principles of fermentation technology second edition. Butterworth-Heinemann, Cornwall, UK.

Stewart, J. D. (2001). Dehydrogenases and transaminases in asymmetric synthesis. *Current Opinion in Chemical Biology*, 5 (2), 120–9.

Stirling, D. I. (1992). The use of aminotransferases for the production of chiral amines and amines, In: Collins AN, Sheldrake, G. N., Crosby, J., editors. Chirality in Industry, UK: John Willey & Sons, 209-222.

Studier, F. W. (2005). Protein production by auto-induction in high-density shaking cultures. *Protein Expression and Purification*, 41 (1), 207–234.

Studier, F. W., Rosenberg, A. H., Dunn, J. J., Dubendorff, J. W. (1990). Use of T7 RNA polymerase to direct expression of cloned genes. *Methods in Enzymology*, 185 (1986), 60–89.

Sutin, L., Andersson, S., Bergquist, L., Castro, M., Danielsson, E., James, S., Henriksson, M., Johansson, L., Kaiser, C., Flyren, K., Williams, M. (2007). Oxazolones as potent inhibitors of 11beta-hydroxysteroid dehydrogenase type 1. *Bioorganic and Medicinal Chemistry*

Letters, 17, 4837–4840.

Sydney, E. B. (2013). Valorization of vinasse as broth for biological hydrogen and volatile fatty acids production by means of anaerobic bacteria. PhD thesis, Universidade Federal Do Parana.

Taconi, K. A., Venkataramanan, K. P., Johnson, D.T. (2009). Growth and solvent production by *Clostridium pasteurianum* ATCC® 6013™ utilizing biodiesel derived crude glycerol as the sole carbon source. *Environmental Progress and Sustainable Energy*, 28, 100-110.

Tang, S., Boehme, L., Lam, H., Zhang, Z. (2009). *Pichia pastori* fermentation for phytase production using crude glycerol from biodiesel production as the sole carbon source. *Biochemical Enginering Journal*, 43, 157-162.

Tang, Y. J., Laidlaw, D., Gani, K., Keasling, J. D. (2006). Evaluation of the effects of various culture conditions on Cr(VI) reduction by *Shewanella oneidensis* MR-1 in a novel high-throughput mini-bioreactor, *Biotechnology and Bioengineering*, 95 (1), 176-184.

Tao, J., Xu, J. H. (2009). Biocatalysis in development of green pharmaceutical processes. *Current Opinion in Chemical Biology*, 13, 1, 43-50.

Thompson, J. C., He, B. B. (2006). Characterization of crude glycerol from biodiesel production from multiple feed stocks. *Applied Engineering in Agriculture*, 22, 261 - 265.

Toeroek, C., Cserjan-Puschmann, M., Bayer, K., Striedner, G. (2015). Fed-batch like cultivation in a micro-bioreactor: screening conditions relevant for *Escherichia coli* based production processes. *SpringerPlus*, 4, 490.

Truppo, M. D., Strotman, H., Hughes, G. (2012). Development of an immobilized transaminase capable of operating in organic solvent. *ChemCatChem*, 4, 1071–1074.

Tyler, R. C., Sreenath, H. K., Singh, S., Aceti, D. J., Bingman, C. A., Markley, J. L., Fox, B. G. (2005). Auto-induction medium for the production of [U-15N]- and [U-13C, U-15N]-labeled proteins for NMR screening and structure determination. *Protein Expression and Purification*, 40, 268–278.

Urban, P.L., Goodall, D.M., Bruce, N.C. (2006). Enzymatic microreactors in chemical analysis and kinetic studies. *Biotechnology Advances*, 24, 42–47.

Vaccari, G., Tamburini, E., Sgualdino, G., Urbaniek, K., Klemeˇs, J. (2005). Overview of the environmental problems in beet sugar processing: possible solutions, *Journal of Cleaner Production*, 13, 499–507.

Valetti, F., Gilardi, G. (2013). Improvements of biocatalysts for industrial and environmental purposes by saturation mutagenesis. *Biomolecules*, 3 (4), 778-811.

Van't Riet, K. (1979). Review of Measuring Methods and Results in Nonviscous Gas-Liquid Mass Transfer in Stirred Vessels. *Industrial and Engineering Chemistry Process Design and Development*, 18 (3), 357–364.

Vera, C., Guerrero, C., Conejeros, R., Illanes, A. (2012). Synthesis of galacto-oligosaccharides by betagalactosidase from *Aspergillus oryzae* using partially dissolved and supersaturated solution of lactose. *Enzyme and Microbial Technology*, 50, 188–94.

Volpato, G., Rodrigues, R. C., Heck, J. X., Ayub, M. A. Z. (2008). Production of organic solvent tolerant lipase by *Staphylococcus caseolyticu* EX17 using raw glycerol as substrate. *Journal of Chemical Technology and Biotechnology*, 83, 821-828.

Walz, A., Demel, R. A., de Kruijff, B., Mutzel, R. (2002). Aerobic sn-glycerol-3-phosphate dehydrogenase from *Escherichia coli* binds to the cytoplasmic membrane through an amphipathic alpha-helix. *The Biochemical Journal*, 365, 471–9.

Wan Isahak, W. N. R., Ramli, Z. A. C., Ismail, M., Mohd Jahim, J., Yarmo, M. A. (2014). Recovery and purification of crude glycerol from vegetable oil transesterification. *Separation and Purification Reviews,* 44 (3), 250 - 267.

Wang, F., Lee, S. Y. (1998). High cell density culture of metabolically engineered *Escherichia coli* for the production of poly(3-hydroxybutyrate) in a defined medium. *Biotechnology and Bioengineering*, 58 (2-3), 325–8.

Wang, L., Wu, D., Chen, J., Wu, J. (2013). Enhanced production of gamma-cyclodextrin by optimization of reaction of gamma-cyclodextrin glycosyltransferase as well as synchronous use of isoamylase. *Food Chemistry*, 141, 3072–3076.

Wang, Z. X., Shi, X. X., Chen, G. R., Ren, Z. H., Luo, L., Yan, J. (2006). A new synthesis of alpha-arbutin via Lewis acid catalyzed selective glycosylation of tetra-O-benzyl-alpha-D-glucopyranosyl trichloroacetimidate with hydroquinone. *Carbohydrate Research*, 341, 1945–1947.

Ward, D. P., Cárdenas-Fernández, M., Hewitson, P., Ignatova, S., Lye, G. J. (2015). Centrifugal partition chromatography in a biorefinery context : Separation of monosaccharides from hydrolysed sugar beet pulp. *Journal of Chromatography A*, 1411, 84–91.

Welch, C. J., Shaimi, M., Biba, M., Chilenski, J. R., Dolling, U., Mathre, D. J., Reider, P. J. (2002). Microplate evaluation of process adsorbents. *Journal of Separation Science*, 25, 847–850.

Werpy, T., Petersen, G. (2004). Top value added chemicals from biomass. Volume I. Results of screening for potential candidates from sugars and synthesis gas. *Office of Scientific and Technical Information (OSTI)*, U. S. Department of Energy.

Weuster-Botz, D., Stevens, S., Hawrylenko, A. (2002). Parallel-operated stirred-columns for microbial process development. *Biochemical Engineering Journal,* 11, 69–72.

Wu, H. C. P. (1967). Role of the galactose transport system in the establishment of endogenous induction of the galactose operon in *Escherichia coli. Journal of Molecular Biology*, 24 (2), 213–223.

Wu, H . C . P ., Kalckar, H . M .(1966). Endogenous induction of the galactose operon in *Escherichia Coli* K12 Source. *Proceedings of the National Academy of Sciences of the United States of America*, 55 (3), 622–629.

Xia, Z., Wu, S. (2012). Cell number as an important variable in optimising inoculum age and size in yeast cultivation. *African Journal of Biotechnology*, 11 (4), 919–922.

Xu, J., Banerjee, A., Pan, S. H., Li, Z. J. (2012). Galactose can be an inducer for production of therapeutic proteins by auto-induction using *E. coli* BL21 strains. *Protein Expression and Purification*, 83 (1), 30–6.

Yachmenev, V. G., Bertoniere, N. R., Blanchard, E. J. (2002). Intensification of the bio-processing of cotton textiles by combined enzyme/ultrasound treatment. *Journal of Chemical Technology and Biotechnology*, 77, 559–67.

Yamamoto, K. O. H., Ishizaki, A., Stanbury, D. P. F. (1993). Reduction in the length of the lag phase of L-lactate fermentation by the use of inocula from electrodialysis seed cultures, *Journal of Fermentation and Bioengineering*, 76 (2), 151–152.

Yang, F., Hanna, M. A., Sun, R. (2012). Value-added uses for crude glycerol - a byproduct of biodiesel production. *Biotechnology for Biofuels*, 5, 13.

Yazdani, S. S., Gonzalez, R. (2007). Anaerobic fermentation of glycerol: a path to economic viability for the biofuels industry. *Current Opinion in Biotechnology*, 18, 213–219.

Yong, M. J., Wang, Y. T., Dong, Z. W. (2007). Effects of induction starting time and Ca2+ on expression of active penicillin G acylase in *Escherichia coli. Biotechnology Progress*, 23 (5),

1031–1037.

Zhang, A., Yang, S. T. (2009). Propionic acid production from glycerol by metabolically engineered *Propionibacterium acidipropionici*. *Process Biochemistry*, 44, 1346–1351.

Zhang, C., Chen, X., Zou, R., Zhou, K., Stephanopoulos, G., Too, H. P. (2013). Combining genotype improvement and statistical media optimization for isoprenoid production in *E. coli*. *PloS One*, 8 (10), e75164.

Zhang, H., Lamping, S. R., Pickering, S. C. R., Lye, G. J., Shamlou, P. A. (2008). Engineering characterisation of a single well from 24-well and 96-well microtitre plates. *Biochemical Engineering Journal*, 40, 138–149.

Zhang, J., Reddy, J., Buckland, B., Greasham, R. (2003). Toward consistent and productive complex media for industrial fermentations: studies on yeast extract for a recombinant yeast fermentation process. *Biotechnology and Bioengineering*, 82 (6), 640–52.

Zheng, Y., Yu, C. Cheng, Y. S., Lee, C., Simmons, C.W., Dooley, T.M., Zhang, R., Jenkins, B.M., VanderGheynst, J.S. (2012). Integrating sugar beet pulp storage, hydrolysis and fermentation for fuel ethanol production. *Applied Energy*, 93, 168–175.

Znabet, A., Polak, M. M., Janssen, E., de Kanter, F. J., Turner, N. J., Orru, R. V. A., Ruijter, E. (2010). A highly efficient synthesis of telaprevir by strategic use of biocatalysis and multicomponent reactions. *Chemical Communications (Camb)*, 46, 7918–7920.

APPENDIX 1 (A1): STANDARD CURVES

$$y = 0.5827x - 0.2515$$
$$R^2 = 0.9932$$
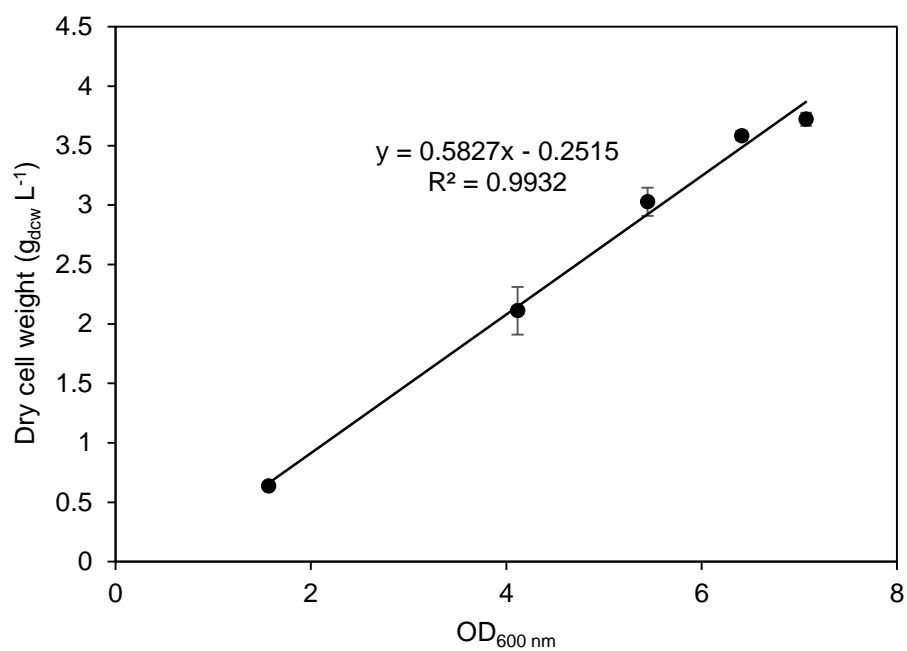
Figure A1.1. Dry cell weight (g_{dcw} L^{-1}) in the function of $OD_{600\ nm}$ in a cultivation using a complex medium. Every point represents the mean value of triplicates. Experiment was performed as described in Section 2.12.1 and 2.12.2.


$$y = 0.3492x + 0.0535$$
$$R^2 = 0.9952$$
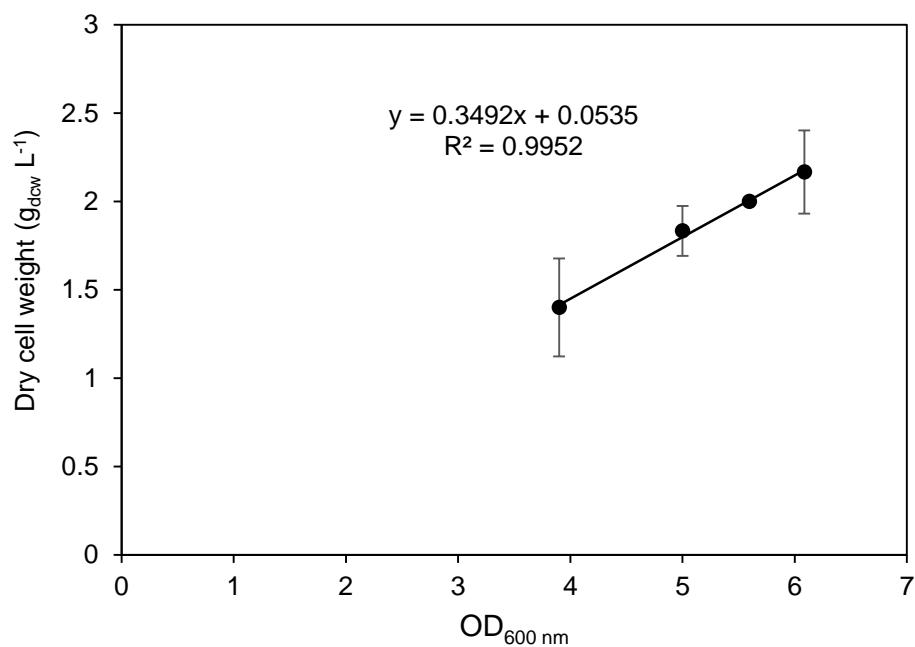
Figure A1.2. Dry cell weight (g_{dcw} L^{-1}) in the function of $OD_{600\ nm}$ in a cultivation using a vinasse medium. Every point represents the mean value of triplicates. Experiment was performed as described in Section 2.12.1 and 2.12.2.
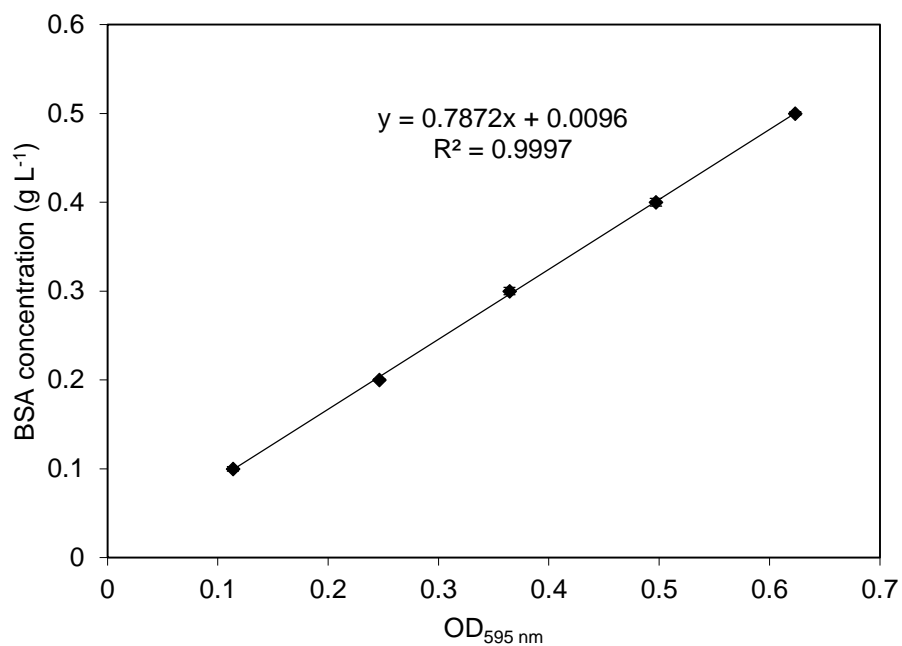
Figure A1.3. BSA (g L^{-1}) in the function of OD$_{595 nm}$. Every point represents the mean value of triplicates. Experiment was performed as described in Section 2.12.3.
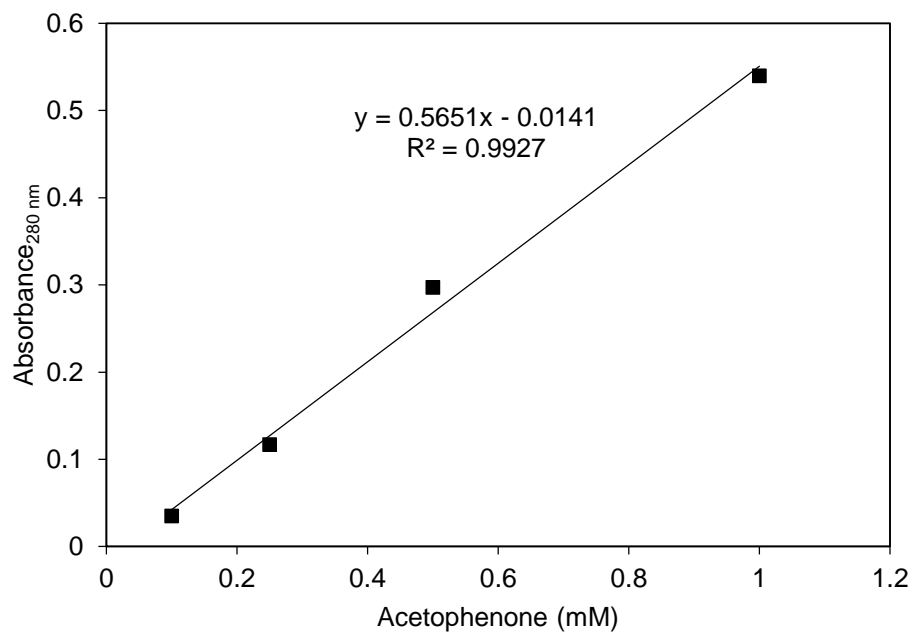
Figure A1.4. Acetophenone (mM) in the function of absorbance at 280 nm. Every point represents the mean value of triplicates. Experiment was performed as described in Section 2.12.5.
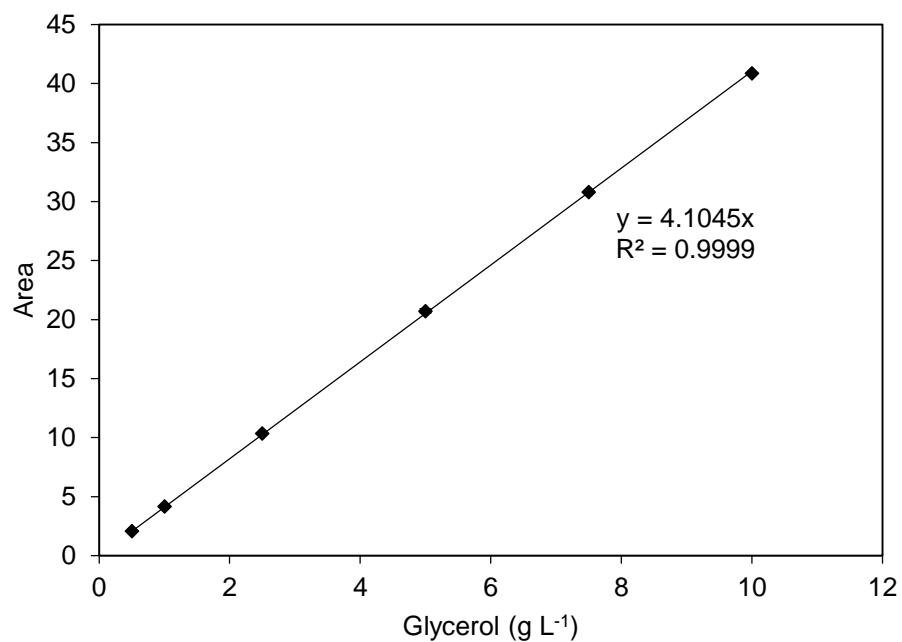
Figure A1.5. Glycerol calibration curve (g L^{-1}) in the function of area. Every point represents the mean value of triplicates. Experiment was performed as described in Section 2.12.6.
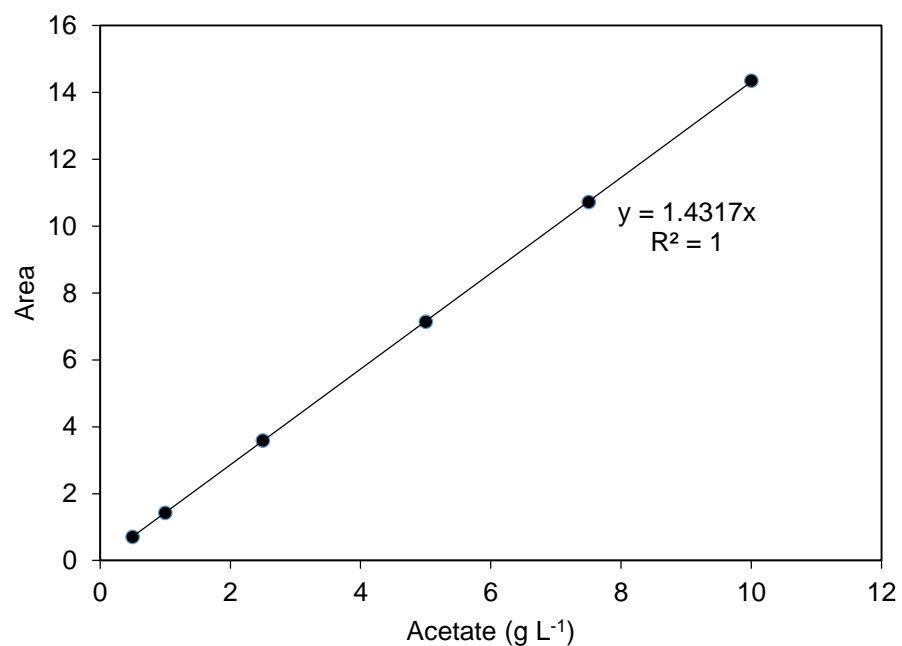
Figure A1.6. Acetate (g L^{-1}) in the function of area. Every point represents the mean value of triplicates. Experiment was performed as described in Section 2.12.6.
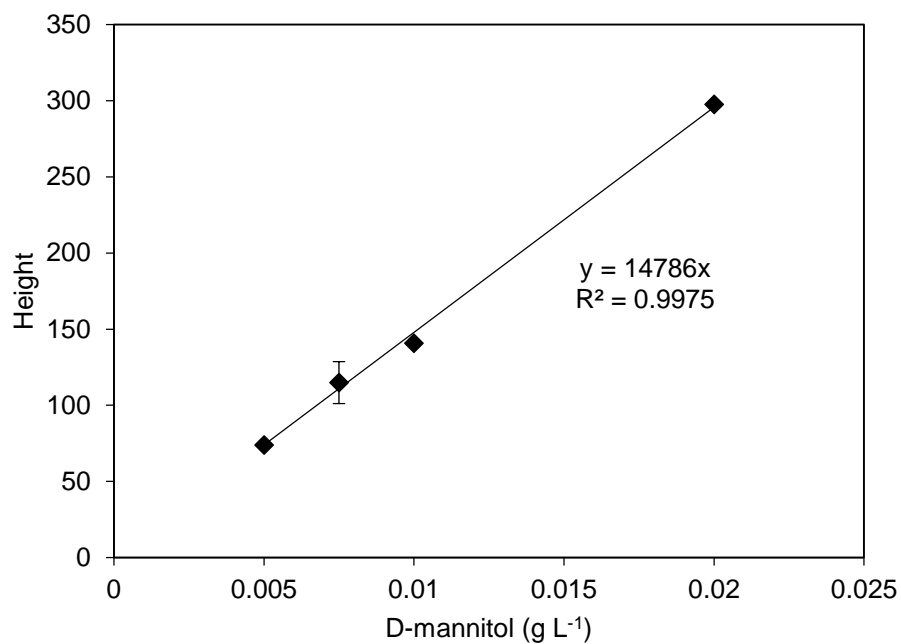
Figure A1.7. D-mannitol (g L^{-1}) in the function of height. Every point represents the mean value of triplicates. Experiment was performed as described in Section 2.12.7.
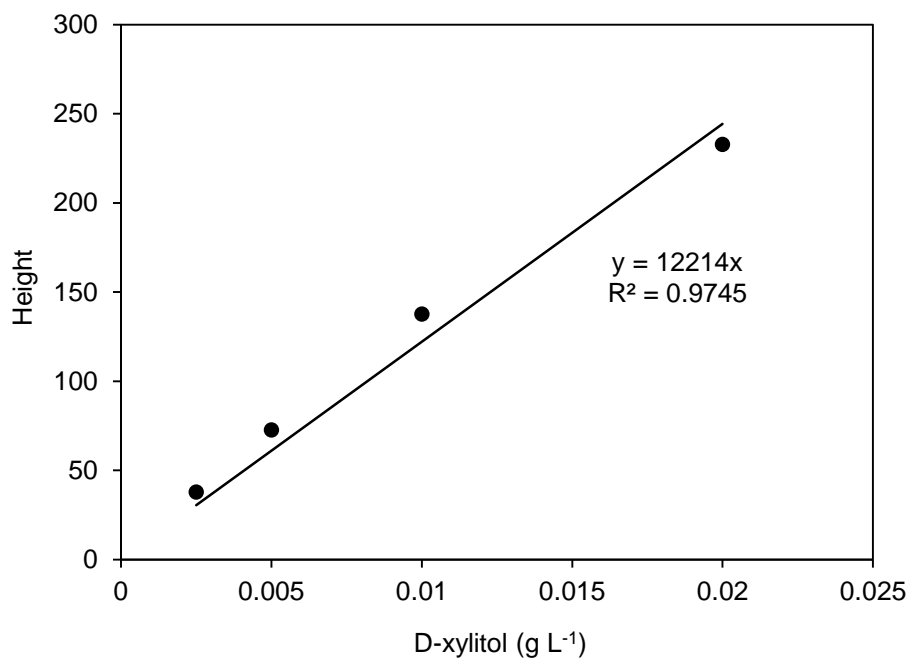
**Figure A1.8.** D-xylitol (g L^{-1}) in the function of height. Every point represents the mean value of triplicates. Experiment was performed as described in Section 2.12.7.
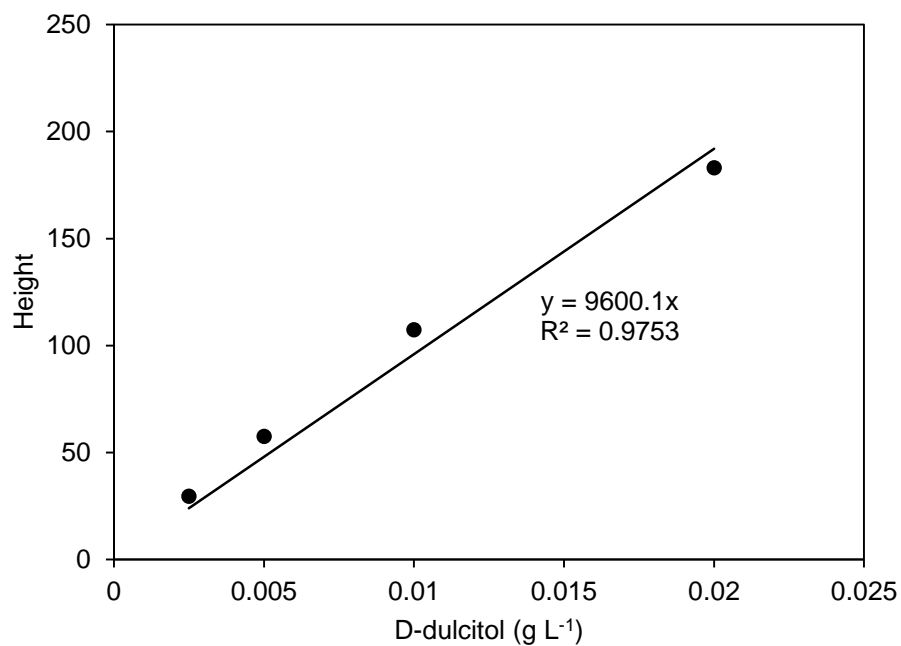
**Figure A1.9.** D-dulcitol (g L^{-1}) in the function of height. Every point represents the mean value of triplicates. Experiment was performed as described in Section 2.12.7.
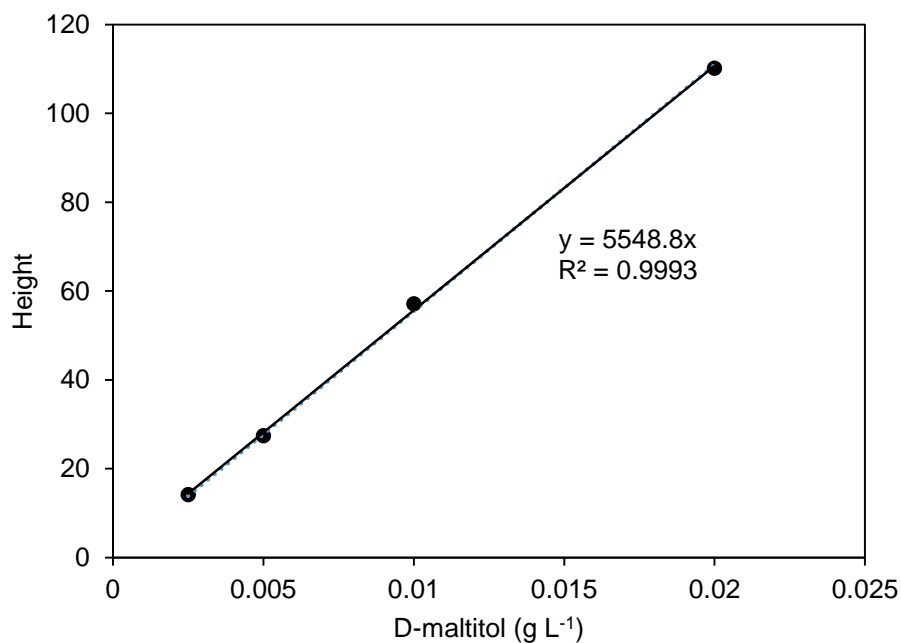
Figure A1.10. D-maltitol (g L^{-1}) in the function of height. Every point represents mean value of triplicates. Experiment was performed as described in Section 2.12.7.
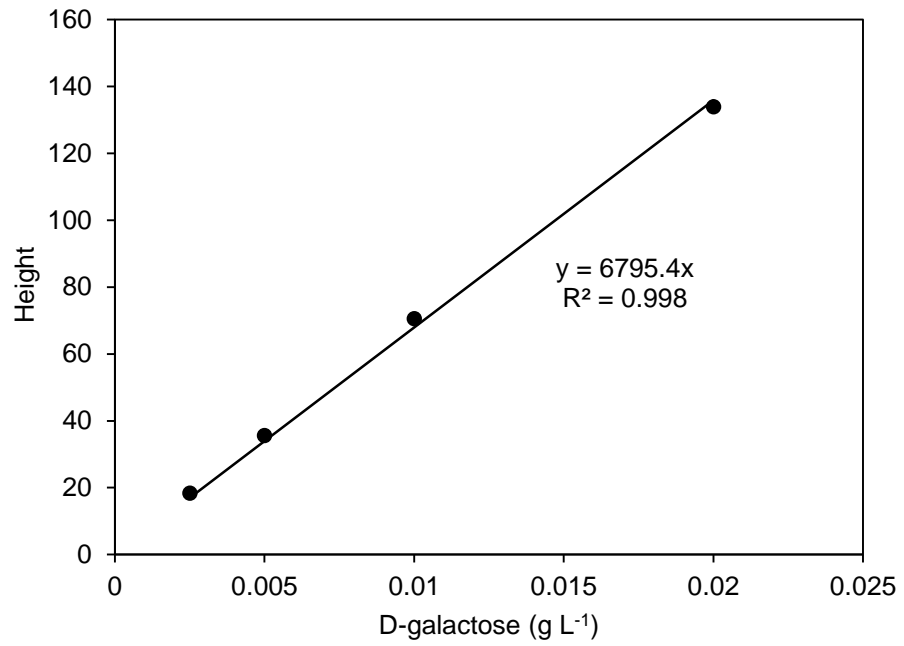
Figure A1.11. D-galactose (g L^{-1}) in the function of height. Every point represents mean value of triplicates. Experiment was performed as described in Section 2.12.7.
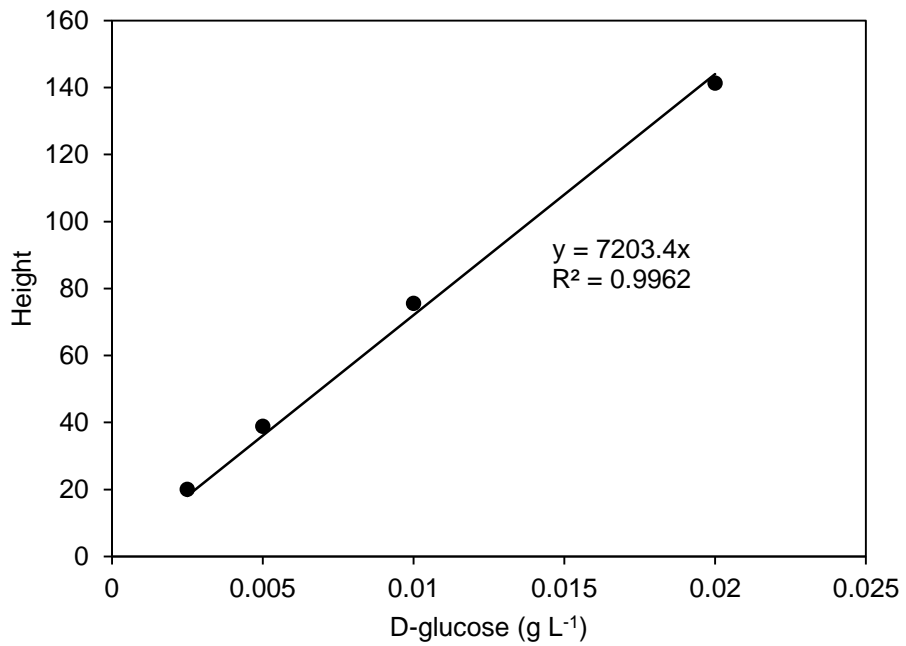

Figure A1.12. D-glucose (g L^{-1}) in the function of height. Every point represents mean value of triplicates. Experiment was performed as described in Section 2.12.7.
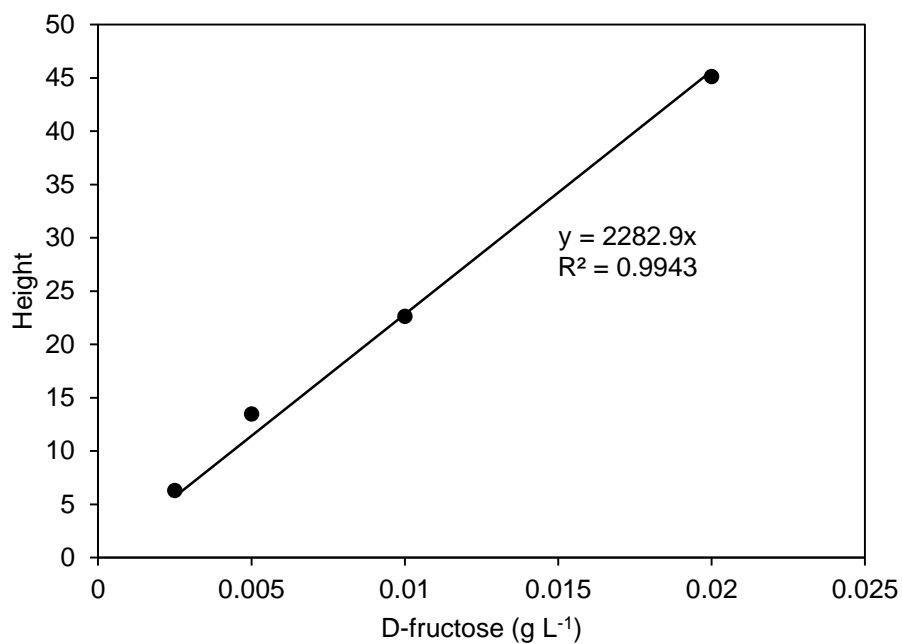
Figure A1.13. D-fructose (g L^{-1}) in the function of height. Every point represents mean value of triplicates. Experiment was performed as described in Section 2.12.7.
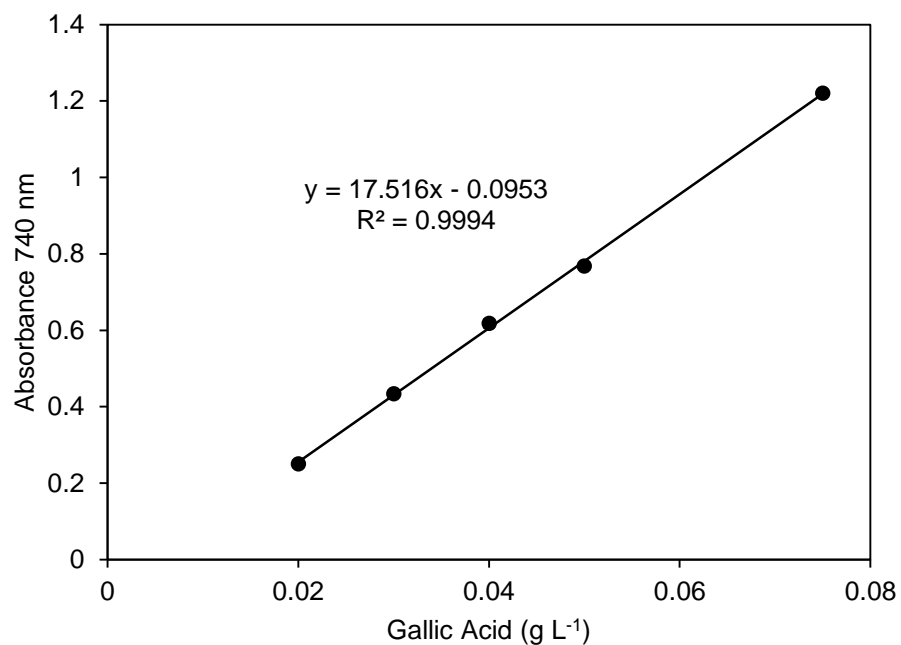
Figure A1.14. Gallic acid (g L^{-1}) in the function of absorbance at 740 nm. Every point represents the mean value of triplicates. Experiment was performed as described in Section 2.12.8.
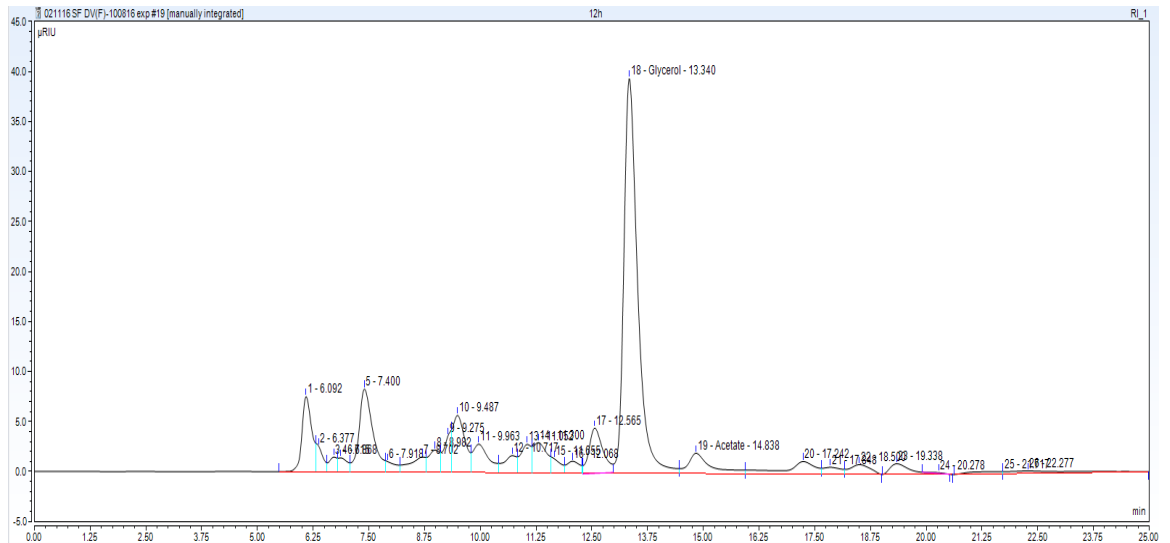
Figure A2.1. Example of an HPLC chromatogram showing the peaks of glycerol (retention time 13.3 min) and acetate (retention time 14.8 min). Experiment was performed as described in Section 2.12.6.
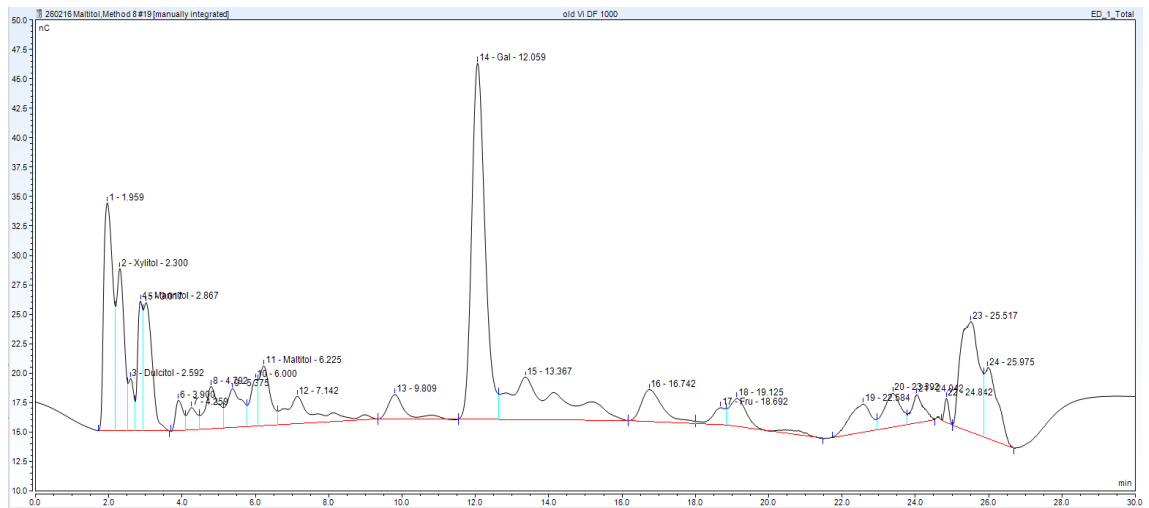

Figure A2.2. Example of an ICS chromatogram showing the peaks of D-xylitol (retention time 2.3 min), D-dulcitol (retention time 2.6 min), D-mannitol (retention time 2.8 min), D-maltitol (retention time 6.2 min), D-galactose (retention time 12.1 min) and D-fructose (retention time 18.7 min). Experiment was performed as described in Section 2.12.7.

APPENDIX 3 (A3): VISCOSITY-SHEAR RATE CURVE
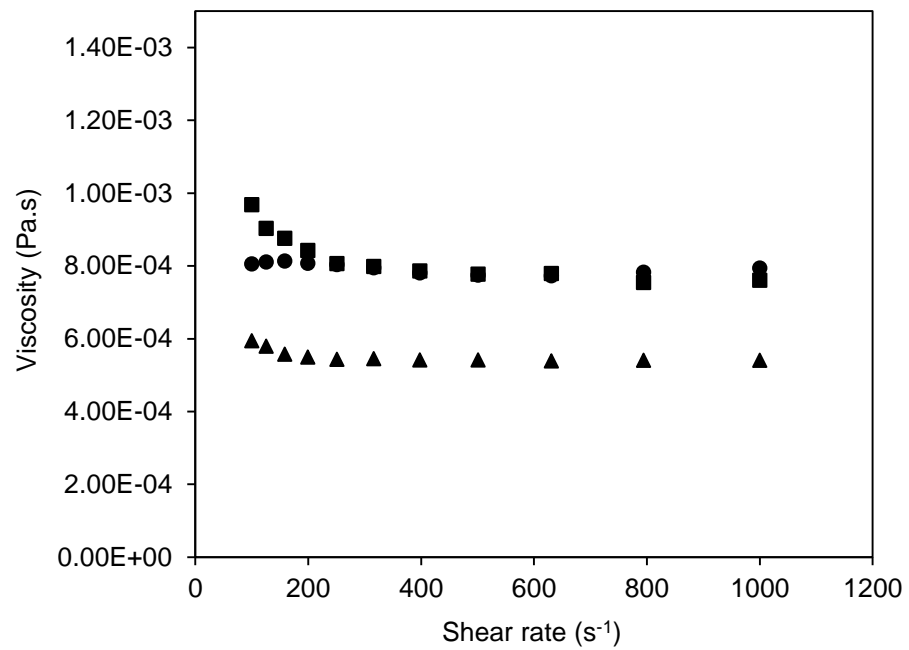
Figure A3.1. Relationship between apparent viscosity and shear rate of (▲) water, (●) complex medium with 1 mL L^{-1} PPG and (■) vinasse medium with 1 mL L^{-1} PPG. Experiment was performed as described in Section 2.12.9.

(A)

$y = 0.0141x + 1.6352$
$R^2 = 0.9807$

$y = 0.0131x + 1.6195$
$R^2 = 0.9687$

(B)

$y = 0.0281x + 1.6483$
$R^2 = 0.9971$

$y = 0.025x + 1.6832$
$R^2 = 0.9585$

(C)

$y = 0.0598x + 1.5872$
$R^2 = 0.9988$

$y = 0.0587x + 1.6358$
$R^2 = 0.959$
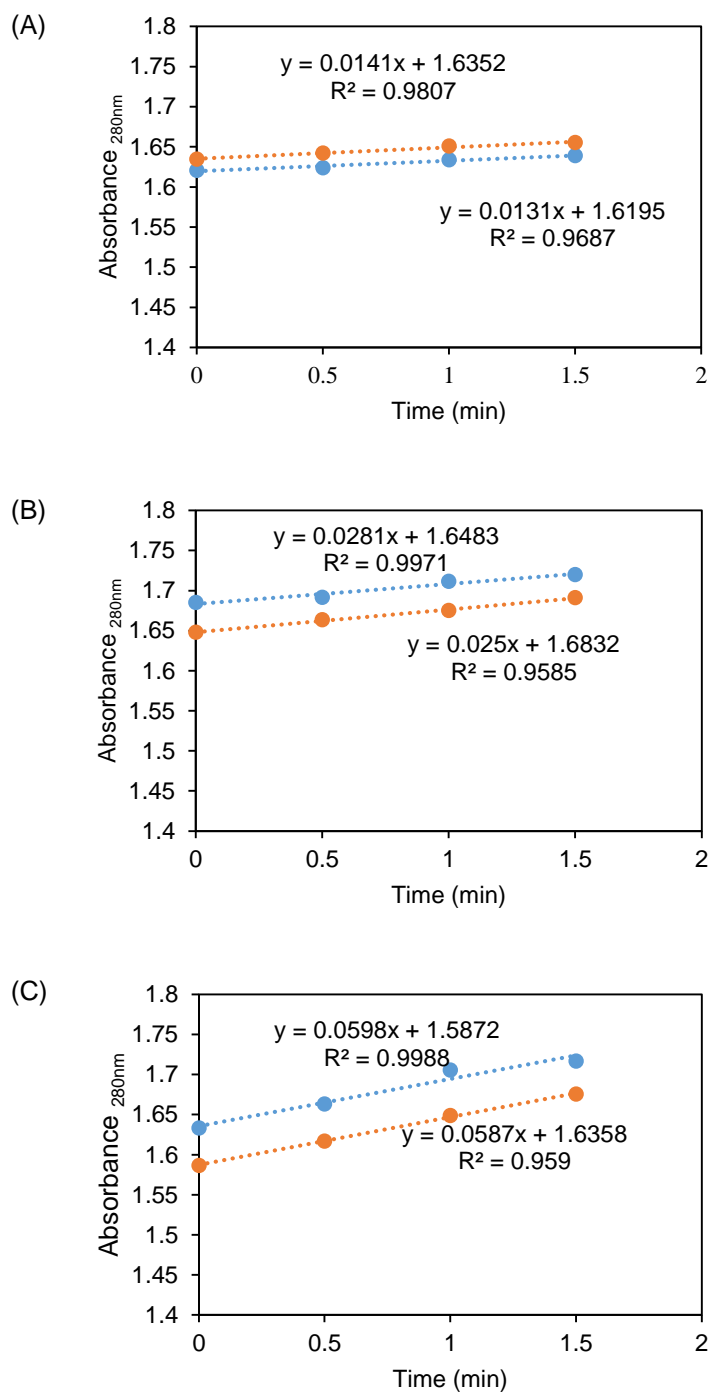
Figure A4.1. Typical time courses of absorbance for duplicate samples with (A) low, (B) intermediate and (C) high CV2025 ω-TAm activity. Experiment was performed as described in Section 2.12.5.

APPENDIX 5 (A5): PRESENTATIONS AND PUBLICATIONS

Suhaili, N., Cárdenas-Fernández, M., Ward, J. M., Lye, G. J. (2016). Potential of sugar beet vinasse as a fermentation feedstock for industrial enzyme production. 38th Symposium of Biotechnology for Fuels and Chemicals, Baltimore, Maryland, USA, April 25 – 28.

Lye, G. J., Cárdenas-Fernández, M., Suhaili, N. (2016). High throughput evaluation of sugar beet vinasse for industrial enzyme production. 2016 SIMB Annual Meeting and Exhibition, New Orleans, Louisiana, USA, July 24 – 30.

Suhaili, N., Cárdenas-Fernández, M., Ward, J. M., Lye, G. J. (2016). Scale-up of industrial biocatalyst production using sugar beet vinasse as a fermentation feedstock. 6th International IUPAC Conference on Green Chemistry, Venice, Italy, September 4 - 8.

Suhaili, N., Cárdenas-Fernández, M., Ward, J. M., Lye, G. J. (2016). Optimisation and scale-up of industrial enzyme production in *E. coli* fermentations using a 24-well single use microbioreactor. 13th Annual bioProcessUK Conference, Newcastle, UK, November 23 - 24.

Cárdenas-Fernández, M., Bawn, M., Bennett, C. E. M., Bharat, P. K. V., Subrizi, F., Suhaili, N., Ward, D. P., Bourdin, S., Dalby, P. A., Hailes, H. C., Hewitson, P., Ignatova, S., Kontoravdi, C., Leak, D. J., Shah, N., Sheppard, T. D., Ward, J. M., Lye, G. J. (2017). An integrated biorefinery concept for conversion of sugar beet pulp into value-added chemicals and pharmaceutical intermediates. *Faraday Discussions*, 202, 415-431.

Suhaili, N., Cárdenas-Fernández, M., Ward, J. M., Lye, G. J. (2017). Evaluation of pre-processing options of sugar beet vinasse as a feedstock for large scale bioproductions. 39th Symposium of Biotechnology for Fuels and Chemicals, San Francisco, California, USA. May 1 – 4.